Sequence Specific Complexation of B DNA at Sites Containing G,C Base Pairs

Thesis by

Warren Stanfield Wade

In Partial Fulfillment of the Requirements

for the Degree of

Doctor of Philosophy

California Institute of Technology

Pasadena, California

1989

(Submitted February 2, 1989)

To Jesus

Acknowledgements

I would like to thank my advisor, Peter Dervan, for the opportunities and challenges of the past few years. His insight, enthusiasm, and insistence on excellence will always be appreciated. Many thanks go to the members of the Dervan group who have made my sojourn both interesting and rewarding. Special thanks are in order for the people who proofread this thesis: Dave Mack, Dr. Jim Reiss, Dr. Jim Maher, Martha Oakley, Kevin Luebke, and Joy Scott. Your comments and suggestions were greatly appreciated. The support of the National Science Foundation for much of this work is gratefully acknowledged.

To my family and good christian friends, thank you for bearing with me through ups and downs. Your support has meant a great deal to me. Lastly, I thank the LORD my God for creating me as I am, and blessing me continually. This thesis is yours in every sense of the word.

Abstract

A series of eight related analogs of distamycin A has been synthesized. Footprinting and affinity cleaving reveal that only two of the analogs, pyridine-2-carboxamide-netropsin (2-PyN) and 1-methylimidazole-2-carboxamide-netropsin (2-ImN), bind to DNA with a specificity different from that of the parent compound. A new class of sites, represented by a TGACT sequence, is a strong site for 2-PyN binding, and the major recognition site for 2-ImN on DNA. Both compounds recognize the G·C bp specifically, although A's and T's in the site may be interchanged without penalty. Additional A·T bp outside the binding site increase the binding affinity. The compounds bind in the minor groove of the DNA sequence, but protect both grooves from dimethylsulfate. The binding evidence suggests that 2-PyN or 2-ImN binding induces a DNA conformational change.

In order to understand this sequence specific complexation better, the Ackers quantitative footprinting method for measuring individual site affinity constants has been extended to small molecules. MPE·Fe(II) cleavage reactions over a 10^5 range of free ligand concentrations are analyzed by gel electrophoresis. The decrease in cleavage is calculated by densitometry of a gel autoradiogram. The apparent fraction of DNA bound is then calculated from the amount of cleavage protection. The data is fitted to a theoretical curve using non-linear least squares techniques. Affinity constants at four individual sites are determined simultaneously. The distamycin A analog binds solely at A·T rich sites. Affinities range from

10^6–10^7 M^{-1}. The data for parent compound D fit closely to a monomeric binding curve. 2-PyN binds both A·T sites and the TGTCA site with an apparent affinity constant of 10^5 M^{-1}. 2-ImN binds A·T sites with affinities less than 5×10^4 M^{-1}. The affinity of 2-ImN for the TGTCA site does not change significantly from the 2-PyN value. At the TGTCA site, the experimental data fit a dimeric binding curve better than a monomeric curve. Both 2-PyN and 2-ImN have substantially lower DNA affinities than closely related compounds.

In order to probe the requirements of this new binding site, fourteen other derivatives have been synthesized and tested. All compounds that recognize the TGTCA site have a heterocyclic aromatic nitrogen *ortho* to the N or C-terminal amide of the netropsin subunit. Specificity is strongly affected by the overall length of the small molecule. Only compounds that consist of at least three aromatic rings linked by amides exhibit TGTCA site binding. Specificity is only weakly altered by substitution on the pyridine ring, which correlates best with steric factors. A model is proposed for TGTCA site binding that has as its key feature hydrogen bonding to both G's by the small molecule. The specificity is determined by the sequence dependence of the distance between G's.

One derivative of 2-PyN exhibits pH dependent sequence specificity. At low pH, 4-dimethylaminopyridine-2-carboxamide-netropsin binds tightly to A·T sites. At high pH, 4-Me_2NPyN binds most tightly to the TGTCA site. In aqueous solution, this compound protonates at the pyridine nitrogen at pH 6. Thus presence of the protonated form correlates with A·T specificity.

The binding site of a class of eukaryotic transcriptional activators typified by yeast protein GCN4 and the mammalian oncogene *jun* contains a strong 2-ImN binding site. Specificity requirements for the protein and small molecule are similar. GCN4 and 2-ImN bind simultaneously to the same binding site. GCN4 alters the cleavage pattern of 2-ImN-EDTA derivative at only one of its binding sites. The details of the interaction suggest that GCN4 alters the conformation of an AAAAAAA sequence adjacent to its binding site. The presence of a yeast counterpart to *jun* partially blocks 2-ImN binding. The differences do not appear to be caused by direct interactions between 2-ImN and the proteins, but by induced conformational changes in the DNA protein complex. It is likely that the observed differences in complexation are involved in the varying sequence specificity of these proteins.

Table of Contents

List of Illustrations

Chapter 1

Recognition of B DNA by Small Molecules

Introduction

It has become apparent over the last 20 years that specific binding to nucleic acids is an important control point for biological processes. The complexation of specific DNA sequences by regulatory molecules can control transfer of information from DNA to RNA to proteins, with far reaching biological consequences. A central challenge to chemists studying DNA is to understand the physical basis for such specific interactions. The studies described here are aimed at designing synthetic molecules that complex specifically to target DNA sequences containing G,C base pairs.

DNA structure

Watson and Crick originally proposed a regular rod-like structure for DNA.[1] This double helix is characterized by flat purine-pyrimidine base pairs (bp) spaced at regular intervals along a sugar phosphate backbone. Hydrogen bonding interactions between the bases on antiparallel strands produce two distinct grooves, which spiral along the helix axis. Information is stored in the sequence of bases along a particular strand. The array of functional groups on each base is such that both the interactions between the strands and the pattern of hydrogen bond donors and acceptors in the grooves are unique for each base.[2,3] Selection of a particular sequence could then be accomplished by maximizing the number of hydrogen bonds and hydrophobic contacts with the edges of the bases. Thus the design of

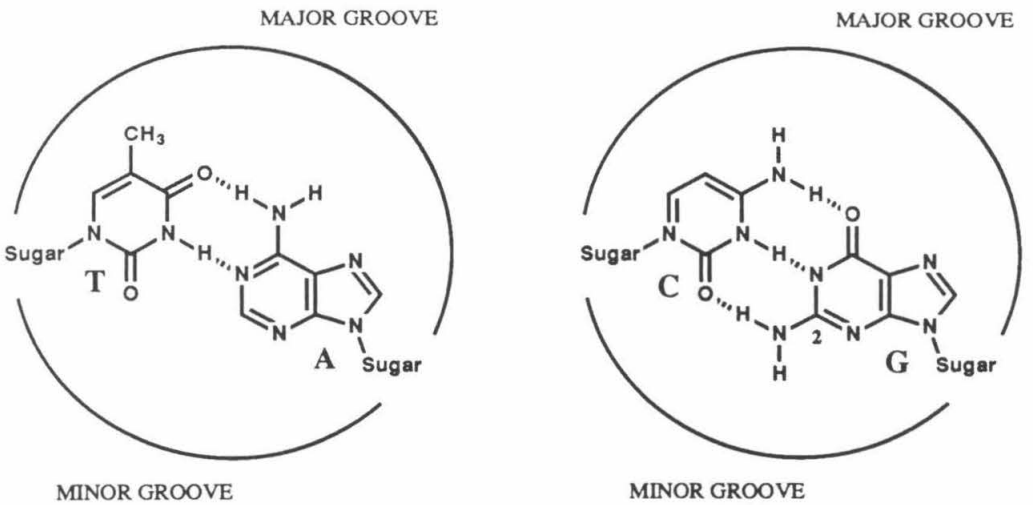

Figure 1 Effects of Watson-Crick base pairing on the availability of base functional groups. Triangles represent potential hydrogen bond interactions in the major and minor grooves.

DNA binding molecules might be reduced to the relatively straightforward task of matching an array of DNA contacts with a complementary set on the ligand.

Discoveries in the past few years have both supported and refined this original model. X-ray structures[4] and solution studies of DNA itself have revealed many sequence dependent variations in DNA structure.[5] In the crystals, base pairs are neither flat nor perpendicular to the helix axis. Instead they are propeller twisted as shown in figure 2, increasing the stacking interactions between the bases. From the minor groove, each base is twisted towards the 5′ end of its own DNA strand. There is also a sequence dependence to the tilt (*i.e.*, rotation about the short axis of the base pair), roll (rotation about the long axis of the base pair) and twist

(rotation about the helix axis between consecutive bp). Instead of a rigid rod, it appears that B DNA should be viewed as a series of local conformations with varying elastic properties. These local structures blend into one another, with each unique sequence having its own unique set of helix parameters.

This ensemble of conformations has important implications for DNA sequence recognition. In addition to the pattern of potential hydrogen bonds and hydrophobic contacts, the distance and orientation of the base functional groups are now unique to a given sequence. Instead of matching all interactions with a given bp, a ligand could select between sequences by requiring a specified distance between interactions. This is especially important in the minor groove, where replacement of A by T or G by C produces only small changes in the functional group pattern.

This more sophisticated approach to sequence specific recognition requires a knowledge of the structure of the target sequence. Recently, detailed models for this sequence specific variation have been developed by Calladine[6] and modified and extended by Dickerson.[7] The authors propose that steric interactions produced by the propeller twist are responsible for such structure variations. For a 5′ purine-pyrimidine sequence, the fact that purines are significantly longer than half a bp produces close van der Waals contacts in the major groove. For a 5′ pyrimidine-purine sequence, the close contacts occur in the minor groove, while for a purine-purine sequence ($\equiv$ pyrimidine-pyrimidine) no unfavorable steric interaction occurs. In addition, the extra width of a G,C bp results in closer contacts than A,T bp.

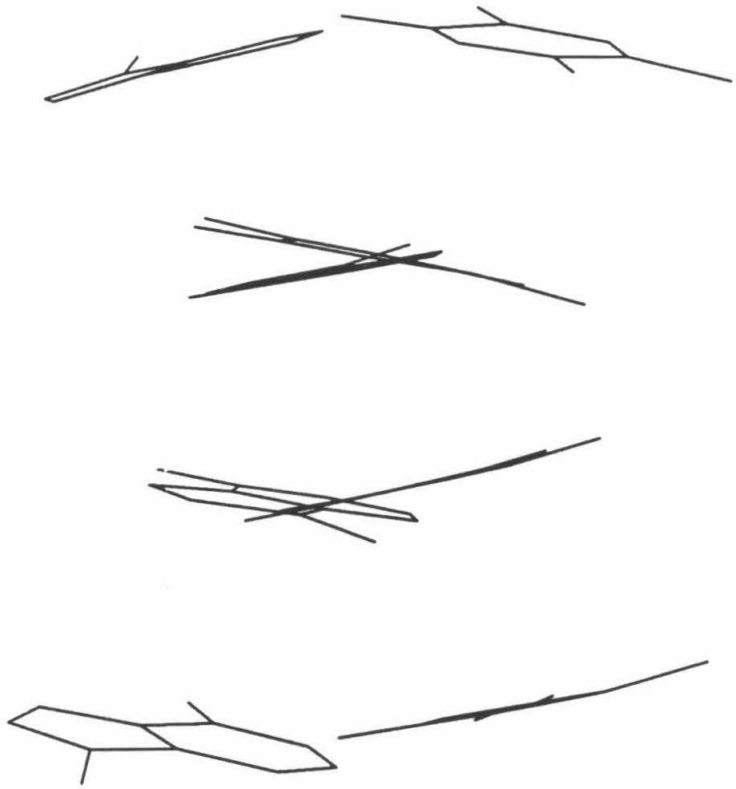

Figure 2 Implications of propeller twist for the sequence dependent structure of DNA, from reference 7. Atom positions of the AATT region of the dodecamer crystal structure are taken from the Brookhaven Protein Databank (only base atoms shown). The major groove is to the left of the figure, and the minor groove is to the right. Propeller twisting towards the 5′ terminus of each strand in the minor groove results in a stacked conformation for each strand.

Unfavorable contacts can be relieved by a number of mechanisms involving the tilt, roll, and twist of the base pair. Significantly, application of the Calladine model to the dodecamer structure determined by Dickerson *et al.* gives a good correlation to the experimental data.[7] A recent paper proposes that this sequence dependent structure is actually due to repulsion of partial charges on neighbor-

ing bases, rather than steric effects.[8] However the small number of independent DNA crystal structures in the database makes the predictive value of these models difficult to assess.

Small Molecule DNA Complexes

A number of test cases for distance dependent sequence recognition already exist. A variety of small molecules (molecular weights less than 1500 daltons) have been observed to bind specifically to DNA. These compounds appear to exert anti-tumor and antibiotic activities by forming tight complexes with their cognate DNA sites, blocking transcription.[9] On such a small molecule, the number of specific contacts is limited. Thus the distance between contacts ought to be an important determinant of specificity.

Three modes of interaction have been observed in the DNA complexes of such small molecules.[10] A common mode involves the intercalation of a flat aromatic molecule between two base pairs. In general this mode has a relatively low specificity, presumably because a major interaction is the relatively nonspecific $\pi - \pi$ stacking interaction. Usually there is a slight preference for G,C bp because of the increased width and flatter conformations of G,C sequences. Intercalation necessitates a change in DNA conformation, and experiments to date reveal no obvious correspondence between the structure of a particular compound and the details of the complex.[11] Because the relevant distances are drastically altered in the complex, distance matching would have to be done on the intercalated conformation.

The other two recognition modes involve interactions within one of the grooves of the helix. Either the major or minor groove could serve as a complexation site, with the appropriate segregation of base recognition elements. Groove binding small molecules examined to date form complexes in the minor groove, presumably because of a closer match in size. The known binding characteristics of these nonintercalative compounds have recently been exhaustively reviewed,[9] and so only the information pertaining to specificity will be repeated here.

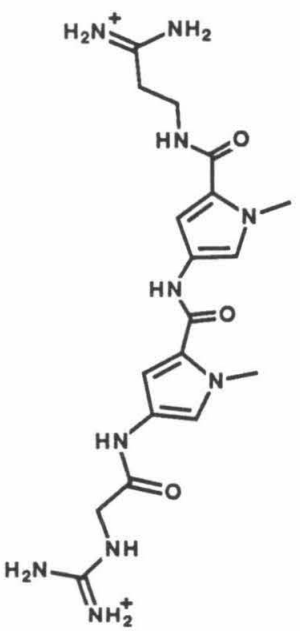

Netropsin

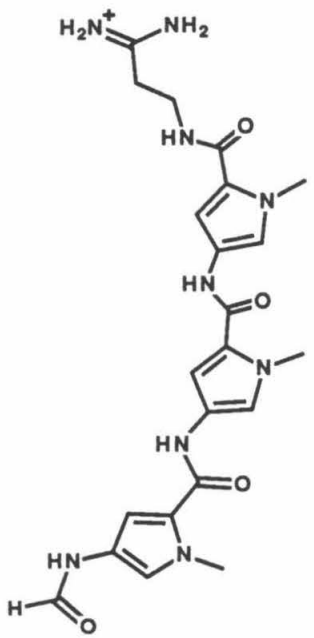

Distamycin A

Figure 3 Naturally occurring polypyrrole antitumor antibiotics.

A,T Sequence Specificity

Netropsin and distamycin A are well studied compounds that bind to A,T rich DNA. As shown in figure 3, they consist of a poly-N-methylpyrroleamide backbone capped with one or more delocalized positively charged groups. Both compounds exhibit strong preferences for double stranded B DNA, with high specificity for A,T bp.[9] Footprinting studies reveal that the polypyrrole antibiotics bind in the minor groove[12] at sites containing 4–5 contiguous A,T bp.[13–16] In general, the binding constant increases with the number of AA dinucleotides present in the bound sequence.[17] Neither netropsin nor distamycin A bind tightly to alternating A,T sequences.[9, 14]

Dodecamer-netropsin[18, 19] and dodecamer-distamycin A[20] complexes have been examined recently by X-ray crystallography (see figure 4). In both cases the antibiotic is set deeply into the minor groove so that the pyrrole amide hydrogens form bifurcated hydrogen bonds with the N3 of adenine and the O2 of thymine on the floor of the groove. In the netropsin complex, the width of the minor groove has increased by an average of 1.7 Å. The adjustment allows the pyrrole rings to fill the groove completely and to form extensive van der Waals contacts with the groove sides. These close contacts require the pyrrole rings to be parallel to the sides of the groove, increasing the overall screw sense of the antibiotic to match that of the groove. The helix axis is bent away from the netropsin molecule by 8°, increasing the distance between the outermost T carbonyls by about 0.5 Å. These

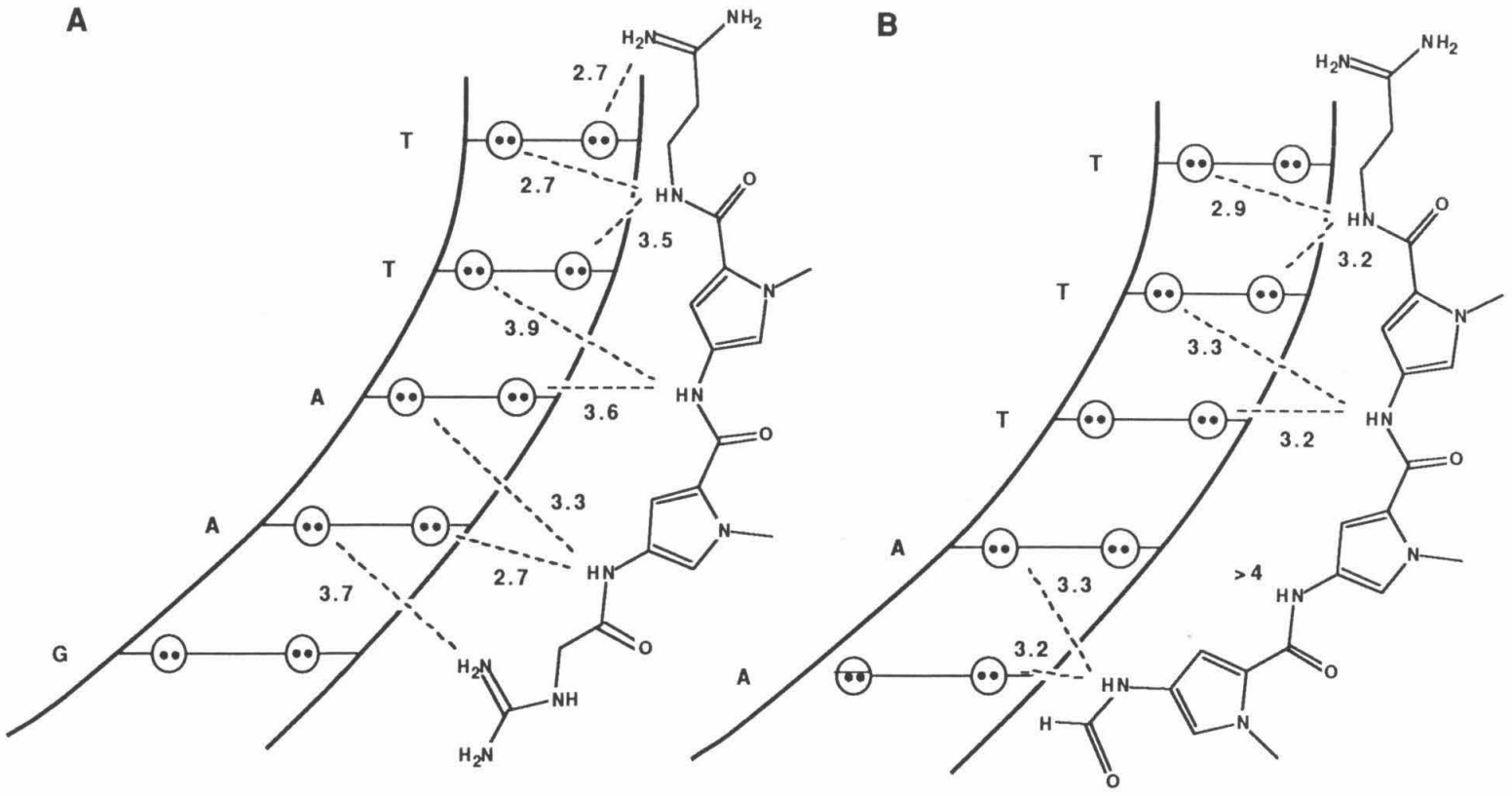

Figure 4 Structural features of the DNA complexes of netropsin and distamycin A.[18,20] The small molecules are set deeply in the minor groove, in close van der Waals contact to the sugar phosphate backbones. Circles represent the lone pair electrons of the thymine O2 and the adenine N3. Dashed lines represent hydrogen bonds existing in the complex. The distance in Å between donor and acceptor atoms is shown beside each interaction.

carbonyls also form the strongest hydrogen bonds to the pyrrole amides, suggesting that the overall distance of the unbound DNA site is smaller than that required for optimum contacts with netropsin.[21] Upon binding, both partners of the complex alter conformation, the DNA by bending away from the minor groove, and the netropsin by twisting around the amide pyrrole single bonds to better match the groove. A similar situation exists in the DNA-distamycin A cocrystal.[20] As a consequence of an increasing mismatch between ligand size and site size, one pyrrole amide cannot form hydrogen bonds to the DNA.

^{1}H NMR studies of a netropsin-GGAATTCC,[22] a netropsin-GGTATACC,[23] and a distamycin-CGCGAATTCGCG complex[24] conclude that the structure in solution is very similar to that found in the solid state. The DNA in the complexes is clearly in the B form, although there are conformational differences between the free DNA and the complex. NOEs between the antibiotic protons and the adenines in the binding site provide strong evidence that the polypyrrole compounds bind to the A,T regions of the oligonucleotides. The concave edge of the pyrrole system lies at the bottom of the groove, with the amide protons forming hydrogen bonds to the bases. Patel and his co-workers find that netropsin at the TATA site exchanges much more rapidly than netropsin at the AATT site, consistent with the footprinting data for this compound.

Breslauer and co-workers have studied the thermodynamic parameters of netropsin and distamycin A binding by Calorimetry and melting temperature

shift studies. Excluding poly(dA)·poly(dT), specific binding of netropsin and distamycin A to A,T rich DNA is enthalpically driven.[25-27] (Binding of most ligands, including intercalators, to poly(dA)·poly(dT) is entropically driven.[27]) This suggests that the ability to form strong hydrogen bonds at A,T sequences is an important factor in the overall specificity of these compounds. A recent study of the ionic strength dependence of netropsin complexation to poly d(AT) and poly d(GC) shows no significant difference, although the free energy of complexation differs by > 5 kcal/mol.[25] This would seem to eliminate electrostatic interactions as a major source of the A,T specificity. To date, no individual binding sites of either compound have been studied by these techniques, so that the enthalpy and entropy contributions to selectivity between A,T sequences are not known.

Taken together, the experimental evidence suggests that specificity for A,T bp is determined by several interacting features. The requirement for hydrogen bonding in the complex means that close contacts are formed between the C2H of adenine and the C3H on the pyrrole rings. The extra bulk of the guanine N2 would disrupt these interactions. The disparity in size between pyrrole compound and the DNA binding site would also tend to select for taller, thinner sequences. Because A,T rich DNA has fewer bp per turn than G,C rich DNA,[28, 29] such sequences would provide hydrogen bonding more in register with the small molecule and increase the Van der Waals interactions between the aromatic rings and the side of the groove.

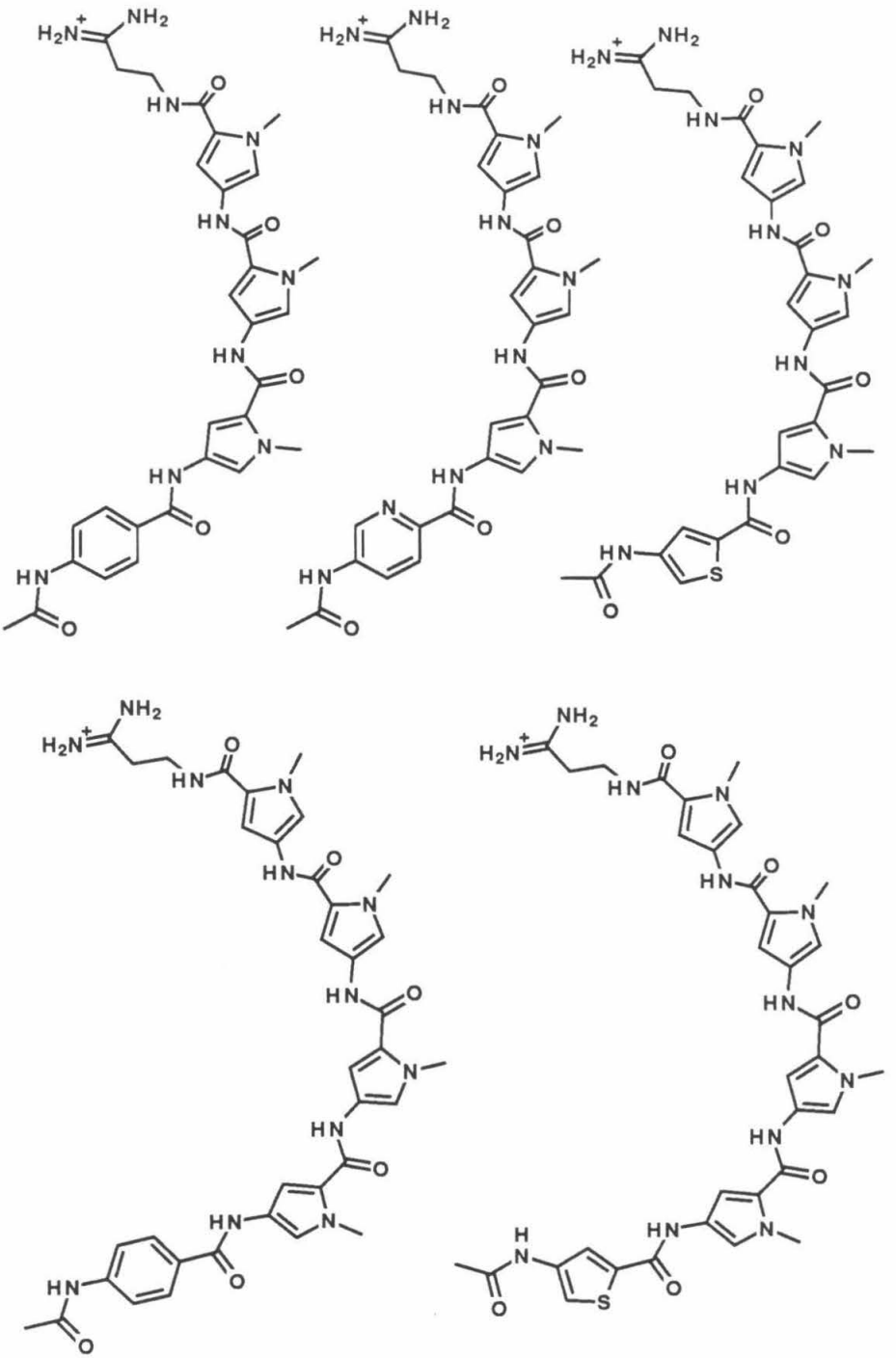

Figure 5 Strong binding heterocyclic analogs of distamycin A prepared by Arcamone and co-workers.[30]

Variations on the positively charged groups[31, 32] or the N-alkyl groups of the pyrrole rings[33] retain the A,T specificity of the parent compounds. A series of analogs of distamycin A with pyrrole rings substituted by other heterocyclic rings have also been prepared by Arcamone and co-workers.[30] Shown in figure 5 are the derivatives whose DNA binding properties have been studied. By CD measurements, these compounds show a distinct preference for A,T homopolymers, though with lower overall specificity than distamycin A. As is observed for netropsin and distamycin, longer derivatives have higher binding constants.

Many other synthetic compounds have been shown to bind preferentially to A,T DNA.[9] As shown in figure 6, these molecules are generally aromatic systems with one or more positive charges. The compounds can be separated by their ability to form a distamycin-like crescent conformation. Compounds in the top row of figure 6 show a strong preference for homopolymer A,T bp over homopolymer G,C bp of B DNA, while the bottom row shows much less specific behavior.[9] The mPD derivative shows intermediate behavior by CD, strongly preferring B DNA of either sequence.[34] Rao *et al.* conclude that the degree of bending in these compounds is a major determinant of A,T specificity.[34] All of these compounds compete with netropsin for DNA sites.[35-37] At this time, it is not known whether this is direct competition for common binding sites or conformational exclusion of nearby sites.

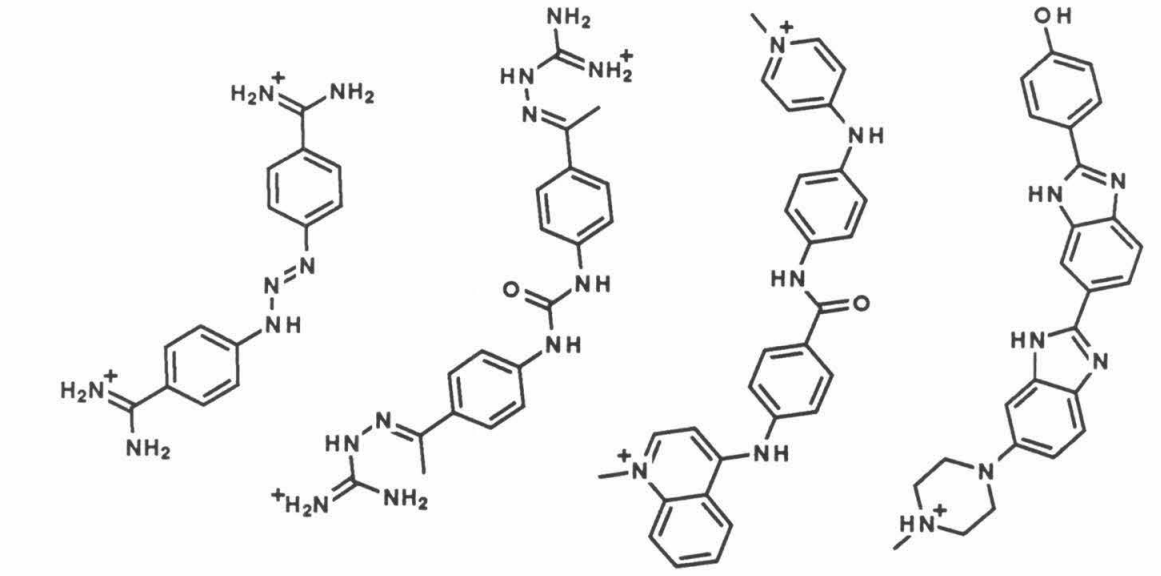

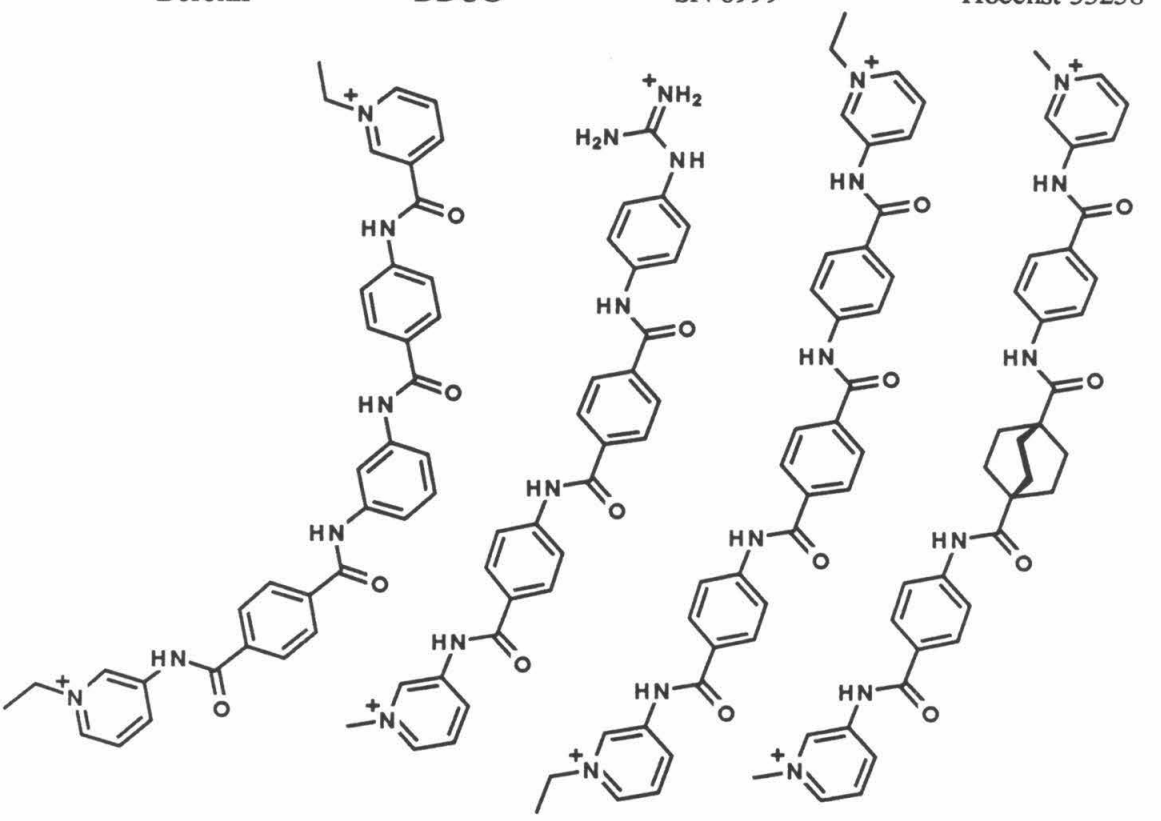

Figure 6 Other synthetic molecules that bind preferentially to A,T sequences.[9]

Recently, the DNA specificity of Hoechst 33258 has been studied by footprinting[38] and crystallography.[39, 40] Although Hoechst 33258 possesses only two potential hydrogen bonding groups, it binds the same sites as distamycin A with the same relative ordering of binding sites.[38] In the cocrystal solved by Dickerson and co-workers, Hoechst 33258 is shifted one bp from the netropsin position on the same oligonucleotide. The position of the piperazine ring is disordered, with equivalent occupancies along the innermost G,C bp and pointing out of the groove.[39] This result has prompted Dickerson to conclude that the extra width of the piperazine ring precludes its binding to an A,T bp. In the structure solved by Wang and coworkers,[40] Hoechst 33258 is complexed to the same oligonucleotide, but the overall complex is more similar to the netropsin complex. The small molecule is located in the AATT region of the minor groove, with a bifurcated hydrogen bonding array similar to netropsin. There is clearly only one orientation in the crystal and only one position for the piperazine ring. Comparing the two complexes, the Wang structure has no disorder in the small molecule and is more consistent with the footprinting data. This complex also demonstrates that the width of the piperazine ring does not necessarily preclude binding in A,T regions. The reason for such dissimilar complexes with the same components is not presently understood.

While no footprinting data has been published to date for the remaining compounds in figure 6, the evidence so far suggests that the key recognition motif for A,T sequences is a positively charged crescent shape. This shape serves to present

hydrogen bond donors at regular intervals, and both X-ray and NMR experiments show that these interactions are present in the complexes. The compounds are also aromatic and fit tightly in the groove of A,T regions, implicating van der Waals contacts as an important stabilizing factor. Clearly, the position of functional groups on the ligands is important for the interaction with the DNA sequence. Netropsin contains a regular array of contacts, each of which interacts with the DNA. This allows the compound to discriminate between A,T sites through better or worse matching to this array. However, the DNA conformation in the complex is not that observed for the free sequence.

G,C Sequence Specificity

Compounds that complex specifically to G,C bp are comparatively rare. Only a single family of antibiotics, the aureolic acids, appears to bind non-intercalatively to G,C sequences.[41] Structures of the original members of this family, chromomycin A_3, mithramycin, and olivomycin, are shown in figure 7. The aureolic acids share a common anthracenone chromophore, which is substituted at both ends with a series of polydeoxygenated sugar residues. The compounds differ from one another by the presence or absence of the C7 methyl group and the substitution pattern of the sugar residues. These compounds are negatively charged at neutral pH, and require magnesium cations to bind DNA.[42,43] Binding does not unwind supercoiled DNA,[44] making an intercalative complex unlikely. The aureolic acids also require

a purine 2′ amino group for strong binding to DNA. Thus most investigators have proposed a minor groove complex for these compounds.[42]

Footprinting studies reveal that these compounds bind to 3 bp sites containing a 5′GC or a 5′GG sequence.[14, 45, 46] Complexation involves both drug and DNA conformational changes as judged by CD[47] and DNase I hypersensitivity[14, 46] respectively. The aureolic acids also alter dimethylsulfate (DMS) reactivity at G residues without a readily interpretable pattern.[46] Interestingly, these compounds appear to bind poly(dG-d^{m}C) in the Z form.[48]

To date, the aureolic acid-DNA complexes have proved refractory to crystallization. NMR studies by two groups favor different structures in the complex. Shafer and co-workers[43, 49-51] propose a major groove complex, with chromomycin complexing preferentially to one strand of the oligonucleotide ATGCAT. Intercalation is ruled out as a binding mode by two lines of evidence. The authors detect a G-C intrastrand NOE, which limits their separation to less than 4.5 Å, much smaller than the minimum distance required for intercalation (7 Å). The temperature dependence of the chemical shifts is also completely different from that found for the known intercalator actinomycin D.[52] However, the authors detect surprisingly few NOEs between chromomycin and the DNA, and no assignments are made for many of the carbohydrate protons of the antibiotic, so that the exact nature of the complex is difficult to establish.

Later work by Gao and Patel provides considerable evidence that the complex contains two chromomycin molecules located in the minor groove.[53] NOEs between

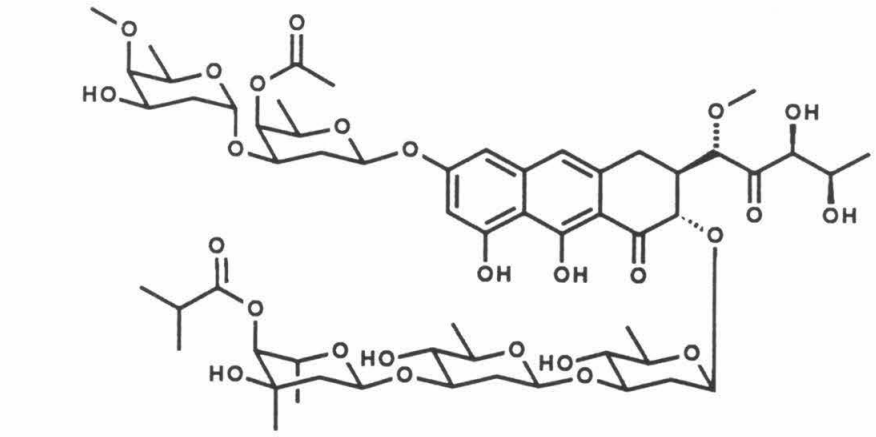

Olivomycin

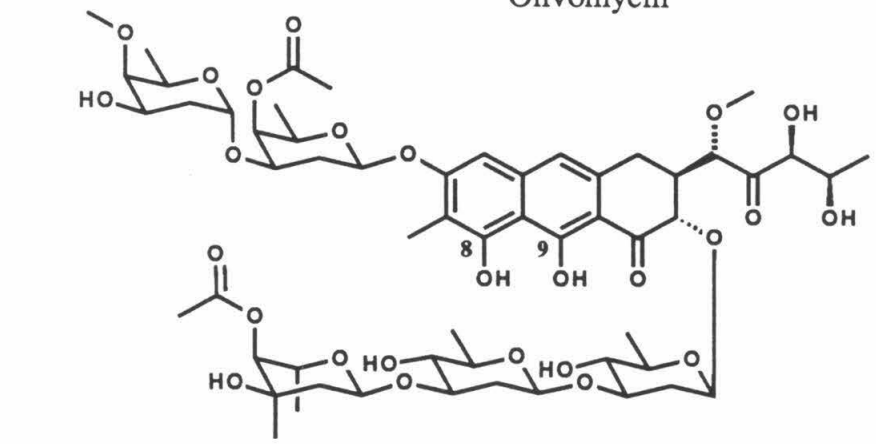

Chromomycin A_3

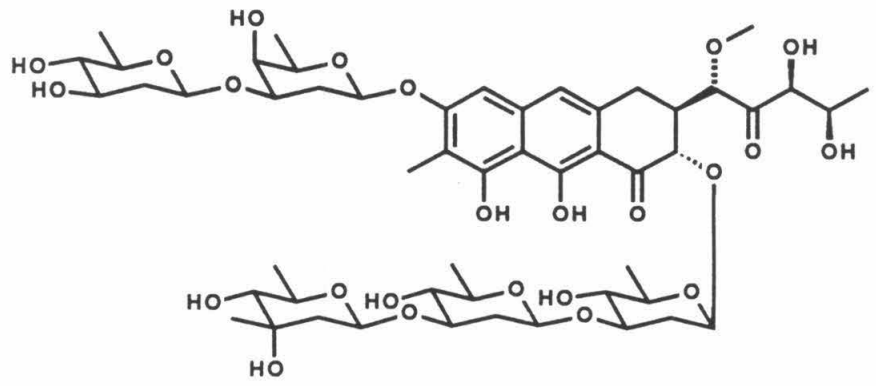

Mithramycin

Figure 7 The aureolic acid family of G,C specific antitumor antibiotics.[41]

the chromophore and protons on the middle sugar of the trisaccharide (which are well separated in space) can be explained by intermolecular interactions between different CHR molecules in a head to tail dimer. The DNA conformation is most consistent with an A form structure, which would allow the bulky dimer to fit into the shallow minor groove of A DNA. This model is completely consistent with the footprinting results, the hypersensitive sites that could be due to B/A junctions, the requirement for 2-aminopurines where the 2-amino group is directly involved in the complex, and the strong preference for oligo GC sequences that have an inherently wider minor groove.

Molecules Designed for Sequence Specificity

The compounds which have been discussed so far have small binding sites (< 5 bp) and therefore relatively low specificities. If the binding site size could be increased while maintaining the specificity of the original compound, it should be possible to produce small molecules with specificities and binding constants in the range of DNA regulatory proteins (9 bp and up). Attachment of a DNA cleaving function would then give compounds that can cut very large DNAs at only a few discrete sites.[54,55]

A,T Sequences

This stategy has been enormously successful for polypyrrole analogs. Increasing the number of pyrroles from 2–9 increases both the binding site size and the specificity for longer regions of A,T bp,[17,54,56] consistent with maintaining the

structural features of the netropsin and distamycin A complexes.[18,20] The longer derivatives require ten or more consecutive A,T bp at high affinity sites, giving these compounds an overall specificity greater than that of a unique 5 bp site.[55] An EDTA derivative of the nine pyrrole compound cuts the ≈50,000 bp lambda phage genome at only two major sites.[16] This is a higher specificity than is expected from the binding site size, and probably represents the nonrandom distribution of long stretches of A,T bp.

As the length of the pyrrole chain increases, the synthesis of these compounds gets progressively more difficult.[16] A possible solution is to connect shorter polypyrrole segments with flexible[56-61] or rigid[62] linkers. This strategy is complicated by the potential for long, flexible linkers to permit independent binding of the polypyrrole subunits.[56] Two different linker design strategies have proved viable. Short rigid linkers, with geometric requirements similar to the replaced pyrrole unit, exhibit similar binding specificities as the same size polypyrrole compound.[62] Specificity for a subset of A,T sequences is also increased by utilizing β-alanine or ethylenediamine as the linker.[63] Thus, limiting the degrees of freedom in the molecule appears to be a major factor in the selectivity between A,T sequences. These studies are complicated by the large number of potential binding sites which need to be observed to establish the specificity. For specificity at the 9 bp level, there are 256 unique all A,T sequences, and considerably more potential binding sites containing one or two G,C bp.[55] Further studies on a larger number of DNA sequences should help establish the exact specificities of these compounds.

G,C Sequences

Groove binding molecules that bind to G,C-containing sequences have proved much more elusive. Design efforts have focused on developing an element that can successfully hydrogen bond to G. The presence of the guanine N2H at the bottom of the minor groove has led several investigators to simultaneously propose that hydrogen bond accepting groups delivered to the bottom of the minor groove ought to favor G,C sequences.[19, 64-67] During the course of the work described in this thesis, Lown and co-workers have synthesized a number of imidazole-containing netropsin analogs to test this proposal. Early reports concern the dicationic compounds shown in figure 8, which are minimal substitutions of the parent compound netropsin.[64, 68] Footprinting studies indicate that these compounds exhibit a lower specificity than netropsin, reflected by an increase in the number of sites bound. The largest decrease is observed for the bis-imidazole compound iii. Consistent with the original proposal, there appears to be an increased tolerance for G,C bp, although the overall preference remains for A,T sequences. NMR studies using the well-studied CGCAATTGCG sequence[69] provide supporting evidence.[68] Like the netropsin complex, the oligonucleotide is in the B conformation, and the largest induced chemical shifts occur in the central A,T bp. Exchange rates increase in the order netropsin << Py-Im < Im-Im, again indicating a general decrease in A,T binding.

Three explanations have been put forth to account for the lack of a clearly defined G,C preference for i–iii. Calculations of the electrostatic potential of DNA

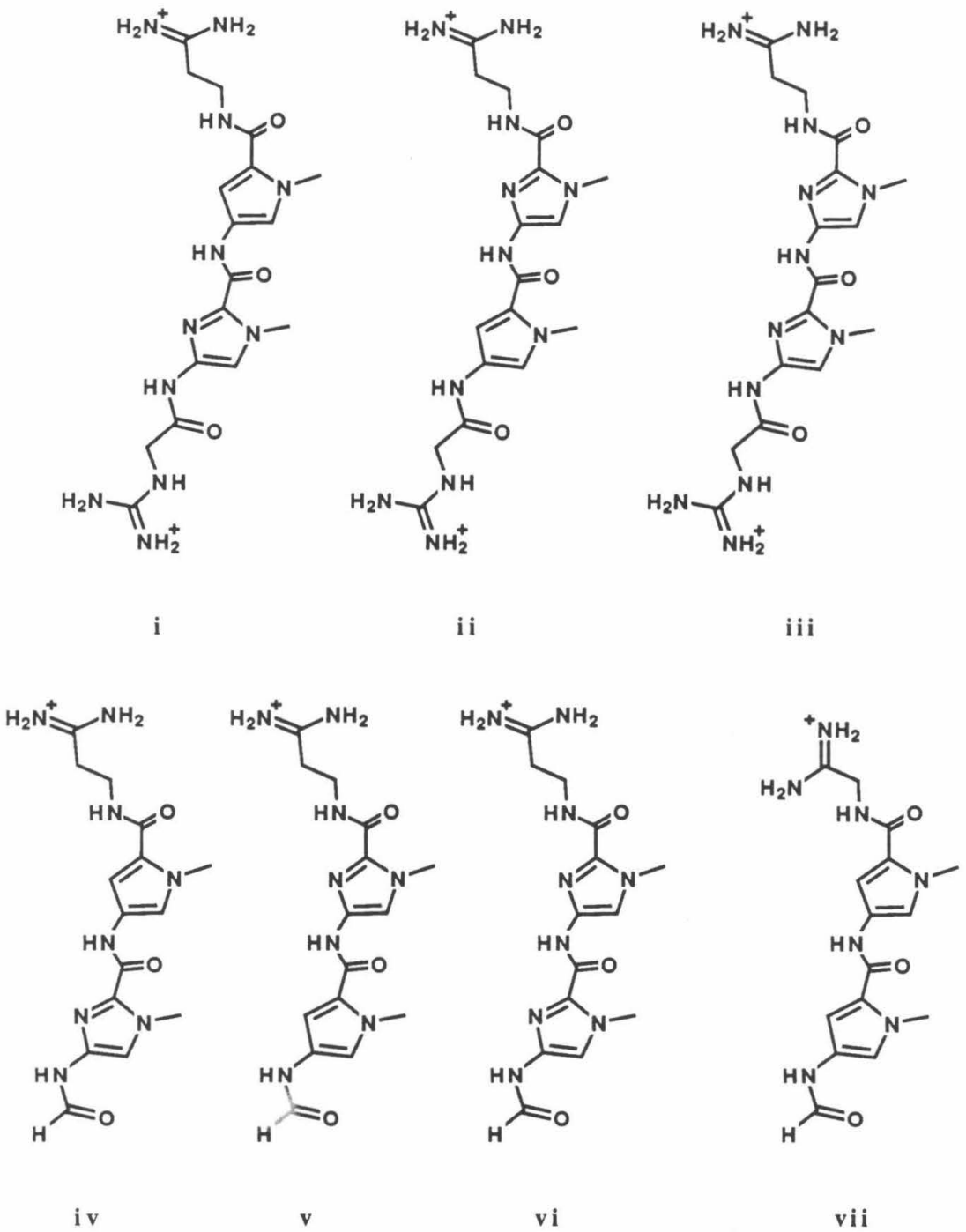

Figure 8 Netropsin analogs studied by Lown and co-workers.[64, 65, 70]

sequences have suggested that the dicationic compounds should prefer A,T sequences on purely electrostatic grounds.[71] A second alternative is suggested by the original design. While replacement of CH by N should result in better fits with G,C sequences, there is no obvious mechanism for the disfavoring of A,T sequences.[39] Indeed, the narrower minor groove of A,T DNA should still provide better contacts to the sides of the pyrrole rings. A third possibility is that the methylenes at both ends of the molecule are also involved in close contacts with A,T bp.[70]

Lown and co-workers have since redesigned the molecules to account for these factors. Recently, they have reported the series of monocationic imidazole containing compounds shown in the bottom row of figure 8.[65] These compounds contain just one positive charge to minimize the electrostatic effects, and a formyl group at the N-terminus to minimize any steric effects. As before, the monoimidazole derivatives **iv** and **v** exhibit a predominantly A,T specificity. The bis-imidazole compound **vi**, however, is complexed most strongly to a pair of CCGT sequences on the probe DNA. Several other oligo G,C sequences are not bound even at very high concentrations of **vi**. As the restriction fragment used does not contain high affinity netropsin or distamycin sites,[17] the overall specificity of this compound is still in question.

Significant binding of **vi** to CCAT and CCGT sites has been confirmed by NMR.[72,73] The NOE data support a minor groove complex with **vi** oriented so

that the formamide group is adjacent to the 5′ C of the binding site. There are some puzzling features about these complexes, especially with that of the more strongly bound sequence.[73] Although the authors use a nonsymmetric DNA sequence, they report peak doubling of the DNA protons in the binding site. Exchange with free ligand seems unlikely because the imidazole protons are not doubled and the millimolar concentrations of DNA and ligand should produce very low concentrations of uncomplexed DNA. Nonetheless, some sort of exchange appears to be occurring because the doubled peaks coalesce at higher temperatures. Additionally, all significant chemical shift changes are localized on one strand, indicating an asymmetric complex. Finally, Lee *et al.* detect an NOE between the protons of the imidazole rings, which are expected to be > 7 Å apart in a crescent shaped conformation. It is hoped that an X-ray structure will clarify this situation in the near future.

The success of this formamide bis-imidazole compound has provided the impetus to produce pyrrole derivatives with potential for mixed G,C and A,T specificity. The complex of netropsin analog **vii**, with a formyl group on the N-terminus and a shorter methylene chain on the C-terminus, has recently been studied by NMR on the usual CGCAATTGCG sequence.[70] The chemical shift data look very similar to that obtained for earlier A,T specific compounds,[68] although the authors do detect NOEs between the compound and the innermost G. No other data are currently available on the specificity of **vii**.

Conclusion

While the work to date delineates a reasonably well understood motif for the sequence specific complexation of all A,T bp sequences, the situation is not so straightforward for the complexation of other sequences. The Lown compounds show no simple correspondence between the number of hydrogen bond acceptor groups on a small molecule and the sequence that it recognizes. It is encouraging however, that binding to the minor groove is not limited to A,T sequences, which appear at present to be the usual sequence preference of groove binding small molecules.

The validity of designed specificity based on contacts and distances is still in question for these small molecules. This design does not take into account the DNA conformational changes that are common features in small molecule complexes. The success of the polypyrrole strategy may mean that the DNA structure need not be completely known to produce results. Clearly, much more investigation is needed to determine the range and molecular details of even the smallest molecules complexed to DNA. It is to this general problem that the rest of this work will be addressed.

Chapter 2

Sequence Specific Complexation of Mixed A,T/G,C Sequences

In order to extend the specificity observed with the longer pyrrole compounds to other sequences, it is necessary to develop a compound that is specific for G,C bp. Two techniques recently developed in the Dervan group hold considerable promise in screening for such specificity. Protection from methidium-propyl-EDTA (MPE·Fe(II)) cleavage or MPE·Fe(II) footprinting[13, 14, 45] is a recent addition to the DNase I[74] and dimethyl sulfate[75] protection experiments. Advantages over previous techniques include the determination of binding sites to nucleotide specificity[14] and the lack of sequence specificity in the cleavage patterns produced.[13] A second recent technique is termed affinity cleaving.[76] An EDTA moiety is attached directly to the molecule of interest, and binding sites are revealed by the sequence specificity of the cleavage patterns produced.

Figure 1 shows the complementary nature of these two experiments in the determination of sequence specificity. Application of both techniques to a target molecule allows for the correlation of specific affinity cleavage sites with the sites of complexation, giving additional information about the orientation of the molecule and the groove that it occupies at each of its binding sites.[77] The high signal to noise ratio of the affinity cleaving experiment allows this technique to be extended to kb sized DNA molecules,[16, 56, 78] giving a more complete picture of the overall specificity and sequence preferences of the compound studied.

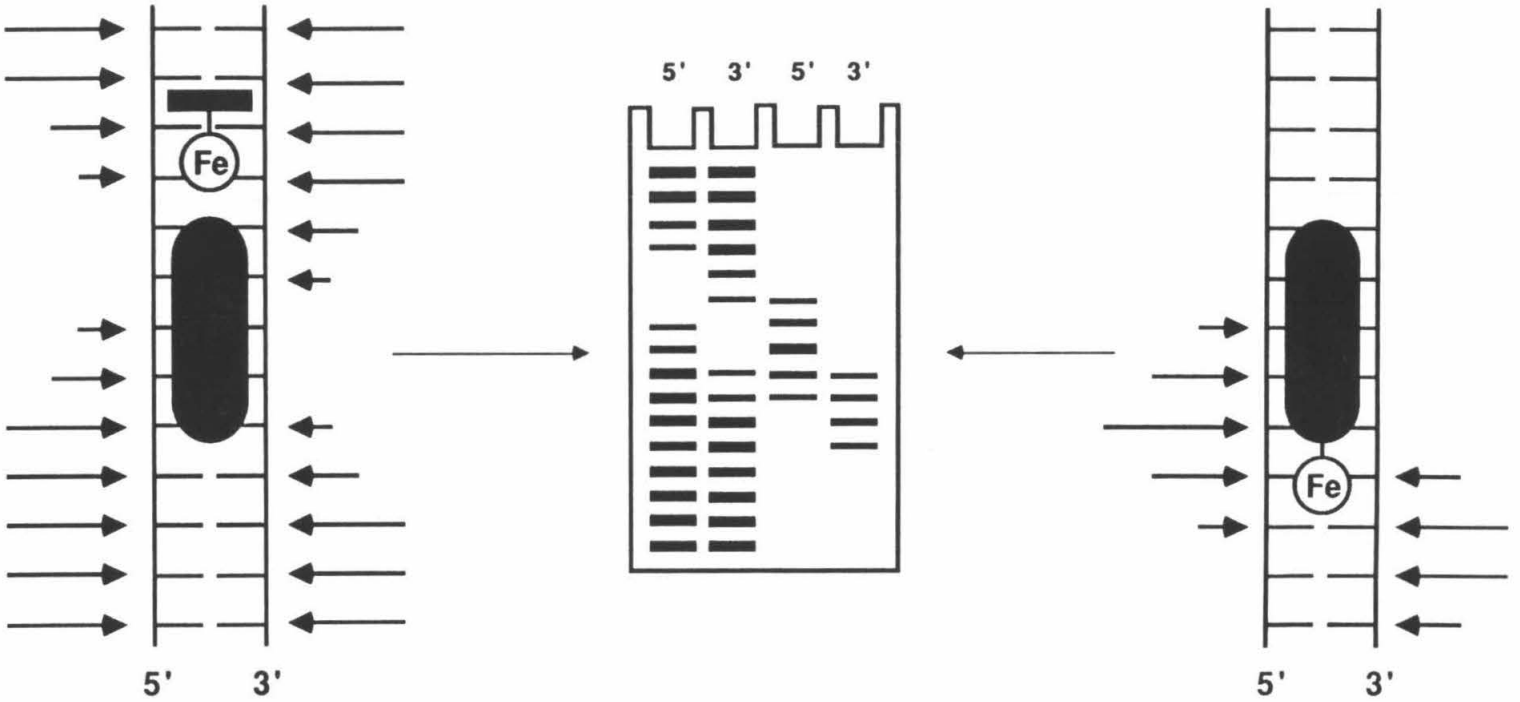

Figure 1 Complementary information provided by the footprinting and affinity cleaving experiments. Footprinting determines the binding site of the small molecule. Affinity cleaving produces a relative ordering of binding site affinities. A 3′ shift in the cleavage pattern (as shown) indicates that the compound binds in the minor groove.[77] A comparison of both experiments determines the orientation of the molecule at its binding sites.

Design of Potential G,C Binding Molecules

All of the groove-binding compounds in chapter 1 have some common features presumably important for their DNA binding activity. The compounds that form tight complexes are aromatic and positively charged, and usually form specific hydrogen bonds with the target DNA. From the minor groove, the major difference between A,T and G,C bp is the presence of the guanine N2 at the floor of the groove. Thus the simplest design for a G,C specific minor groove binding molecule takes advantage of the hydrogen bond donating ability of guanine with an aromatic ring system containing hydrogen bond acceptors and a single positive charge. Several different versions of such compounds have been synthesized, and are shown in appendix D.

Attempts to footprint these compounds reveal two flaws in this simple strategy. The DNA binding assays require a binding constant of at least 10^4 M^{-1}. Affinity cleaving at higher concentrations of cleaving agent needs mM concentrations of iron, resulting in very high backgrounds. MPE·Fe(II) footprinting is complicated by the potential for direct interaction between the intercalator probe and the groove binder. Both experiments suffer from the substantial metal chelating abilities of the synthetic compounds. In addition, such ligands prove labor-intensive to synthesize and study.

For these reasons, a more successful strategy involves the modification of existing DNA binding ligands. The best candidates for such an approach are the

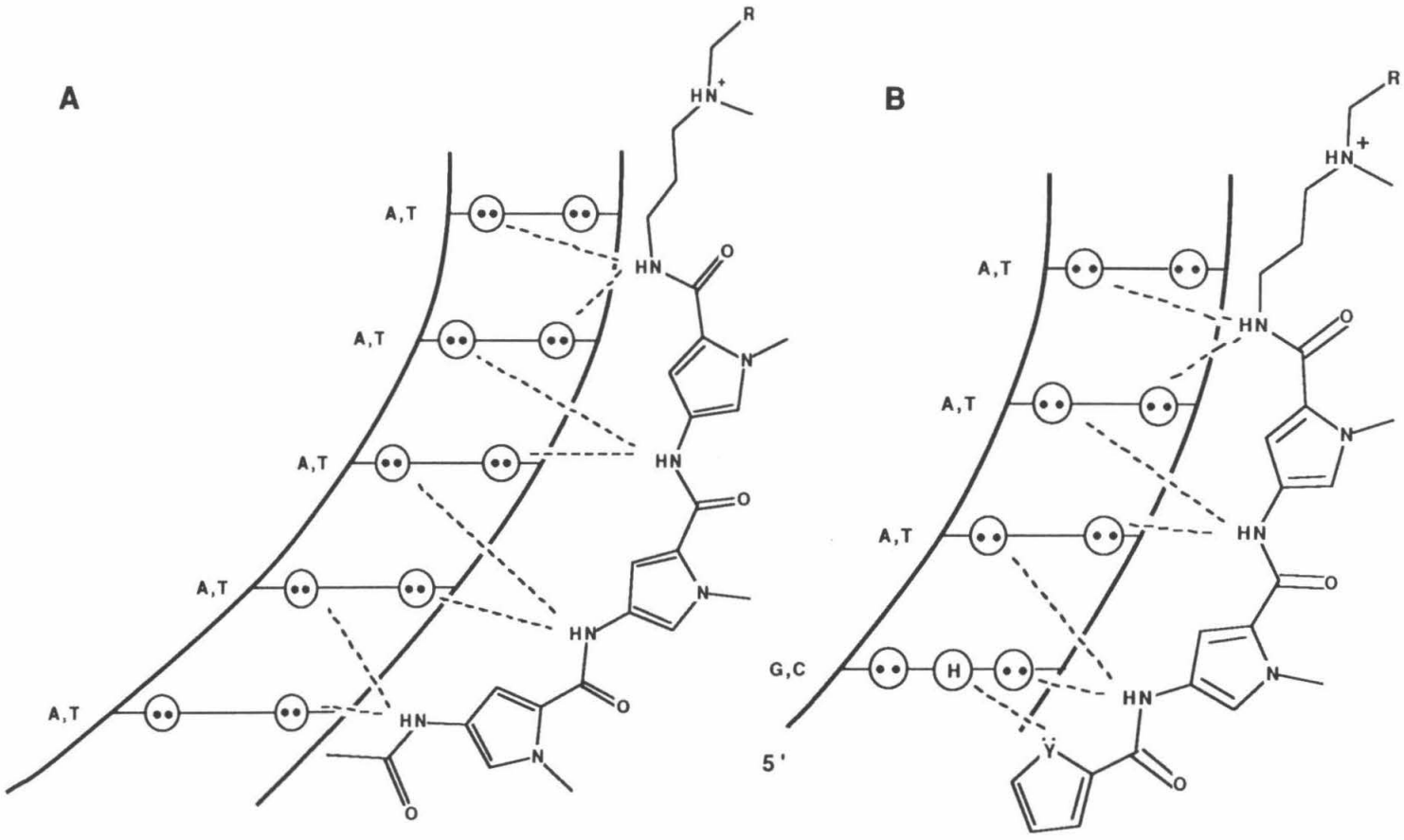

Figure 2 Design of synthetic compounds expected to complex with single G containing sites. Circles represent the lone pair electrons of thymine O2 and adenine N3. Dashed lines represent the expected pattern of hydrogen bonds. A) The putative complex of the distamycin A analog D based on the crystallized complexes.[18,20] B) Hypothetical effect of placing one hydrogen bond acceptor on the floor of the minor groove.

polypyrrole compounds discussed in chapter 1. By utilizing the A,T specificity and high affinity of netropsin or distamycin A to deliver a G,C bp recognizing element to the minor groove of B DNA, it should be possible to produce hybrid molecules that recognize mixed A,T/G,C sequences at micromolar concentrations. The design of such a molecule is shown in figure 2. The first G,C recognition element to be examined is a heterocyclic aromatic ring capable of forming a strong hydrogen bond to the guanine NH. Placement of this ring at the N-terminus of netropsin has two distinct advantages. Many different aromatic acids are commercially available or readily prepared, and the synthesis of all compounds is convergently achieved in one step from a common dipyrrole intermediate. Production of the appropriate C-terminal EDTA compound has also been achieved,[76] so that similar chemistry produces the analogs required for both assays. Earlier studies have shown that the monopyrrole analog of netropsin does not bind DNA,[79] and that the binding constant of these compounds increases with the number of pyrroles.[9, 17] Two pyrroles appear to offer the best compromise between the requirement for large binding constants and the lowest possible A,T bp preferences. Similarly, a single positive charge appears to offer the best electrostatic compromise. As shown in figure 2, a successfully designed compound is envisioned as binding to one G,C bp, followed by 3–4 A,T bp, having a strong preference for the orientation that gives a hydrogen bond between the N2H of G and the N-terminal heterocycle. Such binding should produce detectable differences from binding and cleavage patterns of the distamycin A analog D shown in figure 2.

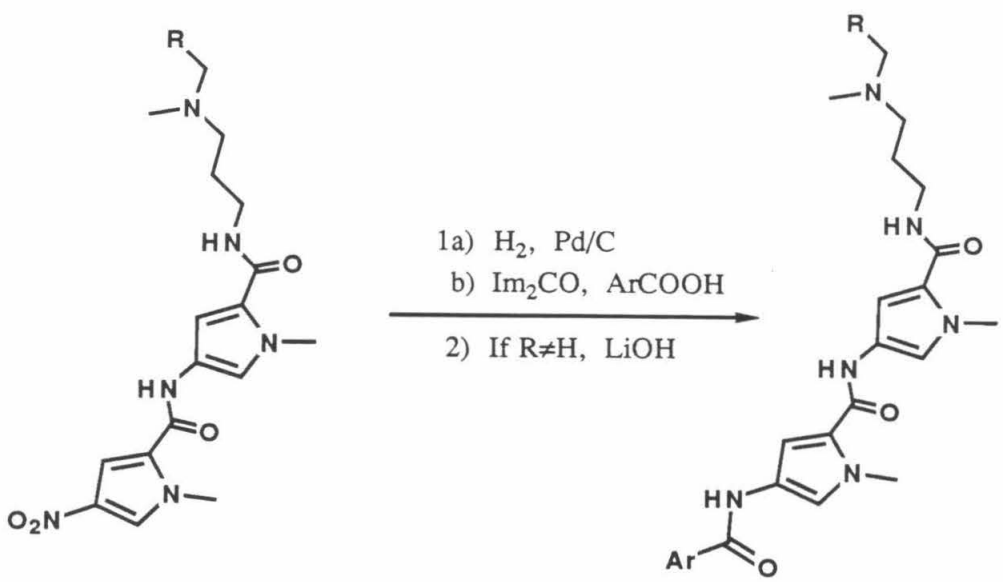

1 R = H
2 R = $(CH_2)_2$NHEDTA$(OEt)_3$

ArN R = H
ArNE R = $(CH_2)_2$NHEDTA$(OH)_3$

Scheme 1 Synthesis of ArN and ArNE.

Synthesis

The synthesis of this class of compounds is shown in scheme 1. The precursor nitro-dipyrrole compounds **1** and **2** are available from pyrrole-2-carboxylic acid in five or eight steps, in approximately 8% overall yield.[76] Carbonyldiimidazole activated coupling of the reduced dipyrrole amine and the appropriate heterocyclic aromatic acid gives clean products in 60–85% yield. Other coupling agents gave higher yields but less pure products. While **1** is readily reduced at atmospheric pressure, it was necessary to hydrogenate **2** for 24 h at 50 psi in the presence of

a large amount of palladium catalyst.[76] The first compounds prepared are shown in figure 3. Coupling of 1-methylimidazole-2-carboxylic acid to the amine derived from **2** by several different methods fails completely. The synthesis of the imidazole EDTA compound is shown in scheme 2.

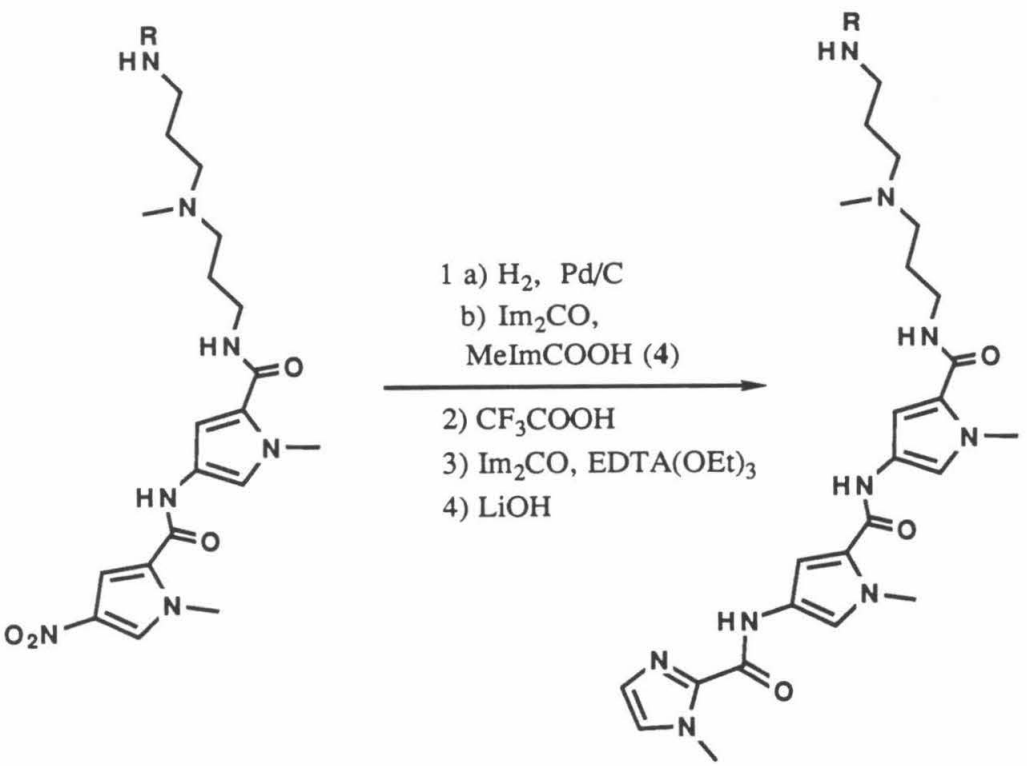

5 R = t-Boc

6	R = t-Boc	84 %
7	R = H	87 %
8	R = $EDTA(OEt)_3$	15 %
2-ImNE	R = $EDTA(OH)_3$	27 %

Scheme 2 Synthesis of 2-ImNE.

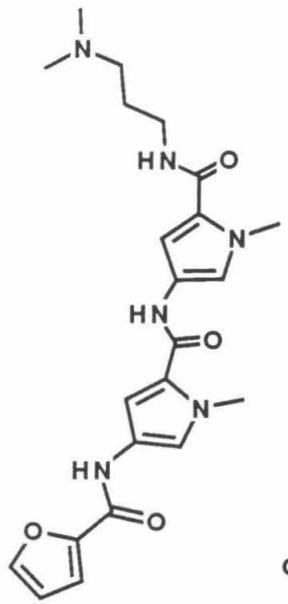

2-FuN

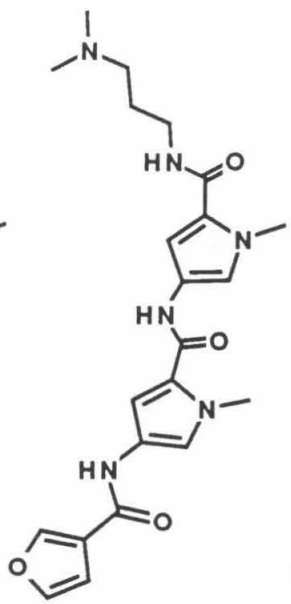

3-FuN

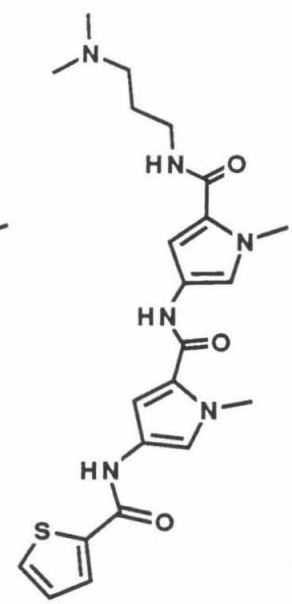

2-ThN

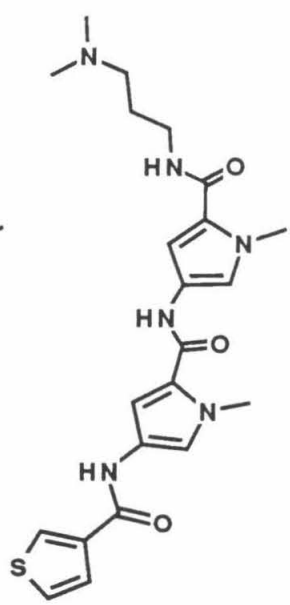

3-ThN

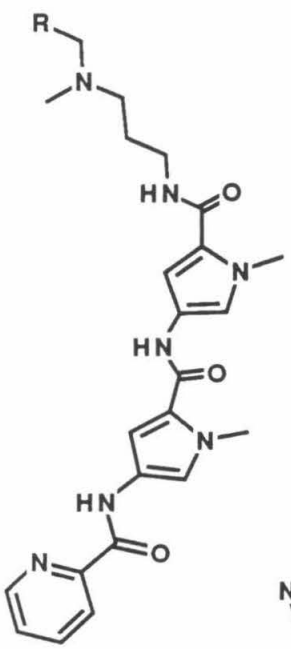

2-PyN, 2-PyNE

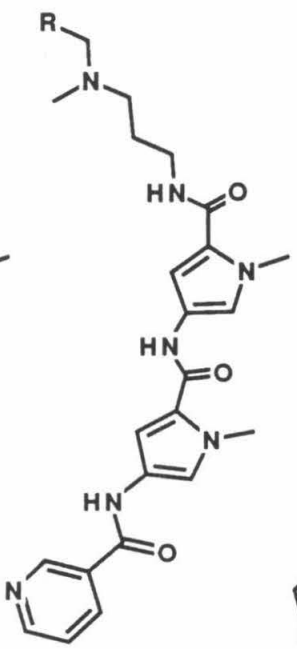

3-PyN, 3-PyNE

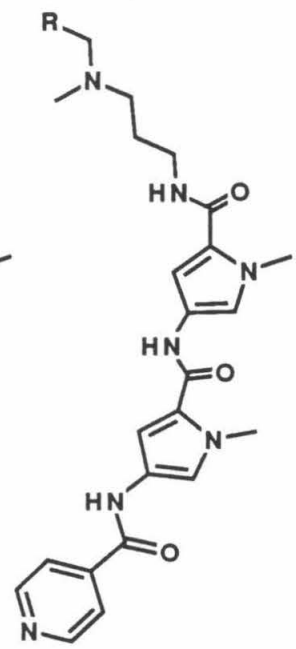

4-PyN, 4-PyNE

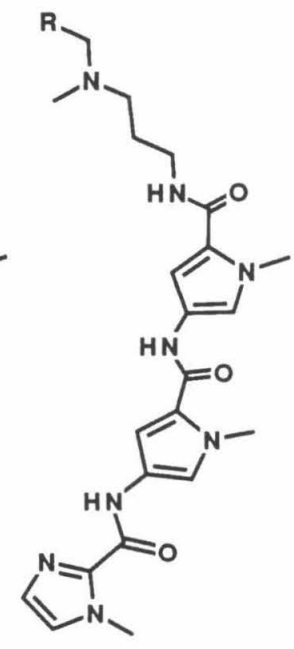

2-ImN, 2-ImNE

Figure 3 Synthetic compounds to be tested for G,C recognition.

DNA Binding Assays

The behavior of these compounds on the 517 bp *EcoR* I/*Rsa* I restriction fragment of pBR322 is shown in figures 4, 5, and 6. Analysis of these compounds by MPE·Fe(II) footprinting reveals that μM concentrations of all the compounds protect distinct 5–6 bp regions from MPE·Fe(II) induced cleavage. The location of protected regions is determined by the published method.[77] An autoradiogram of the high resolution sequencing gel is scanned by densitometer. The footprinting lane is compared to a standard lane obtained from MPE·Fe(II) cleavage in the absence of any ligand, and the nucleotides protected from cleavage are identified. The extent of protection is measured by subtracting the protected peak heights from the height of the nearest unaffected peak. These protection patterns are plotted in histogram form in figures 7 and 8. Binding sites are determined by the published model[13, 14] with MPE·Fe(II) cleavage protection shifted by one bp to the 3′ end of the DNA.

On this restriction fragment, distamycin A and its analog D (figure 2) bind to five readily interpretable sites. The 5′-TTTTT-3′ site is clearly the highest affinity site, detected at 0.5 μM. Two other sites are detected at 2 μM, and the last two show only weak protection at concentrations below 10 μM.[13, 84] This same pattern is observed for the thiophene-2-carboxamide-netropsin, thiophene-3-carboxamide-netropsin, furan-2-carboxamide-netropsin, furan-3-carboxamide-netropsin, pyridine-3-carboxamide-netropsin, and pyridine-4-carboxamide-netropsin derivatives.

Figure 4 MPE·Fe(II) footprinting of the furan and thiophene analogs of D. Autoradiogram of an 8% high resolution denaturing polyacrylamide gel. All reactions contain 4 mM DTT, 100 μM-bp calf thymus DNA, and 12 kcpm 5′ labeled 517 bp restriction fragment in 40 mM Tris·acetate pH 7.9 buffer. Lane 1, intact DNA; lane 2, Maxam-Gilbert G reaction;[80] lanes 3–10 contain 4 μM MPE·Fe(II), lane 3, MPE·Fe(II) standard, lane 4, 2 μM D; lanes 5–6, 20 μM and 10 μM 2-FuN respectively; lanes 7–8 20 μM and 10 μM 3-FuN respectively; lane 9, 5 μM 2-ThN, lane 10, 5 μM 3-ThN.

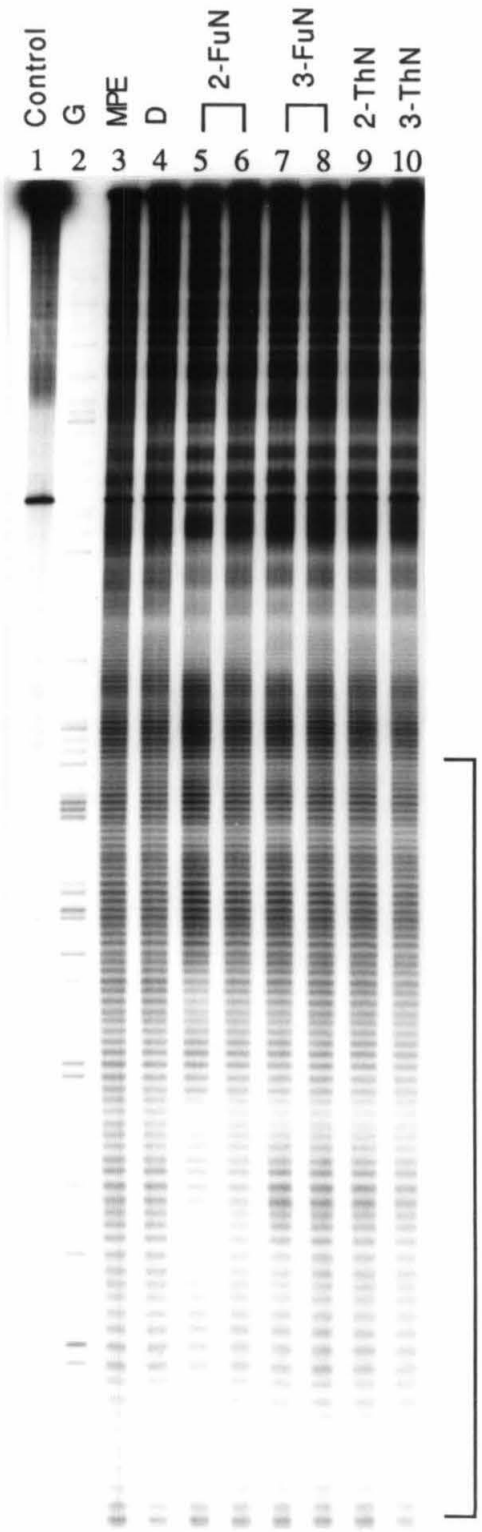
Control
G
MPE
D
2-FuN
3-FuN
2-ThN
3-ThN
1 2 3 4 5 6 7 8 9 10

Figure 5 A) MPE·Fe(II) footprinting of the pyridine analogs of D. Autoradiogram of an 8% high resolution denaturing polyacrylamide gel. All reactions contain 4 mM DTT, 100 μM-bp calf thymus DNA, and 12 kcpm 5′ labeled 517 bp restriction fragment in 40 mM Tris·acetate pH 7.9 buffer. Lane 1, intact DNA; lane 2, Maxam-Gilbert G reaction;[80] lane 3, A reaction;[81] lanes 4–13 contain 4 μM MPE·Fe(II): lane 4, MPE·Fe(II) standard; lane 5, 4 μM D; lane 6, 20 μM 2-PyN; lane 7, 20 μM 2-ImN; lanes 8–10 contain 35 μM, 10 μM, and 1 μM 3-PyN respectively; lanes 11–13, 35 μM, 10 μM, and 1 μM 4-PyN respectively. B) Specific Cleavage by the pyridine analogs of D. Autoradiogram of an 8% high resolution gel. All reactions contain 4 mM DTT, 100 μM-bp calf thymus DNA, and 12 kcpm 5′ labeled 517 bp restriction fragment in 40 mM Tris·acetate pH 7.9 buffer. Lane 1, intact DNA; lane 2, Maxam-Gilbert G reaction;[80] lane 3, A reaction;[81] lane 4, 2 μM ED; lane 5, 50 μM 2-PyNE; lane 6, 70 μM 2-ImNE; lane 7, 10 μM 3-PyNE; lane 8, 7 μM 4-PyNE.

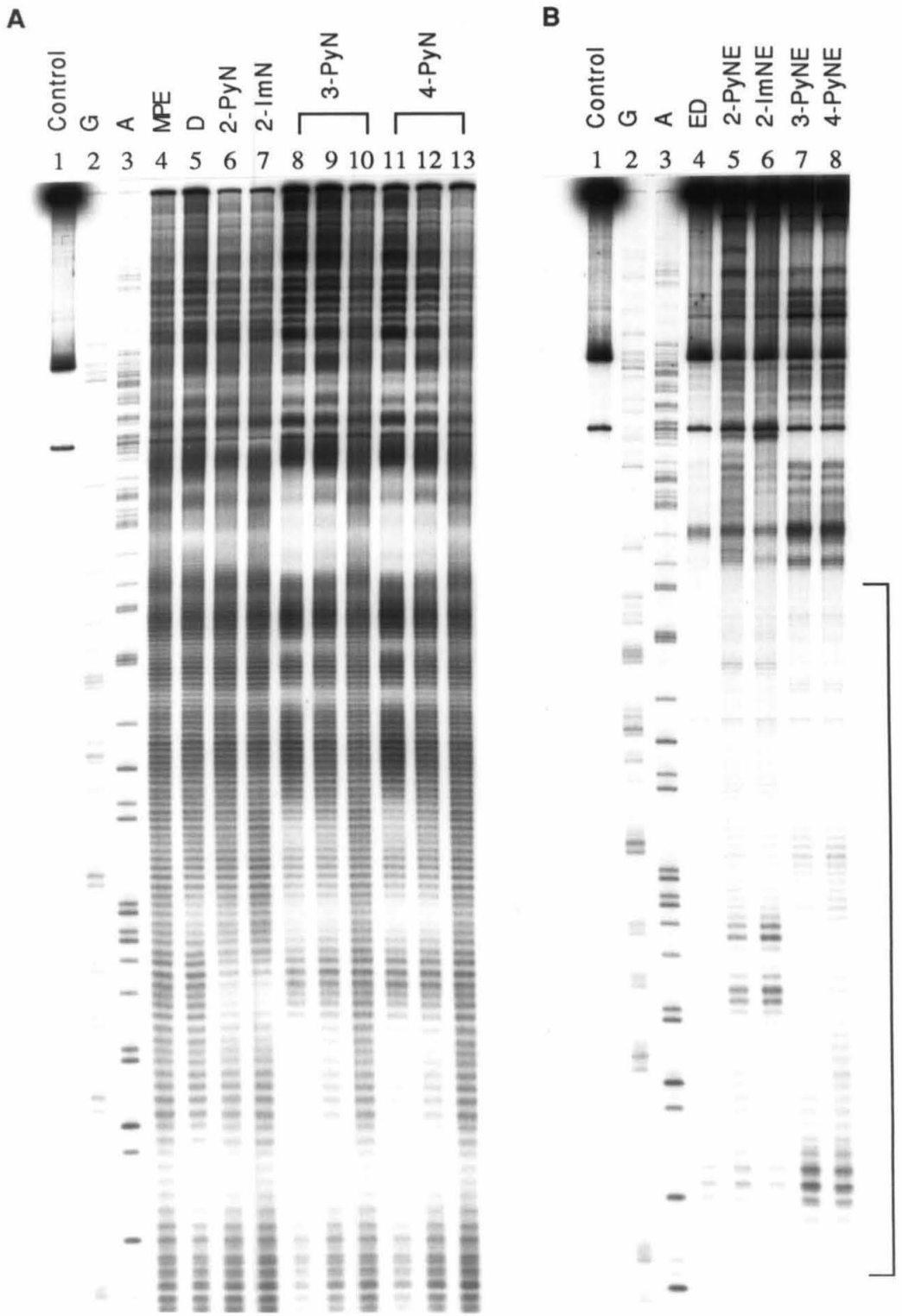
A
Control
G
A
MPE
D
2-PyN
2-ImN
3-PyN
4-PyN
1 2 3 4 5 6 7 8 9 10 11 12 13
B
Control
G
A
ED
2-PyNE
2-ImNE
3-PyNE
4-PyNE
1 2 3 4 5 6 7 8

Figure 6 Footprinting and affinity cleaving of 2-PyN and 2-ImN. Autoradiogram of an 8% high resolution denaturing polyacrylamide gel. All reactions contain 4 mM DTT, 100 μM-bp calf thymus DNA, and 12 kcpm 5′ labeled 517 bp restriction fragment in 40 mM Tris·acetate pH 7.9 buffer. Lane 1, intact DNA; lane 2, Maxam-Gilbert G reaction;[80] lanes 3–10 contain 4 μM MPE·Fe(II): lane 4, 2 μM D; lanes 5–7 2-PyN at 35, 20, and 10 μM respectively; lanes 8–10, 2-ImN at 35, 20, and 10 μM respectively; lane 11, 2 μM ED; lane 12, 50 μM 2-PyNE; lanes 13–14, 70 and 50 μM 2-ImNE respectively.

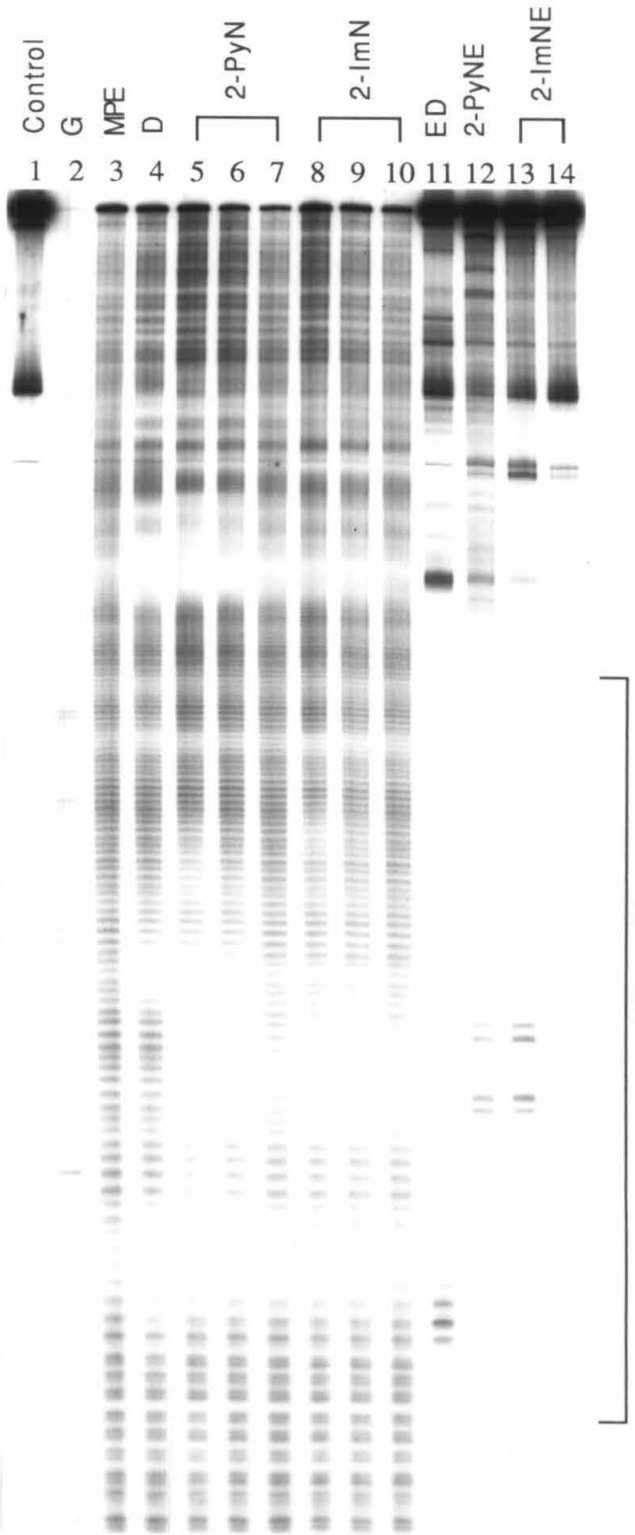
Control
G
MPE
D
2-PyN
2-ImN
ED
2-PyNE
2-ImNE
1 2 3 4 5 6 7 8 9 10 11 12 13 14

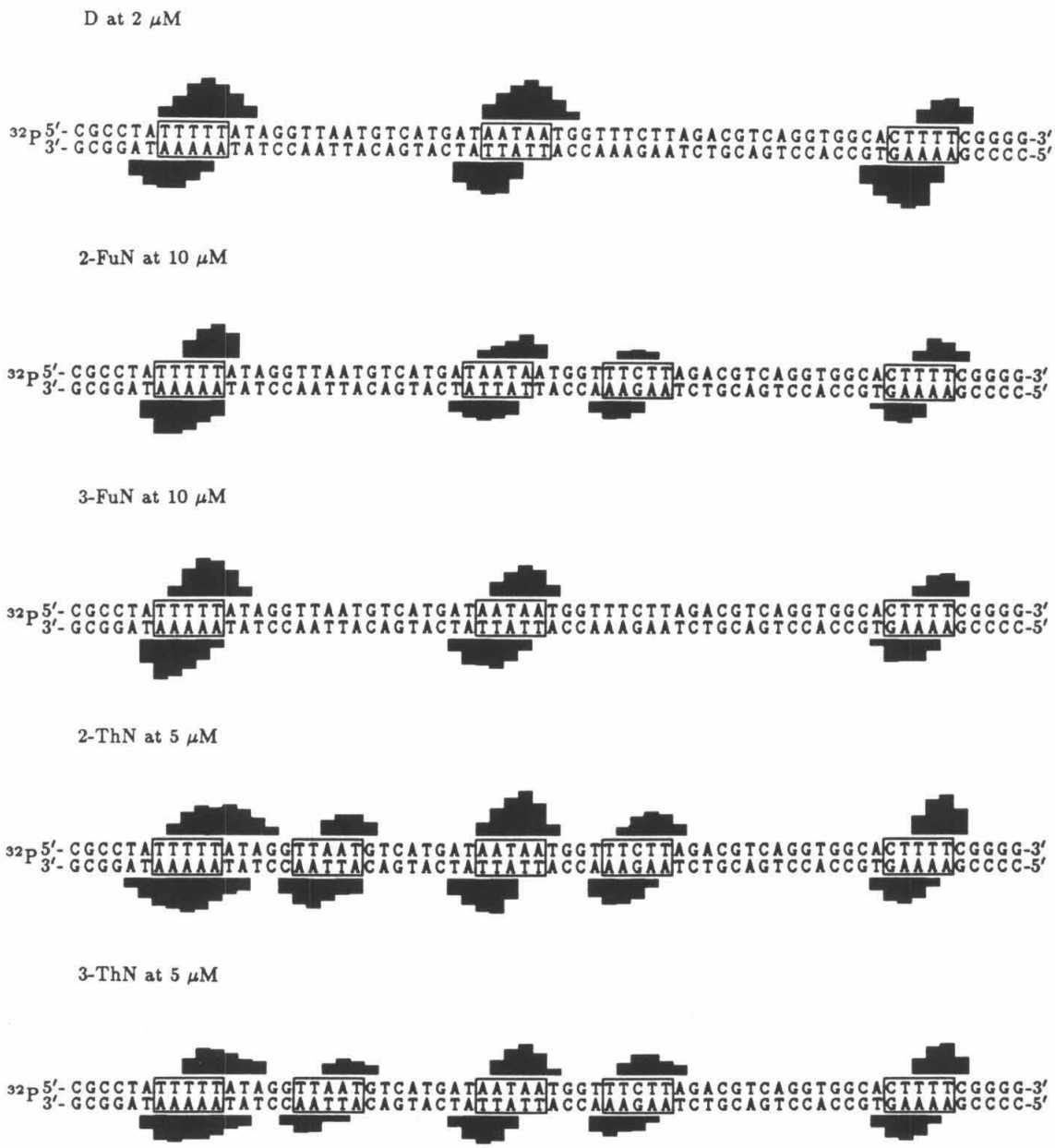

Figure 7 MPE protection patterns for the furan and thiophene compounds of figure 3 on the 517 bp fragment of pBR322, bp 4268–335.[82, 83] 5′ labeled data are from figure 4; 3′ data are compiled in appendix A. Bar heights are proportional to the protection from cleavage at each band, determined by the published method (see text).[77] Boxes represent equilibrium binding sites determined by the published model.[13, 14]

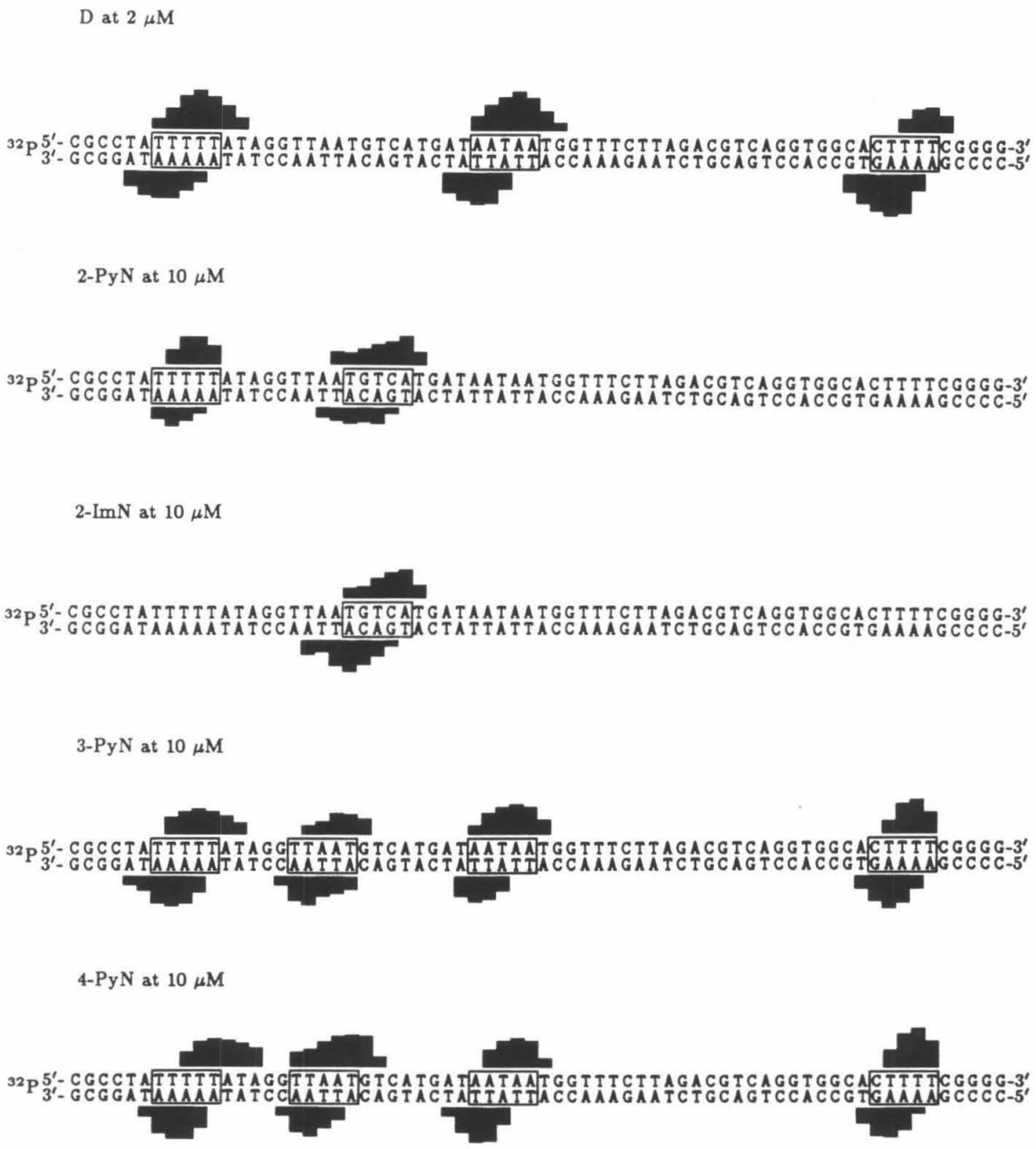

Figure 8 MPE protection patterns for the pyridine and 1-methylimidazole containing compounds of figure 3 on the 517 bp fragment of pBR322, bp 4268–335.[82,83] 5′ labeled data are from figures 5 and 6, 3′ data are compiled in appendix A. Bar heights are proportional to the protection from cleavage at each band, determined by the published method (see text).[77] Boxes represent equilibrium binding sites determined by the published model.[13,14]

These compounds give generally lower binding constants and less selectivity between sites than does D. The pyridine-3-carboxamide-netropsin compound is typical, with all five normal D sites protected at 10 μM and no detectable binding at 1 μM. The lower specificity and binding affinity for these compounds is probably a result of the removal of the N-terminal amide of D, representing the effect of loss of one bifurcated hydrogen bond on the overall complex stabilities at various sites.[20]

Two compounds exhibit significantly different binding properties that can be readily observed in the affinity cleaving lanes of figure 6. The data are summarized in histogram form in figure 9. Both the pyridine-2-carboxamide-netropsin (2-PyN) and the 1-methylimidazole-2-carboxamide-netropsin (2-ImN) compounds bind to a new site on the 517 bp fragment that maps to a TGTCA sequence. The cleavage patterns of the EDTA derivatives, 2-PyNE and 2-ImNE, indicate one binding site with two equivalent orientations. This correlates with the approximate two-fold symmetry of the new site. The cleavage is shifted toward the 3′ end of the DNA, consistent with the presence of these compounds in the minor groove. The affinity at all sites is reduced by at least a factor of 10. Both 2-PyNE and 2-ImNE cleave this restriction fragment less efficiently at 50 μM than ED at 2 μM or the pyridine isomers 3-PyNE and 4-PyNE at 10 μM.

Several minor sites, most notably the CTTTT sequence in figure 9, show the binding and cleavage patterns expected from the original model. Both compounds cleave this site with a strong preference for the orientation that puts the heterocyclic nitrogen near the G,C bp. This specificity is reversed from the behavior of

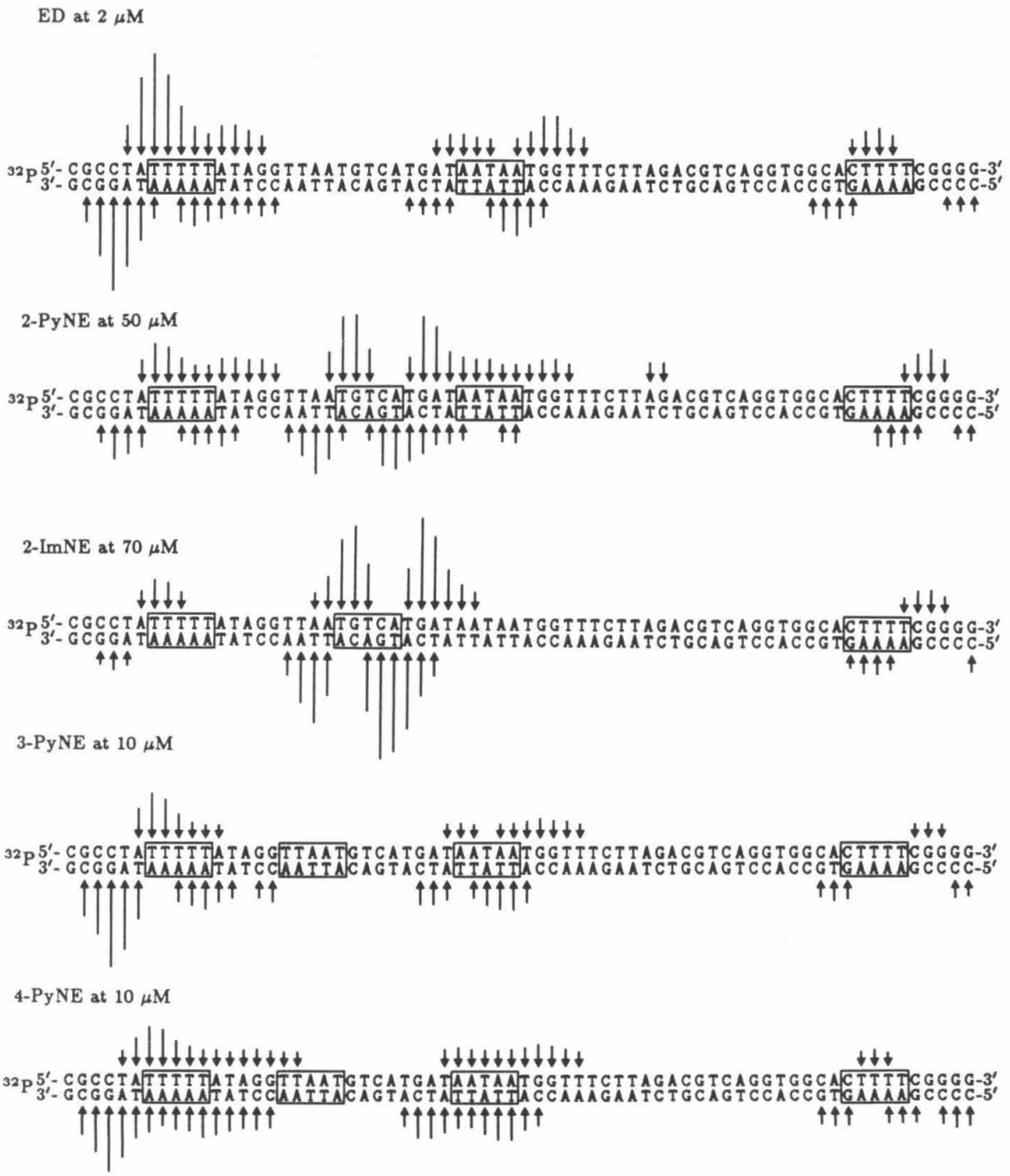

Figure 9 Cleavage of the 517 bp fragment of pBR322, bp 4268–335,[82,83] by the EDTA substituted analogs of figure 3. 5′ labeled data are from figures 5 and 6, 3′ data are compiled in appendix A. Arrows are proportional to the maximum densities of the cleavage bands. Boxes represent binding sites determined by the published method.[77]

ED at the same site, and thus probably represents the expected binding mode. However, it is clear that the major binding site of these compounds on the 517 bp fragment unexpectedly contains a second G,C bp.

The three pyridine isomers differ only by the relative position of the nitrogen atom in the pyridine ring, yet the DNA binding behavior changes radically for the 2 isomer. Both 3-PyN and 4-PyN exhibit normal behavior for this type of compound. They bind strongly to A,T rich sites at 10 μM with orientation preferences and relative site preferences identical to the parent compound D. When the pyridine nitrogen is adjacent to the amide carbonyl, however, the binding of A,T is strongly disfavored and the new site appears. This change in binding on isomer substitution implicates the pyridine nitrogen in both the recognition of the TGTCA site and the disfavoring of A,T rich sites. It also suggests that the proximity of the amide and the heterocyclic nitrogen is important for the altered behavior of 2-PyN.

Comparison of the cleavage patterns of 2-PyNE and 2-ImNE reveals that the imidazole compound is more selective for the TGTCA site. Although cleavage at the new site is the same (within experimental error), cleavage at all A,T sites is considerably reduced. There are only two major cleavage sites visible on the 517 bp fragment, the TGTCA site and a slower running site that maps to an AGACA sequence. Again, the differences between the compounds imply an active role for the heterocyclic nitrogen in the disfavoring of A,T sites. Simple geometric arguments for the specificity difference are eliminated by the similar geometry

of the two compounds, the range of observed donor acceptor angles of hydrogen bonds[85] and the fact that the compound with a five-membered ring binds less well to A,T regions.

A possible explanation for this behavior lies in the ability of the pyridine ring to form two isomeric complexes with any DNA sequence. The pyridine nitrogen can either face the floor of the minor groove, where it could form a hydrogen bond with the bases, or face out of the groove, where it is available only to solvent. In the second conformation, 2-PyN should be very similar to 4-PyN, which binds only A,T rich sequences. It seems reasonable that the 2-PyN/TGTCA complex is formed with the pyridine nitrogen facing the floor of the groove (giving a putative hydrogen bond to the N2H of G), while the 2-PyN/TTTTT complex is formed with the ring nitrogen facing out. This N out conformation is inaccessable to 2-ImN because of close contacts between the 1-methyl group and the floor of the minor groove. Free in solution, these compounds are presumed to be completely hydrogen bonded to solvent. If the complex at A,T sites is similar to that of distamycin A, then the imidazole nitrogen must be desolvated to form a tight complex, whereas the pyridine nitrogen facing out does not lose a hydrogen bond.

TGTCA Site Structure

Strong sites for D binding, such as the TTTTT site on the 517 bp fragment, are known to exhibit unusual reactivity[86] and structure,[87] which induces local bending.[88] On binding distamycin A, the binding site undergoes a conformational

Figure 10 Structural features of 2-PyN and 2-ImN binding. Autoradiogram of an 8% high resolution denaturing polyacrylamide gel. All reactions contain 12 kcpm 3′ labeled 517 bp restriction fragment. Lanes 1, 3–6, and 12–24 contain 200 μM-bp calf thymus DNA in 40 mM tris acetate pH 7.9 buffer; Lanes 7–11 contain 200 μM-bp calf thymus DNA in TKMC buffer; Lane 1, intact DNA; lane 2, Maxam-Gilbert G reaction;[80] lanes 3–6 contain 4 μM MPE·Fe(II), and 4 mM DTT, cleavage time 20 min at 37°C; lane 7, intact DNA; lanes 8–11 contain 0.33 ng DNase I reacted for 3 min at 25°C; lanes 12–15 contain 100 μM calf thymus DNA, 100 μM potassium permanganate, 15 min at 37°C; lanes 16–19 contain 100 μM calf thymus DNA, 136 mM diethyl pyrocarbonate, 10 min at 37°C; lanes 20–23 contain 53 mM dimethyl sulfate, reacted for 5 min at 25°C, then A>G workup;[80] lanes 4, 9, 13, 17, and 21 contain 20 μM D; lanes 5, 10, 14, 18, and 22 contain 20 μM 2-PyN; lanes 4, 9, 13, 17, and 23 contain 20 μM 2-ImN.

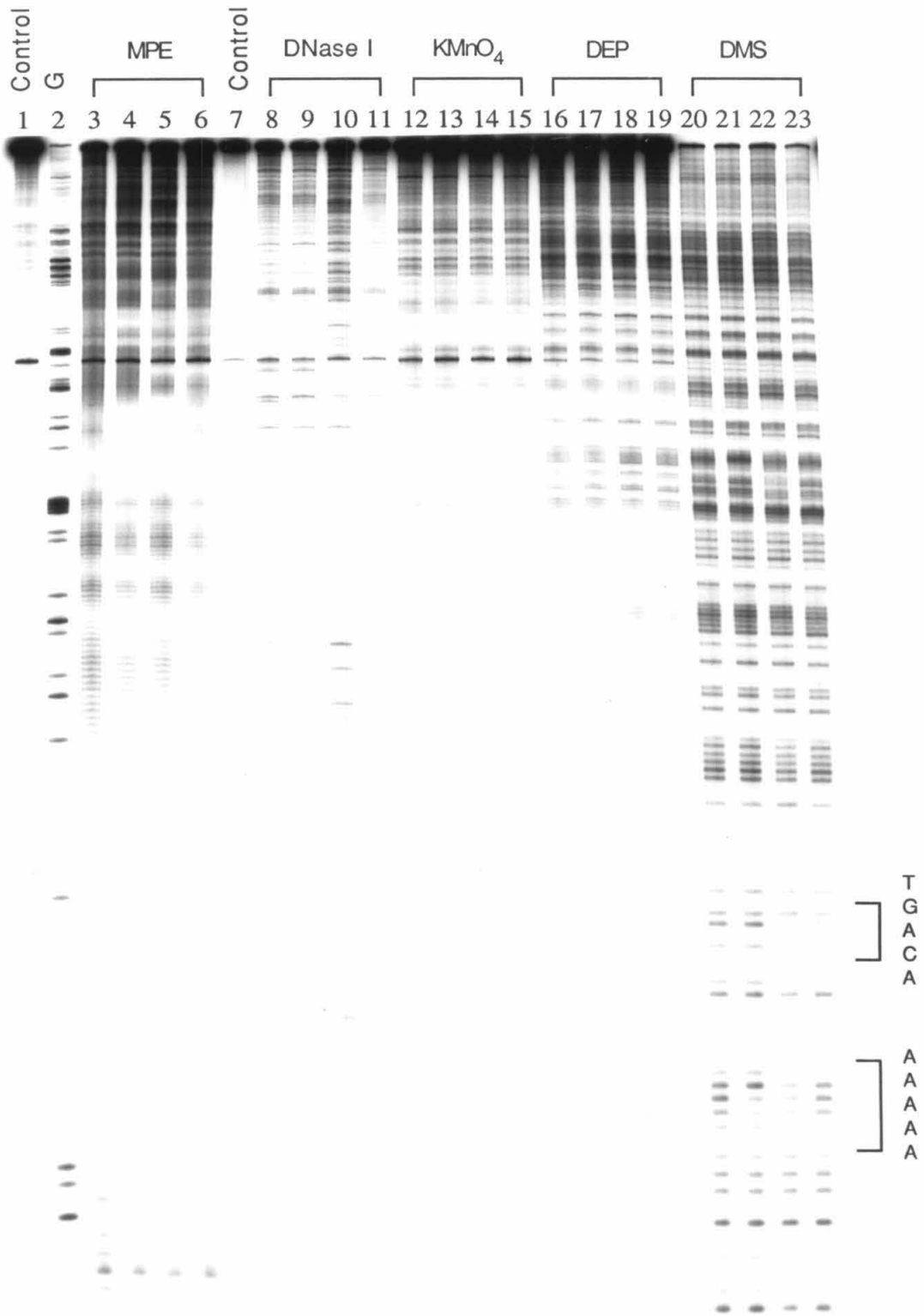
Control
G
MPE
Control
DNase I
KMnO4
DEP
DMS
1 2 3 4 5 6 7 8 9 10 11 12 13 14 15 16 17 18 19 20 21 22 23
T
G
A
C
A
A
A
A
A
A

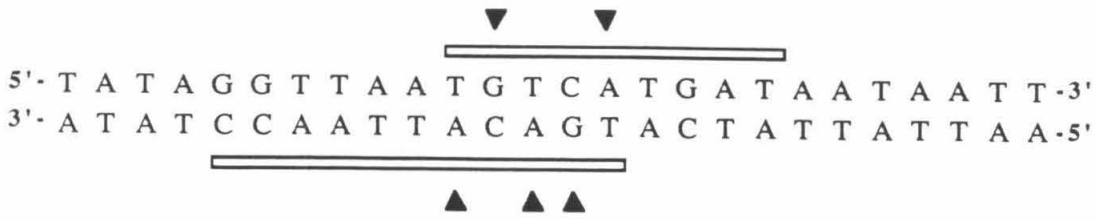

Figure 11 Footprinting of 2-ImN by DNase I and DMS. Bars represent extent of bases protected from DNase I cleavage. Triangles represent significant protection from DMS. The 3′ data are from figure 10, the 5′ data are compiled in appendix A. No significant changes were observed on treatment with potassium permanganate or diethyl pyrocarbonate.

transition to an unbent, more B-like form.[88] To assess the importance of altered structure in the sequence selectivity of 2-PyN and 2-ImN, 517 bp fragment DNA was treated with a variety of structure sensitive reagents in the presence and absence of the small molecules.

D, 2-PyN and 2-ImN all footprint with DNase I and dimethyl sulfate at the same sites determined for MPE·Fe(II) footprinting. Upon addition of D, a hypersensitive site appears at the TTTTT sequence (see lane 21), consistent with previous observations.[84] At the TGTCA site, there is no evidence for hypersensitivity to DNase, dimethyl sulfate, diethyl pyrocarbonate or potassium permanganate in either the 2-PyN, the 2-ImN or the control lanes of figure 10. A summary of the footprinting results for 2-ImN at the TGTCA site is shown in figure 11. DNase I produces a larger footprint that includes the MPE·Fe(II) protection pattern, as expected from previous results.[14] All purines in the site are protected from dimethyl sulfate by 2-PyN or 2-ImN binding. Since G reacts predominantly at N7 in the

major groove and A reacts predominantly at N3 in the minor groove,[89] this is most consistent with a DNA structural transition on complexation. The negative results obtained with the other structure-sensitive reagents are taken as evidence that any change in DNA conformation remains in the B family.

Double Stranded Cleavage of pBR322

It appears from the high resolution gel data that 2-PyN and 2-ImN exhibit a completely different DNA specificity than the other ArN compounds. However, in the resolvable region of the 167 and 517 bp fragments of pBR322, only 36% of the 512 unique five bp sequences and only 11% of the 2080 unique six bp sequences are present. Since high resolution gels can scan only a small fraction of the potential binding sequences in a reasonable time period, an assay capable of examining larger DNAs has been developed[16] (figure 12). A small molecule equipped with an EDTA cleaving moiety will produce double-stranded breaks whenever two cleavage events occur within eight bp of one another on opposite strands.[90] Frequently occupied sites will then be revealed as cleavage bands on an agarose gel. Using two singly labeled strands and averaging the band sizes determined for each strand gives site positions accurate to $\pm$40 bp on a 4000 bp DNA molecule as judged by the known high affinity sites found on restriction fragments.[16] Conditions used for the double stranded assay are essentially the same as those used for high resolution, except that the decreased background permits longer cleavage times (2 h) and the use of ascorbate as a reductant.

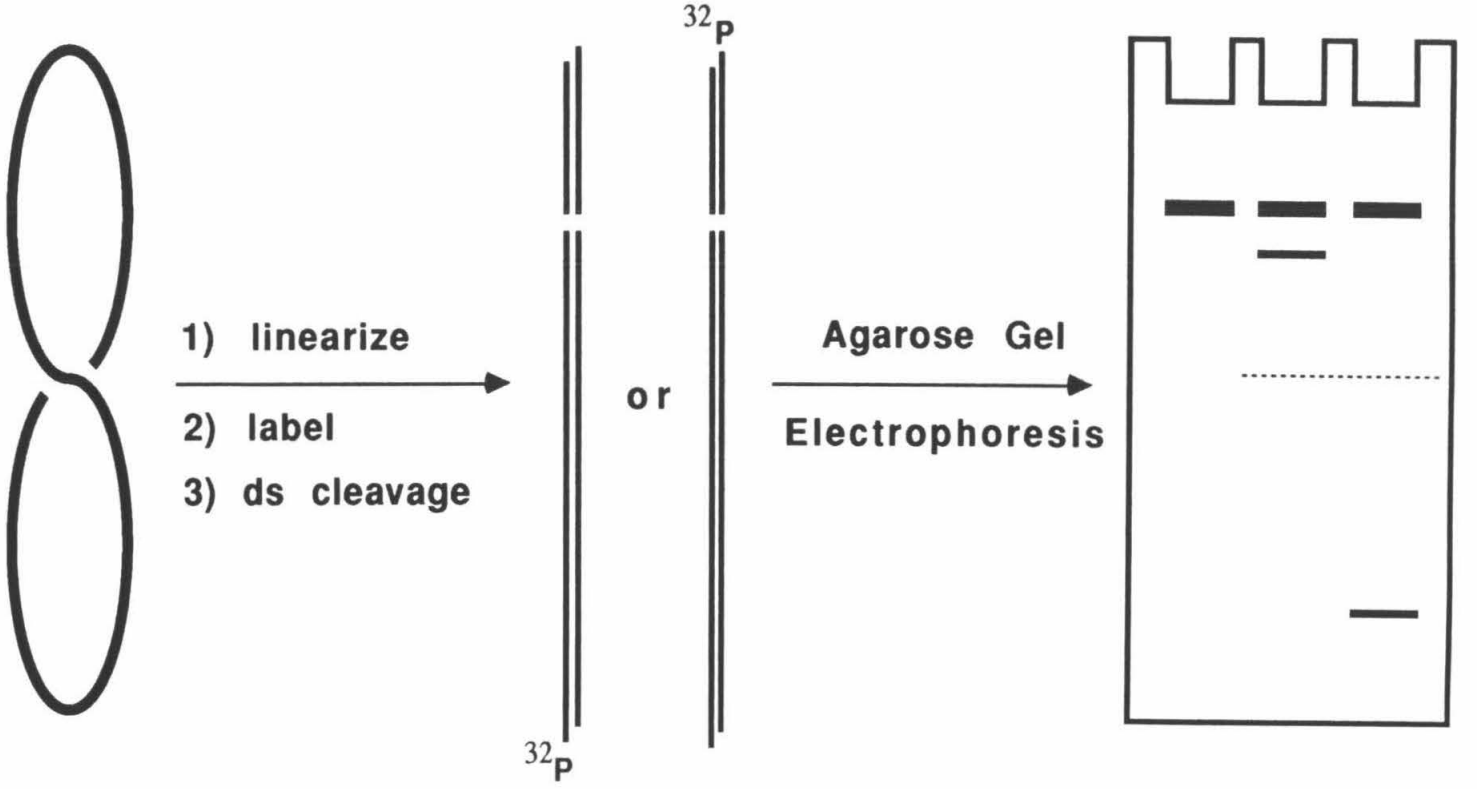

Figure 12 Double stranded cleavage specificity assay. A circular DNA is linearized with a restriction enzyme that gives differentiable termini. Labeling with Klenow fragment of DNA polymerase I at one terminus and treatment with the specific cleavage agent gives a set of double stranded fragments (only one shown) which can be resolved on an agarose gel. Comparison of both labeled ends gives two independent determinations of the cleavage site locations.

Table 1 Sequence determining capabilities of available DNA.

DNA	Size (bp)	Unique Five bp Sequences[a] (%)	Unique Six bp Sequences[b] (%)
167 fragment[c]	167	26	7
517 fragment[c]	517	60	22
Plasmid pSN2	1288	76	37
Plasmid pBR322	4363	99	84
Bacteriophage ΦX174	5386	99	83
Bacteriophage M13	6407	99	83
Plasmid pAA3.7X	9583	99	94
Bacteriophage PZA	19366	99	95
Adenovirus	35937	100	100
Bacteriophage λ	48502	100	99

[a] Determined by the program Fivmer. (see text) [b] Determined by the program Sixmer. [c] *Eco R* I/*Rsa* restriction fragments of pBR322.

Table 1 shows the potential of several available DNA sequences to determine specificities at the five and six bp level. The numbers shown are from actual counts using the FORTRAN program MERS. This program moves linearly through the data sequence, tabulates five and six bp sequences, and produces a frequency table containing the count of each of the 512 unique five bp sequences (Fivmer) or 2080 unique six bp sequences (Sixmer). To be confident that the observed binding sites are representative of all DNA binding sites, it appears necessary to examine about 5000 bp for a five bp binding site and about 10,000 bp for a six bp binding site.

Cleavage of *Sty* I linearized pBR322 by ED, the three pyridine isomers, and 2-ImNE is shown in figure 13. The size in bp of each band is then calculated by

Figure 13 Double-stranded cleavage of pBR322 by ED, 2-PyNE, 3-PyNE, 4-PyNE, and 2-ImNE. Autoradiograms of 1% agarose gels. All reactions contain 1 mM sodium ascorbate, 100 μM-bp calf thymus DNA, and 24 kcpm 3′ labeled pBR322 linearized with *Sty* I and labeled at only one terminus with Klenow fragment. A) Lanes 1–5 are labeled on the clockwise strand with [α-^{32}P] dATP. Lanes 6–8 are labeled on the counterclockwise strand with [α-^{32}P] TTP. Lane 1, intact DNA; lane 2, molecular weight standards; lanes 3 and 6, 2 μM ED; lanes 4 and 7, 50 μM 2-PyNE; lanes 5 and 8, 70 μM 2-ImNE. B) Labeled on the clockwise strand with [α-^{32}P] dATP, lane 1, intact DNA; lane 2, molecular weight standards; lane 3, 2 μM ED; lane 4, 50 μM 2-PyNE; lane 5, 70 μM 2-ImNE; lane 6, 10 μM 3-PyNE; lane 7, 7 μM 4-PyNE. C) Labeled on the counterclockwise strand with [α-^{32}P] TTP. Lane 1, intact DNA; lane 2, molecular weight standards; lane 3, 2 μM ED; lane 4, 50 μM 2-PyNE; lane 5, 70 μM 2-ImNE; lane 6, 10 μM 3-PyNE; lane 7, 7 μM 4-PyNE.

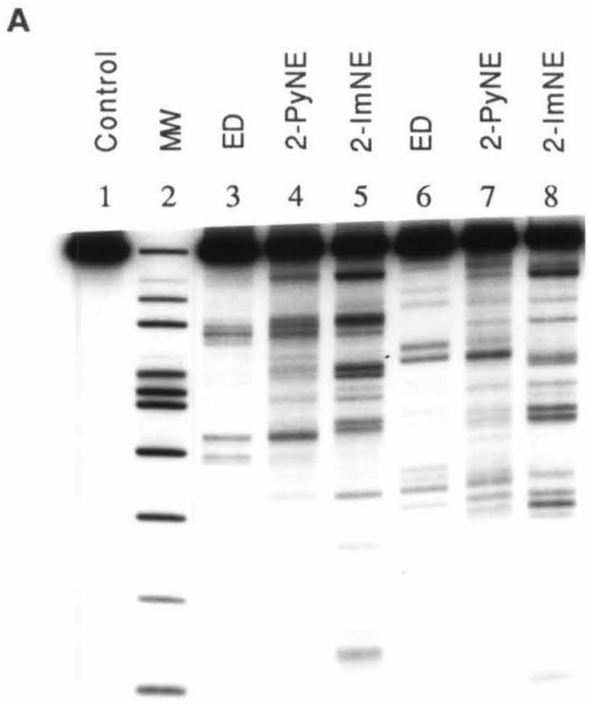
A
Control
MW
ED
2-PyNE
2-ImNE
ED
2-PyNE
2-ImNE
1 2 3 4 5 6 7 8

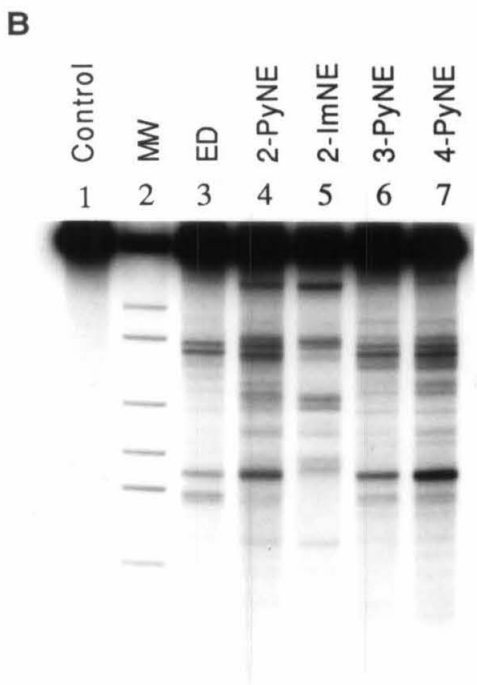
B
Control
MW
ED
2-PyNE
2-ImNE
3-PyNE
4-PyNE
1 2 3 4 5 6 7

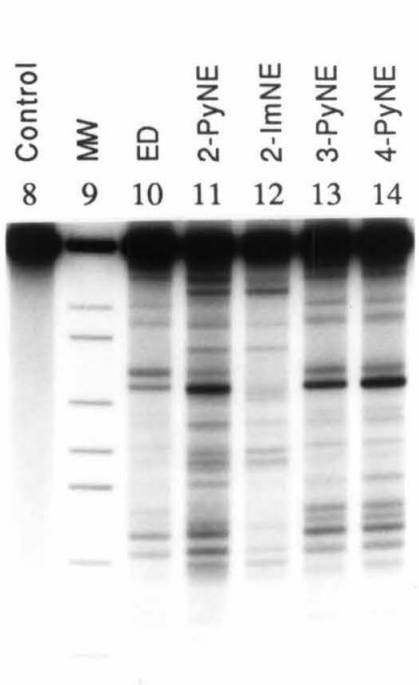
C
Control
MW
ED
2-PyNE
2-ImNE
3-PyNE
4-PyNE
8 9 10 11 12 13 14

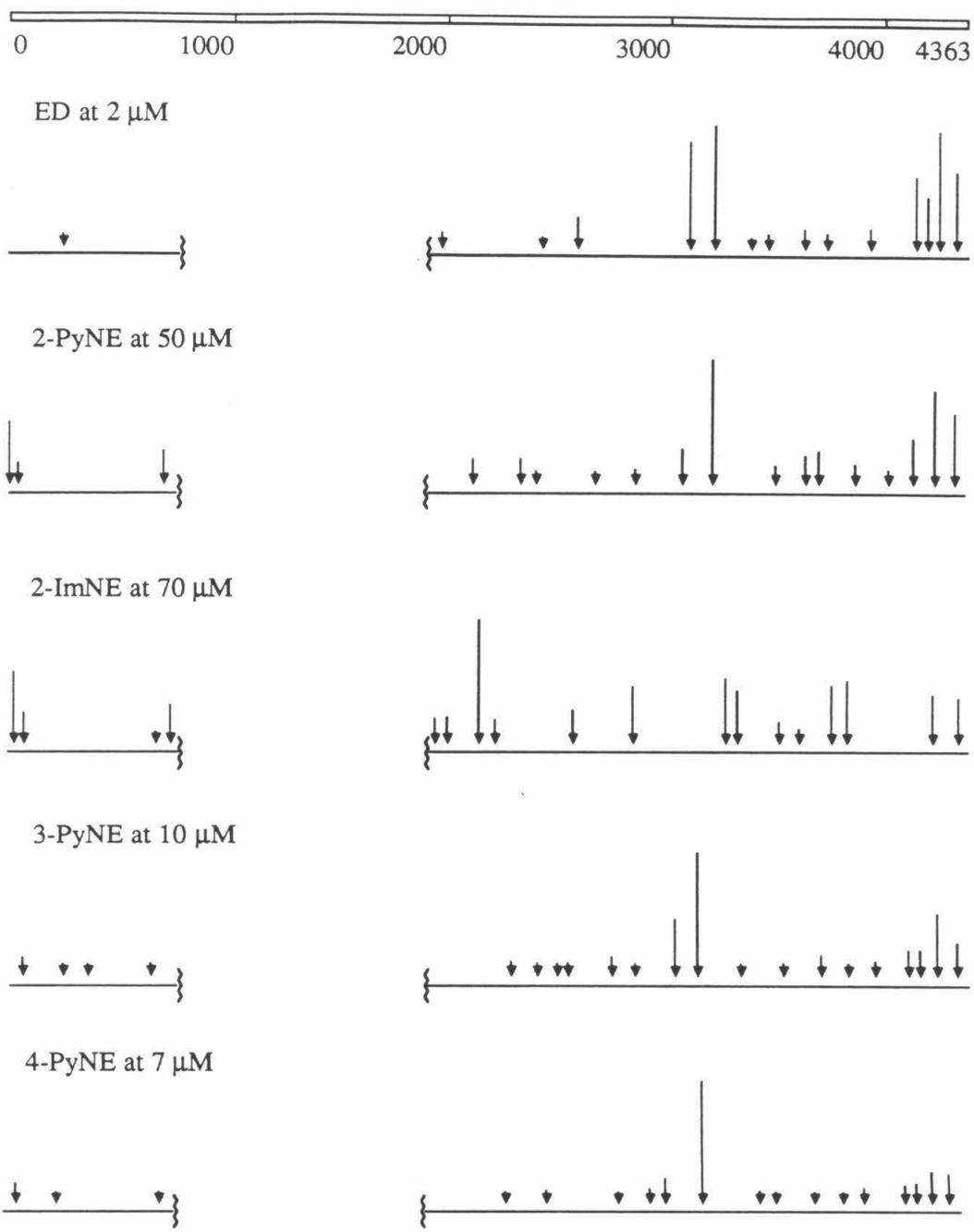

Figure 14 Cleavage sites on pBR322. Arrows represent the extent of cleavage in each lane for figure 13. Band densities are averaged between labels, then normalized to the most intense band. Arrow positions represent approximate binding site locations accurate to within 40 bp. Cleavage bands within 700 bp of the labeled ends are not resolved on the gel.

linear interpolation from the logarithmic sizes of the standards, the numbers are translated into a position on pBR322, and the data from the two labels is averaged to give the approximate cleavage positions shown in figure 14. The cleavage patterns of all five compounds are consistent with the high resolution data. Only 2-ImNE shows a markedly different cleavage pattern from ED. All three pyridine isomers contain bands that match those of the ED lane and additional bands. The 2-PyNE lane appears to be a linear combination of the ED and 2-ImNE lanes, while 3-PyNE and 4-PyNE appear to have only a few bands in common with 2-ImNE.

To determine the specificity of each compound, the portion of pBR322 within 40 bp of the strong cleavage bands was analyzed for sequence content by comparing the list of sequences present near the cleavage bands to the list of all possible sequences resolved on the gel. After using MERS to produce the required frequency tables, the data are screened by stepwise comparison looking for frequencies above a defined threshold. A single class of efficiently cleaved sites should result in a distribution of sequences appearing at frequencies significantly greater than chance. The highest frequency sequence is predicted to be the cleavage site, followed by one bp shifts, followed by two bp shifts, and so forth. Because 2-PyN and 2-ImN show efficient cleavage at both a TGTCA and an AGACA sequence on the 517 bp fragment, the analysis is performed for both five and six bp sequences with each base counted separately or with A and T being interchangeable (W in IUPAC nomenclature[91]).

Acetamide-distamycin-EDTA (ED)

Of the four analyses run, highest frequencies for the distamycin A analog are obtained by tabulating six bp sequences with A and T treated separately. In the 427 bp close to the strong cleavage bands, only the sequences shown in table 2 are present at frequencies significantly above average. As published,[16] ED shows a strong preference for stretches of homopolymer A longer than five bp. Sequences that best fit the observed specificity with positions near the assigned cleavage sites are shown in table 3. The distribution of the proposed sites is plotted against the cleavage patterns in figure 15. For ED, efficient double-stranded cleavage correlates well with A,T sequences at least eight bp long containing at least five consecutive A's. A stretch of six A's is not sufficient for strong cleavage. One such stretch at 3707, surrounded by G,C bp, does not give a strong cleavage band (table 3). The two stretches of seven A's also appear to give less cleavage. The band that contains the cleavage from both is only as intense as the band that maps to the TTTTT site on the 517 bp fragment. Assuming a seven bp A,T sequence containing an AAAAA stretch is the minimum requirement for efficient cleavage at 2 μM, D has a specificity of $4/8192 = 0.05\%$. This is the equivalent of a unique six bp site. Because only 36% of all possible seven bp A,T sequences appear on pBR, the actual specificity could easily be lower.

Table 2 Six bp sequences found at significantly nonrandom frequencies near ED cleavage bands[a].

Sequence	Within ±40 bp of Bands	Resolvable on gel	Frequency
A A A A A A	5	6	0.83
A A A G G A	3	5	0.60
A G A A A A	3	5	0.60
G A A A A A	3	5	0.60
A A A A A G	3	7	0.43

[a] Expected single site frequency is $427/3162 = 0.135$

Pyridine 3- and 4-carboxamide-netropsin-EDTA (3-PyNE and 4-PyNE)

The cleavage patterns of 3-PyNE and 4-PyNE are quite similar to ED, although the total number of cleavage bands has increased. Both compounds give a single major cleavage site at 3140. This band corresponds to the region on pBR322 richest in A,T bp, a 54 bp sequence that is 80% A,T. In addition, the two seven bp homopolymer A tracts on pBR322 occur within 60 bp of calculated position of this band. Because of the abnormal width of the band, a 160 bp segment centered on the calculated size is used in the frequency analysis. The analysis (tables 4 and 5) reveals a lower selectivity for the homopolymer A sites that ED cleaves most efficiently. 4-PyNE cleaves at more sites, and the band at 3140 represents a larger fraction of the total cleavage. This suggests that the specificity of this compound is lower than 3-PyNE.

Table 3 Probable ED sites on pBR322.[a]

Cleavage Position[b]	Site Position[c]	Sequence	Strength
240[d]	252	T T G A T G C A A T T T C T A T G C G C	w
1970	1930	A A A C A G G A A A A A A A C C G C C C T	w
2432	2512	G G A A C C G T A A A A A A G G C C G C G	w
2592	2570	G C A T C A C A A A A A A T C G A C G C T	w
2689	2613	A C A G G A C T A T A A A A G A T A C C A	m
3109	3076	G C G G T G G T T T T T T T G T T T G C	s
	3109	C G C G C A G A A A A A A A A G G A T C T	s
3221	3231	G A T C C C T T T T A A A T T A A A A A A T...	s
	3246	G A A G T T T T A A A T C A A T C T A A	s
3459	3468	T A T C A G C A A T A A A C C A G C C A	w
3633	3579	T C G C C A G T T A A T A G T T T G C G	w
3731	3707	G T T G T G C A A A A A A G C G G T T A	w
3931	3943	G C A G A A C T T T A A A A A G T G C T C	w
4136	4090	G G T G A G C A A A A A A C A G G A A G G	s
	4114	A T G C C G C A A A A A A A G G G A A T A	s
4185	4164	C T C T T C C T T T T T C A A T A T T A	m
4244[d]	4233	T A T T T A G A A A A A A T A A A C A A A A	s
4324[d]	4325	T A A C C T A T A A A A A A T A G G C G T	s

[a] Underlined sequences represent A,T regions predicted to contain strong binding sites. [b] Calculated cleavage band positions averaged between labels, pBR322 numbering.[82, 83] [c] Lowest numbered bp of the A,T region. [d] Cleavage site observed on a high resolution sequencing gel.

1-Methylimidazole-2-carboxamide-netropsin-EDTA (2-ImNE)

The composite cleavage lane shown in figure 14 contains fifteen bands sufficiently intense to permit accurate size estimation. One third of the 3160 resolvable bp on pBR322 are within 40 bp of a strong cleavage site. Table 6 shows all sites that appeared more than 70% of the time within this subset. The highest frequency is found for WWGWCW, the consensus sequence for strong 2-PyNE and 2-ImNE

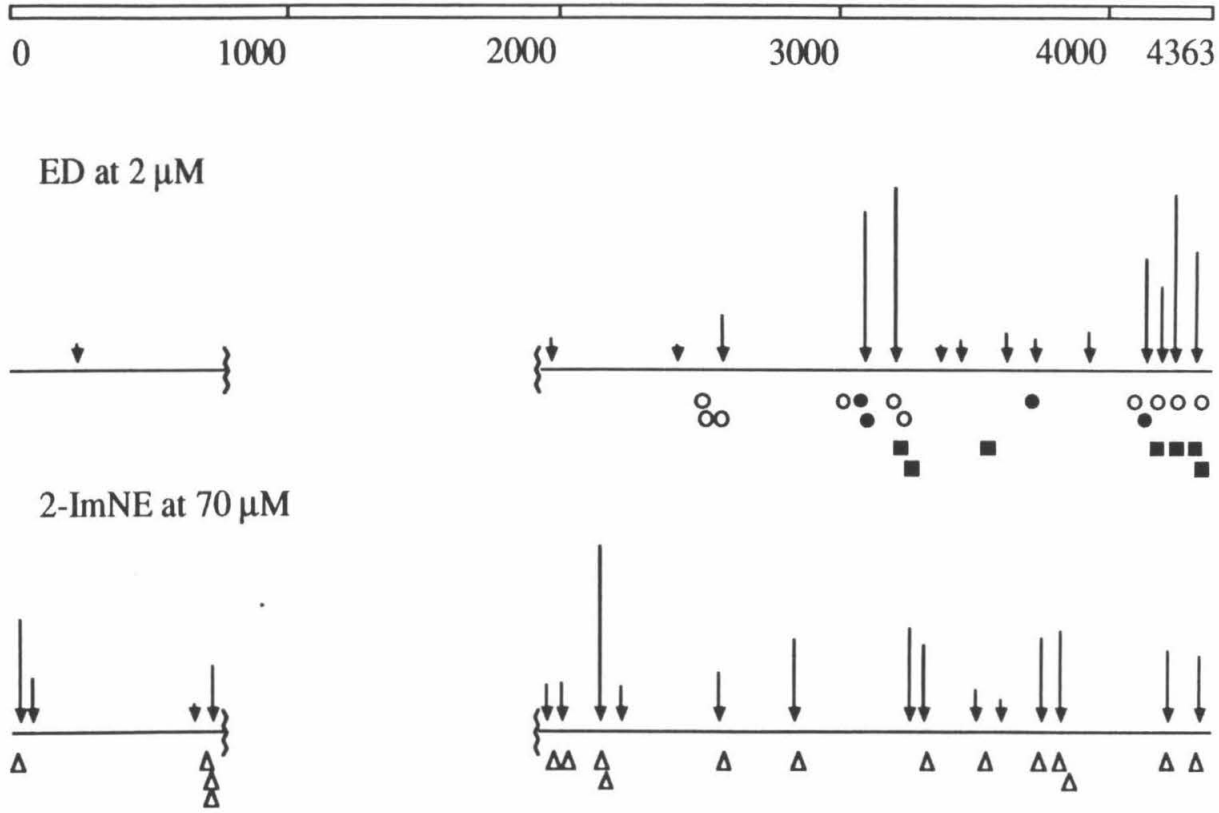

Figure 15 Top) Position of ED cleavage bands in relation to long A,T sequences. ○ – AAAAA sites, • – AAAAAA sites, ■ – WWWWWWWW sites. Bottom) Position of 2-ImNE cleavage bands in relation to WWGWCW sequences (△).

Table 4 Five and six bp sequences found at significantly nonrandom frequencies near 3-PyNE cleavage bands.[a]

Sequence	Within ±40 bp of Bands	Resolvable on Gel	Frequency
G G A A A	6	7	0.86
A A A A A	16	20	0.80
C A A A A	7	10	0.80
A A A T A	7	9	0.78
G C A A A	7	9	0.78
C A G A A	7	9	0.78
G A A A A	10	13	0.77
A A A A C	6	8	0.75
G C A A A A	6	6	1.00
A A A A A A	6	6	1.00
A A A A A G	5	7	0.71

[a] Expected single site frequency is $1121/3162 = 0.354$

binding on the high resolution gels. Most other table entries are one or two bp shifts of this sequence, providing good evidence that WWGWCW represents the only major class of binding sites for 2-ImNE on pBR322.

Table 7 contains a summary of the proposed binding sites. The correlation of these sites with the observed cleavage bands is shown in figure 15. Only one of the 16 intense 2-ImNE bands is not near a WWGWCW sequence. Its position corresponds to the strong cleavage band found at 3270 in ED and 2-PyNE or 3140 in 3-PyNE and 4-PyNE lanes. Of the 21 detectable bands, only one very weak site is not near a WGWCW sequence. Nearly every potential site is within 20 bp of the band sizes determined from the gel. The strongest cleavage bands are positioned

Table 5 Five and six bp sequences found at significantly nonrandom frequencies near 4-PyNE cleavage bands.[a]

Sequence	Within ±40 bp of Bands	Resolvable on gel	Frequency
T T A A A	9	9	1.00
A T A A A	8	9	0.89
A A A A G	13	15	0.87
A G T G C	6	7	0.86
A T C A T	6	7	0.86
A A T A C	6	7	0.86
T A T C A	9	11	0.82
G A T A A	13	16	0.81
C A A A A	8	10	0.80
A A A T A	7	9	0.78
G C A A A	7	9	0.78
C A G A A	7	9	0.78
A A A G G	9	12	0.75
A A A A A	14	20	0.70
A A A A G G	7	8	0.88
T G A T A A	7	8	0.88
A A A A A G	6	7	0.86

[a] Expected single site frequency is 1394/3162 = 0.441

within 50 bp of more than one copy of the consensus sequence. Single WWGWCW sites appear to give nearly the same amount of cleavage. The one exception, the site at 29, cleaves much better than average. Thus, it is likely that WWGWCW is the major site of 2-ImN binding on DNA. There are 16 unique WWGWCW sequences, giving 2-ImN a specificity of 16/2080 = 0.8%, the equivalent of a four bp unique site.

Several of these cleavage sites have been checked by examining high resolution

gels of the appropriate restriction fragment. In all cases examined (see table 7), the cleavage bands map directly to WGWCW sites. All sites are cleaved without orientation preference, and the relative cleavage intensities match those found on the agarose gel. In addition, neither WGWGW nor WGWWWW nor WCWGW sites bind 2-ImN to a measurable extent at 20 μM, as shown by high resolution gels on the 517 bp fragment and others.

Table 6 Six bp sequences found at significantly nonrandom frequencies near 2-ImNE cleavage bands.[a]

Sequence	Within ±40 bp of Bands	Resolvable on gel	Frequency
W G W G W C	6	6	1.00
W W G W C W	19	20	0.95
W W W G W C	11	13	0.85
C W W G W C	8	10	0.80
W G W C W G	18	24	0.75
W G W C C W	5	7	0.71

[a] Expected single site frequency is 1026/3162 = 0.324

Pyridine-2-carboxamide-netropsin-EDTA (2-PyNE)

Application of the same analysis in the pyridine case does not give clear-cut results. As expected from the high resolution data, the cutting pattern is a mixture of those obtained with 2-ImNE and ED. The strongest 2-PyNE cleavage bands correspond to ED sites, but some bands are found only in the 2-PyNE and 2-ImNE lanes. Indeed, a high resolution gel of the *Sal* I/*Sty* I 720 bp restriction

Table 7 Probable 2-ImNE binding sites on pBR322.[a]

Cleavage Position[b]	Site Position[c]	Sequence	Strength
29	10[d]	A T G T T T G A C A G C T T A	s
86	71[d]	A A C G C A G T C A G G C A C	m
196	212	T C G C C A G T C A C T A T G	w
666	682[d]	A A C C C A G T C A G C T C C	w
730	710[d]	G G G C A T G A C T A T C G T	
	732[d]	A C T T A T G A C T G T C T T	
	736[d]	A T G A C T G T C T T C T T T	m
1901	1915	C A T C A A G T G A C C A A A	w
1935	1969	A A G C C A G A C A T T A A C	m
1993	2021	C A G G C A G A C A T C T G T	m
2137	2106	A C C T C T G A C A C A T G C	
	2139	C A G C T T G T C T G T A A G	
	2163	G G A G C A G A C A A G C C C	s
2215	2224	G A C C C A G T C A C G T A G	m
2359	2374	C T C A C T G A C T C G C T G	w
2573	2585	G C T C A A G T C A G A G G T	m
2844	2861	C G G T A A G A C A C G A C T	m
3269	3231	C C T T T T A A A T T A A A A...	
		A T G A A G T T T T A A T C A...	
		A T C T A A A G T A T A T A T...	
		G A G T A A A C T T G	s
	3289	T G G T C T G A C A G T T A C	s
3326	3335	C G A T C T G T C T A T T T C	m
3513	3534	C A T C C A G T C T A T T A A	m
3601	3624	C G T G G T G T C A C G C T C	w
3749	3742	A T C G T T G T C A G A A G T	m
3823	3808	C T T A C T G T C A T G C C A	
	3837	T T C T G T G A C T G G T G A	
	3858	A A C C A A G T C A T T C T G	s
4215	4199[d]	G T T A T T G T C T C A T G A	m
4332	4311[d]	T A T C A T G A C A T T A A C	m

[a] Underlined sequences represent putative or actual binding sites. [b] Calculated cleavage band positions averaged between labels, pBR322 numbering.[82, 83] [c] Lowest numbered bp of the A,T region. [d] Cleavage site observed on a high resolution sequencing gel.

fragment that contains the cleavage sites near 700 shows efficient cutting by 2-PyNE only at three WWGWCW sites (see appendix A).

In contrast to the nearly equal WWGWCW:AAAAA site preference seen on the 517 bp fragment, the strongest sites for 2-PyNE on pBR322 tend to match those of ED. This can be explained by different distributions of the two types of sites. WWGWCW sites are normally single and isolated. There are only three places on pBR322 where two or more sites exist within 50 bp of one another. However, with a poly A sequence there is nearly a 25% chance (on pBR322) that the stretch will continue and create a stronger affinity site. This tends to produce ED cleavage intensities that vary considerably with the actual sequence. In contrast, 2-ImNE should cleave all WWGWCW sites to the same extent.

Of the five compounds, it appears that only two, ED and 2-ImNE, exhibit cleavage patterns consistent with a single class of high affinity binding sites. Paradoxically, while the 3-PyNE and 4-PyNE compounds have lower specificities than ED, they produce the most selective cleavage. Almost 25% of the total cleavage products are found in the band at 3140. Such an example of anomalously high specificity has been observed with ED on bacteriophage λ,[16] where it has been attributed to the uneven distribution of cleavage sites. Thus, this strong cleavage band that appears in all compounds is likely to be the superposition of a large number of lower affinity sites. High resolution studies on other compounds support

this conclusion.[92] 2-ImNE is the only compound where another site gives significantly more cleavage. This indicates that A,T site binding must be quite strongly disfavored before a shift in overall specificity occurs.

A Model for the 2-ImN Complex Conformation

Any binding model developed for 2-ImN binding at its major site must explain a number of separate observations.

1. A GAC sequence must be present in the binding site.
2. 2-ImN binds a five bp sequence but recognizes a six bp sequence.
3. 2-ImNE cleaves non C_2 symmetric sites with no orientation preference.
4. A,T bp are interchangeable within the recognition site, but are strictly required.
5. The heterocyclic nitrogen is required and must be *ortho* to the amide carbonyl.
6. The binding affinity if 2-ImN to DNA is significantly lower than related compounds.
7. Dimethyl sulfate protection occurs in both the minor and major grooves.

The interchangeability of the A,T bp in the site indicates that the major interactions responsible for sequence specific complexation must occur between 2-ImN and the G,C bp in the site. This is borne out by the specificity for GAC sequences over CAG and GAG. For all WWGWCW sites to be cleaved symmetrically, the DNA site recognition element must also be C_2 symmetric. In the minor groove, only the O2 of C, the N2H of G and the N3 of G are potential candidates. The most accessible is the N2 of guanine, which is also the only hydrogen bonding donor in the minor groove. Two changes have been made in designing 2-ImN. The N-terminal amide has been removed and the pyrrole 3CH has been replaced by

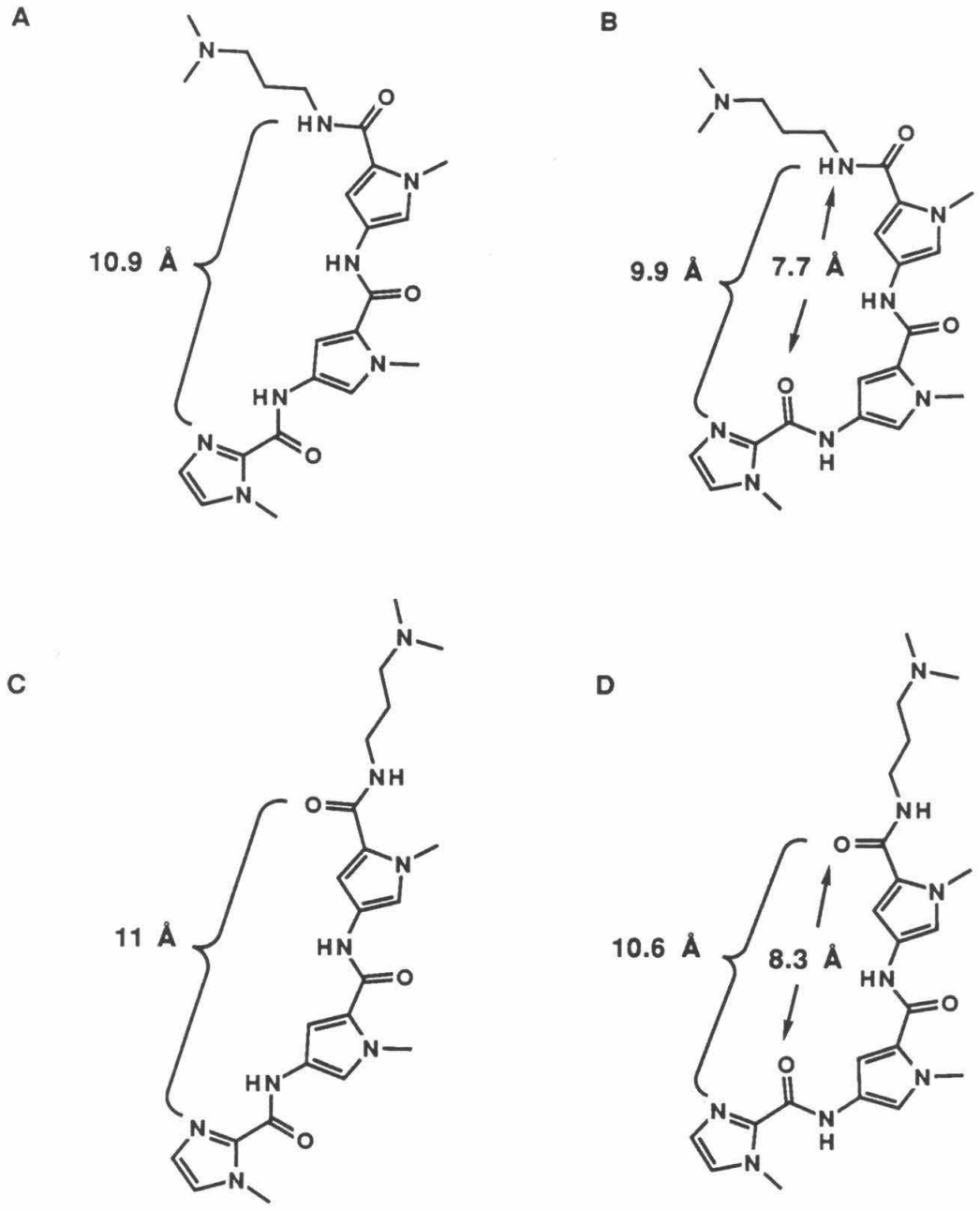

Figure 16 Low energy conformers of 2-ImN capable of fitting in minor groove of B DNA. Distances are measured using the program Macromodel and the AMBER forcefield parameters.[93] The planar conformation shown has the shortest distance between hydrogen bonding moieties.

nitrogen. The change in specificity cannot be due to the loss of the amide, for 2-FuN, 2-ThN, 3-PyN, and 4-PyN do not show the same pattern. Thus it is probable that a hydrogen bond is formed between the imidazole nitrogen and the guanine exocyclic amine. To give two fold symmetry, a second G,C hydrogen bond must be formed at the other end of the binding site. The four conformations of 2-ImN capable of occupying the minor groove are shown in figure 16. For comparison purposes, the distances shown are for the planar conformations, representing the minimum distance between hydrogen bonding groups. In the actual complex, the aromatic rings would be twisted 10–20° out of planarity, increasing the distance slightly, as has been observed for netropsin[18, 19] and distamycin A.[20]

There is no obvious reason to choose or eliminate any of these conformations. Conformation A is that observed in the netropsin and distamycin A crystal structures. Conformations B + D have the virtue of decreasing the distance between the ends of 2-ImN to a value more closely matching the idealized B DNA distance (approximately 8 Å).[94] Conformations C + D have the advantage of placing a second hydrogen bond acceptor at the bottom of the groove so that the 2-ImN to G hydrogen bonds are actually symmetric.

With respect to the DNA target site, the remaining observations can be explained by postulating a conformational change upon small molecule binding. An induced fit could decrease the accessability of the guanine N7's to dimethyl sulfate. If the bound sequence is favored by A,T bp, this would also explain the A,T

requirement outside the binding site. An induced fit would also require energy, lowering the total free energy of complexation.

This putative conformational change also provides an explanation for the selective complexation of GAC sequences over CAG or GAG. The rigidity of 2-ImN and the requirement for binding in the minor groove means that the positions of G,C bp in the complex are tightly constrained. If complexation of 2-ImN induces a conformational change, then the sequence selectivity can be explained by the relative abilities of GAC, CAG, and GAG sequences to achieve the proper conformation. From computer modeling,[95] it appears that the relevant distances for 2-ImN are at least one Å larger than the DNA distance. For better matching, the guanine nitrogens must move farther apart. This could be accomplished by increasing the twist at the site to make the DNA longer and thinner, bending the helix axis towards the major groove or changing the propeller twist of the G,C bp. The first two possibilities offer no obvious difference between the the three sequence isomers. However, the propensity for propeller twisting is predicted to vary between these three sequences.[6] To increase the distance between guanine N2's, a GAC sequence must increase the propeller twist at both G,C bp, for a GAG sequence, one G must increase and the other must decrease the propeller twist, and a CAG sequence must decrease both. Increased propeller twist will tend to be favored by A,T bp that have an average 5° larger twist than G,C bp.[4] The observed selectivity of A,T bp outside the binding site can then be explained as

a preference for the more propeller twisted conformation, which would lower the reorganization energy of the complex.

Recent studies of 434 repressor support the above outline. Like 2-ImN, 434 repressor binds with higher affinity to sequences that contain additional A,T bp at the center of the dimeric binding site.[96] An examination of the protein-DNA cocrystal reveals that there are no specific contacts to these bp. Further, the DNA region between monomers is overtwisted, compressing the minor groove and producing larger propeller twists than are usually observed.[97] Nicking the center of the operator site relaxes the specificity requirement for the noncontacted bp,[98] consistent with the postulated conformational role of these bp.

It is encouraging to find that a recognition mechanism similar to that proposed is used by Nature. While the actual details of the complex await the use of more powerful structural methods such as NMR or X-ray crystallography, the general outlines of this model can be tested by chemical and biological techniques. This will be the general focus of the following chapters.

Summary

To search for altered DNA sequence specificity, a series of distamycin A analogs have been prepared. The majority of these compounds bind only to the A,T rich sites of the parent compound. Two analogs, pyridine-2-carboxamide-netropsin (2-PyN) and 1-methylimidazole-2-carboxamide-netropsin (2-ImN), bind a TGTCA sequence. The pyridine isomers 3-PyN and 4-PyN do not bind this sequence. The

compounds are present in the minor groove, but protect the binding site from dimethyl sulfate in both grooves. Two equivalent orientations are observed at this binding site. The specificity of 2-ImN is higher than that of 2-PyN. Although both compounds bind equally well to the TGTCA site, 2-ImN has significantly lower affinity to all A,T sites. On pBR322, the EDTA derivative of 2-ImN (2-ImNE) efficiently cleaves a single class of sites with the consensus sequence WWGWCW (W is either A or T). An induced DNA conformational change is proposed to fit this data.

Chapter 3

Quantitative MPE·Fe(II) Footprinting

The assays used in chapter 2 to measure DNA specificity give only relative preferences for 2-PyN and 2-ImN binding sites. For comparison between DNA substrates, it is necessary to describe the sequence specificity in absolute terms. This corresponds to the measurement of the binding constant at the sites to be compared. Moreover, by measuring the binding constant of identical sites in different environments, it should be possible to precisely delineate the effect of flanking sequences.

Methods capable of measuring individual site binding constants are rare. Most binding assays, such as equilibrium dialysis, measure macroscopic properties. Measurement of single site affinities is only possible for oligonucleotides containing a single site. The relevance of the numbers produced then depends on the correspondance of oligonucleotide properties to those of longer DNA. Recently a method has been developed by Ackers and co-workers that is capable of determining individual site binding constants on restriction fragments.[99] The method uses standard DNase I footprinting techniques to report the occupancy of binding sites over a range of ligand concentrations. With the appropriate DNA sequence, affinity constants for several binding sites can be determined from a single gel.

Theoretical Basis

The association constant for DNA binding of a general ligand is defined as

$$K_a = \frac{[DNA \cdot L]}{[DNA]_{free}[L]_{free}}$$

This can be redefined using Y, the fraction of DNA bound, as follows

$$Y = \frac{[DNA \cdot L]}{[DNA]_{total}}$$

$$K_a = \frac{[DNA \cdot L]}{[DNA]_{total}} \left(\frac{[DNA]_{total}}{[DNA]_{free}} \right) \frac{1}{[L]_{free}}$$

$$K_a = \frac{Y}{1 - Y} \cdot \frac{1}{[L]_{free}}$$

In the ideal case, Y will vary from 0 at very low concentrations of ligand to 1 at saturation. The binding constant can then be determined at a given site by plotting the Y value versus the ligand concentration. At $Y = 0.5$, the association constant will be the reciprocal of the free ligand concentration.

These equations lead to two conclusions important to the footprinting experiment. First, the amount of DNA need not be measured, because the final equation for K_a is independent of the DNA concentration. This permits the use of radioactive DNA, because it not necessary to know the specific activity. Second, an accurate determination of the binding constant depends only on accurate measurements of the free ligand concentration and the fraction of DNA bound.

The Ackers group determines $[L]_{free}$ by lowering the DNA concentration. When the concentration of DNA binding sites is $< 1\%$ of the total ligand concentration, even site saturation will have no significant effect on the total ligand concentration. This is readily achieved with labeled DNA by increasing the specific activity. Incorporation of four radioactive deoxynucleotides into a single restriction fragment lowers the final concentration of radioactive probe DNA to < 50 pM-bp.

However, > 99% of the DNA in the footprinting experiment is nonradioactive carrier, usually present at 100 μM-bp or higher concentration. To minimize carrier DNA effects, the final DNA concentration is lowered to 2 μM. If the average binding constant to carrier is $\leq 10^4$ M^{-1} and the binding site size is greater than five bp, then < 3% of the ligand will be bound at any concentration. These conditions usually hold for the binding proteins to calf thymus DNA, so that no special carrier is needed to measure the protein-DNA affinity constant. The properties of the protein-DNA complex also permit direct measurement of carrier binding by a nitrocellulose filter assay.[100]

Y, the fraction of DNA bound, can then be determined from the footprinting gel. If the cleavage events are independent, the length of the DNA molecules remains constant over the course of the reaction, and all labeled DNA molecules are equivalent targets, then nicking by DNase I should be described by a Poisson distribution. Cleavage at the binding site is then proportional to the occupancy at the site, and thus a direct measure of the percentage of that site bound. Ackers *et al.* find that cleavage varies exponentially with DNase I concentration, as expected for this distribution.

Under conditions that give a linear X-ray film response, the amount of cleavage at any given site will then be proportional to the optical density of the corresponding band on the film. To ensure a linear film response with the best signal to noise

ratio, Ackers *et al.* use preflashed X-ray film exposed with one calcium tungstate intensification screen.[101]

The optical density at a site is determined by scanning the entire gel in two dimensions. The total volume (AU x mm^2) of the bands in question can then be measured. Because the amount of cleavage at well-protected sites is close to the background value of the film, it is necessary to apply a local background correction. Panel A of figure 1 shows the procedure that Ackers and co-workers use. A special gel comb is constructed with teeth spaced at 6 mm intervals instead of 3 mm. This ensures that DNA lanes are far enough apart so that the optical density between them reaches a true background value. The most probable value midway between lanes is averaged between the two sides of a given lane, and the resultant background is subtracted from the optical density of the site to give the actual amount of cleavage at a given site.

The apparent fraction bound is then calculated, correcting for differences in the total amount of cleavage by using an unbound sequence as an internal standard, as shown below:

$$Y_{app} = 1 - \frac{OD_{site}/OD_{ref}}{OD_{site,std}/OD_{ref,std}}$$

where OD_{site} refers to the site to be measured, OD_{ref} refers to a set of bands that are not bound by the ligand, and $OD_{ref,std}$ and $OD_{site,std}$ refer to the same bands in a lane without any added ligand. In actual practice Y_{app} does not reach either 0 or 1, so that the binding constant is determined by a non-linear least squares

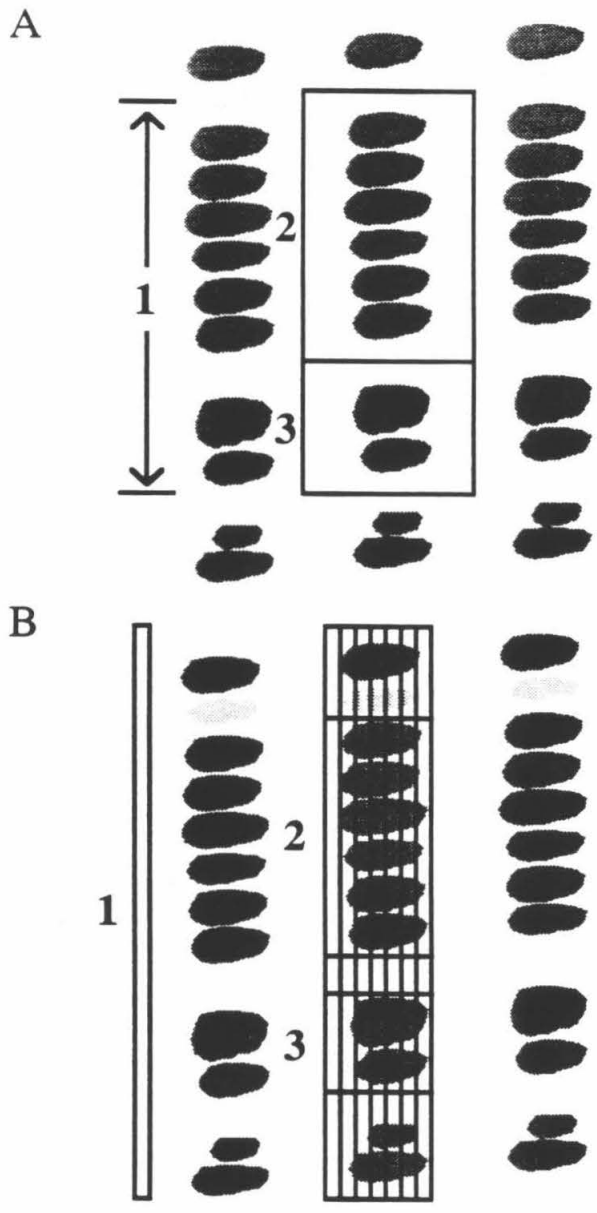

Figure 1 Determination of band optical densities. A) Two dimensional scanning method of Ackers and coworkers.[99] Background 1 is determined by the most probable value between gel lanes. Footprint block 2 and reference block 3 extend to the middle of each lane, and are chosen to minimize the OD at the lane crossings. B) One dimensional scanning equivalent. Background 1 is determined by a single 1 mm scan between lanes. Band densities are determined by a series of seven consecutive 1 mm scans which are averaged. Blocks 2 and 3 are calculated by adding the areas of the appropriate peaks.

fitting procedure. A single independent site binding curve is fit to the experimental data using the Y value at saturation binding (Y_H), the Y value at no binding (Y_L), and the K_a as adjustable parameters.

In studying the binding of lambda repressor to its operator sequence, Ackers *et al.* have found that the measured affinities agree well with measurements made by other methods.[100] Importantly, the measured numbers are also relatively insensitive to variations in the concentration of DNase I or the amount of total cleavage.

Modifications for Small Molecules

In order to use the Ackers procedure to determine small molecule-DNA binding constants, several modifications need to be made. The large size of DNase I footprints does not give sufficient resolution to separate individual D or 2-PyN footprints. Either MPE·Fe(II) or EDTA·Fe(II) has better resolution, and like DNase I, these reagents give a Poisson distribution of cleavage fragments.[86, 102] Initial experiments using EDTA·Fe(II) reveal that the 9 mM hydrogen peroxide required destroys nearly 50% of the 2-PyN and 2-ImN chromophores over the standard reaction time. No significant loss is observed when MPE·Fe(II) is used as the footprinting agent. Apparently the presence of millimolar concentrations of DTT in the MPE·Fe(II) cleavage reaction protects the small molecule from oxidative degradation.

The high specificity of protein binding allows native DNA to be used as a carrier because high affinity sites have very low frequencies. However, the specificity

studies of chapter 2 show that strong binding sites for D, 2-PyN, and 2-ImN are common on random DNA sequences. All observed binding sites contain A,T bp, so the best candidate for a weakly bound carrier is poly(dG)·poly(dC). The binding constant of distamycin A to this polymer has been measured by CD to be 5 x 10^4 M^{-1} at 50 mM salt.[103] At higher salt concentrations, the total amount of compound bound drops rapidly.[104] 2-PyN and 2-ImN do not bind GGGG sequences at 50 μM on the sequencing gels in chapter 2, indicating that the binding constant for all three compounds is below the 10^4 M^{-1} cutoff.

The size of small molecule binding sites (~5 bp), is much smaller than most protein binding sites (~14 bp), and in general the binding constants are lower. This has important implications for the accuracy of the experiment. Ackers *et al.* find that the more bands included in the blocks used to calculate Y_{app}, the better the precision of the experiment. Precision is also enhanced by the larger size of DNase I footprints[74] that increase the number of cleavage bands averaged, and the partial sequence specificity of DNase I that allows the edges of sites to be determined precisely at light cleavage bands. In contrast to the large footprints found with proteins and DNase, the MPE·Fe(II) footprints of the three compounds are five bp in length, with maximal inhibition only at the middle 2–3 bp (see chapter 2). The relatively uniform cleavage pattern of MPE·Fe(II) also means that the film density between any two bands never reaches the background value. Because the sites used to calculate Y_{app} are smaller and the edges are less well defined, quantitative

MPE·Fe(II) footprinting should produce binding curves having more scattered data points than DNase I curves.

The Footprinting Experiment

Unlike 14 other candidate fragments of pBR322, the 517 bp fragment contains a representative D site (TTTTT) and a representative 2-ImN site (TGTCA) within 20 bp of one another. Labeling at the 3′ terminus with the Klenow fragment of DNA polymerase I following the Ackers *et al.* guidelines gives a fragment with 3–4 radioactive deoxynucleotides present in each molecule. For all experiments run, the final DNA concentration is no greater than 50 nM-bp, and is often considerably less. There are 10 potential strong binding sites for D on the restriction fragment, giving a final site concentration of 1 nM and 10^8 M^{-1} as an upper limit for accurate binding constant measurements.

Using a comb similar to that of the Ackers group, the maximum number of footprinting lanes is nineteen. At three points per order of magnitude in small molecule concentration, this gives a five order of magnitude concentration range. A practical upper limit for sample concentrations is 200 μM. Above this limit, the surfactant properties of the compounds and the potential for base catalyzed cleavage at apurinic sites[105] make quantitation difficult.

To minimize electrostatic interactions, the footprinting reactions are performed in pH 7.0 tris·hydrochloride buffer containing 100 mM sodium chloride. For 2-PyN and 2-ImN, final concentrations range from 200 μM to 200 pM. For D,

the final concentrations range from 20 μM to 20 pM. Optimum conditions for MPE cleavage are 2.5 μM-bp poly(dG)·poly(dC), 1 μM MPE·Fe(II), and 2 mM DTT, incubating for 14 min at 37°C.

Poly (dG)·(dC) is difficult to resuspend.[106] The following conditions are found to give the best results. Upon reaction completion, 1 μg tRNA is added. The reactions are ethanol precipitated *without added salt*, and resuspended in formamide with sonication. By following this procedure, an average of only one lane per gel did not resuspend properly. The dried gel is then exposed to preflashed X-ray film as in the Ackers procedure.

A typical film exposure of a 2-PyN gel is shown in figure 3. As expected from previous experiments, there are four sites in close proximity near the bottom of the gel, which correspond to the TTTTT, TTAAT, TGTCA, and AATAA sites mapped in the previous section. As the amount of 2-PyN increases, the total amount of cleavage by MPE·Fe(II) decreases. Above 100 μM, cleavage drops precipitously (data shown only for 200 μM), consistent with a nonspecific binding constant of 2-PyN to DNA on the order of 10^3 M^{-1}. Typical film exposures of a D gel and a 2-ImN gel are shown in figures 2 and 4, respectively. Similar protection at all sequences is observed for D above 10 μM and 2-ImN above 100 μM.

A one dimensional scan through the center of each band is shown in figure 5. Qualitatively, the relative binding constants at each site match the order in which they appear in the normal footprinting experiment and the relative cleavage efficiencies of the EDTA derivatives. For 2-PyN, the TTTTT and TGTCA sites are

Figure 2 Quantitative MPE·Fe(II) footprinting of D. Preflashed film exposure of an 8% polyacrylamide gel. All reactions contain 2 mM DTT, 2.5 μM-bp poly(dG)·poly(dC), and 12 kcpm high specific activity 3′ labeled 517 bp restriction fragment in 40 mM Tris·HCl, 100 mM sodium chloride, pH 7.0 buffer. Lane 1, intact DNA; lane 2, A reaction;[81] lanes 3–23 contain 1 μM MPE·Fe(II): lanes 3 and 23 are **MPE**·Fe(II) standards; lanes 4–22 contain 20 μM, 10 μM, 5 μM, 2 μM, 1 μM, 500 nM, 200 nM, 100 nM, 50 nM, 20 nM, 10 nM, 5 nM, 2 nM, 1 nM, 500 pM, 200 pM, 100 pM, 50 pM, and 20 pM D respectively.

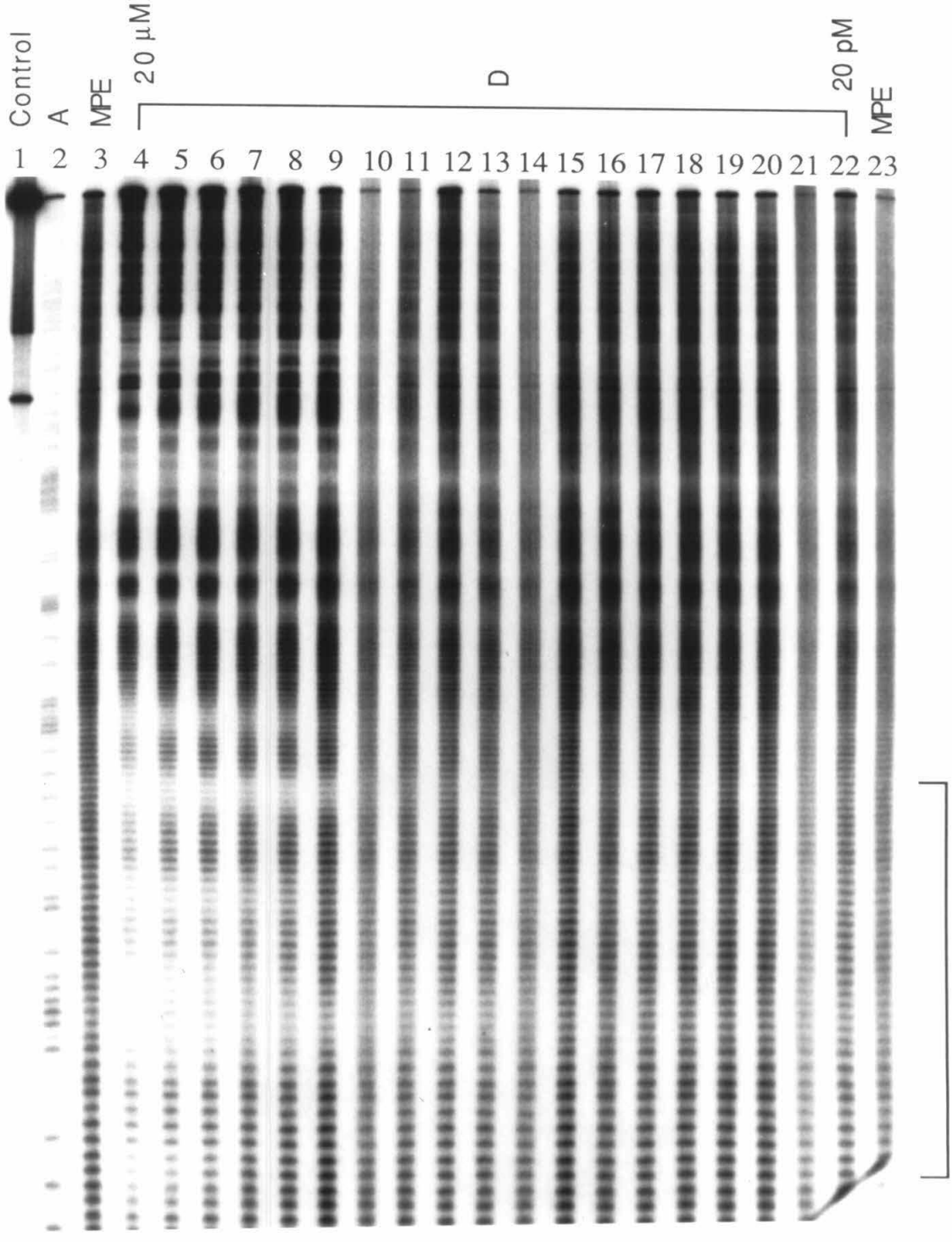
Control
A
MPE
20 μM
D
20 pM
MPE
1 2 3 4 5 6 7 8 9 10 11 12 13 14 15 16 17 18 19 20 21 22 23

Figure 3 Quantitative MPE·Fe(II) footprinting of 2-PyN. Preflashed film exposure of an 8% polyacrylamide gel. All reactions contain 2 mM DTT, 2.5 μM-bp poly(dG)·poly(dC), and 12 kcpm high specific activity 3′ labeled 517 bp restriction fragment in 40 mM Tris·HCl, 100 mM sodium chloride, pH 7.0 buffer. Lane 1, intact DNA; lane 2, A reaction;[81] lanes 3–23 contain 1 μM MPE·Fe(II): lanes 3 and 23 are **MPE**·Fe(II) standards; lanes 4–22 contain 200 μM, 100 μM, 50 μM, 20 μM, 10 μM, 5 μM, 2 μM, 1 μM, 500 nM, 200 nM, 100 nM, 50 nM, 20 nM, 10 nM, 5 nM, 2 nM, 1 nM, 500 pM, and 200 pM 2-PyN respectively.

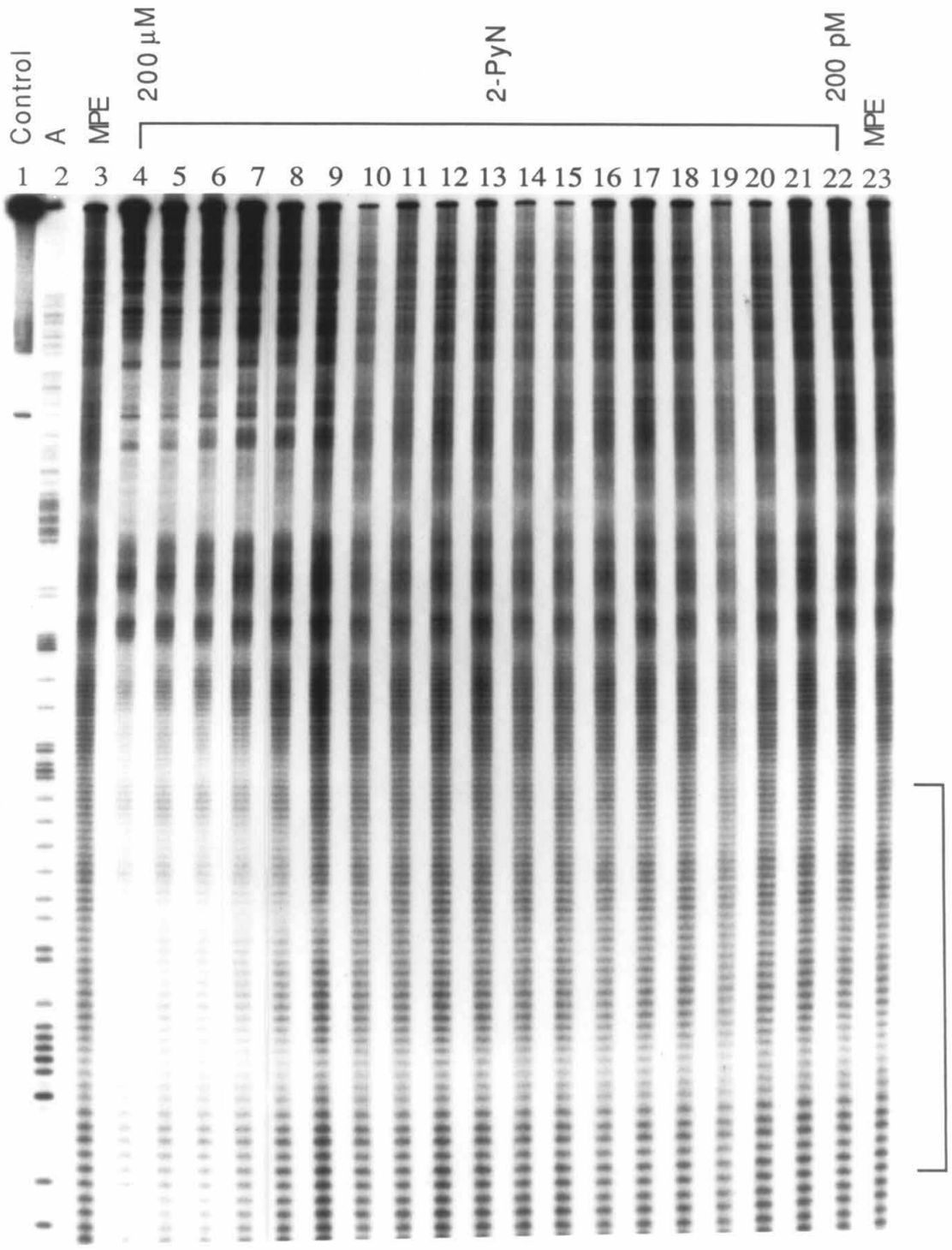
Control
A
MPE
200 µM
2-PyN
200 pM
MPE
1 2 3 4 5 6 7 8 9 10 11 12 13 14 15 16 17 18 19 20 21 22 23

Figure 4 Quantitative MPE·Fe(II) footprinting of 2-ImN. Preflashed film exposure of an 8% polyacrylamide gel. All reactions contain 2 mM DTT, 2.5 μM-bp poly(dG)·poly(dC), and 12 kcpm high specific activity 3′ labeled 517 bp restriction fragment in 40 mM Tris·HCl, 100 mM sodium chloride, pH 7.0 buffer. Lane 1, intact DNA; lane 2, A reaction;[81] lanes 3–23 contain 1 μM MPE·Fe(II): lanes 3 and 23 are **MPE**·Fe(II) standards; lanes 4–22 contain 200 μM, 100 μM, 50 μM, 20 μM, 10 μM, 5 μM, 2 μM, 1 μM, 500 nM, 200 nM, 100 nM, 50 nM, 20 nM, 10 nM, 5 nM, 2 nM, 1 nM, 500 pM, and 200 pM 2-ImN respectively.

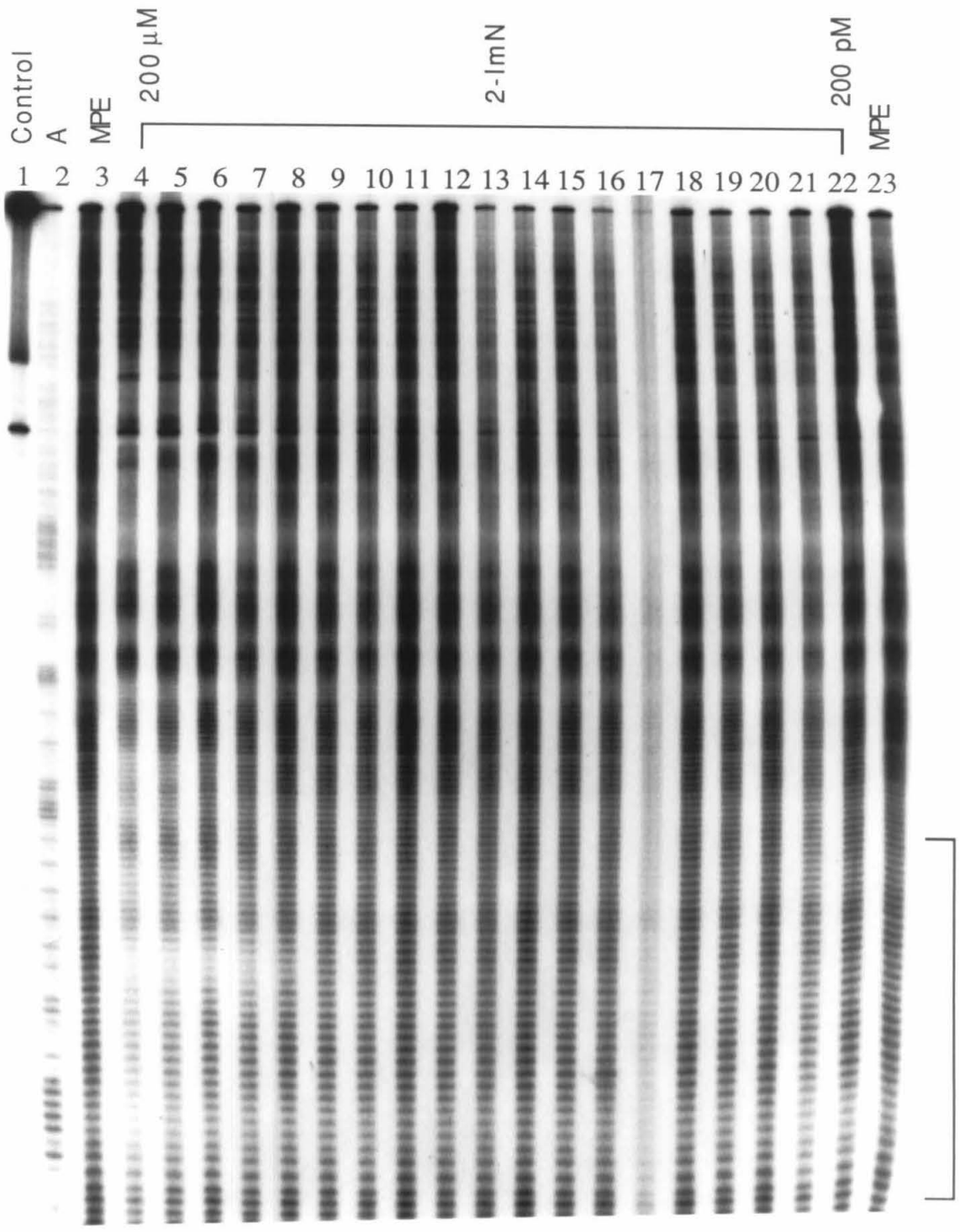
Control
A
MPE
200 µM
2-ImN
200 pM
MPE
1 2 3 4 5 6 7 8 9 10 11 12 13 14 15 16 17 18 19 20 21 22 23

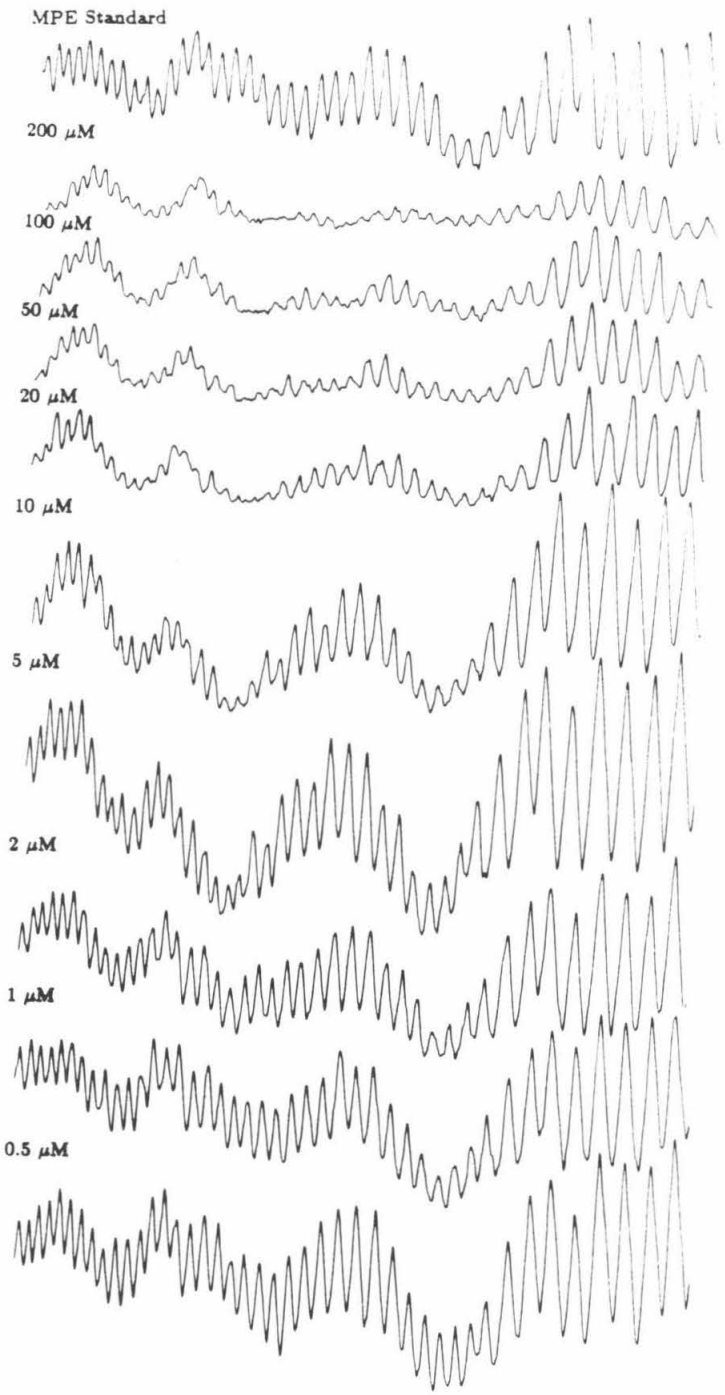

Figure 5 One dimensional densitometry scans of the gel lanes in figure 2. Peaks to the right are at the bottom of the gel, basepairs 4229 to 4342 of pBR322.

bound at the lowest concentrations, with detectable protection at 2 μM. At higher concentrations, the AATAA site is protected, while the TTAAT site is bound only at 50 μM and above.

Analysis

Two dimensional densitometer scanning is currently unavailable. However, the LKB laser densitometer used has the capability of scanning the width of an entire band and averaging to give a one-dimensional result. As shown in panel B of figure 1, this is equivalent to the two dimensional procedure. Due to the averaging function, the optical density values will be an order of magnitude smaller and thus more susceptible to measurement errors. The scanned lanes are fed directly from the densitometer to the LKB analysis program GSXL. The baseline for each cleavage lane is determined by generation of an average baseline from 1 mm background scans on either side of the lanes in question. The program outputs a list of peaks with the area under each peak (in AU x mm) corresponding to the optical density. Site densities are calculated by summing the appropriate bands on a Microsoft Excel worksheet, and Y_{app} values calculated on the same worksheet using the previously discussed equation.

Taking the CGC site of the 517 fragment as the reference, the apparent fraction bound (Y_{app}) can be calculated at each position of the sequence. The Y_{app} values averaged over three gels are plotted in figures 6, 7, and 8. The protection patterns are in general agreement with the patterns observed with calf thymus carrier DNA

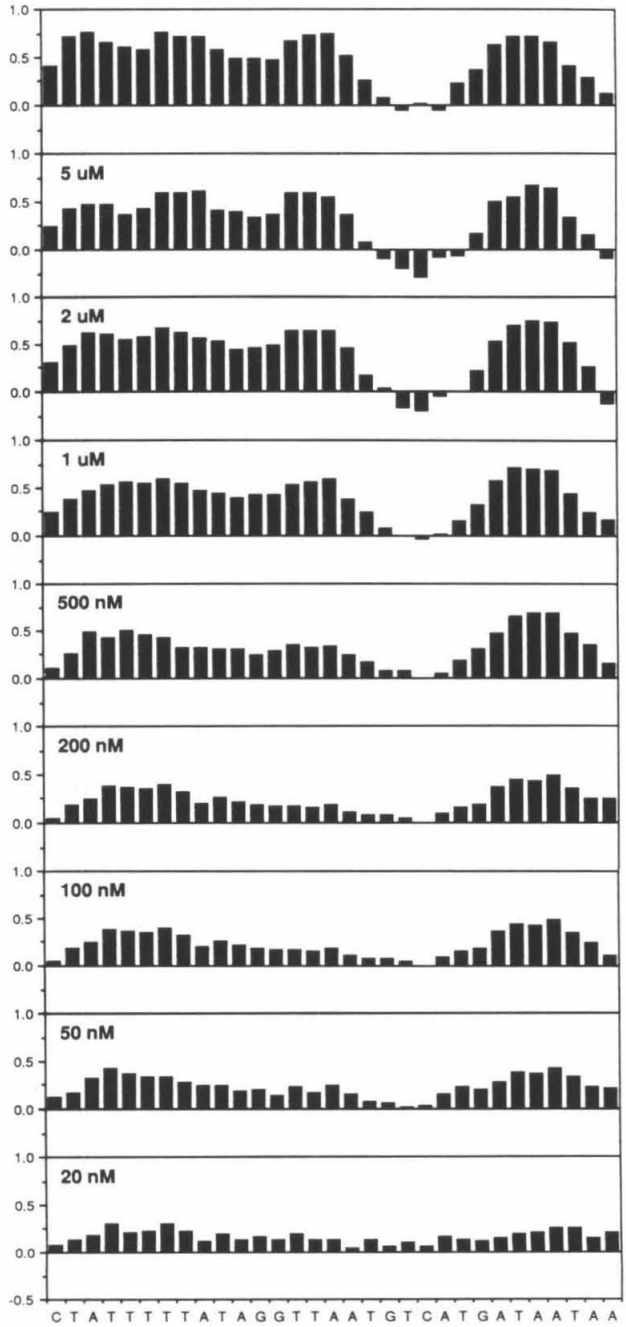

Figure 6 Quantitative MPE·Fe(II) footprints of D on bp 4332 to 4302 of pBR322. The apparent fraction bound (Y_{app}) for each cleavage band is averaged over three experiments, and plotted as a function of sequence. The CGC sequence adjacent to the 5′ end of the plotted sequence is used as the internal standard.

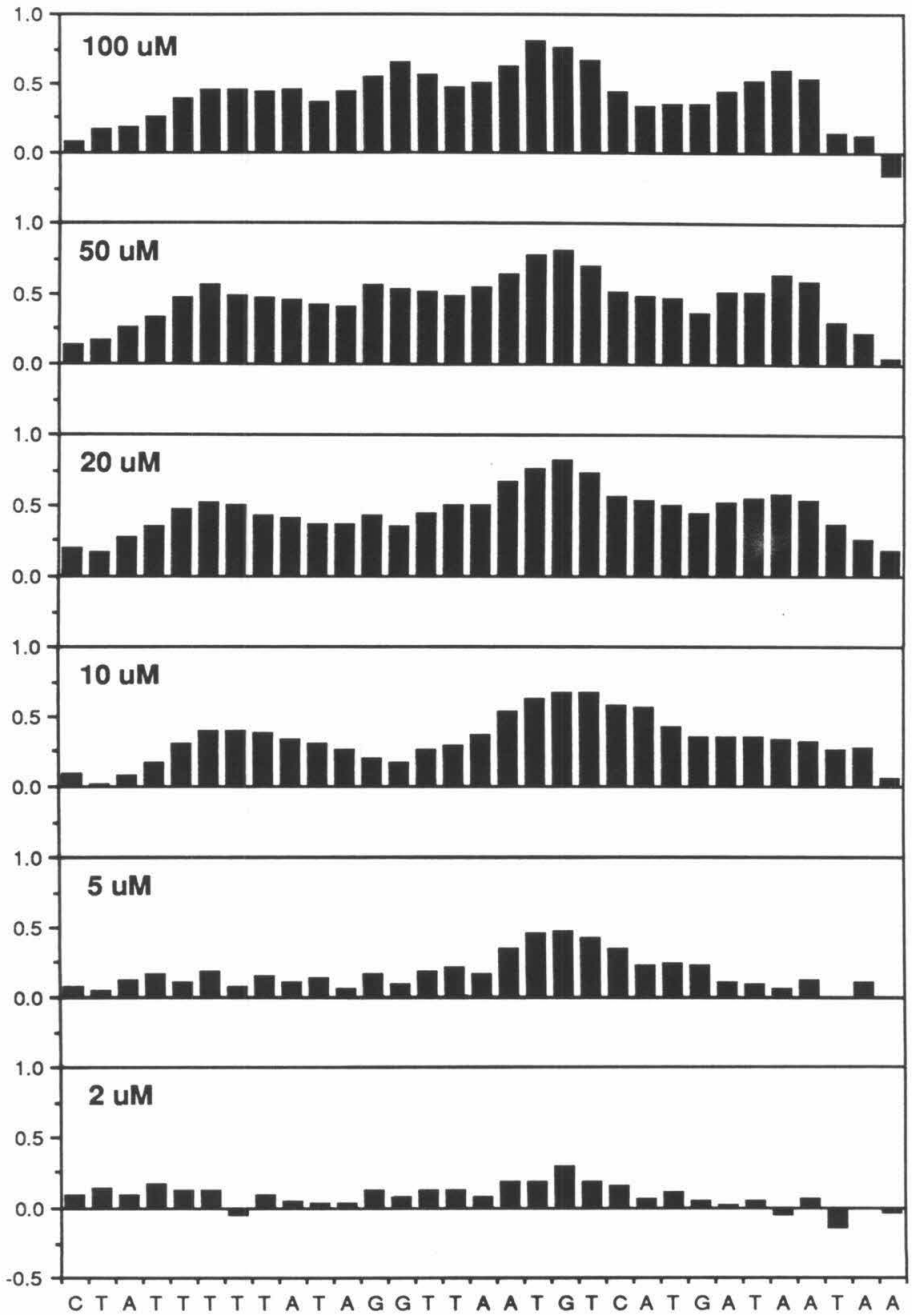

Figure 7 Quantitative MPE·Fe(II) footprints of 2-PyN on bp 4332 to 4302 of pBR322. The apparent fraction bound (Y_{app}) for each cleavage band is averaged over three experiments, and plotted as a function of sequence. The CGC sequence adjacent to the 5′ end of the plotted sequence is used as the internal standard.

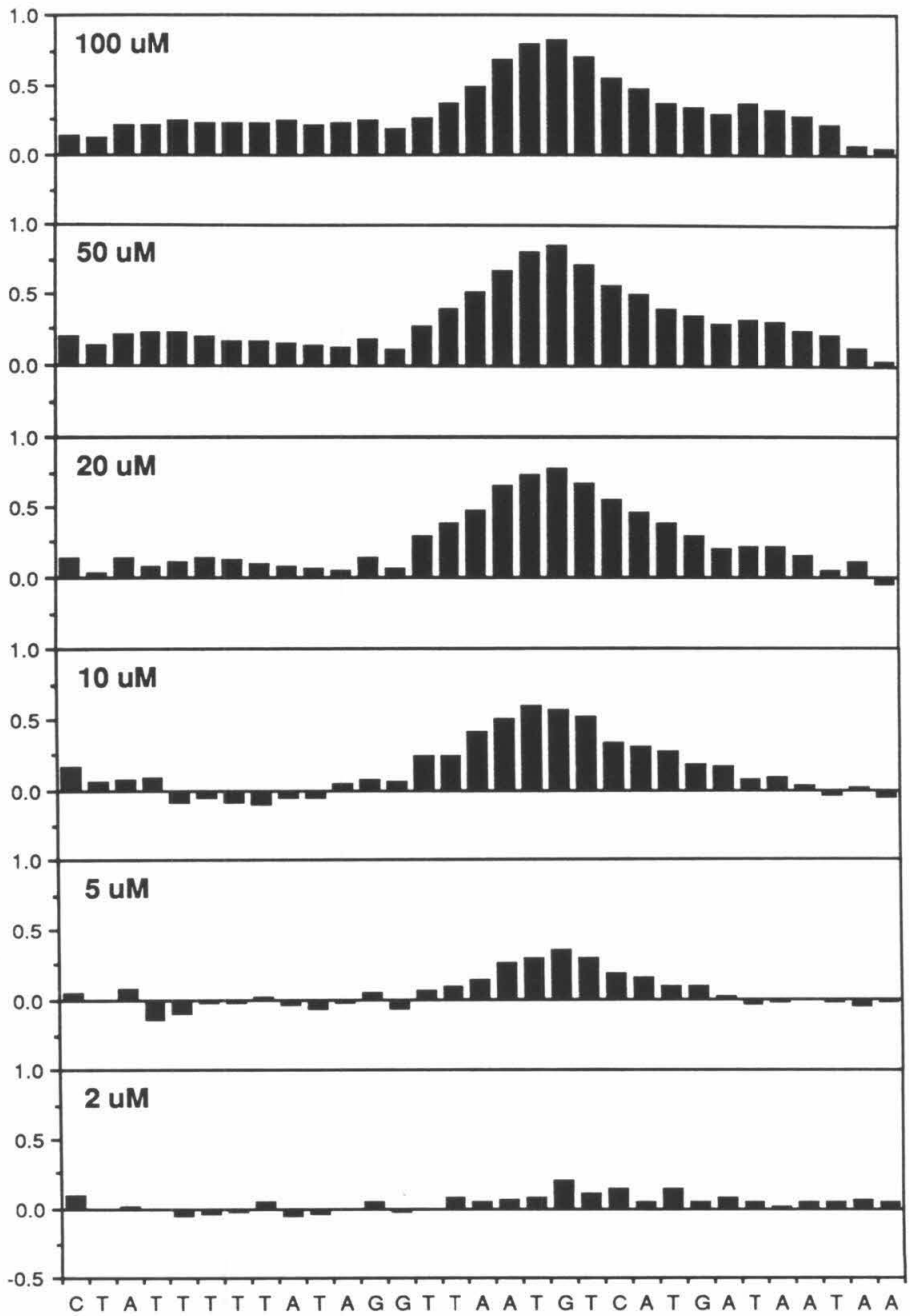

Figure 8 Quantitative MPE·Fe(II) footprints of 2-ImN on bp 4332 to 4302 of pBR322. The apparent fraction bound (Y_{app}) for each cleavage band is averaged over three experiments, and plotted as a function of sequence. The CGC sequence adjacent to the 5′ end of the plotted sequence is used as the internal standard.

(see chapter 2). Again, D and 2-ImN give complementary protection, while 2-PyN appears to be a linear combination of the two other patterns.

At intermediate binding densities, D protects the same TTTTT, TTAAT, and AATAA sites that are observed in previous work.[45, 76] There is no significant protection of the mixed G,C, A,T sequences. Above 2 μM, the protection pattern of D changes, with two defined footprints in the TTTTT region. This is consistent with end to end binding of two D molecules in the 10 bp A,T region. The negative values for D protection at these densities are probably due to cleavage protection at the reference site. There are weak D binding sites directly adjacent to both sides of the CGCC sequence (5′ site not shown). However, it is not possible to rule out cleavage enhancement at this sequence.

As already observed, 2-ImN shows a strong preference for the TGTCA site, although there is clearly some protection of the AATAA and TTTTT sites at high concentrations. Assuming that the maximum protection value at these sites is similar to that of D places an upper limit of 5 x 10^4 M^{-1} for the association constant at the TTTTT site and 2 x 10^4 M^{-1} at the AATAA site. No significant negative values are observed. This could be due to the lack of strong footprints near the reference block. The specificity of 2-PyN is so low that all positions are protected at intermediate binding densities. Although some decrease in Y_{app} is presumably occurring, it is not possible to determine the extent.

The higher specificity of D and 2-ImN allows an estimation of the maximum distance for MPE·Fe(II) cleavage inhibition. For both compounds, the cleavage

pattern > 3 bases away from the end of a binding site is essentially normal. In general the protection patterns are in close agreement to those determined by the published model,[77] although protection at the most distant bp is not usually observed. The similarity in pattern sizes between D and 2-ImN again suggests that both compounds are binding to a DNA conformation in the B family.

To determine association constants at individual sites, the optical density areas of the bands that show maximum protection in figures 6, 7, and 8 are added. The Y_{app} values are then calculated for each concentration by the previous equation. The affinity constants of each compound are measured on at least three independent gels. Different samples of the small molecule are used on each gel, with at least two different labelings in each set of three experiments, and at least two different MPE·Fe(II) samples in each set. For 2-PyN and 2-ImN, calculation of Y_{app} uses the density at the CCG sequence as a reference. For D, the TCA sequence that shows the minimum protection in figure 6 is chosen.

Fitting Procedure

Quantitative MPE·Fe(II) footprinting experiments do show increased scattering of data points, with an occasional point well separated from the points on either side. All data points are included in the fitting procedure unless they meet one of the following conditions.

1. Visual inspection of the film revealed a flaw at either the site or the standard block.
2. The peak heights of the reference block are less than 0.2 AU above background.

3. Y values of a given lane were greater than two standard deviations away from average of several points on both sides.

Most gels contain at least one data point rejected by the first condition and one point rejected by the second. The median for all gels discussed is 16 points. A gel is rejected if the number of valid points is lower than 14 or if more than one of the eight highest concentration points is unusable. About two thirds of the gels run produce acceptable data. Because of the altered protection pattern at high concentrations of D, lanes with D concentrations above 5 μM are not used. This lowers the total number of data points to just above the 14 point limit.

Site values are then fitted to a single site binding curve using non-linear least squares techniques. Generation of the analytical function for Y used in the fitting procedure is straightforward.[99] If Y_L is the apparent fraction bound at $Y = 0$ and Y_H is the apparent fraction bound at saturation, then Y, the true fraction of DNA bound, is related to Y_{app} by the following equation.

$$Y = \frac{Y_{app} - Y_L}{Y_H - Y_L}$$

From the previous equations and using $[L]_{free} = [L]_{total} = [L]$,

$$Y = \frac{K_a[L]}{1 + K_a[L]}$$

Substitution and rearrangement gives a function for Y in terms of [L].

$$Y_{fit} = (Y_H - Y_L)\left(\frac{K_a[L]}{1 + K_a[L]}\right) + Y_L$$

The difference between Y_{fit} and Y_{app} for all ([L], Y_{app}) data points is minimized using a standard algorithm implemented by Bevington in his book *Data Reduction and Error Analysis for the Physical Sciences.*[107] The data points are fitted by a gradient fit combined with a linear expansion of the function Y_{fit} as described by Marquardt[108] with K_a, Y_H, and Y_L as adjustable parameters.

The goodness of fit of the binding curve to the data points is evaluated by the χ^2 criterion. Fits are judged acceptable if the χ^2 at a site other than the TTTTT site is 1.5 or less. Fits generally converge in less than five cycles. An examination of parameter space near the best fit results using the Excel worksheet Ka_map confirms that a true minimum is reached. Binding isotherms determined for the gel in figure 2 at the sites studied are shown in figure 9. The equivalent 2-PyN and 2-ImN isotherms are shown in figures 10 and 11 respectively.

The TGTCA site consistently gives much worse fits than the other sites on the 2-PyN gels. Similarly poor fits are consistently found for 2-ImN at the same site. Visual inspection of the binding curves reveals that in all cases, the increase in Y_{app} is steeper than expected from the fitted curve. Such a situation is normally indicative of cooperativity or the presence of more than one ligand at the binding site.[109] Therefore the previous data has been fitted to a series of cooperative curves using the function shown below,

$$Y_{fit} = (Y_H - Y_L)\left(\frac{K_a^n[L]^n}{1 + K_a^n[L]^n}\right) + Y_L$$

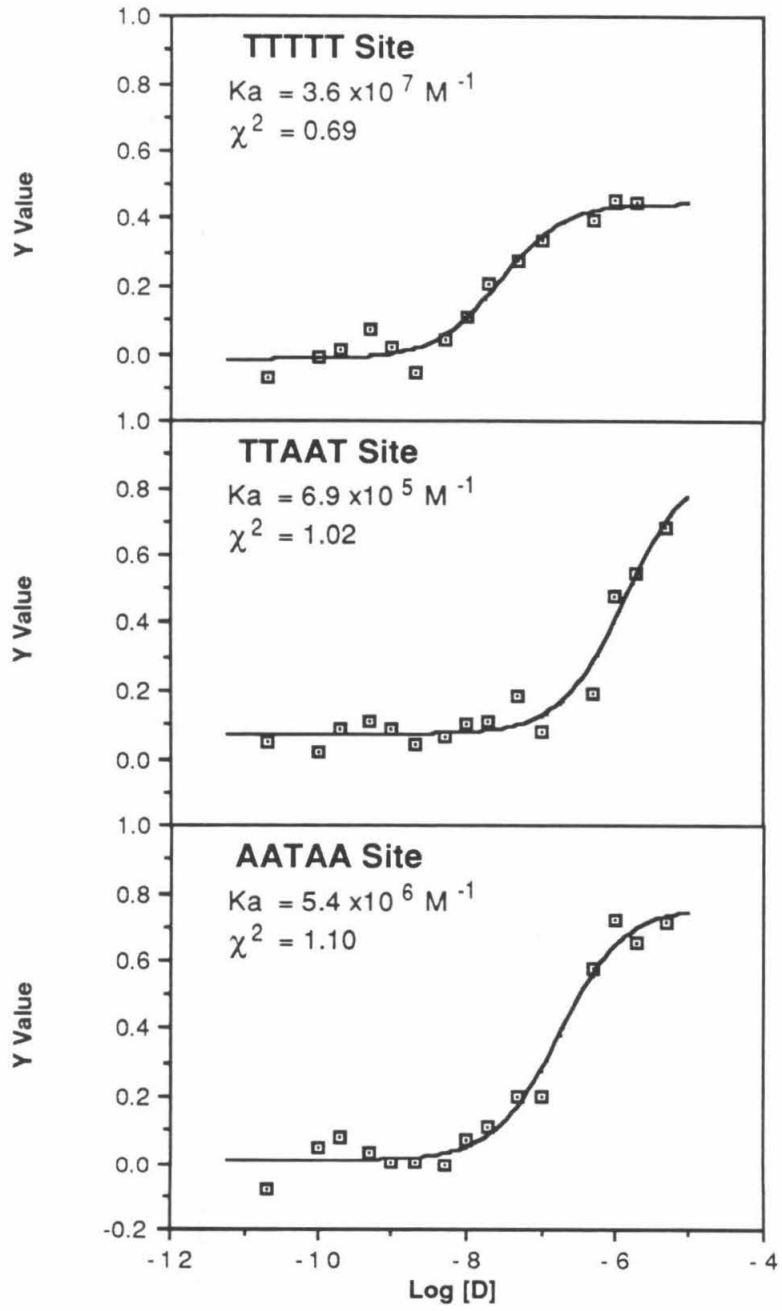

Figure 9 Best fit D binding isotherms from the gel in figure 2.

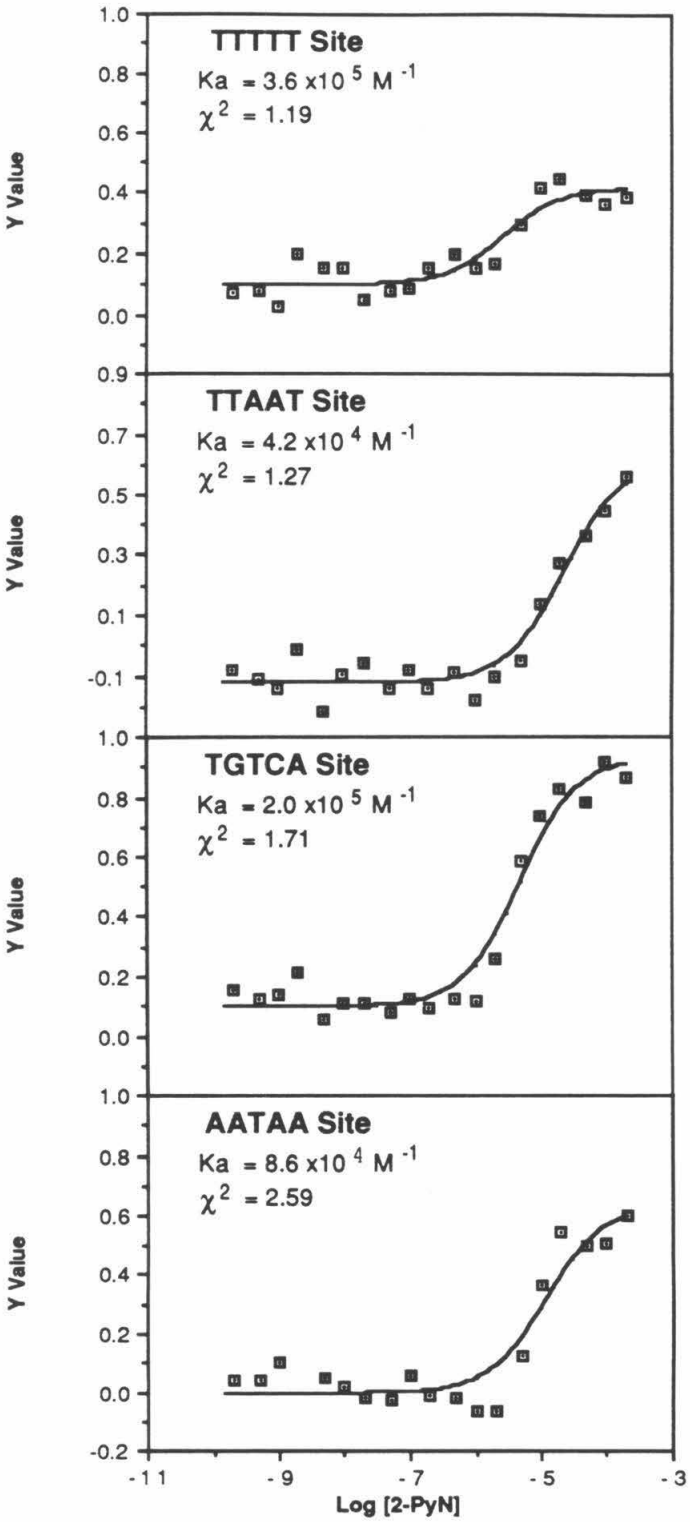

Figure 10 Best fit 2-PyN binding isotherms from figure 3.

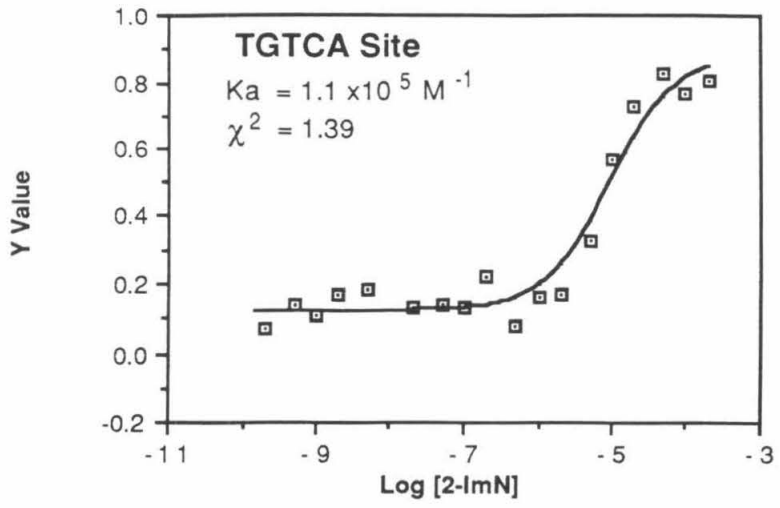

Figure 11 Best fit isotherm of 2-ImN at the TGTCA Site in figure 4.

where n is the Hill cooperativity coefficient. Over the range $1 \leq n \leq 3$, the χ^2 values are lowest for an exponent near 2. However, the general flatness of the χ^2 function and the degree of scatter in the binding curves allows for considerable leeway in the exponent. The fit is clearly worse for $n = 1$ and $n = 3$, but there is only a small difference in χ^2 over the $1.5 \leq n \leq 2.5$ range.

As a check of the quality of the fits, the residual $(Y_{app} - Y_{fit})$ averaged over the three experiments is shown in figures 12, 13, and 14. For both 2-PyN and 2-ImN at the TGTCA site, the best fit curve with $n = 1$ shows significant deviations from random scatter, while the $n = 2$ case shows no significant deviations and smaller residuals. At low but non-zero binding densities, the fitted values are consistently larger than the observed data points. Near the saturation point, the fitted values are consistently smaller than observed. The opposite is true for D at

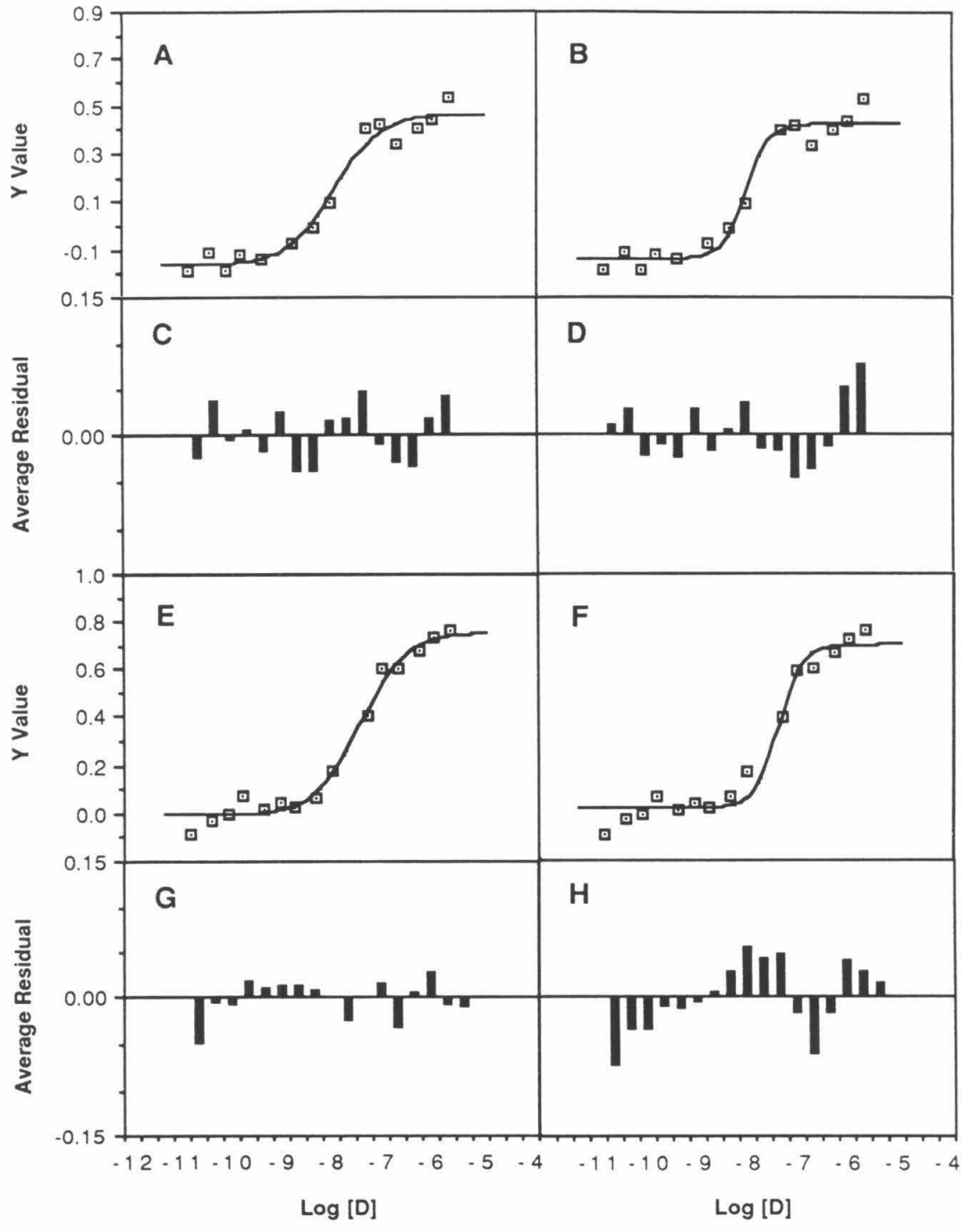

Figure 12 Comparison of single site and cooperative fitting functions for D binding. A) Noncooperative fitting to the TTTTT site data. B) Cooperative fitting to the same data. C) Noncooperative residuals ($Y_{app} - Y_{fit}$) averaged over four experiments. D) Cooperative curve residuals averaged over four experiments. E–H) The same data for the AATAA site.

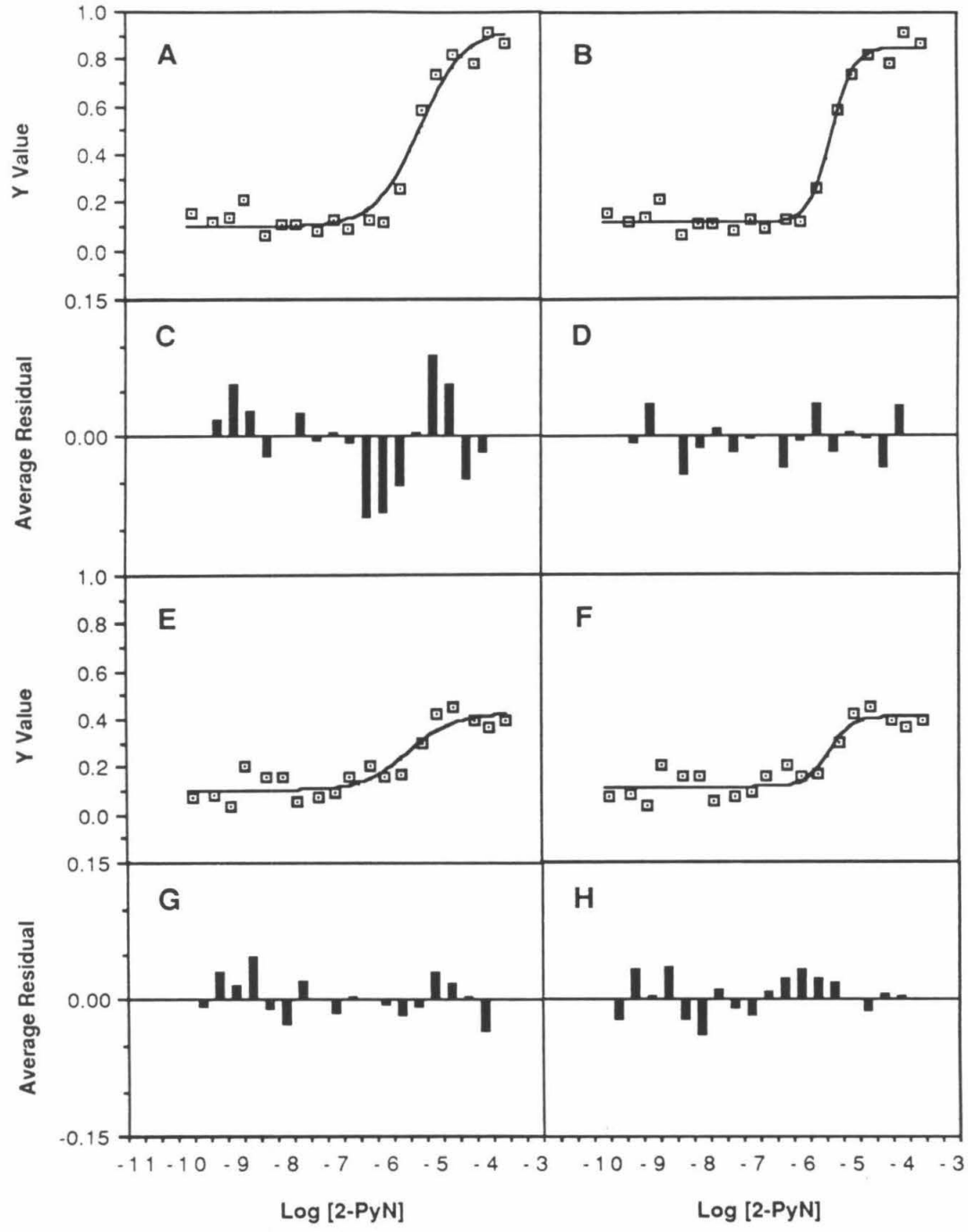

Figure 13 Comparison of single site and cooperative fitting functions for 2-PyN binding. A) Noncooperative fitting to the TGTCA site data. B) Cooperative fitting to the same data. C) Noncooperative residuals ($Y_{app} - Y_{fit}$) averaged over three experiments. D) Cooperative curve residuals averaged over three experiments. E–H) The same data for the TTTTT site.

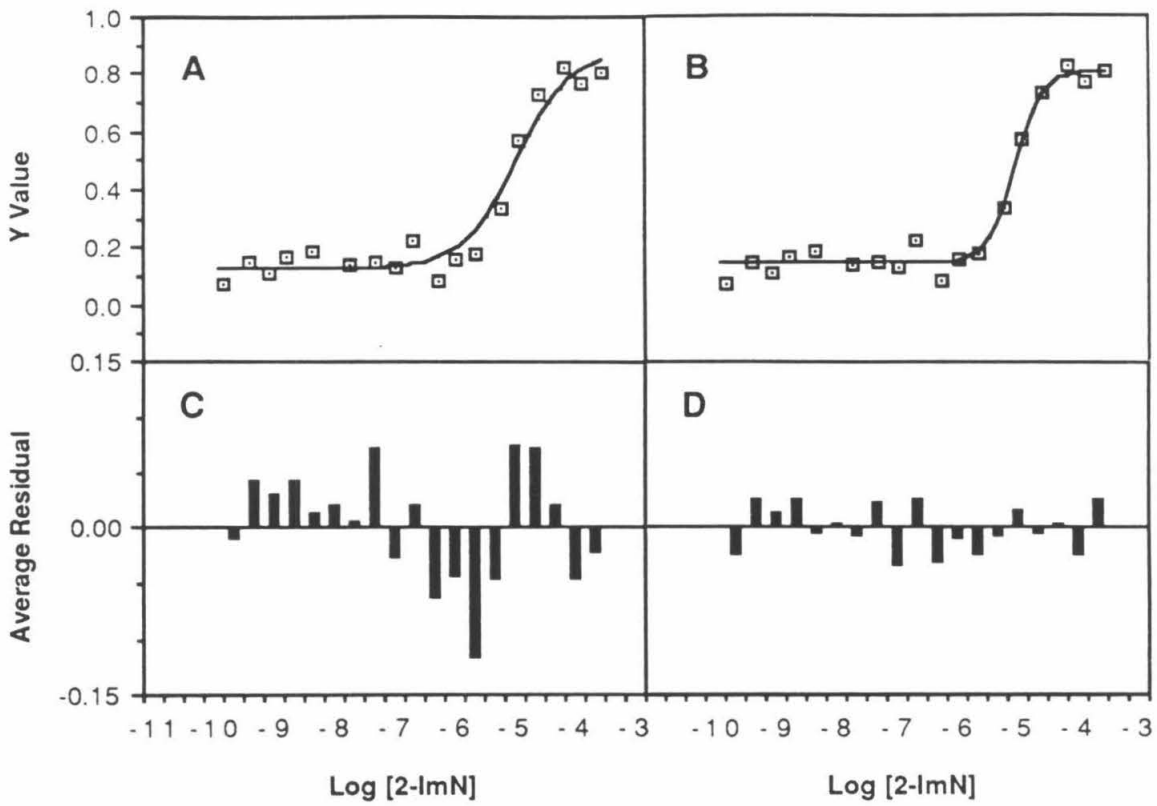

Figure 14 Comparison of single site and cooperative fitting functions for 2-ImN binding. A) Noncooperative fitting to the TGTCA site data. B) Cooperative fitting to the same data. C) Noncooperative residuals ($Y_{app} - Y_{fit}$) averaged over three experiments. D) Cooperative curve residuals averaged over three experiments.

the TTTTT and AATAA sites. Consistently better fits are observed for n = 1. The residuals plotted in figure 12, while barely significant, also appear to show nonrandom behavior in the n = 2 case. The binding constant of the TTAAT site is too low to satisfactorily determine the curve shape. Both curves fit the 2-PyN data equally well at the A,T sites, which is also observed for D when the CGC sequence is used as the reference. This is the expected result if significant protection of the CGC site occurs at high binding densities, since the top of curve will tend to

Table 1 Apparent First Order Affinity Constants[a]

Compound	TTTTT	TTAAT	TGTCA	AATAA
D	5.1×10^7 (1.8)	1.7×10^6 (.83)	$<1 \times 10^5$	1.6×10^7(.91)
2-PyN	2.3×10^5 (1.2)	5.7×10^4 (1.6)	2.2×10^5 (0.3)	8.3×10^4(0.4)
2-ImN	$<5 \times 10^4$	$<1 \times 10^4$	1.4×10^5 (0.3)	$<2 \times 10^4$

[a] Average of three separate experiments (standard deviation).

flatten without altering the bottom. The lack of clear cut results for the pyridine compound leaves open the possibility that all weak binding compounds would fit a monomer binding curve poorly.

Affinity Constants

The apparent first order association constants are shown in table 1. The binding curves for all gels used are shown in appendix B. Standard deviations are large for D at all sites and 2-PyN at the TTTTT and TTAAT sites. For D, the observed lack of precision is caused by a single gel with best fit affinity constants consistently half the average value of the other three gels. While this is suggestive of a dilution error, there is insufficient evidence to remove the gel from consideration. The low precision measurement of 2-PyN binding at the TTTTT site is probably the result of the reduced cleavage at this site which leads to a smaller range in Y_{app} and increased contribution by random errors. The 2-PyN TTAAT site measurement suffers from the presence of the adjacent TGTCA site, which presumably contributes to the observed protection value. This does not significantly affect the

TGTCA site measurement, for protection has almost reached the Y_H value before significant TTAAT protection is observed.

The binding constant of D to TTAAT site is within the range of values (3.0 x 10^5–1.1 x 10^6) reported for distamycin A binding to low affinity sites on calf thymus DNA.[110, 111] The binding constant of D to the TTTTT site is also quite similar to the values measured for distamycin A and poly(dA)·poly(dT), 5.5 x 10^7 and 4.3 x 10^7, at similar salt concentrations.[26, 79, 103] An equilibrium dialysis measurement of D itself binding to a fifteen bp oligonucleotide containing a TTTAT site (8.8 x 10^5) is also close to the TTAAT value.[112] Thus binding constants measured by quantitative MPE·Fe(II) footprinting are in the range of values measured by other techniques, suggesting that this method produces valid isotherms.[100]

Error Analysis

The precision in the experiments is reasonably good, indicating that sources of random error are relatively well controlled. To estimate the accuracy of the derived affinity constants, it is necessary to consider potential sources of systematic error present in the experiment. Due to experimental difficulties in the pyrrole compound purification[113] and complete water removal,[16] measured molar extinction coefficients are generally too small by as a much as 10%. This will tend to underestimate the binding constant, because the concentration of ligand will be smaller than expected:

$$A_{obs} = \epsilon_{obs}[L]_{obs}$$

$$A_{obs} = \epsilon_{real}[L]_{real}$$

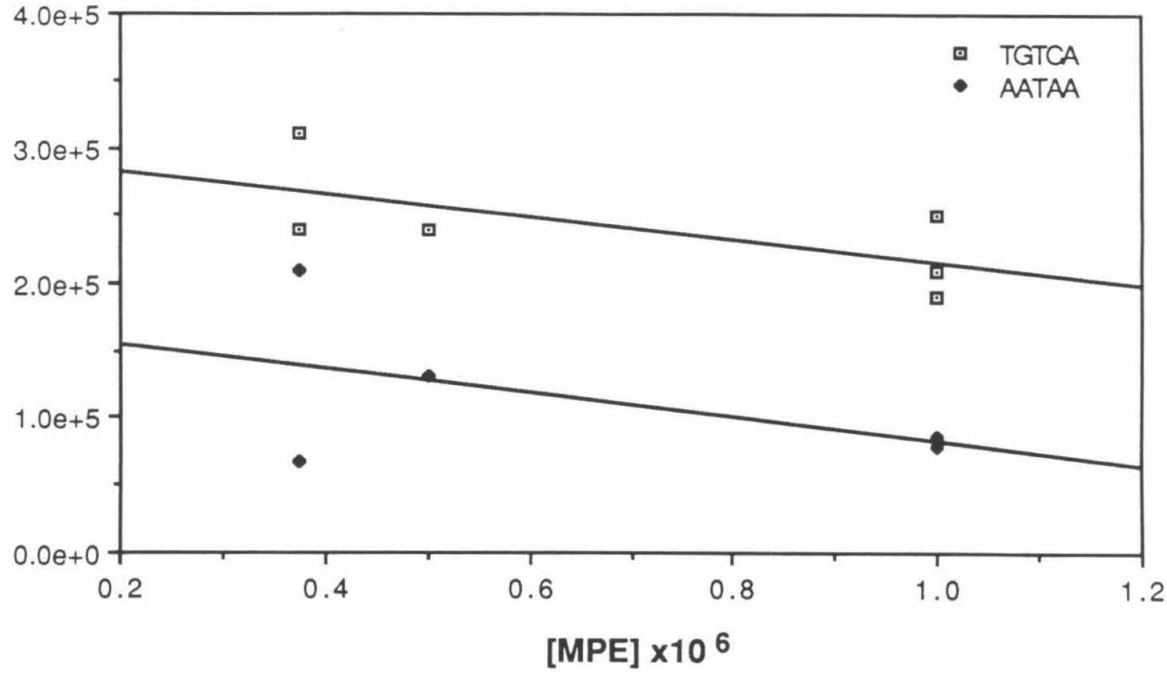

Figure 15 Change of the 2-PyN apparent first order affinity constant with MPE·Fe(II) concentration.

If $\epsilon_{obs} < \epsilon_{real}$, then $[L]_{obs} > [L]_{real}$, and since $K_a \propto 1/[L]$, $K_{a(obs)} < K_{a(real)}$.

A second possible source of error is the potential for direct interactions between MPE·Fe(II) and the bound small molecules. Ackers *et al.* showed the absence of direct interactions with DNase I by demonstrating that the measured association constants are independent of DNase I concentration. The equivalent case for MPE·Fe(II) is shown in figure 15. Low concentration MPE·Fe(II) footprinting gels are considerably more difficult to perform. The binding constant of MPE·Fe(II) is approximately 10^5, leading to a sharp drop in total cleavage at concentrations below 1 μM.[102] Shown in figure 15 are all points with $\chi^2 < 3$. There appears to be

a slight negative interaction between MPE·Fe(II) and 2-PyN. Linear extrapolation to zero MPE·Fe(II) concentration suggests that the high concentration values are underestimated by about 20%.

The third source of error stems directly from the fitting procedure. Because the number of points at the high concentration end of the binding curve is limited, the fitting program can increase the Y_H parameter to fit lower concentration points better with only a small penalty. This will also tend to underestimate the true value of the association constant. Typically, Y_{app} varies between 0 and 0.8. Taking $Y_{H(real)} = 0.8$ and setting Y_H to its maximum value 1, substituting into the previous equations gives $K_{a(fit)} \geq 2/3K_{a(real)}$, equivalent to a maximum error of 30%. The actual error is almost certainly smaller, since Y_H is usually 0.9 or less.

The fourth source of error rests in the assumptions defining the experiment. The theoretical treatment depends on the total number of backbone cleavage events not being significantly altered at saturation binding; the total amount of cleavage must be nearly constant. This is clearly not true in figures 2–4, presumably because most of the fragment is bound at high concentration. When MPE·Fe(II) cleaves a well protected fragment, it normally cleaves unprotected regions more frequently.[16] This will lead to reference blocks that are darker than expected, which will increase the measured protection value and result in reduced binding constants. The magnitude of this effect is difficult to estimate. The total effect is probably small however, because 2-ImN has both the fewest sites on the 517 fragment and the lowest measured binding constant at all sites.

Table 2 Relative Binding Affinities[a]

Compound	Site	TTTTT:Site	TTAAT:Site	TGTCA:Site
D	TTTTT	–	–	–
	TTAAT	30:1	–	–
	TGTCA	> 500:1	> 15:1	–
	AATAA	3:1	1:9	< 1:150
2-PyN	TTTTT	–	–	–
	TTAAT	4:1	–	–
	TGTCA	1:1	1:4	–
	AATAA	3:1	1:1	3:1
2-ImN	TTTTT	–	–	–
	TTAAT	*b*	–	–
	TGTCA	< 1:3	< 1:15	–
	AATAA	*b*	*b*	> 7:1

[a] Ratios of the binding constants displayed in table 1. [b] Binding constants not well determined.

All these sources of nonrandom error tend to decrease the observed binding constant, therefore the values shown in table 1 represent lower bounds on the actual values. Taking all mentioned sources of error into account, a reasonable estimate is that the true association constant is within a factor of three of the observed one. Consequently, the following discussion will refer to the binding constants in order of magnitude terms, which are expected to be significant.

Discussion

The individual specificities of each compound are shown in table 2. They match the qualitative picture determined from the assays in chapter 2 remarkably

well. Most importantly, removal of the N-terminal amide and replacement of a single aromatic CH by N results in a change in relative specificity of over three orders of magnitude. As observed on high resolution gels with calf thymus DNA as carrier, 2-PyN has equal affinities to the TGTCA and TTTTT sites. 2-PyN and 2-ImN also have nearly equal affinities to the TGTCA site. The selective disfavoring of A,T sites by 2-PyN compared to D and 2-ImN compared to 2-PyN is also reproduced. However, the magnitude of these effects is much larger than in the calf thymus case. 2-PyN binds two orders of magnitude less strongly than D at A,T sites, compared to a factor of < 25 on previous gels. Likewise, 2-ImN binds A,T sites at least an order of magnitude less strongly than 2-PyN, as compared to a factor of < 5 on previous gels.

Calculations using a three site model for calf thymus binding reveal that this observation is caused by the fact that the free ligand concentration is not proportional to the added ligand concentration over the measured concentration range.[114] While it is obvious that a substantial portion of the added ligand will be bound to carrier, it is not as obvious that the presence of micromolar concentrations of carrier sites will tend to compress the apparent binding constants towards lower values. The magnitude of these effects is illustrated in table 3. Depending on the exact distribution of sites, ratios between site affinities determined from the added ligand concentration can be inaccurate by more than an order of magnitude in a normal footprinting experiment. The sequence of calf thymus DNA is not known,

Table 3 Effect of significant binding to carrier DNA on relative site affinities.

Case	[Site] (μM)	True K_a[a]	Apparent K_a[b]	True K_{rel}[c]	Apparent K_{rel}[d]
1	10	1.0×10^5	4.9×10^4	1	1
	5	1.0×10^6	1.9×10^5	10	4
	1	1.0×10^7	8.7×10^6	100	18
2	0.1	1.0×10^5	9.8×10^4	1	1
	0.1	1.0×10^6	8.7×10^5	10	9
	0.1	1.0×10^7	6.3×10^6	100	64
3	1	1.0×10^5	8.7×10^4	1	1
	1	1.0×10^6	4.0×10^5	10	5
	1	1.0×10^7	1.4×10^6	100	18
4	10	1.0×10^5	3.0×10^4	1	1
	10	1.0×10^6	6.2×10^5	10	2
	10	1.0×10^7	1.6×10^5	100	6
5	1	1.0×10^5	4.1×10^4	1	1
	5	1.0×10^6	7.8×10^4	10	2
	10	1.0×10^7	1.8×10^5	100	5
6	10	1.0×10^3	9.9×10^2	1	1
	5	1.0×10^4	9.6×10^3	10	10
	1	1.0×10^5	9.1×10^4	100	91
7	1	1.0×10^3	1.0×10^3	1	1
	1	1.0×10^4	9.9×10^3	10	10
	1	1.0×10^5	9.4×10^4	100	95
8	10	1.0×10^3	9.8×10^3	1	1
	10	1.0×10^4	8.7×10^3	10	9
	10	1.0×10^5	6.3×10^4	100	64
9	0.1	1.0×10^7	2.9×10^6	1	1
	0.1	1.0×10^8	6.3×10^6	10	2
	0.1	1.0×10^9	1.6×10^7	100	6

[a] $1/[L]_{free}$ at half protection. [b] $1/[L]_{total}$ at half protection, the number measured on a typical footprinting gel. [c] Ratio of the true K_a at a site to the true K_a at the weakest site. [d] Ratio of the apparent K_a at a site to the apparent K_a at the weakest site.

and 25% of the genome is significantly non-random,[115] so that no quantitative model is currently available. Thus a footprinting or affinity cleaving experiment in the presence of carrier can give only the relative ordering of binding sites. Given the low specificities and potentially high site concentrations of these small molecules, an observed change in affinity of a factor of two on a gel could correspond to an order of magnitude change in binding constant.

The 2-PyN and 2-ImN results, while not conclusive, are at least suggestive that TGTCA site binding is not a simple 1:1 complex. The fact that this effect is observed at a single site severely limits the possible explanations. Cooperativity based on the binding to adjacent sites is clearly excluded by the 2-ImN case. Similarly, the observation of the same behavior over a range of MPE·Fe(II) concentrations would tend to rule out the intercalator as a cause. This leaves two possible explanations. The results could be an artifact of the footprinting procedure, or 2-PyN and 2-ImN could bind as a dimer to the TGTCA site. It is certainly true that these experiments are performed at much higher compound:DNA ratios than usual.[9] If 2-ImN is binding as a dimer, the observed footprint is not large enough to fit two molecules end to end. This either puts one molecule in the minor groove and one in the major, or both in the minor groove. A head to tail dimer in the minor groove is most consistent with data of the previous section. It also neatly explains the always symmetrical cleavage pattern and the interchangeability of the A,T bp in the consensus binding sequence. To eliminate the possibility of an artifact, it

will be necessary to examine this system by an independent method like NMR, or possibly a gel mobility shift experiment modified for fast exchange conditions.[116] Both of these experiments have the advantage that detection of ternary complexes is independent of the fitting method used to determine the binding constants.

A decrease in the binding affinity of 10 reflects a difference in binding free energy of about 1.4 kcal/mol at 37°C. This is consistent with the lower affinity of 2-ImN to A,T sites being produced by the loss of a single hydrogen bond to solvent. The source of the lower affinity of 2-PyN to A,T sequences is more difficult to explain. Certainly the loss of one amide hydrogen bond from D to 2-PyN is responsible for some of the decrease in binding at A,T rich sites, but it is unlikely to account for all 3 kcal/mol as seen from the results with 3-PyN and 4-PyN in chapter 2. The apparent free energy of interaction at the TGTCA site is about -7 kcal/mol. This is below normal for DNA-binding small molecules, and well below that of similar minor groove binding compounds.[9] It is tempting to attribute this loss to structural rearrangement, but other explanations cannot be ruled out at this time. Clearly, more data on the precise structure of the 2-ImN/TGTCA complex is needed before this complex situation will be understood.

Summary

A footprinting method for measuring individual protein-DNA affinity constants is extended to small molecules. The method uses MPE·Fe(II) to report the fraction of DNA bound over a large range in free ligand concentration. The experimental data are then fitted to individual site isotherms using a non-linear least

squares procedure. At the TGTCA site, the data for 2-PyN and 2-ImN fit best to a cooperative binding curve. This may indicate that the compounds bind as a dimer. At 100 mM salt, the affinity of the distamycin A analog D to its strongest site is 10^7 M^{-1}. The apparent affinity of 2-PyN and 2-ImN to the TGTCA site is 10^5 M^{-1}. The affinity of 2-PyN for the distamycin A sites is of similar magnitude. Binding constants of 2-ImN at distamycin A sites are 5×10^4 or less. Removal of one amide and substitution of the N-terminal pyrrole ring of D by imidazole has changed the relative specificity by a factor of 1000.

Chapter 4

The Scope of WGWCW Sequence Specificity

While the preceding chapters provide a detailed analysis of the DNA specificity of 2-ImN and a reasonable model for WGWCW sequence selection, there is no clear candidate for a molecular complex. To learn more about the details and the scope of this complexation, a series of 2-PyN and 2-ImN derivatives have been synthesized, and are shown in figure 1.

Substituted Pyridine Derivatives

4-Chloropyridine-2-carboxamide-netropsin (4-ClPyN) and 4-dimethylamino-pyridine-2-carboxamide-netropsin (4-Me_2NPyN) are designed to test the role of hydrogen bonding in the complex by changing the electron density at the ring nitrogen. 3-Methoxypyridine-2-carboxamide-netropsin (3-MeOPyN) and imidazo[1,2-a]pyrazinecarboxamide-netropsin (CycN) are designed to assess the role of the carbonyl oxygen in the complex. CycN requires the carbonyl and ring nitrogen to be *cis*. 3-MeOPyN should prefer *cis* because of the weak hydrogen bond between the methoxy O and the amide NH in this conformation. 3-MeOPyN and pyrimidine-2-carboxamide-netropsin (2-PmN) are also designed to test the proposed model for selection against A,T sites. Both modify the putative N-out conformation of 2-PyN. 3-MeOPyN blocks a tight complex with the methoxy group. 2-PmN replaces the CH at the bottom of the groove with N.

Synthesis

Synthesis of these compounds follows the procedures described earlier. The final compounds are prepared from the common intermediates **1** and **2** described in

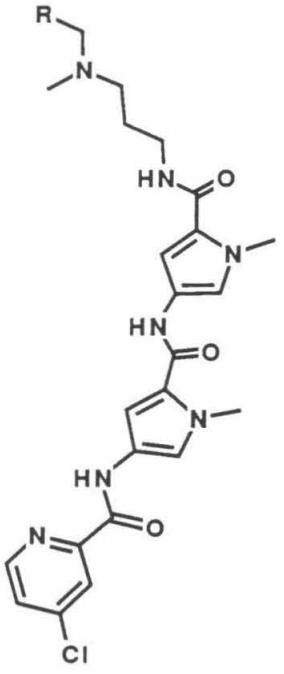

4-ClPyN, 4-ClPyNE

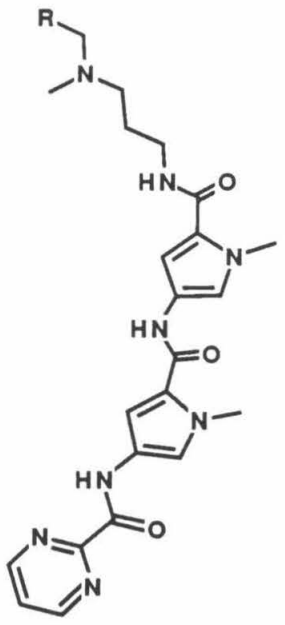

2-PmN, 2-PmNE

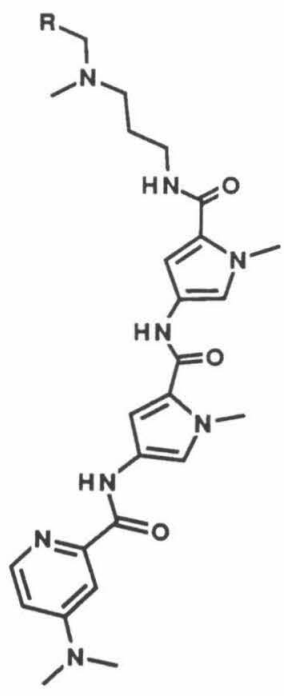

4-Me_2PyN, 4-Me_2PyNE

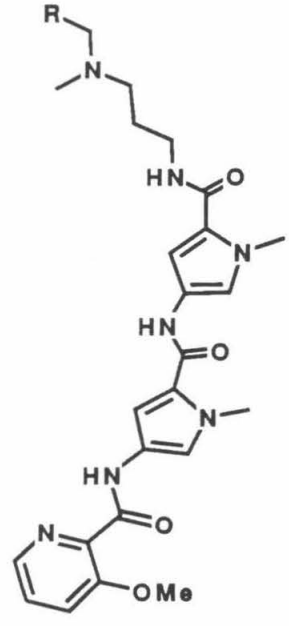

3-MeOPyN, 3-MeOPyNE

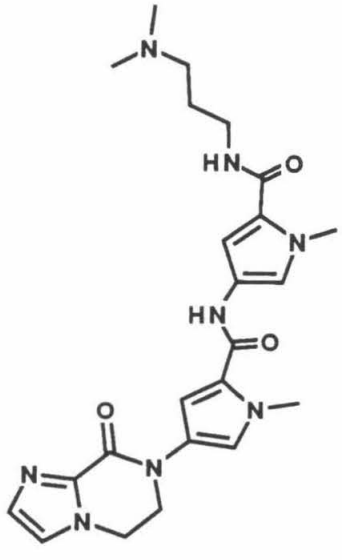

CycN

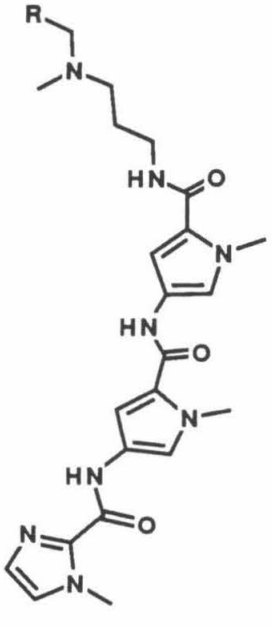

2-ImN, 2-ImNE

Figure 1 Substituted pyridine and imidazole compounds.

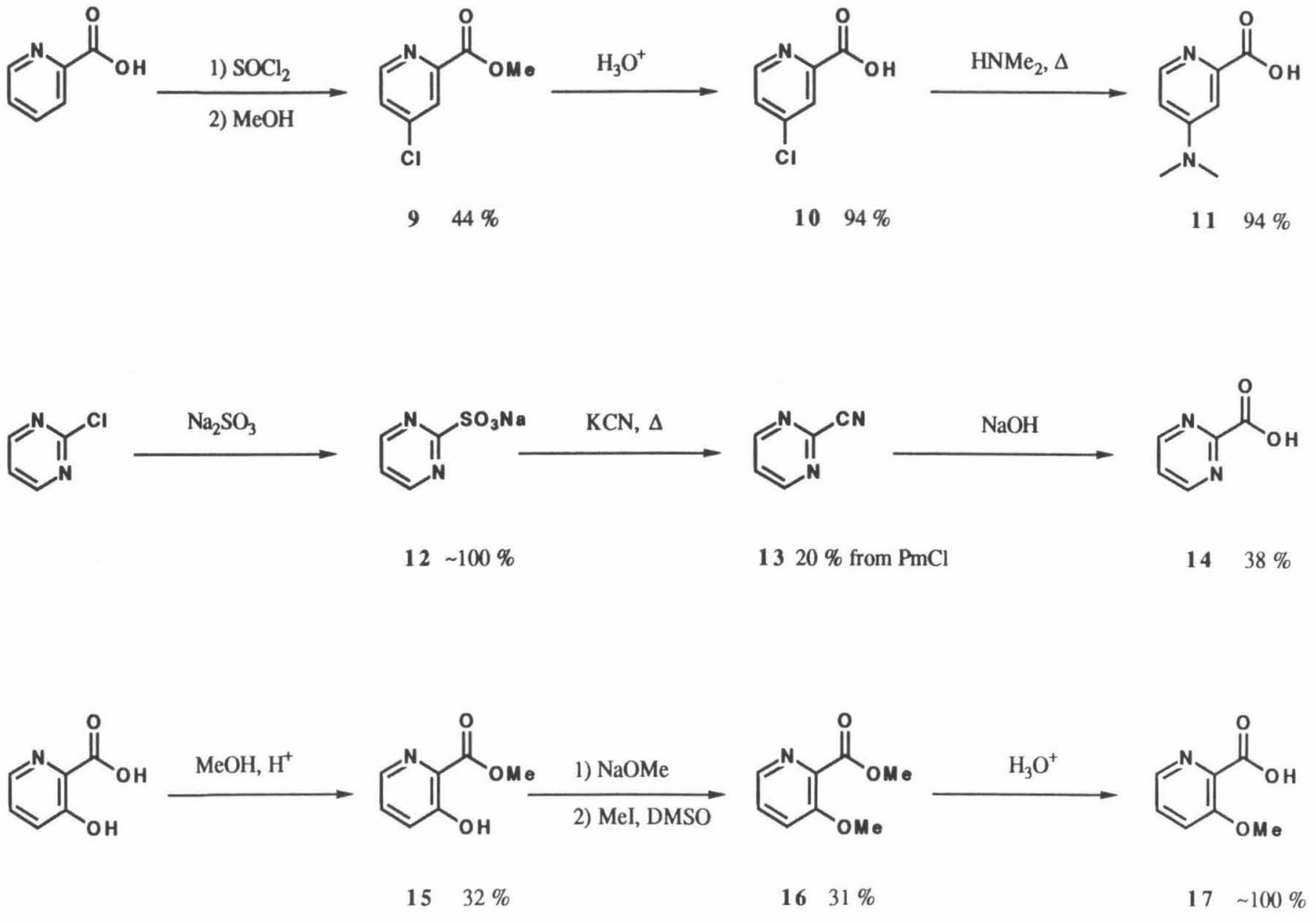

Scheme 1 Synthesis of substituted pyridine acids.

chapter 2. The required acids are not commercially available, but can be prepared by the methods shown in scheme 1. All could be obtained in 1–2 steps from literature starting materials. Preparation of **10** is best accomplished through the methyl ester **9**,[117] which can be recrystallized, then hydrolyzed in acid. Preparation of **11** then follows the procedure for the 4-aminopyridine-3-carboxylic acid.[118] The pyrimidine acid **14** is best synthesized by the method of Ochia and Yamanaka[119] as adapted by Deady *et al.*[120] Compound **17** is readily obtained by acid hydrolysis of the known ester.[121]

Coupling of these acids to the amine derived from **1** is difficult by the N,N′-carbonyldiimidazole procedure. For each compound, a standard sequence of coupling reactions is attempted. The acid is first activated as the imidazolide. If coupling fails, the acid is activated with dicyclohexylcarbodiimide and N-hydroxybenzotriazole. If coupling still fails, the acid is activated as the acid chloride. Several of these compounds, most notably 2-PmN, have the same R_f as the amine derived from **1**. To purify these compounds, the residual amine is acetylated before chromatography. Coupling of the same acids to the amine derived from **2** by the most successful procedure for **1** provides the EDTA derivatives.

The synthesis of the bicyclic imidazole derivative is shown in scheme 2. Alkylation of imidazole at N1 and preparation of the ester follow standard procedures.[122] Compound **18** is apparently unstable at low pH, as has been found for other 1-methylimidazole-2-carboxylic acids.[123] Best coupling yields are achieved by titrat-

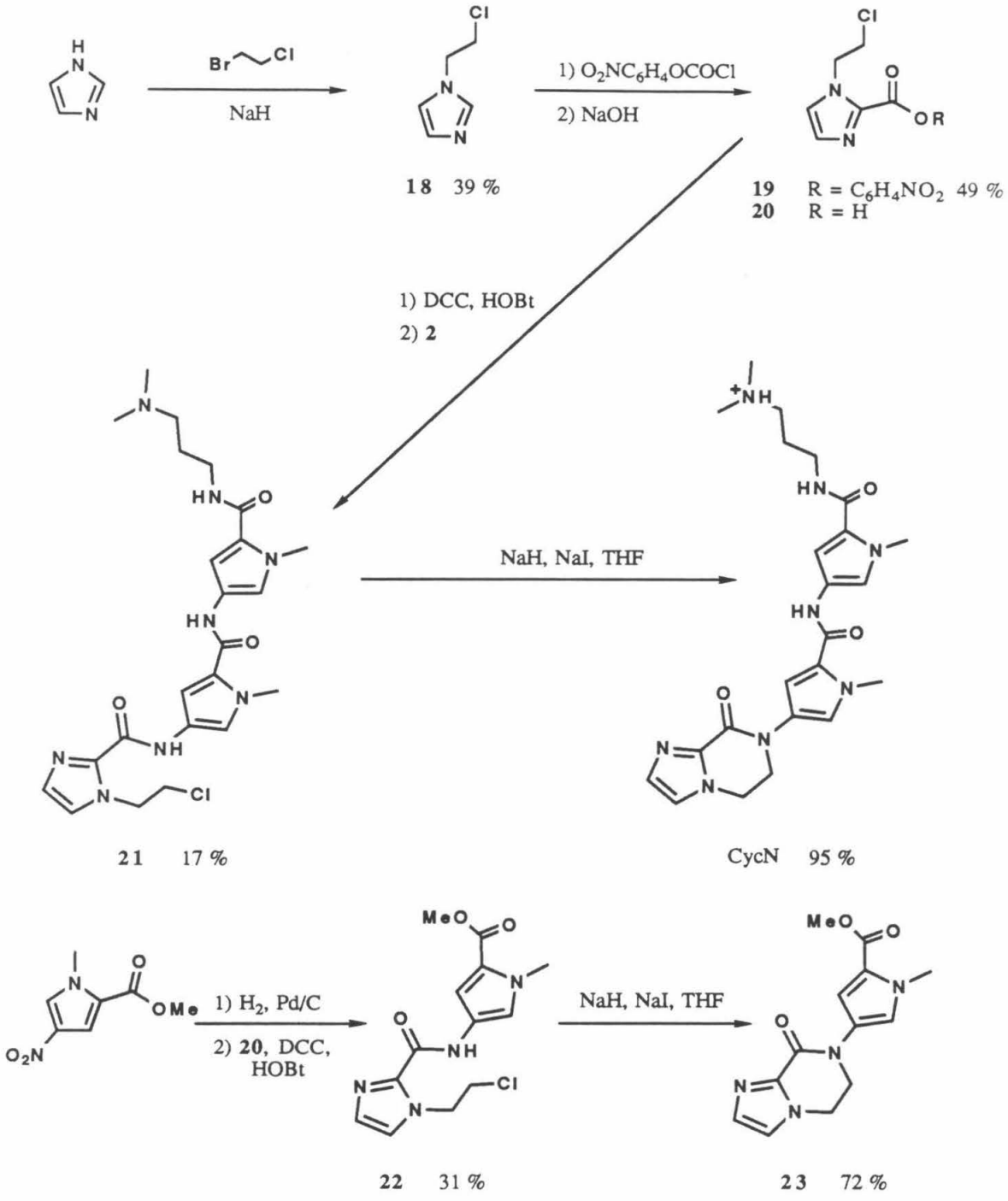

Scheme 2 Synthesis of CycN and model compound **23**.

ing the alkaline hydrolysis reaction mixture of **19** until clear, extracting the nitrophenol with dichloromethane, evaporating the solvent, then immediately activating and coupling with the amine from **1**. Under N-alkylation conditions,[124] cyclization occurs to give the target compound. The mass spectrum and the loss of one amide proton in the ^{1}H NMR spectrum are consistent with either N to C or O to C bond formation. Cyclization occurs on nitrogen as judged by the following evidence. The ^{1}H NMR spectrum of CycN is very similar to the model compound **23** shown in scheme 2. Compound **23** shows both an amide stretch and an ester stretch in the IR spectrum, and the bicyclic portion of the molecule is unaffected by refluxing sodium hydroxide. It is unlikely that the oxygen cyclized product would be stable to these conditions, thus both compounds are probably correct as displayed. As in the 2-ImN case, all attempts to couple **20** to the EDTA amine have failed.

Footprints of these compounds on the 517 bp fragment is shown in figure 2, and the affinity cleaving is shown in figure 3. As observed for the 2-PyN, high concentrations of these analogs show nonselective protection over most of the fragment. Histograms of cleavage and protection sites were determined by the same method used in chapter 2, and are shown in figures 4 and 5. Each compound gives a different binding and cleavage pattern, and will be discussed separately.

4-Chloropyridine-2-carboxamide-netropsin (4-ClPyN)

4-ClPyN protects the same sites as 2-PyN at about the same concentration. 4-ClPyNE cleaves A,T rich sites less efficiently at a slightly higher concentration

Figure 2 Footprinting of substituted derivatives of 2-PyN and 2-ImN. Autoradiogram of an 8% denaturing polyacrylamide gel. All reactions contain 4 mM DTT, 100 μM-bp calf thymus DNA, and 12 kcpm 5′ labeled 517 bp restriction fragment in 40 mM Tris·acetate pH 7.9 buffer. Lane 1, intact DNA; lane 2, G reaction;[80] lane 3, A reaction;[81] lanes 4–22 contain 4 μM MPE·Fe(II): lane 4, MPE·Fe(II) standard; lane 5 4 μM D; lane 6, 20 μM 2-PyN; lane 6, 20 μM 2-ImN; lanes 8–10 contain 35 μM, 10 μM, and 1 μM 4-ClPyN respectively; lanes 11–13, 35 μM, 10 μM, and 1 μM 2-PmN respectively; lanes 14–16, 35 μM, 10 μM, and 1 μM 4-Me_2NPyN respectively; lanes 17–19, 35 μM, 10 μM, and 1 μM CycN respectively.

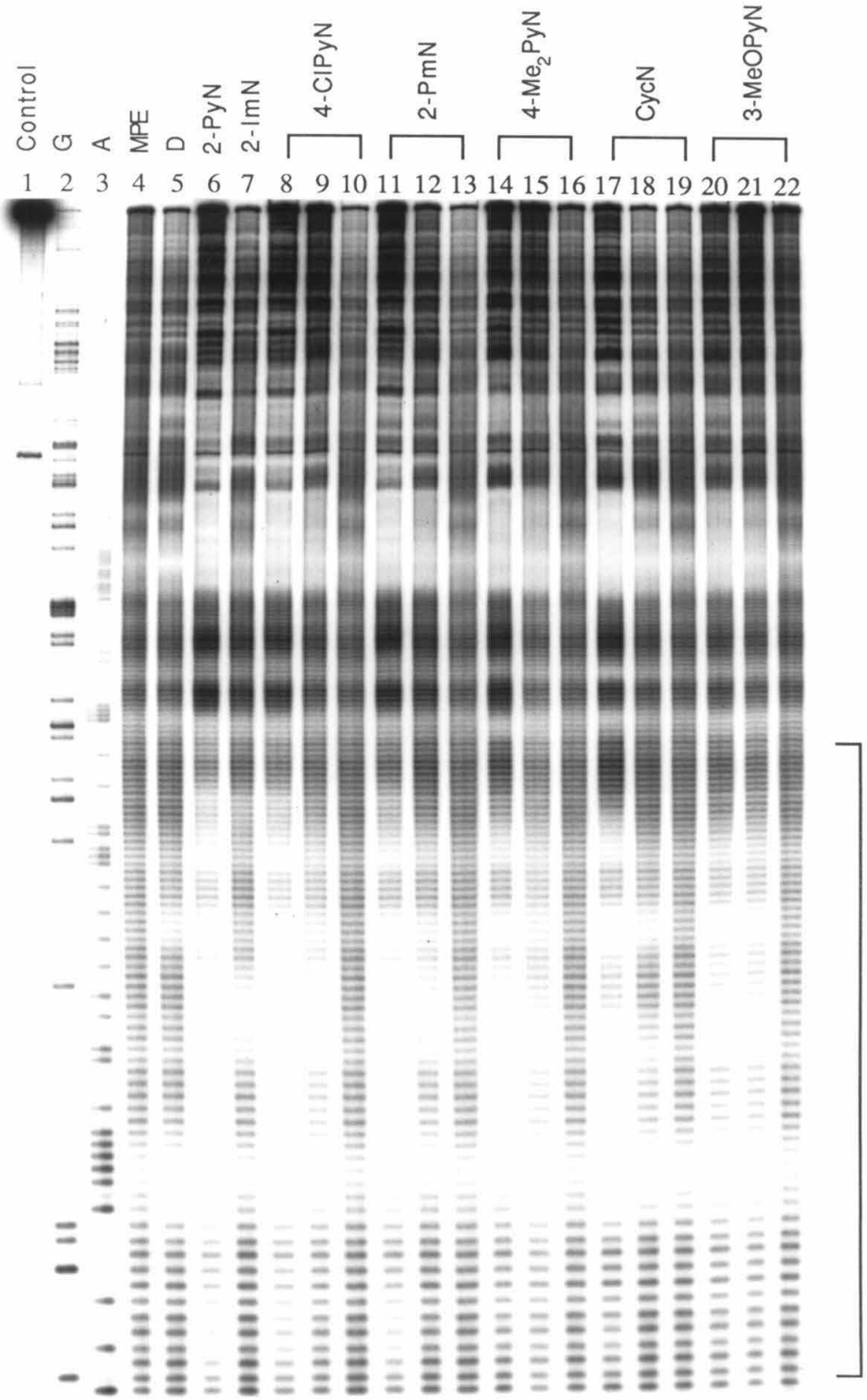
Control
G
A
MPE
D
2-PyN
2-ImN
4-ClPyN
2-PmN
4-Me2PyN
CycN
3-MeOPyN
1 2 3 4 5 6 7 8 9 10 11 12 13 14 15 16 17 18 19 20 21 22

Figure 3 Affinity cleaving of substituted pyridine derivatives of 2-PyN. Autoradiogram of an 8% denaturing polyacrylamide gel. All reactions contain 4 mM DTT, 100 μM-bp calf thymus DNA, and 12 kcpm 5′ labeled 517 bp restriction fragment in 40 mM Tris·acetate pH 7.9 buffer. Lane 1, intact DNA; lane 2, G reaction;[80] lane 3, A reaction;[81] lane 4, 2 μM ED; lane 5, 50 μM 2-PyNE, lane 6, 70 μM 2-ImNE; lane 7, 10 μM 3-PyNE; lane 8, 7 μM 4-PyNE; lane 9, 70 μM 4-ClPyNE; lane 10, 25 μM 2-PmNE; lane 11, 50 μM 4-Me_2NPyNE; lane 12, 70 μM 3-MeOPyNE.

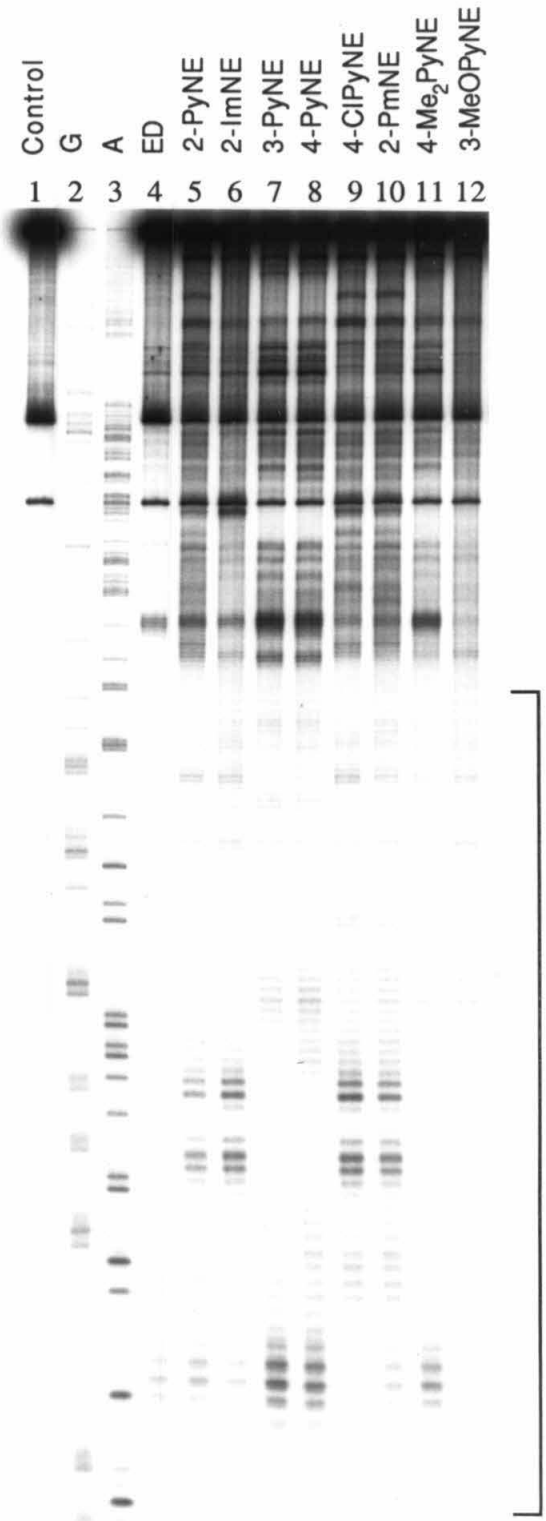
Control
G
A
ED
2-PyNE
2-ImNE
3-PyNE
4-PyNE
4-ClPyNE
2-PmNE
4-Me2PyNE
3-MeOPyNE
1 2 3 4 5 6 7 8 9 10 11 12

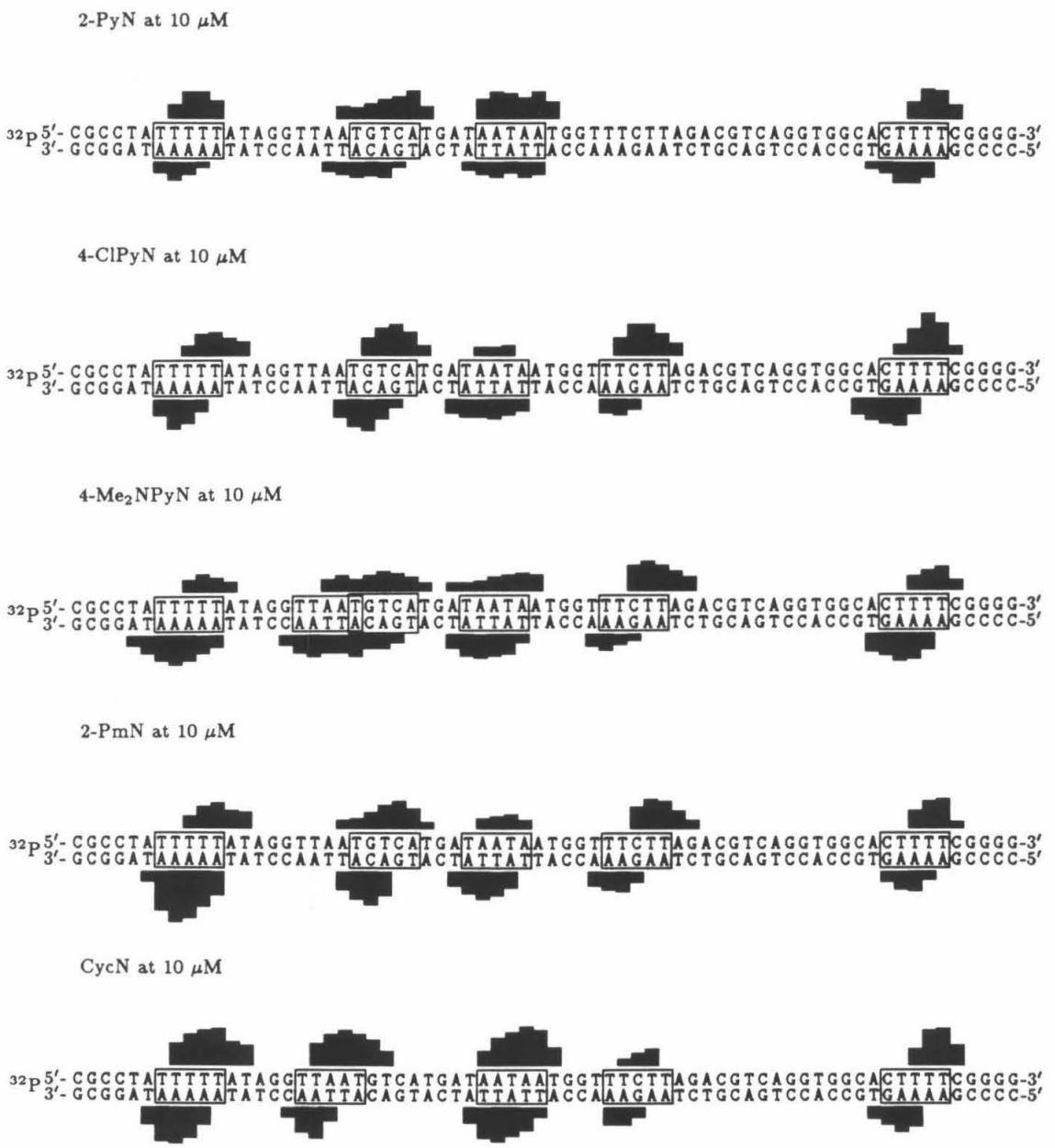

Figure 4 MPE·Fe(II) footprinting protection for the substituted pyridine and imidazole compounds in figure 1.

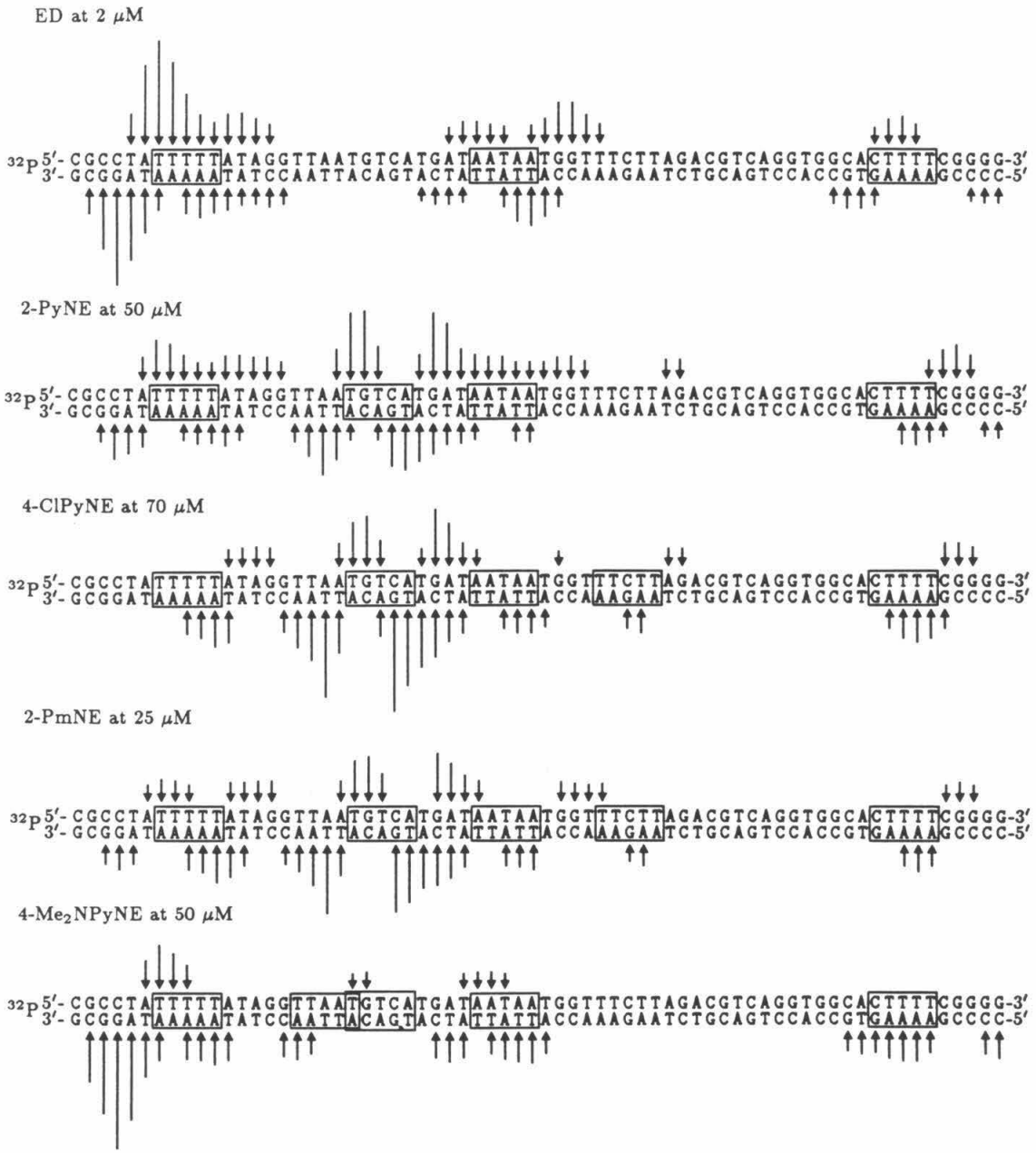

Figure 5 Affinity cleaving of 517 bp fragment of pBR322 by the compounds of figure 1.

than 2-PyNE. This produces a slightly higher TGTCA specificity than the parent compound. 4-ClPyN also binds at the TTTTT site in the opposite orientation from that observed for all compounds in chapter 2. Like 2-PyN and 2-ImN, 4-ClPyN prefers the orientation at the CTTTT site that can hydrogen bond to G.

Pyrimidine-2-carboxamide-netropsin (2-PmN)

The pyrimidine compound protects the TGTCA site and all but one of the A,T rich sites at 10 μM. As judged by the amount of cleavage by 2-PmNE, the binding constant is higher than that of 2-PyN by more than a factor of two. On this fragment, the cleavage specificity of 2-PmNE is identical to 2-PyNE except for the TTTTT site. At the TTTTT site, 2-PmNE cleavage reveals that both orientations are equally favored.

4-Dimethylaminopyridine-2-carboxamide-netropsin (4-Me_2NPyN)

The protection pattern for 4-Me_2NPyN suggests that A,T rich sites are more favored by this compound. Unlike the parent compound at 10 μM, 4-Me_2NPyN at 10 μM prevents MPE·Fe(II) cleavage at the TTAAT site. Almost all cleavage by the EDTA derivative occurs at the TTTTT site in the orientation generally found for ED and 4-PyNE. There is little cleavage at the TGTCA site, consistent with the favoring of A,T rich sites and the disfavoring of the TGTCA site relative to 2-PyN. There is no orientation preference at the CTTTT site, which is also consistent with an overall lower preference for G,C binding.

3-Methoxypyridine-2-carboxamide-netropsin (3-MeOPyN)

This compound does not give detectable footprints on the 517 fragment at concentrations up to 50 μM. Control experiments establish that this is not due to decomposition of the compound, sample packaging or misloading errors. The ^{1}H NMR spectrum of the final compound is clearly that of the 3-methoxy-2-carboxamide compound. The aromatic region has a coupling pattern indicative of three adjacent ring protons. Chemical shift data show one proton next to the ring nitrogen, and large upfield shifts for two protons (*ortho* and *para* to the methoxy) with respect to 2-PyN.

Imidazo[1,2-a]pyrazinecarboxamide-netropsin (CycN)

CycN binds only the usual A,T rich sites at 35 or 10 μM. Despite having only two amide hydrogens, its binding selectivity appears similar to 3-PyN or 4-PyN.

Cleavage Specificity on pBR322

The cleavage specificity of these compounds on larger DNA is determined by the same procedure used in chapter 2. An autoradiogram of the agarose gels is shown in figure 6 and the band sizes and relative cleavage efficiencies are shown in figure 7. The pyrimidine compound gives a cleavage pattern that is identical to the 2-PyNE pattern within the resolution of the experiment. By comparison, 4-ClPyNE shows enhanced cleavage at sites that correlate with the 2-ImNE cleavage bands (*i.e.*, the sites at 10 and 1900), while 4-Me_2NPyN shows decreased cleavage at the same bands. Matching its behavior on the restriction fragment, 3-MeOPyNE cleaves pBR322 very poorly.

Figure 6 Double-stranded cleavage of pBR322 by substituted pyridine compounds. Autoradiogram of a 1% agarose gel. All reactions contain 1 mM sodium ascorbate, 100 μM-bp calf thymus DNA, and 24 kcpm 3′ labeled pBR322 linearized with *Sty* I and labeled at only one end with Klenow fragment. Top) Labeled on the clockwise strand with [α-^{32}P] dATP; Bottom) Labeled on the counterclockwise strand with [α-^{32}P] TTP. Lane 1, intact DNA; lane 2, molecular weight standards; lane 3, 2 μM ED; lane 4, 50 μM 2-PyNE; lane 5, 70 μM 2-ImNE; lane 6, 50 μM 4-ClPyNE; lane 7, 50 μM 4-Me_2NPyNE; lane 8, 25 μM 2-PmNE; lane 9, 70 μM 3-MeOPyNE.

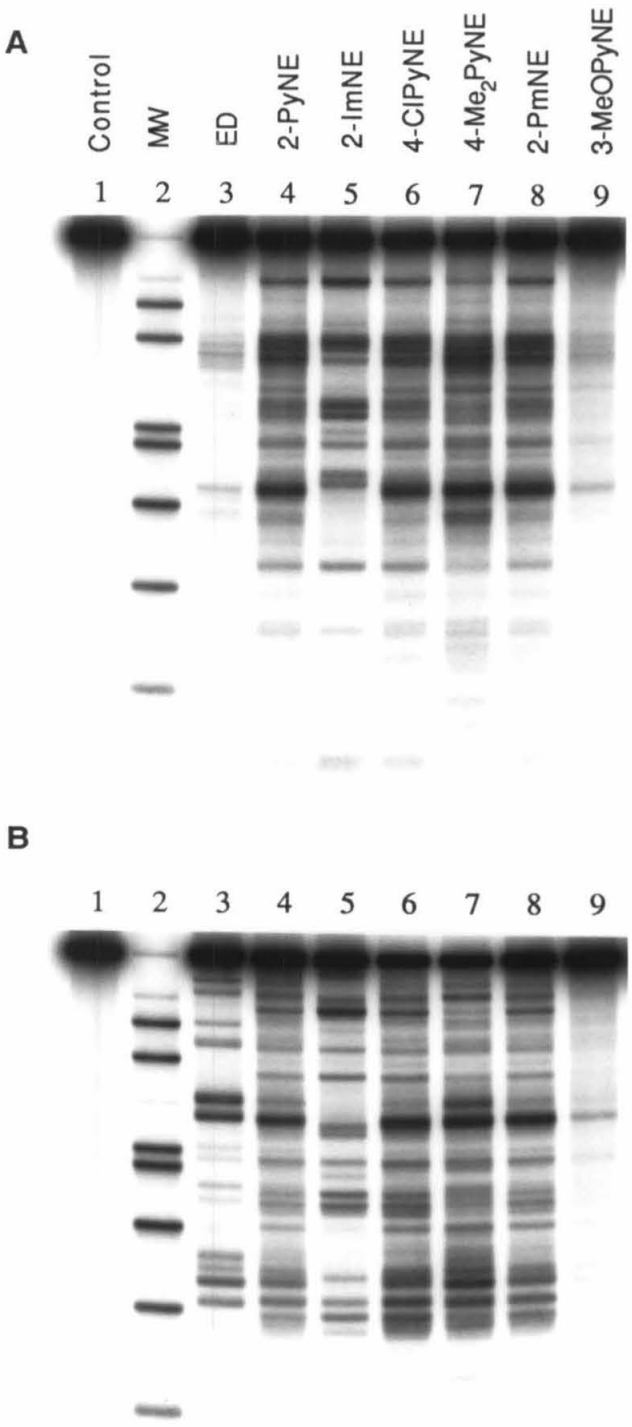
A
Control
MW
ED
2-PyNE
2-ImNE
4-ClPyNE
4-Me2PyNE
2-PmNE
3-MeOPyNE
1 2 3 4 5 6 7 8 9
B
1 2 3 4 5 6 7 8 9

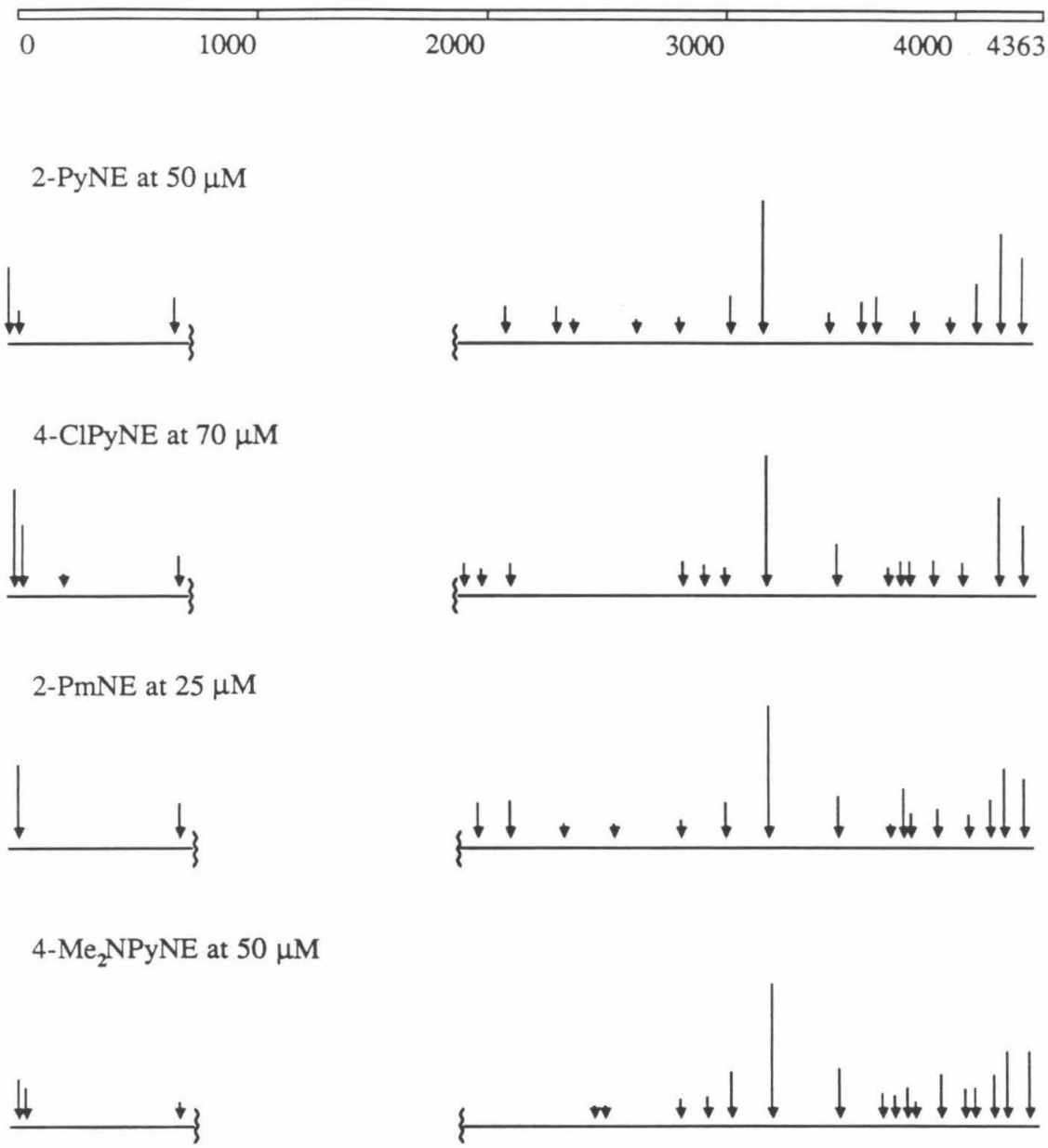

Figure 7 Cleavage sites on linearized pBR322. Arrows represent the extent of cleavage in each lane of figure 6. Arrow positions represent approximate binding site locations, accurate to within 40 bp. Cleavage bands within 700 bp of the labeled termini are not resolved on the gel.

Discussion

While the pyrimidine compound shows no change in specificity from 2-PyN, the binding constant at the TGTCA site is significantly higher. This can be readily explained by an entropic argument. There are now two degenerate conformations each of which can hydrogen bond to G. An identical increase in binding affinity at A,T rich sites could be explained by the same effect if only one of the pyrimidine nitrogens is hydrogen bonded in water solution. This is reasonably consistent with the low basicity of pyrimidine derivatives. Such a bonding scheme would give two degenerate N-out complexes and the entropic contribution would be the same at all sites. Alternatively, the difference in affinity may be caused by the change in dipole or electronic structure between pyridine and pyrimidine, with the similar magnitude at different sites being fortuitous.

Both CycN and 3-MeOPyN provide evidence against the participation of the N-terminal amide carbonyl in the WGWCW complex. Neither shows detectable binding at the TGTCA site. The methoxy compound also shows no detectable binding at A,T sites, consistent with the solvent hydrogen bond model for disfavoring such sites. Because of the methoxy group, 3-MeOPyN must have the pyridine nitrogen at the floor of the groove at all sites. Thus it should behave like 2-ImN at all A,T sites. CycN, however, could rotate so that the two methylene groups are present on the floor of the groove. Such a conformation looks very similar to the piperazine ring of Hoechst 33258 in the crystal structure of the DNA complexes.[39, 40]

If the specificity of 2-PyN and 2-ImN is due mostly to hydrogen bonding patterns, as proposed in chapter 2, then an increase in hydrogen bond strength should increase the selectivity for TGTCA by two different mechanisms. The G/aromatic N hydrogen bond should be stronger, increasing the WGWCW binding affinity. A similar increase in the aromatic N to water hydrogen bond strength should decrease the affinity at A,T sites. Substitution of the 4 carbon of the pyridine ring should have the strongest effect on the aromatic nitrogen, but other factors can intervene. It is expected that bulky groups at the 4 position prefer the N-in conformation, thus selecting against A,T binding sites. For a bulky electron-withdrawing group, these factors will compete with one another. Steric factors will favor WGWCW sites, and hydrogen bonding will favor A,T sites. For a bulky electron donating group, both factors tend to favor WGWCW sequences.

Experimentally, the opposite trend is observed. 4-ClPyN is more specific for the TGTCA site by disfavoring A,T sites. 4-Me_2NPyN is less specific for the TGTCA site by both favoring A,T sites and disfavoring the TGTCA site. For 4-ClPyN, the results are consistent with the enhanced preference for the N-in conformation dominating over the loss in hydrogen bond strength. The 4-Me_2NPyN results cannot be explained by this argument. However, to obtain sharp ^{1}H NMR peaks for 4-Me_2NPyN and its precursors, it is necessary to add trifluoroacetic acid. This suggests that a protonation event occurs near neutral pH. NMR studies have shown that the protonation of dimethylaminopyridines occurs at the ring

nitrogen.[125, 126] Such a protonation event would favor A,T sites at low pH, since the pyridine nitrogen can now hydrogen bond to A and T.

The UV absorbance of 4-Me_2NPyN with varying pH is shown in figure 8. At low pH, the absorbance maxima at 270 nm shifts to longer wavelength. The three isosbestic points at 278, 313, and 328 nm indicate that a single process is occuring in this pH range. Plotting the difference in absorbance at 265 nm and 300 nm versus pH gives an approximate pK_a of 6.2, consistent with the literature values of this class of compounds.[127-129] The electronegative environment of DNA should raise the pK_a, so that it is quite reasonable to expect 4-Me_2NPyN to be at least partially protonated under typical footprinting conditions. To test this hypothesis, 4-ClPyN, 2-PyN, 4-Me_2NPyN, and 2-ImN have been footprinted over a range of pH values. As the pH of the reaction increases, the binding affinity of all compounds should decrease as the C-terminal amino group deprotonates. At the lowest pH, it is possible that the DNA itself is partially protonated. In the absence of another protonation site on the ligand, there should be a gradual decrease in the number of protected sites with increasing pH.

Because MPE·Fe(II) cleaves extremes of pH at considerably lower efficiencies,[102] sodium ascorbate is used as the reductant. The cleavage time is varied from 4 min at pH 7 or 8 to 30 min at pH 10. An autoradiogram of the 517 fragment is shown in figure 9, and the footprints are shown in figures 10 and 11. Detection of light footprints is problematic. Any diminution of cleavage at the sites present at pH 6 was considered to be evidence for binding at that site, and is shown in the histograms.

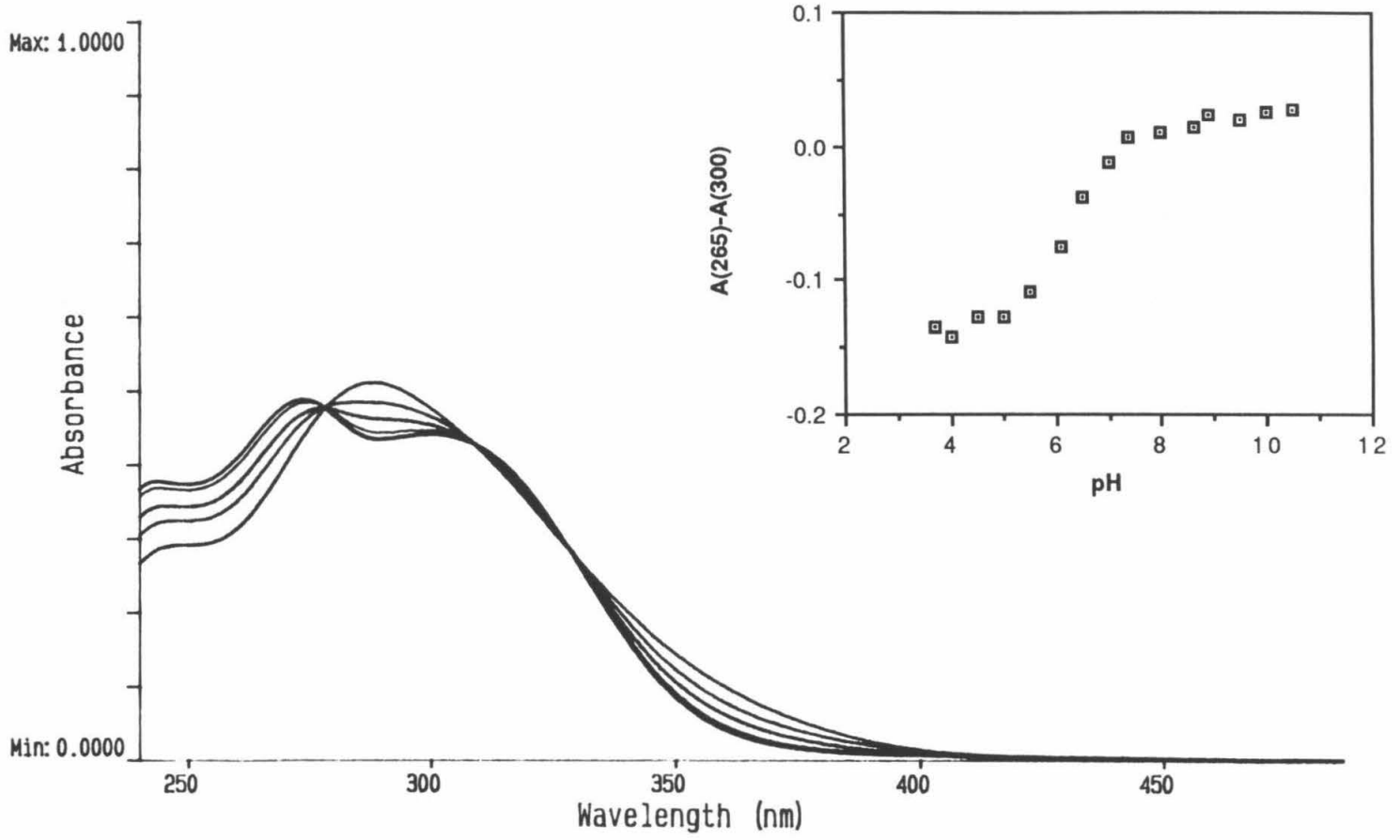

Figure 8 pH titration of 4-Me_2NPyN. UV-visible absorbance spectra at pH 5, pH 5.5, pH 6, pH 6.5 and pH 7. Insert) Titration curve for 4-Me_2NPyN, as determined by the relative change in absorbance between 265 and 300 nm.

Figure 9 pH dependence of 4-Me_2NPyN, 2-PyN, 4-ClPyN, and 2-ImN footprints. Autoradiogram of an 8% denaturing polyacrylamide gel. All reactions contain 1 mM sodium ascorbate, 100 μM-bp calf thymus DNA, and 12 kcpm 3′ labeled 517 bp restriction fragment in 40 mM Tris·acetate pH 7.9 buffer. Lanes 1–3, intact DNA at pH 6, 8, and 10 respectively; lane 4, G reaction;[80] lane 5, A reaction;[81] lanes 6–30 contain 4 μM MPE·Fe(II): lanes 6–10 contain the products of MPE·Fe(II) cleavage for 18 min at pH 6; lanes 11–15, cleavage for 4 min at pH 7; lanes 16–20, cleavage for 4 min at pH 8; lanes 21–25, cleavage for 8 min at pH 9; lanes 26–30, cleavage for 30 min at pH 10; lanes 6, 11, 16, 21, and 26 are MPE·Fe(II) standards; lanes 7, 12, 17, 22, and 27 contain 20 μM 4-Me_2NPyN; lanes 8, 13, 18, 23, and 28, 20 μM 2-PyN; lanes 9, 14, 19, 24, and 29, 20 μM 4-ClPyN; lanes 10, 15, 20, 25, and 30, 20 μM 2-ImN.

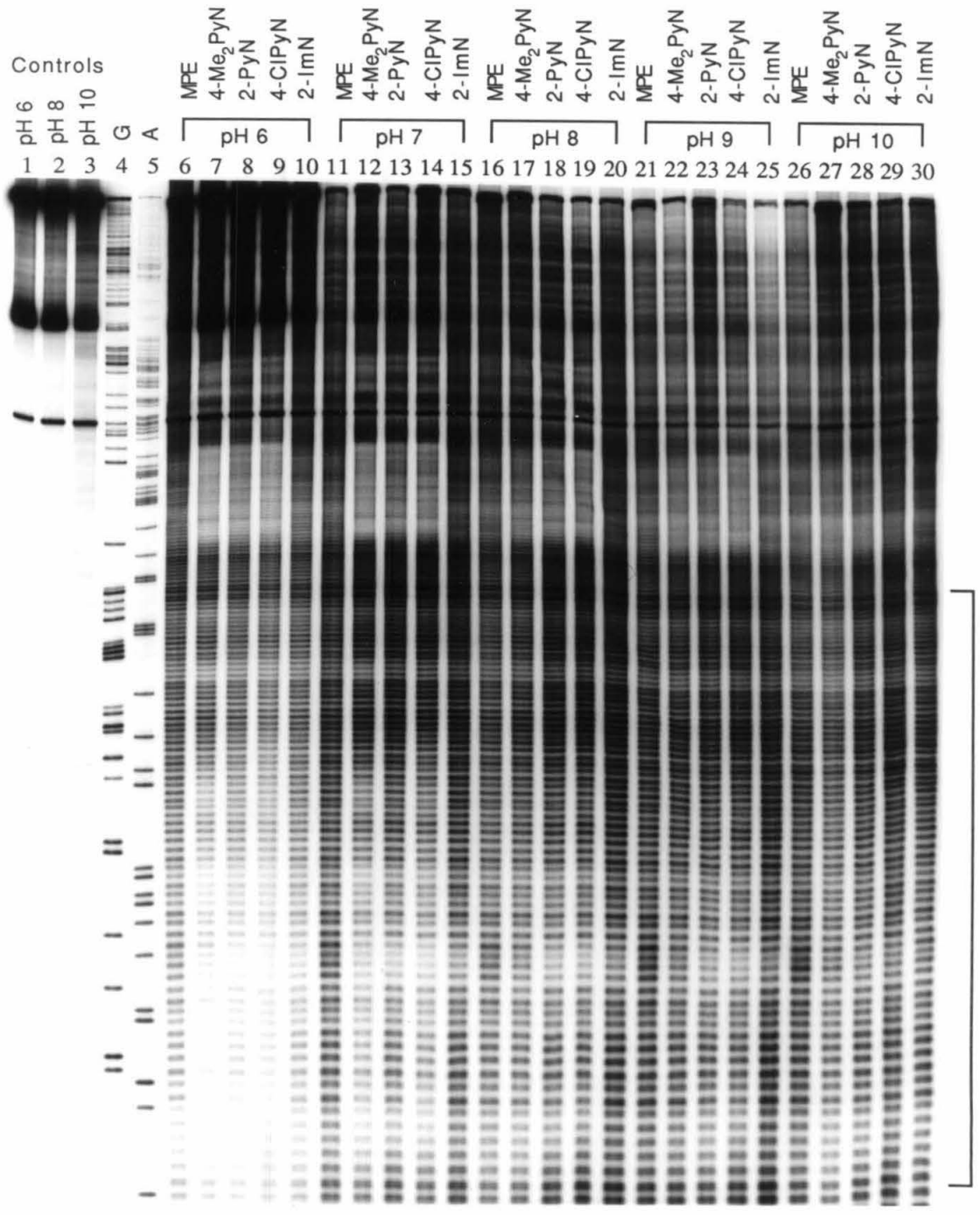
Controls
pH 6
pH 8
pH 10
G
A
MPE
4-Me2PyN
2-PyN
4-ClPyN
2-ImN
pH 6
pH 7
pH 8
pH 9
pH 10
1 2 3 4 5 6 7 8 9 10 11 12 13 14 15 16 17 18 19 20 21 22 23 24 25 26 27 28 29 30

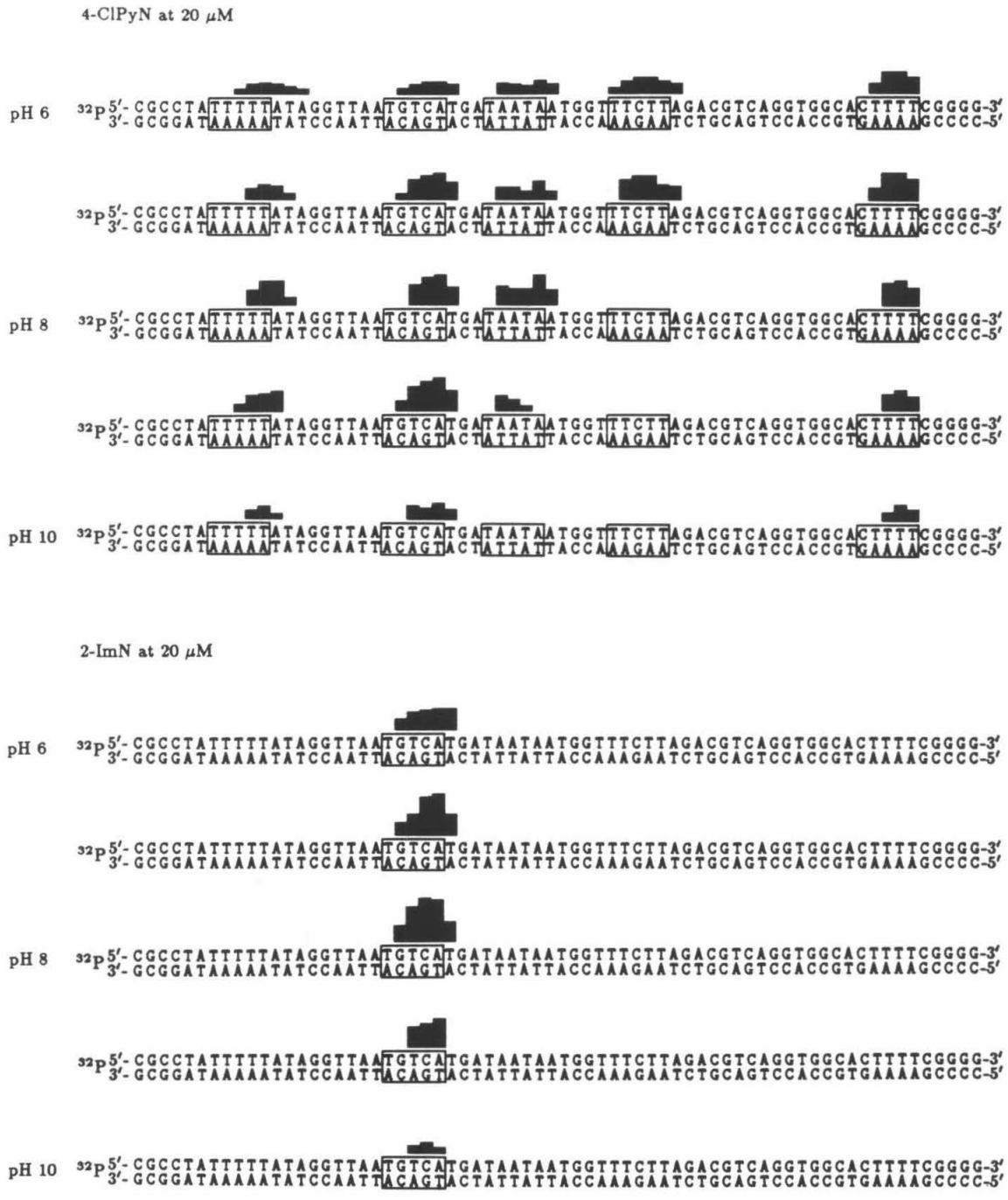

Figure 10 pH dependence of 4-ClPyN and 2-ImN footprinting. Boxes represent sites bound by the compounds at pH 6.

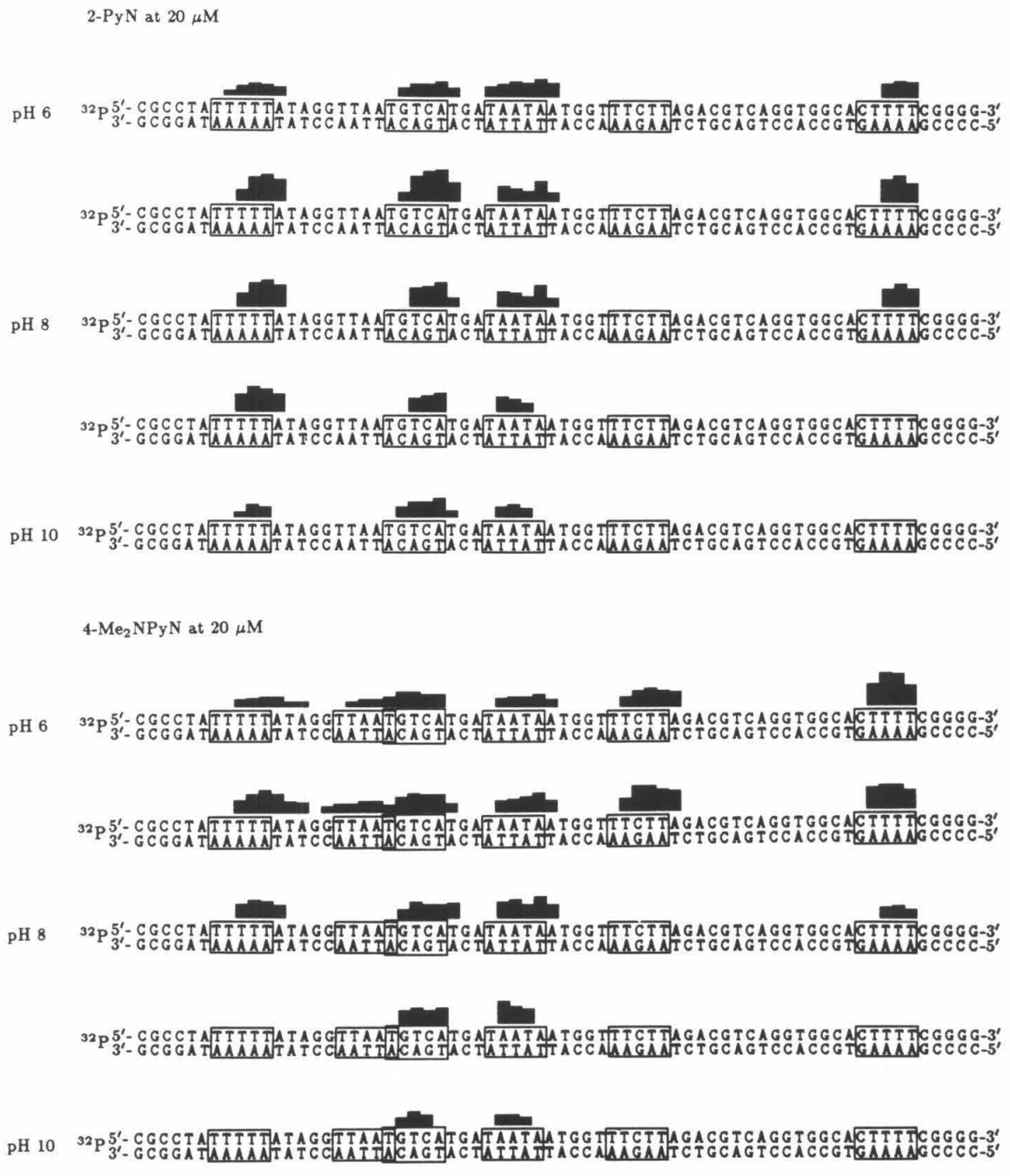

Figure 11 pH dependence of 2-PyN and 4-Me_2NPyN footprinting. Boxes represent sites bound by the compounds at pH 6.

As expected, all four compounds protect fewer sites at high pH. TGTCA site complexes are stable over the entire pH range for all compounds. 2-PyN and 4-ClPyN complexes are also reasonably stable. One binding site is not detected at pH 8 and another is very weakly protected at pH 10. The protection pattern of 4-Me_2NPyN changes markedly with pH. Below pH 8, 6 sites are bound, including the TTAAT site that is not bound by 2-PyN at this concentration. At pH 8, the same 4 sites bound by 2-PyN are protected. Above pH 8, only two sites are detected, one of them the TGTCA site. At pH 9, there is no detectable footprint at the TTTTT site, unlike both 2-PyN and 4-ClPyN. Thus, it is likely that the originally measured specificity corresponds to the protonated form. At higher pH, 4-Me_2NPyN is more specific for the TGTCA site than 2-PyN, as expected from the original hydrogen bonding argument.

Length Dependence of WGWCW Site Specificity

Studies of a series of polypyrrole analogs of distamycin A have shown that the binding site size increases incrementally with the number of pyrroles, while the A,T specificity of the molecules remains in force.[17] This has been formulated as the *n+1* rule, where *n+1* A,T bp are recognized by *n* amides on the small molecule. If 2-ImN binds at the TGTCA site in the distamycin-like conformation, then the same trend should hold. In contrast, the model proposed in chapter 2 predicts that analogs containing two aromatic rings should have no TGTCA site affinity, and

that longer analogs should have potential for recognizing larger distances between G,C bp.

In order to examine the susceptability of WGWCW sequence binding to variations in small molecule length and number of amides, the series of compounds shown in figure 12 has been synthesized. All compounds are readily available from the appropriate nitroamine precursors by the standard reduction and coupling sequence.[16] Synthesis of AcImN requires the 4-nitro-1-methylimidazole-2-carboxylic acid **25**, which can be prepared by the literature method[113] as shown in scheme 3. After coupling of **25**, the nitro group is reduced and acetylated to give AcImN. The specificity of one of the compounds in this series (**iv** in chapter 1) has been reported to be solely A,T,[65] and therefore is not examined further here.

As shown in table 1, these compounds constitute two series with incremental variations. The footprinting gel of these compounds is shown in figure 13, and the derived histograms are shown in figures 14 and 15. The series containing only pyrrole rings behaves as expected. There appears to be only a small increase in binding affinity associated with the attachment of the third pyrrole ring in 2-PrN. This is consistent with the affinity of the complex being determined by the amide hydrogen bonds.

The imidazole-containing series shows a more variable selectivity. 2-ImP binds only A,T rich sites as predicted by the WGWCW binding model. Binding affinities are low, consistent with the lack of amides and the disfavoring of A,T sites by the

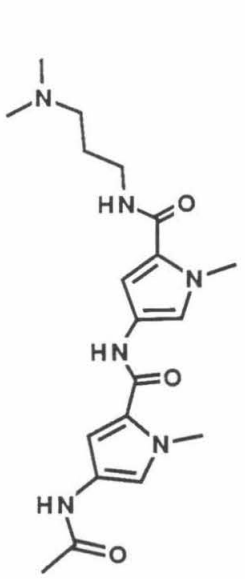

N

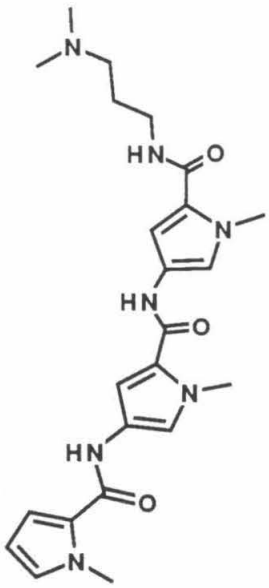

2-PrN

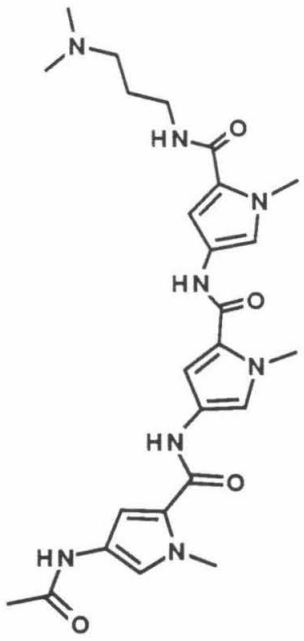

D

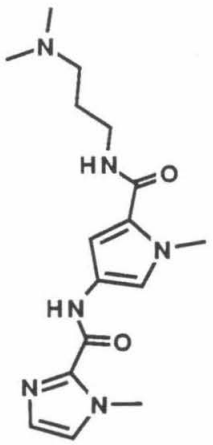

2-ImP

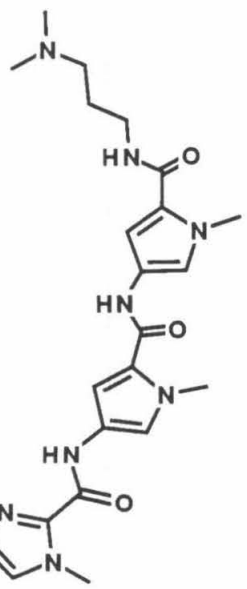

2-ImN

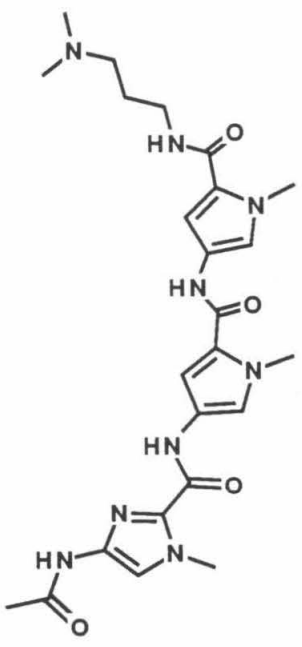

AcImN

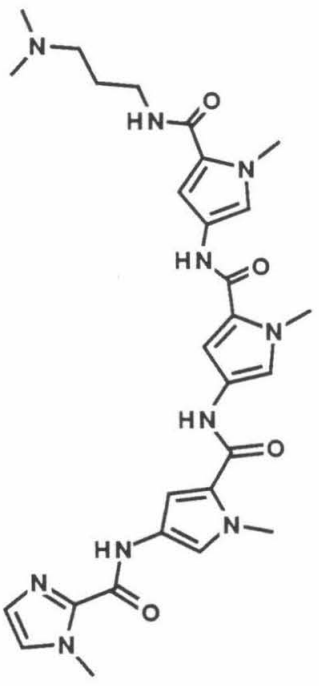

2-ImD

Figure 12 Variable Length Analogs of 2-ImN.

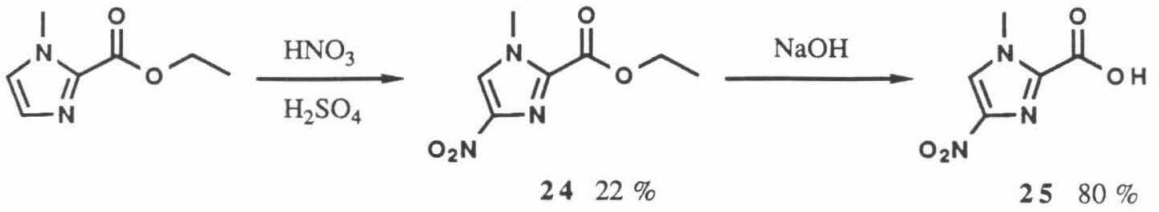

24 22 %

25 80 %

Scheme 3 Synthesis of 1-methylimidazole-2-carboxylic acids.

Table 1 Expected Site Sizes for Variable Length Analogs.

Compound	Aromatic Rings	Amides	Site Size[a]
N	2	3	4
2-PrN	3	3	5
D	3	4	5
2-ImP	2	2	4
HCOImP, iv[b]	2	3	4
2-ImN	3	3	5
AcImN	3	4	5
2-ImD	4	4	6

[a] Based on the number of aromatic rings. [b] See chapter 1.

imidazole ring. AcImN does not bind detectably to the TGTCA site even at 50 μM. It binds A,T sites with roughly the same affinity as 2-PrN. Thus the addition of a single amide to 2-ImN has two significant effects. The fourth amide counteracts the disfavoring of A,T sites by the imidazole ring, and disfavors WGWCW binding. If the 2-ImN binding conformation is similar to distamycin A, this is difficult to explain. If 2-ImN is binding so that the amide carbonyl faces inward, then the lack of TGTCA site binding could be due to close contacts between the extra amide

Figure 13 Footprinting of varying length D and 2-ImN derivatives. Autoradiogram of an 8% denaturing polyacrylamide gel. All reactions contain 4 mM DTT, 100 μM-bp calf thymus DNA, and 12 kcpm 3′ labeled 517 bp restriction fragment in 40 mM Tris·acetate pH 7.9 buffer. Lane 1, intact DNA; lane 2, G reaction;[80] lane 3, A reaction;[81] lanes 4–22 contain 4 μM MPE·Fe(II): lane 4, MPE·Fe(II) standard lanes 5–7 contain 35 μM, 10 μM, and 1 μM N respectively; lanes 8–10, 35 μM, 10 μM, and 1 μM 2-PrN respectively; lanes 11–13, 5 μM, 2 μM, and 1 μM D respectively; lanes 14–16, 50 μM, 35 μM, and 10 μM 2-PrN respectively; lanes 17–19, 35 μM, 10 μM, and 1 μM 2-ImN respectively; lanes 20–22, 35 μM, 10 μM, and 1 μM AcImN respectively; lanes 23–25, 35 μM, 10 μM, and 1 μM 2-ImD respectively.

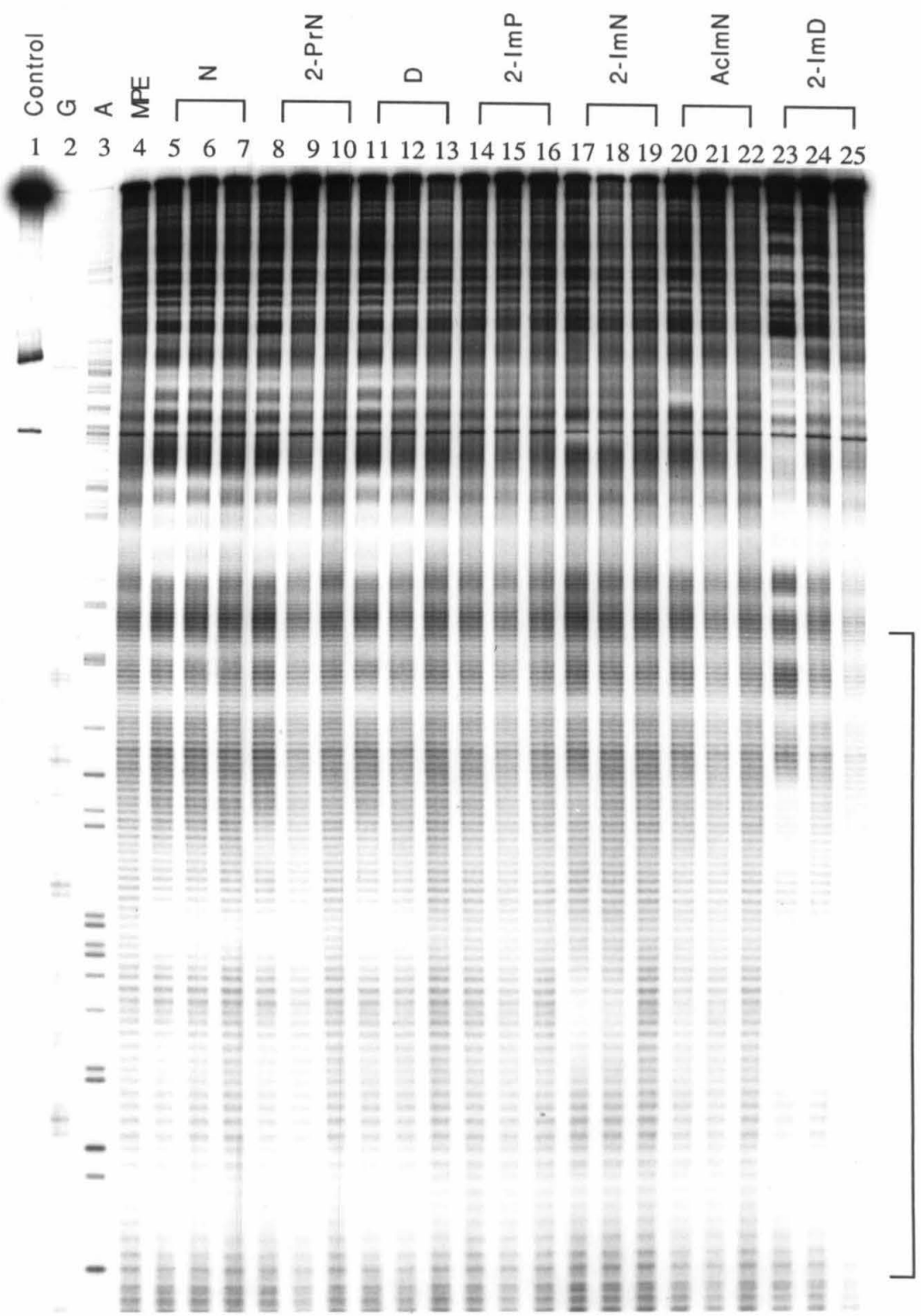
Control
G
A
MPE
N
2-PrN
D
2-ImP
2-ImN
AcImN
2-ImD
1 2 3 4 5 6 7 8 9 10 11 12 13 14 15 16 17 18 19 20 21 22 23 24 25

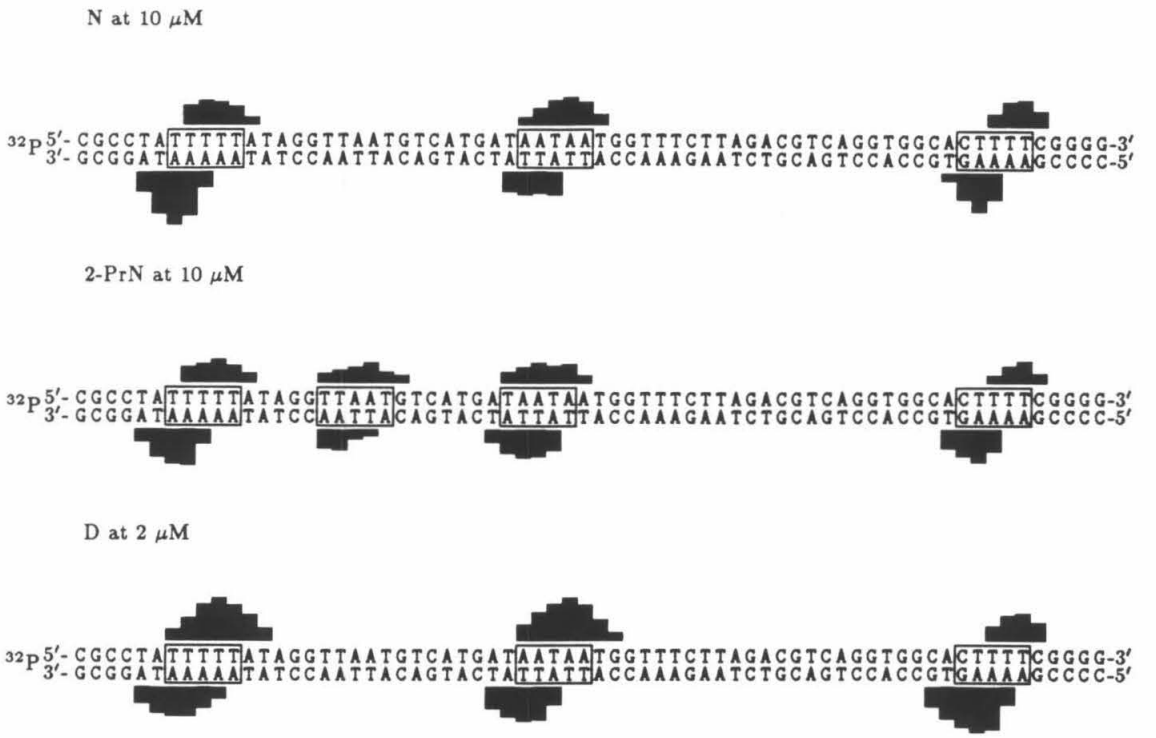

Figure 14 Footprinting of the distamycin A series.

and the bases.

Like 2-ImN, 2-ImD also shows altered sequence specificity. As predicted by the *n+1* rule, 2-ImD binds to 6 bp sites. 2-ImD also binds A,T rich sequences better than 2-ImN. As with AcImN, the addition of another amide appears to counteract the effect of the imidazole ring. At 10 μM, this compound protects an extended region on the 517 bp fragment. This sequence contains the TGTCA and TAATAA sites observed previously as well as the TCATGA site in between. The limited resolution of this footprint precludes convincing evidence of TCATGA site binding, but the degree of protection is much higher than normally found for

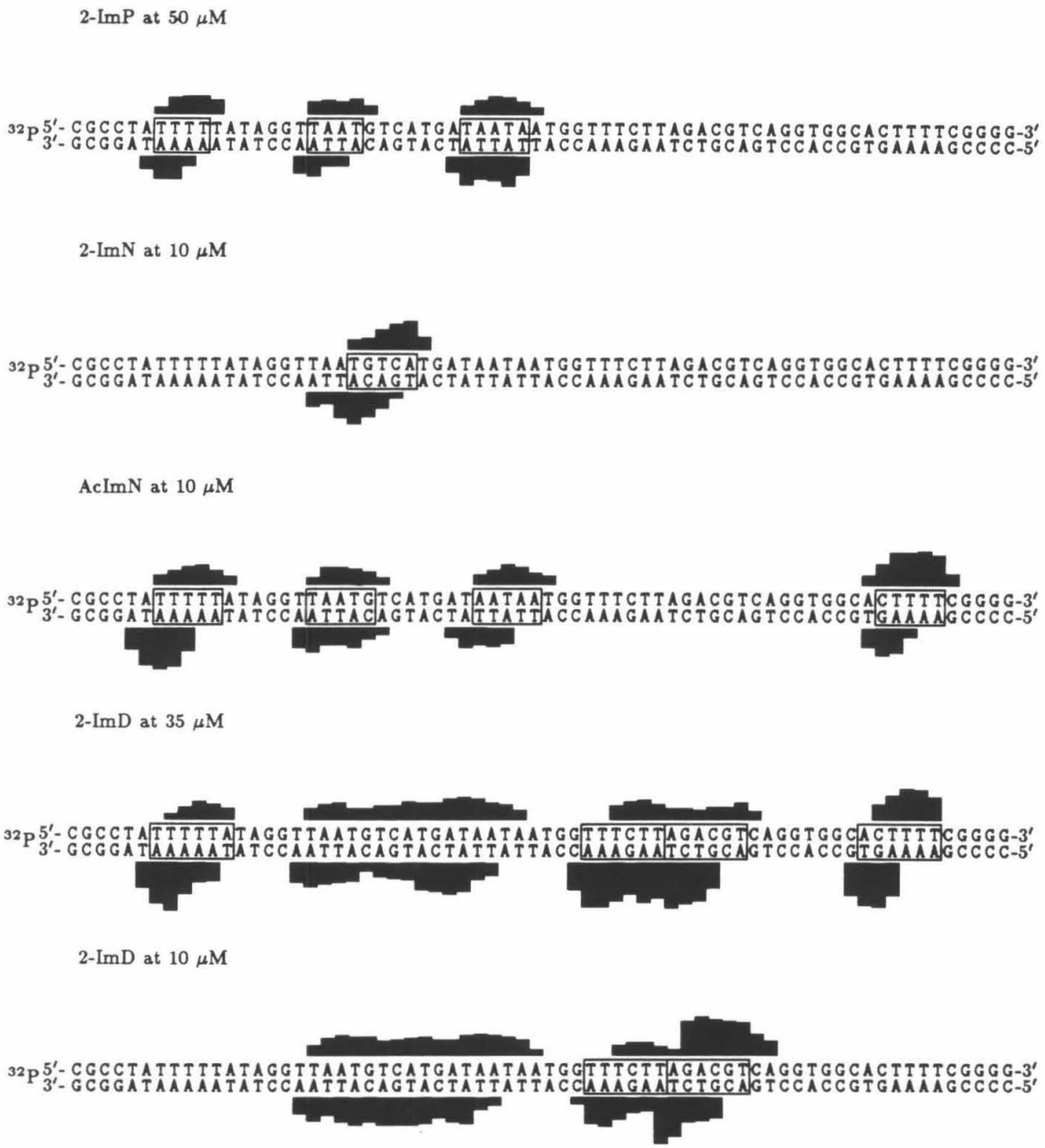

Figure 15 Footprinting of the 2-ImN series on bp 4268-4335 of pBR322.

the other compounds studied. In addition, 2-ImD binds to a AGACGT sequence farther up on the 517 bp fragment. These observations suggest that 2-ImD can recognize sequences with longer distances between the G,C bp.

Carboxyterminal Derivatives

To gather a final set of information about the WGWCW complex, a series of C-terminal 2-PyN and 2-ImN analogs has been synthesized. Compounds in this series, as shown in figure 16, have an additional atom between the amide carbonyl and the heterocyclic nitrogen. As a consequence, the L shape of the carbonyl-in conformation of the N-terminal analog does not occur for the same conformation at the C-terminus. An extra atom between partners will also necessarily alter the geometry of the hydrogen bonds.

The synthesis of the first three compounds in figure 16 is shown in scheme 4. Acylation of 2-aminopyridines is difficult, but could be accomplished in refluxing pyridine following literature precedent.[130] 2-Amino-1-methylimidazole can be prepared by the method of Lawson,[131] and is acylated under the same conditions. Compound **30** could then be N-methylated using the standard method.[124] Elaboration of these compounds to the distamycin analogs uses the standard reduction/amide coupling sequence.[76]

Placement of an aromatic ring at each end of the netropsin unit requires another position for the positive charge. The synthesis of a postively charged derivative of the nitropyrrole building block **38** and its incorporation into the final

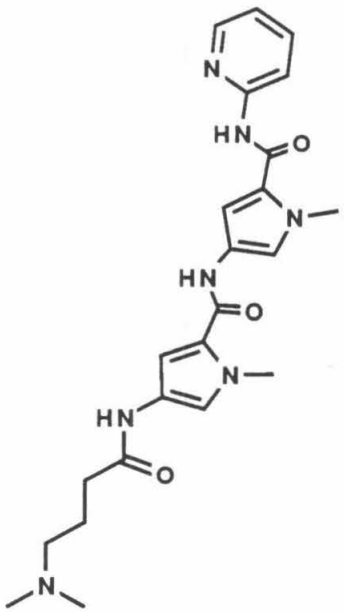

NPy

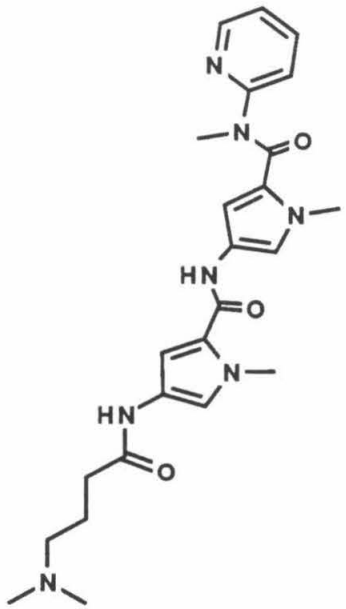

NMePy

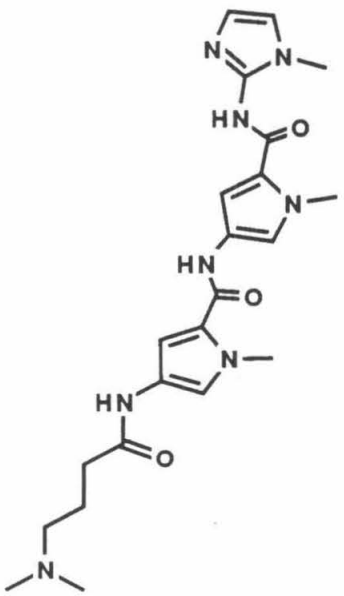

NIm

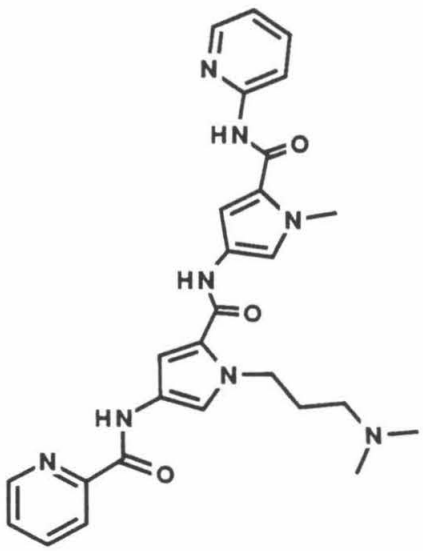

$PyP^{+}PPy$

Figure 16 C-terminal 2-PyN and 2-ImN analogs.

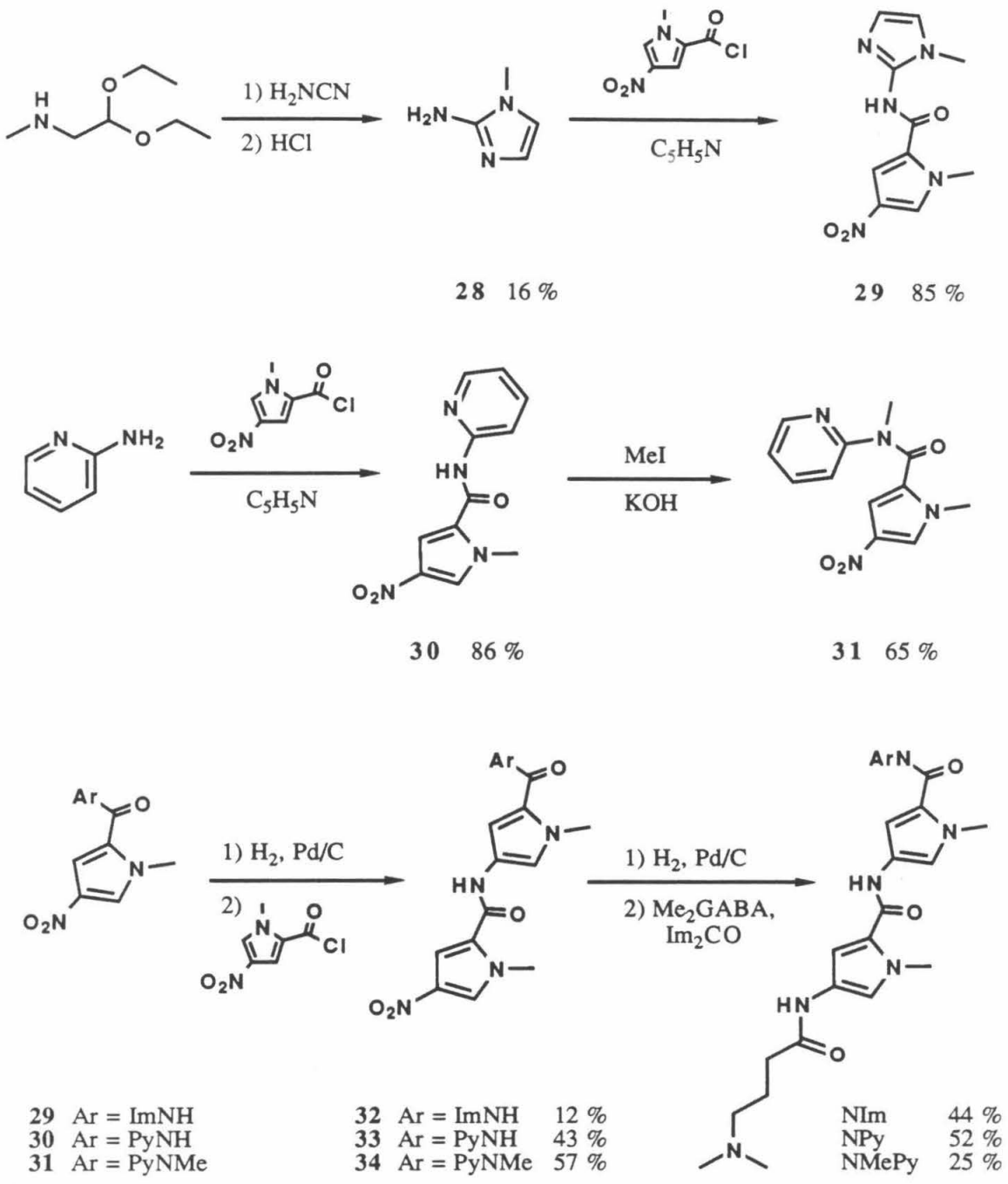

Scheme 4 Synthesis of simple C-terminal analogs of 2-PyN and 2-ImN.

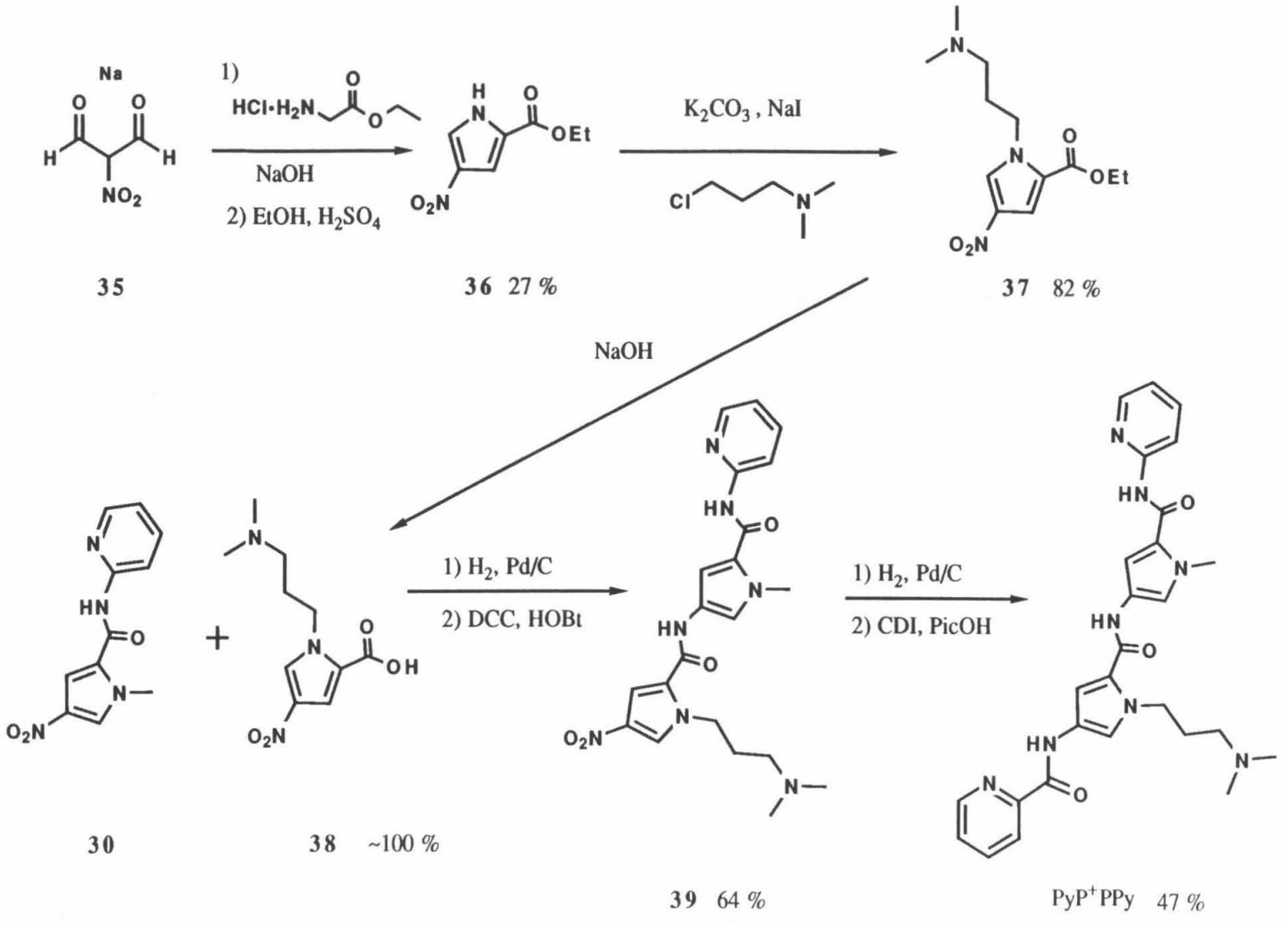

Scheme 5 Synthesis of $PyP^{+}PPy$.

compound PyP^+PPy is shown in scheme 5. Compound **36** is prepared by the literature procedure,[132] then alkylated by the procedure developed in the group by Sam Gellman.[133] Coupling to the previous precursor **30** follows standard procedures.

The footprinting gel with these compounds is shown in figure 17. Histograms are collected in figure 18. Neither NIm nor NMePy exhibit any detectable binding to the TGTCA site. Both NPy and PyP^+PPy bind to the TGTCA site, but have lower specificities than 2-PyN. PyP^+PPy also has substantially lower binding affinities to all sites, giving no detectable footprints at 10 μM. Like 2-ImD, PyP^+PPy recognizes the AGACG site.

The lower specificity of NPy is probably not due to protonation, becausesince the pK_a of 2-benzamidopyridine is 3.3.[134] Clearly, separation of the amide carbonyl and the heterocycle by one atom does not prevent WGWCW sequence binding as does a one atom separation along the pyridine ring. As in the previous cases, the lower specificity is produced by an increased affinity for A,T sites.

The lower specificity of PyP^+PPy could be due solely to a lower binding constant at the TGTCA site. There are several possible explanations. The positive charge on PyP^+PPy is not at the bottom of the groove where the largest negative electrostatic potential is calculated to be.[135] Alternatively, the distance between the two pyridine rings may not allow for simultaneous interactions with the DNA. The second aromatic ring would then tend to disfavor WGWCW sites in the same way that 2-PyN disfavors A,T sites. This second interpretation is supported by

Figure 17 Footprinting of C-terminal analogs of 2-PyN and 2-ImN. Autoradiogram of an 8% denaturing polyacrylamide gel. All reactions contain 4 mM DTT, 100 μM-bp calf thymus DNA, and 12 kcpm 5′ labeled 517 bp restriction fragment in 40 mM Tris·acetate pH 7.9 buffer. Lane 1, intact DNA; lane 2, G reaction;[80] lane 3, A reaction;[81] lanes 4–25 contain 4 μM MPE·Fe(II): lane 4, MPE·Fe(II) standard; lane 5 4 μM D; lane 6, 20 μM 2-PyN; lane 6, 20 μM 2-ImN; lanes 8–10 contain 35 μM, 10 μM, and 1 μM 3-PyN respectively; lanes 11–13, 35 μM, 10 μM, and 1 μM 4-PyN respectively; lanes 14–16, 35 μM, 10 μM, and 1 μM NPy respectively; lanes 17–19, 35 μM, 10 μM, and 1 μM NMePy respectively; lanes 20–22, 50 μM, 35 μM, and 10 μM PyP^+PPy respectively; and lanes 23–25, 35 μM, 10 μM, and 1 μM NIm respectively.

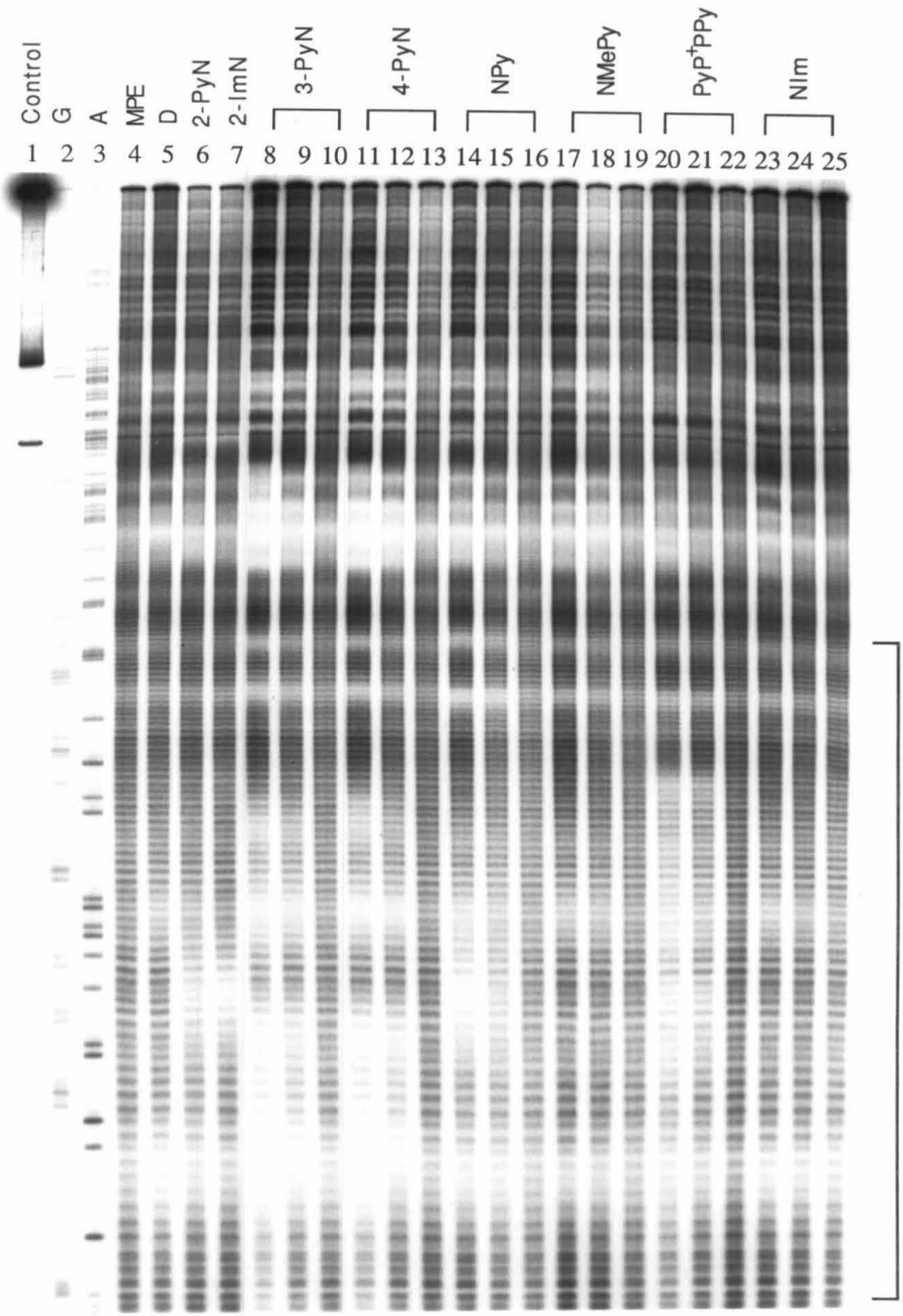
Control
G
A
MPE
D
2-PyN
2-ImN
3-PyN
4-PyN
NPy
NMePy
PyP+PPy
NIm
1 2 3 4 5 6 7 8 9 10 11 12 13 14 15 16 17 18 19 20 21 22 23 24 25

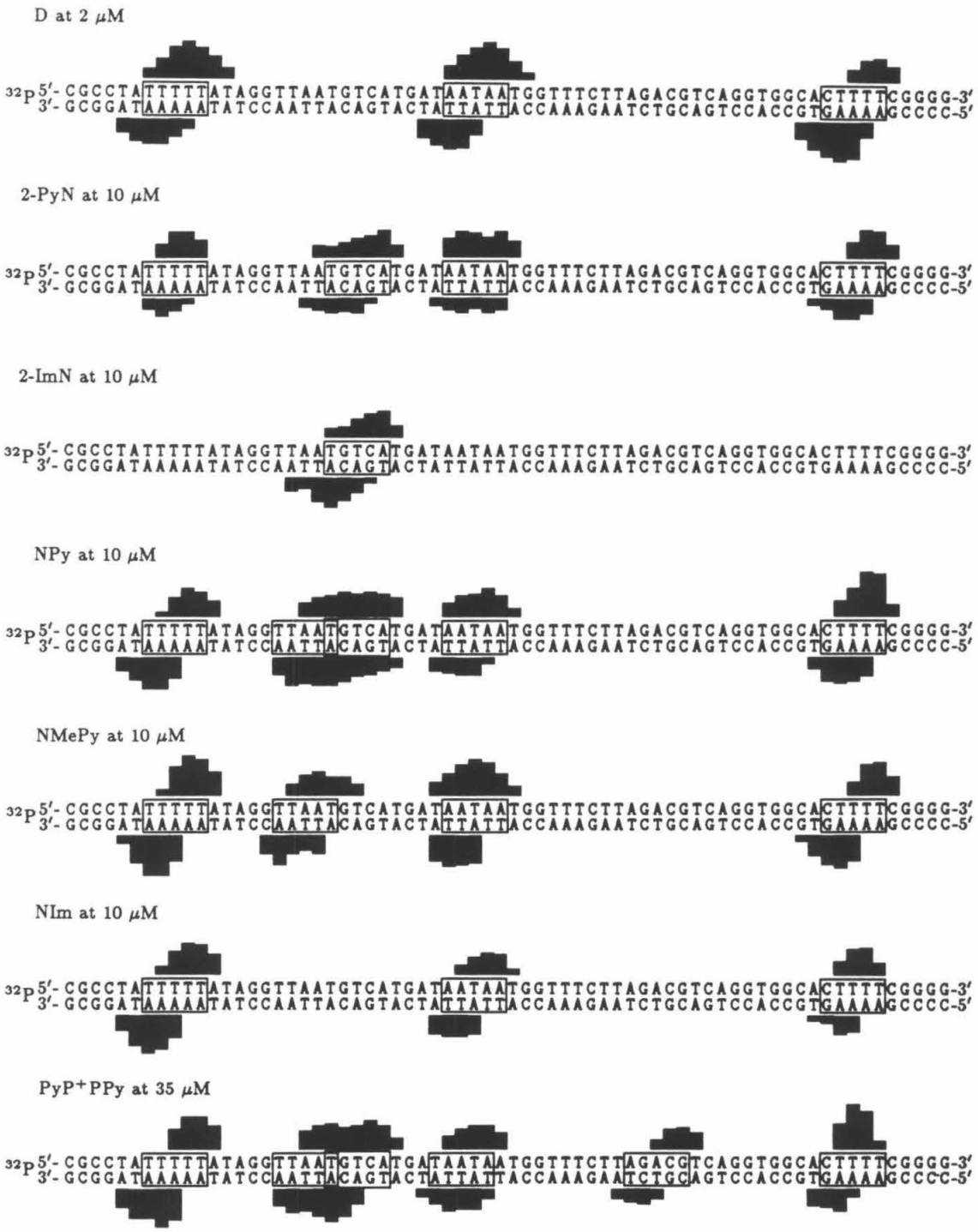

Figure 18 MPE·Fe(II) protection patterns of the C-terminal analogs of 2-PyN and 2-ImN.

presence of the AGACG binding site. It is possible that this compound could hydrogen bond with 3 G's, the first two exactly as in the 2-ImN complex, with the third G being picked up by the second pyridine nitrogen. Such a complex is predicted to show a strong orientation preference with the affinity cleaving derivative.

The behavior of NIm is also puzzling. Although this compound should be able to bind to WGWCW sequences, it does not. UV-visible spectra show no change between pH 5 and pH 11, thus it is unlikely that a protonation event is responsible for the A,T preference.

Methylation of the C-terminal amide is predicted to limit substantially the number of conformations available to NPy. From CPK and molecular modeling,[93] all *trans* methyl amide conformations are strongly disfavored by contacts between the amide methyl and the pyrrole ring. However, no such conformation can be fitted into a normal B DNA minor groove. The lowest energy conformers of NMePy that can fit apparently give A,T specificity.

Chemical Evidence for a Binding Conformation

From all of the compounds studied, some general conclusions can be drawn. The minimum requirement for WGWCW sequence binding is a heterocyclic nitrogen attached to two pyrrole rings. The nitrogen atom must be next to the amide, and better results are achieved when the carbonyl is directly attached to the heterocycle. The factors that determine 2-ImN like specificity are relatively weak, and

can easily be overwhelmed by other effects. It is instructive that only one compound, 2-ImN, binds only WGWCW sequences. Because the overall specificity of this class of compounds relies on the disfavoring of the normal binding sites, longer derivatives should show further decreases in specificity unless the imidazole to pyrrole ratio can be increased. At present, the imidazole must cap the N terminus of the polypyrrole subunit. To recognize more G's (*i.e.*, a TGACTCA site), it will be necessary to develop an imidazole linkage that can be used in the middle of a pyrrole chain.

The binding constant at WGWCW sites also seems to be independent of compound structure. Only one analog binds significantly more strongly than 2-PyN or 2-ImN. It might be possible to increase the binding constant by increasing the number of positive charges on the small molecule, but even simple electrostatic interactions appear to lower the binding specificity.[65, 135] If WGWCW binding is actually dominated by two hydrogen bonds, as the model suggests, than the best way to increase binding would be to increase the number of G's recognized. Again, this requires the development of a middle chain imidazole derivative with the proper specificity.

A recurring theme of this entire investigation is that simple substitutions lead to far-reaching consequences. Conservative changes of 2-PyN and 2-ImN have led to compounds that do not bind to DNA, compounds that prefer new mixed G,C, A,T sites, and compounds that revert to distamycin A specificity. The four

simplest compounds have a WGWCW sequence preference decreasing in the order 2-ImN > 2-PyN > NPy > NIm. However, it is clear that WGWCW sequence binding is characteristic of a family of synthetic compounds with varied structure. From this database, it should be possible to design similar molecules with good potential for complexation to other G,C-containing sites. A key problem with this class of compounds is the basicity of the final products. A protonation event at near neutral pH can easily shift a G,C binding molecule to an A,T binder. Fortunately, an analog with a pK_a near 7 is usually detected by the broad peaks of its ^1H NMR spectrum. To minimize this effect, the best choices are to use either 2-carboxyimidazole or pyrimidine rings for G recognition. Both have pK_as significantly below biologically relevant pH. Some potential targets that incorporate these design principles are shown in appendix C. The success of these designs would show that it is possible to use the specificity found in 2-ImN to complex to sequences in a rational manner. Judging from progress to date, however, it would seem that there are many surprises still waiting to be discovered.

Lastly, evidence for a particular 2-ImN conformation in the WGWCW complex is equivocal. The behavior of 3-MeOPyN and CycN favors models that use the crescent-shaped carbonyl-out conformations. In contrast, the data from AcImN and 2-ImD suggests that the carbonyl-in conformers that place a bend in the small molecule could be correct. There is no chemical evidence that addresses the possibility of dimer formation at the TGTCA site. There is also little evidence

for the amide conformation at the C-terminus of the pyrrole rings, although the behavior of PyP^+PPy slightly favors the carbonyl-in form.

It will take more direct observations to establish the details of the 2-ImN/TGTCA complex. With the specificity of 2-ImN firmly in hand, it should be possible to study the major DNA complex by physical techniques. ^1H NMR has been used with similar compounds to determine complex structure.[72] In this particular case, the analysis will almost certainly be complicated by the near C_2 symmetry of the binding site, and the asymmetry of 2-ImN. At saturation binding, there will be equal amounts of two diastereomeric complexes that differ from one another only in the orientation of 2-ImN with respect to the A,T bp. This will lead to four nonequivalent but closely related strands to be deconvoluted.[72] However, a minor groove dimer would be readily detected and might increase the symmetry of the complex. Better options are probably X-ray crystallography or resonance Raman, but degenerate orientations could still create serious difficulties.

A potential solution is shown in scheme 6. ImP^+P^+Im is completely C_2 symmetrical, and computer modeling indicates that there is potential for interaction with symmetric sites with sequence TGATCA. This compound has been synthesized from 1-methylimidazole-2-carboxylic acid , **36** and 1,2-diaminoethane, as shown in scheme 6. At present, little is known about its DNA binding specificity. ImP^+P^+Im does not bind well to the 517 bp fragment, but then the predicted site does not occur. Future experiments, especially with an affinity cleaving derivative,

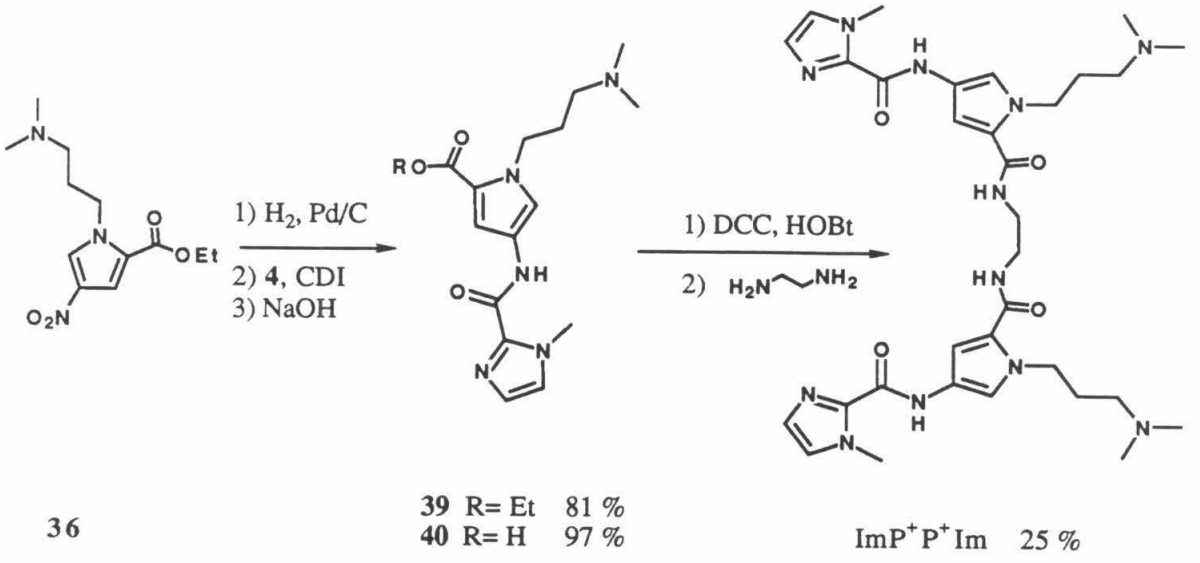

Scheme 6 Synthesis of ImP^+P^+Im.

should settle this question, and provide a derivative that can be more easily studied by other physical techniques.

Summary

A series of 2-PyN and 2-ImN derivatives has been prepared. The 4-chloropyridine derivative shows enhanced specificity for WGWCW sites (W is A or T). Replacement of the pyridine ring by pyrimidine increases the binding affinity without increasing the specificity. The 4-dimethylaminopyridine derivative binds with a pH sensitive specificity. At low pH, this compound binds tightly to A,T

rich sites. At high pH, the same compound binds most tightly to the TGTCA site. The 3-methoxypyridine derivative binds weakly to DNA. A bicyclic imidazole derivative binds only A,T sites.

Shorter analogs of 2-ImN do not bind the TGTCA sequence. The 4-acetamido derivative of 2-ImN also does not bind this site. An analog containing one imidazole ring and three pyrrole rings appears to bind the TGTCA site, but other G,C-containing binding sites are also observed. All of these analogs consist of a heterocyclic ring at the N-terminus of a polypyrrole subunit. Derivatives have also been prepared with a heterocyclic ring at the C-terminus. The C-terminal pyridine compound binds to the TGTCA site with lower specificity than 2-PyN. The imidazole compound binds only A,T rich sites. An N-methylamide pyridine compound binds solely to A,T sites. A compound with pyridine rings at both the N- and C-termini does bind the TGTCA site with lower affinity, as well as a three G-containing site. The only required structure for WGWCW sequence binding is the presence a heterocyclic nitrogen next to a carboxamide.

Chapter 5

Biological Implications of WGWCW Sequence Binding

As shown in the previous chapters, the key requirement for WGWCW sequence complexation is the imidazole or pyridine nitrogen. With a one atom C→N change, the specificity changes from A,T to WGWCW. It appears that WGWCW sequences have a unique conformation that allows for ready recognition by the small molecule. As nature tends to utilize recognizable structural features as control elements,[136] it seems likely that WGWCW sequences would also be complexed by proteins. A literature search reveals that this is indeed true, with a WGWCW sequence present in the consensus recognition sequence TGACTCA of both the eukaryotic transcriptional activator GCN4 and the AP-1 family of eukaryotic transcriptional activators/oncogenes.

Background

GCN4

Under conditions of amino acid starvation, GCN4 activates the *de novo* synthesis of new amino acids by increasing transcription at the appropriate genes.[137, 138] Deletion mutants of the 281 aa protein show that DNA binding is localized in the 60 aa terminal region.[139] GCN4 binds as a nonexchangeable dimer, with each monomer presumably binding specifically to half of the pseudosymmetric recognition site.[140] Activation occurs in both orientations of the binding site,[139] and is mediated by a 19 aa region that is highly negatively charged.[141]

Table 1 Effect of single mutations on the binding of GCN4 at *his3*.

Activity[a]	Sequence
Increased	A
Wild type	G G A T G A C T C T T T T T T T T T
Unchanged	C G A A G T
Decreased	C A A G G G T
No Detectable Activity	A A C A A G C C C G G C G T T T G

[a] Activity measured by resistance to aminotriazole and GCN4 binding ability.

The binding properties of GCN4 are quite similar to those of 2-ImN. The protein gives a 9 bp footprint at its binding site,[159] much smaller than a helix-turn-helix dimer ($\approx$ 28 bp). Saturation mutagenesis in the *his3* promoter region reveals that the TGACT sequence is required for strong binding.[146] As shown in table 1, additional bp give weaker effects, resulting in a TGACTCA consensus sequence for high affinity sites. A survey of a number of amino acid gene promoter regions reveals a similar pattern.[146] Like 2-ImN, A,T bp are usually present adjacent to the footprinted sequence (see tables 2 and 3).

AP-1

AP-1 is a family of related proteins that also appear to be transcriptional activators. There are at least four different species that bind to AP-1 like recog-

Table 2 Sequences similar to the *his3* GCN4 binding site found in other GCN4 inducible promoter regions.

Gene	Sequence	Position[a]	Ref
	Class I		
arg3	G T C G T G A C T C A T A T G	*−296*	142
arg4	T G A A T G A C T C A C T T T	*−183*	143
cpa1	T G T T T G A C T C A T C A T	*−488*	144
cpa2	C G A A T G A C T C T T A T T	*−297*[b]	144
his1	A G C G T G A C T C T T C C C	*−285*	145
his1	G A G G T G A C T C A C T T G	*−188*	145
his3	C G G A T G A C T C T T T T T	*−141*	146
his4	A C A G T G A C T C A C G T T	*−221*	147
his5	C T G T T G A C T C A C T T C	*−206*	148
ils1	A T G A T G A C T C T T A A G	*−80*	146
ilv1	G A G A T G A C T C T T T T T	*−137*[b]	149
ilv2	G C G A T G A T T C A T T T C	*−358*[b]	150
leu1	T A G A T G A C T C A G T T T	*−308*	151
leu3	C A T A T G A C T C A C A A C	*−423*	152
leu4	T A A G T G A C T C A G T T C	*−105*	153
trp2	T T G C T G A C T C A T T A C	*−166*	154
trp3	T C G T T G A C T C A T T C T	*−67*	155
A	3 5 4 8 0 0 17 0 0 0 12 0 4 4 0		
C	4 3 2 1 0 0 0 16 0 17 0 5 2 2 6		
G	4 5 9 5 0 17 0 0 0 0 0 2 1 0 3		
T	6 4 2 3 17 0 0 1 17 0 5 10 10 11 8		
	− − r r T G A C T C W Y w w −		

[a] relative position of the upstreammost bp with respect to the start codon. [b] Oriented in the opposite direction.

nition sequences, with varying specificities.[160] These proteins are involved in oncogenesis,[161] the biological activity of phorbol esters,[162] and the cellular response to growth factors.[163] The proto-oncogenes *jun* and *fos* have been shown

Table 3 Probable GCN4 binding sites similar to the SV40 enhancer sequence.[156]

Gene	Sequence	Position[a]	Ref
	Class II		
his3	T C C C <u>T G A C T A A</u> T G C C	*−233*[b]	146
his5	G A G A <u>T G A C T A A</u> A C T A	*−276*	148
his5	T T A A <u>T G A C T A A</u> T C C G	*−337*	148
leu2	T T C A <u>T G A C T A A</u> A T G C	*−162*	157
leu4	G C G A <u>T G A C T A A</u> C C T A	*−426*[b]	153
trp2	A A C A <u>T G A C T A A</u> A G G G	*−111*	154
trp5	A G A A <u>T G A C T A A</u> T T T T	*−66*	158
A	2 2 2 6 0 0 7 0 0 7 7 3 0 0 2		
C	0 2 3 1 0 0 0 7 0 0 0 1 3 2 2		
G	2 1 2 0 0 7 0 0 0 0 0 0 2 2 2		
T	3 2 0 0 7 0 0 0 7 0 0 3 2 3 1		
	− − − A T G A C T A A w − − −		

[a] relative position of the upstreammost bp with respect to the start codon. [b] Oriented in the opposite direction.

to be constituents of AP-1/DNA complexes.[164, 165] There is almost 50% homology between the DNA-binding regions of *jun*, *fos*, and GCN4, and *jun* can activate transcription at GCN4 sites.[141] Because the identity of AP-1 varies with the preparation,[160, 163] much less is known about the DNA specificities of these proteins. However, a TGACT sequence is almost always present in the observed binding sites.[165]

A Cleavage Assay for Specific DNA Complexes

A recent report from the Parker group has identified a yeast equivalent of AP-1 with similar binding properties to the mamalian proteins.[159] DMS footprinting

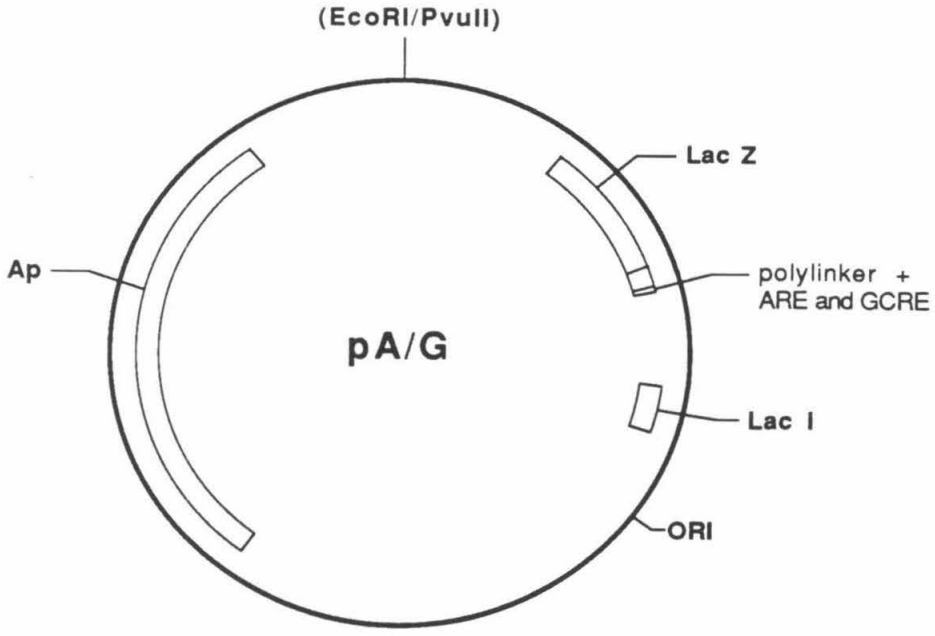

Figure 1 pAG plasmid as described by Harshman *et al.*[159]

shows protection for GCN4, AP-1, and yAP-1 only in the major groove.[159] Thus it might be possible to bind 2-ImN to the DNA-protein complex. Because the apparent binding affinity of the protein is a factor of 10^5 higher than 2-ImN, the presence of 2-ImN should have minimal effects on the protein complex. 2-ImN and 2-ImNE then become structural probes of the DNA conformation in the complex. Moreover, the 2-ImN binding site is placed asymmetrically in the protein binding site. If there is a direct interaction between protein and small molecule, binding and cleavage should also be affected asymmetrically.

The plasmid used for these studies is shown in figure 1. As reported by Harshman *et al.*, it consists of a pUC19 plasmid with the SV40 AP-1 recognition

element (ARE) inserted into the *BamH* I site of the polylinker, and the *his3* GCRE inserted into the *Pst* I site. The *EcoR* I/*Pvu* II restriction fragment of this plasmid allows simultaneous examination of GCN4 and yAP-1 binding. GCN4 binds with nearly equal affinity to both sites, whereas yAP-1 prefers the ARE by at least a factor of 20.[159]

The behavior of 2-ImN and 2-ImNE in the presence of yAP-1 and GCN4 is shown in figure 2. No attempt has been made to remove the proteins from the reaction mixture, so that a substantial portion of the DNA exhibits altered mobility in the protein-containing lanes. This probably could be avoided by phenol extraction before electrophoresis. The 2-ImNE used for these experiments is only 50% as active as expected. Figure 2 is a two-week exposure with concommitant increase in background. This is most noticeable in the yAP-1 lanes, where a faint purine lane is superimposed on the cleavage pattern.

Histograms of the footprinting data are shown in figure 3. 2-ImN binds specifically to the two protein binding sites, both of which contain the WWGWCW high affinity consensus sequence. As expected at these binding densities, GCN4 binds well to both sites, while yAP-1 is only detected at the ARE. Addition of 50 μM 2-ImN does not prevent protein binding, and appears to increase the amount of protection at the GCRE.

The 2-ImNE results are summarized in figure 4. Without added protein, 2-ImNE cleavage is very similar to sites on fragments previously reported. At the

Figure 2 Interactions between 2-ImN and GCN4 or yAP-1. Autoradiogram of an 8% denaturing polyacrylamide gel. All reactions contain 4 mM DTT, 100 μM-bp calf thymus DNA, and 12 kcpm 5′ labeled 280 bp *EcoR* I/*Pvu* II restriction fragment of plasmid pA/G[159] in 40 mM Tris·acetate pH 7.9 buffer. Lane 1, intact DNA; lane 2, G reaction;[80] lane 3, A reaction;[81] lanes 4–7 contain 4 μM MPE·Fe(II): lane 4, MPE·Fe(II) standard; lane 5 contains 50 μM 2-ImN; lane 6, 5 binding units of yAP-1[159]; lane 7, 50 μM 2-ImN and 5 units yAP-1; lanes 8–10 contain 2-ImNE at 75 μM, 50 μM, and 25 μM respectively; lanes 11–13 contain 5 units yAP-1 and 75 μM, 50 μM, and 25 μM 2-ImN respectively; lanes 14–16 contain 5 binding units GCN4 and 75 μM, 50 μM, and 25 μM 2-ImNE respectively; lanes 17–20 contain 4 μM MPE·Fe(II): lane 17 contains 5 units GCN4 and 50 μM 2-ImN; lane 18, 5 units GCN4; lane 19, 50 μM 2-ImN; lane 20, MPE·Fe(II) standard.

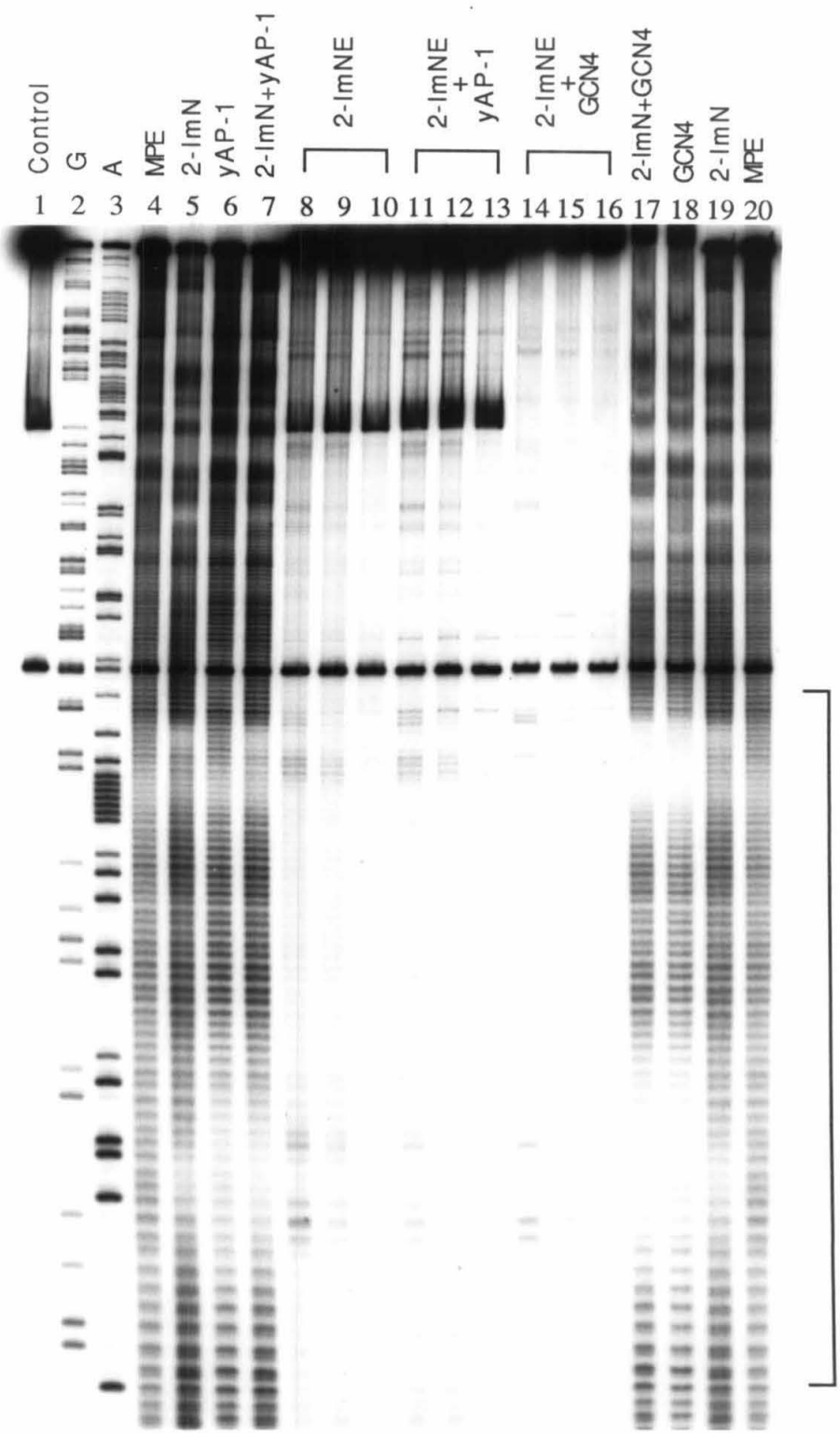
Control
G
A
MPE
2-ImN
yAP-1
2-ImN+yAP-1
2-ImNE
2-ImNE + yAP-1
2-ImNE + GCN4
2-ImN+GCN4
GCN4
2-ImN
MPE
1 2 3 4 5 6 7 8 9 10 11 12 13 14 15 16 17 18 19 20

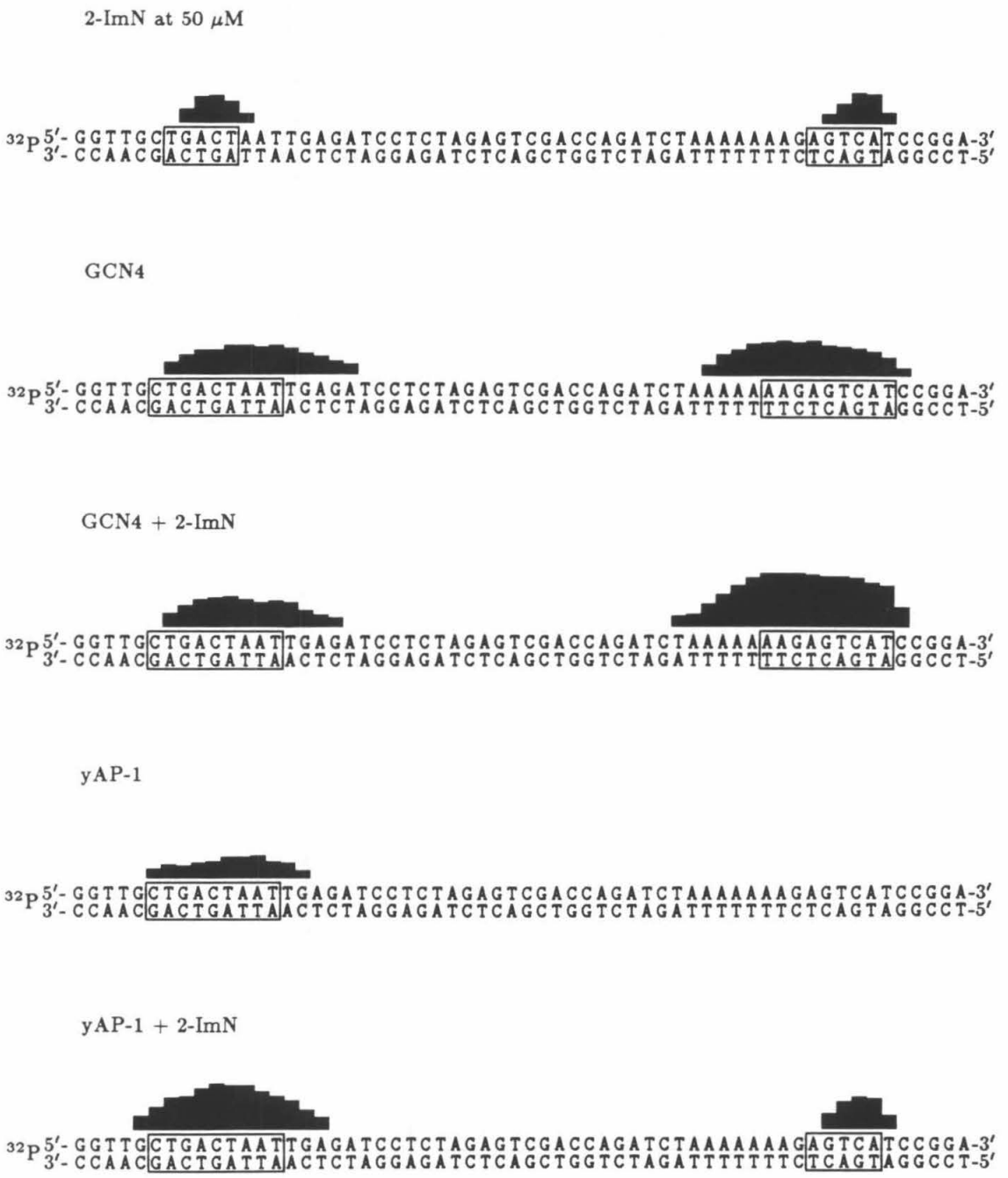

Figure 3 Protection of the ARE and GCRE by 2-ImN, GCN4, and yAP-1.

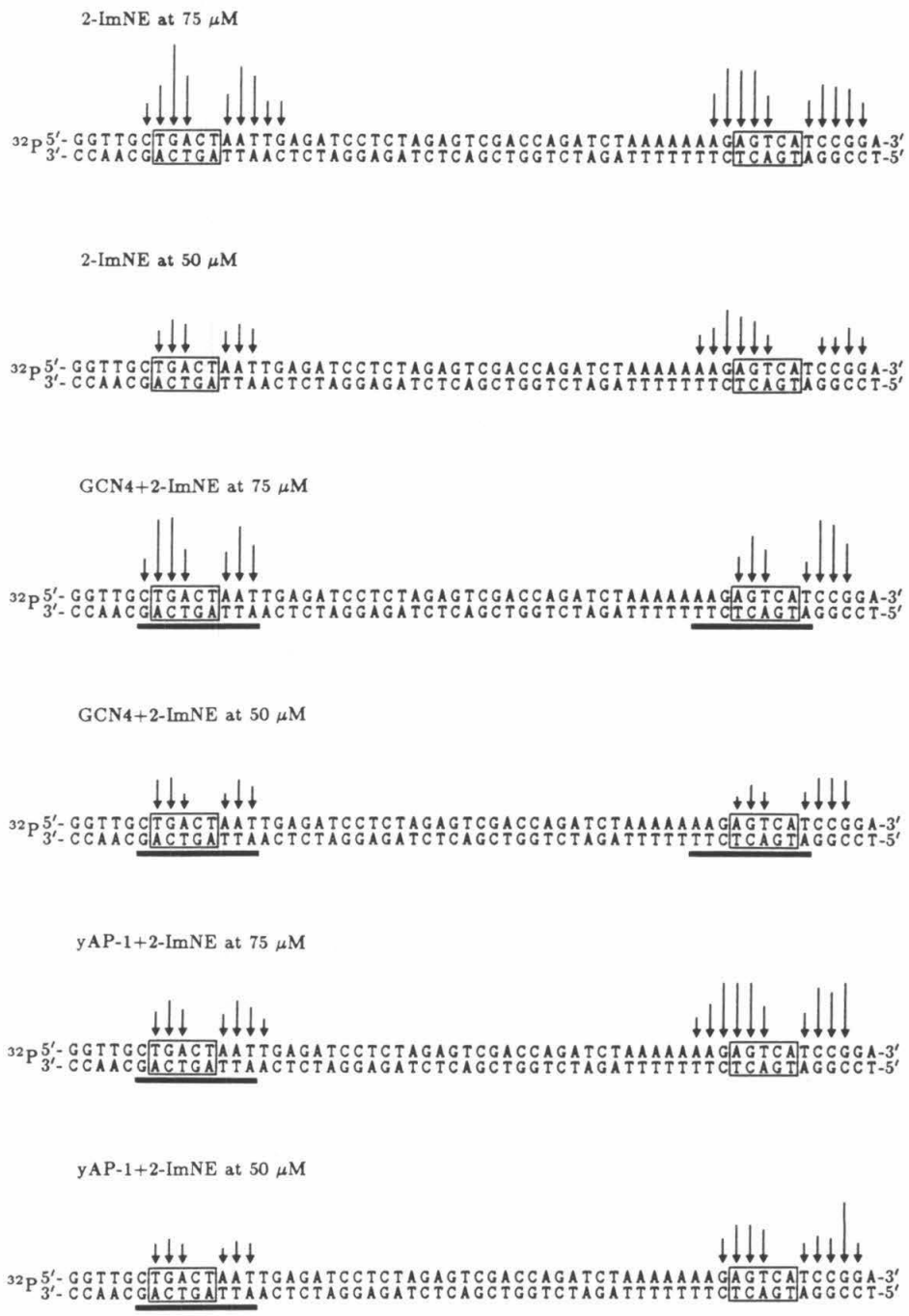

Figure 4 2-ImNE cleavage in the presence of GCN4 and yAP-1. Arrows represent the maximum density of 2-ImNE cleavage bands. Bars represent the protein footprints from reference 159 and figure 3.

GCRE, there appears to be a small orientation preference, with better cleavage at the AAAAAAA end of the site. Cleavage is much diminished at 50 μM, and nonexistent at 25 μM. Addition of 5 binding units of yAP-1 to the affinity cleaving reactions gives an identical cleavage pattern at the GCRE, but substantially reduces cleavage at the ARE. The shape of the cleavage patterns remains the same in the presence of the protein. Therefore yAP-1 inhibits 2-ImNE cleavage symmetrically at its binding site. Addition of GCN4 produces completely different results. The cleavage pattern at the 5′ end of the GCRE sharpens considerably, but the overall cleavage efficiency is only slightly lower at either site. In both cases, the inhibition of MPE·Fe(II) cleavage is much greater than the inhibition of 2-ImNE cleavage. This implies that 2-ImN and the proteins are binding simultaneously to the same binding site from opposite grooves. Thus *the DNA conformation found in the GCN4 complex is identical, (within experimental error) to that found in the 2-ImN complex.*

The altered pattern at the GCRE cannot be due simply to a change in orientation preference, because the amount of cleavage at the 3′ end of the site remains essentially constant, and cleavage at the first two bands of the 5′ end is close to the level seen without GCN4. Instead, the missing cleavage maps exactly to the end of the poly A stretch. MPE·Fe(II) also shows enhanced protection over the complete homopolymer A sequence. This effect is seen in a region where there is relatively low homology between GCN4 binding sites, which argues against direct protection

by the protein. Instead it suggests that the region undergoes a conformational change upon GCN4 binding.

It is well known that runs of homopolymer A exhibit altered structure in the solid phase,[87] and a decreased susceptibility to oxidative cleavage in solution.[166, 167] Recently, Klug and co-workers have solved the structure of a B DNA dodecamer containing an AAAAAA sequence.[87] In the crystal, the A,T bp are propeller twisted by an average of 20° with almost no tilt or roll between bp. This allows for maximum stacking between the bases. The minor groove is considerably narrower (9.5 Å) than expected for random sequence DNA (11 Å).[94] A key feature is the presence of interbase-pair bifurcated hydrogen bonds, which appear to stabilize the highly twisted conformation. The presence of an AAA sequence is the minimum structural requirement, with only the interior bp capable of bifurcation. This same feature has also been observed in the A,T sequence of the distamycin A-DNA cocrystal.[20] In solution, Tulius has shown that stretches of A's longer than three bp show diminished cleavage when treated with EDTA·Fe(II), presumably an effect of the narrower minor groove.[166] The effect is strongest at the 3′ end of the stretch of A's, which would place the most altered structure directly adjacent to the GCN4 site. A reasonable hypothesis is that the presence of the poly(dA)·poly(dT) sequence at the GCRE increases the GCN4 affinity by favoring a more propeller twisted complex. GCN4 binding would in turn favor the bifurcated conformation of the poly A segment by increasing the propeller twist of adjacent bp.

This hypothesis is also supported by the biological evidence. The stretch of A's is not well conserved over GCN4 binding sites, consistent with an indirect role in complexation (table 1). At *his3*, presence of at least three T's to the 5′ of the binding site is necessary to increase GCN4 binding and *his3* transcription levels. Presence of more than 6 T's gives no further increase in binding or transcription,[146] the expected result if a stable altered conformation has been reached. A similar role for A,T bp has been observed in the 434 repressor crystal structure.[97] The central A,T bases of the DNA sequence do not contact the protein directly, yet they are highly twisted and appear to form a very similar bifurcated array. This allows the protein to maximize dimer interactions. At the center of this region, the minor groove is only 9 Å wide, similar to the Klug DNA structure. G,C bp present in this region are highly propeller twisted, unlike the G,C bp at the ends of the binding site.

Differences between the effects of yAP-1 and GCN4 on 2-ImNE cleavage could be due to a number of factors. It is unlikely that yAP-1 directly blocks 2-ImN binding, because the cleavage inhibition is symmetric over the binding site. However, either a complex with a different DNA conformation or a simple electrostatic effect, where yAP-1 neutralizes the DNA negative potential more effectively than GCN4, would satisfactorily explain the differences. To be able to evaluate these possibilities, it is necessary to consider the structure of these proteins and their DNA complexes in more detail.

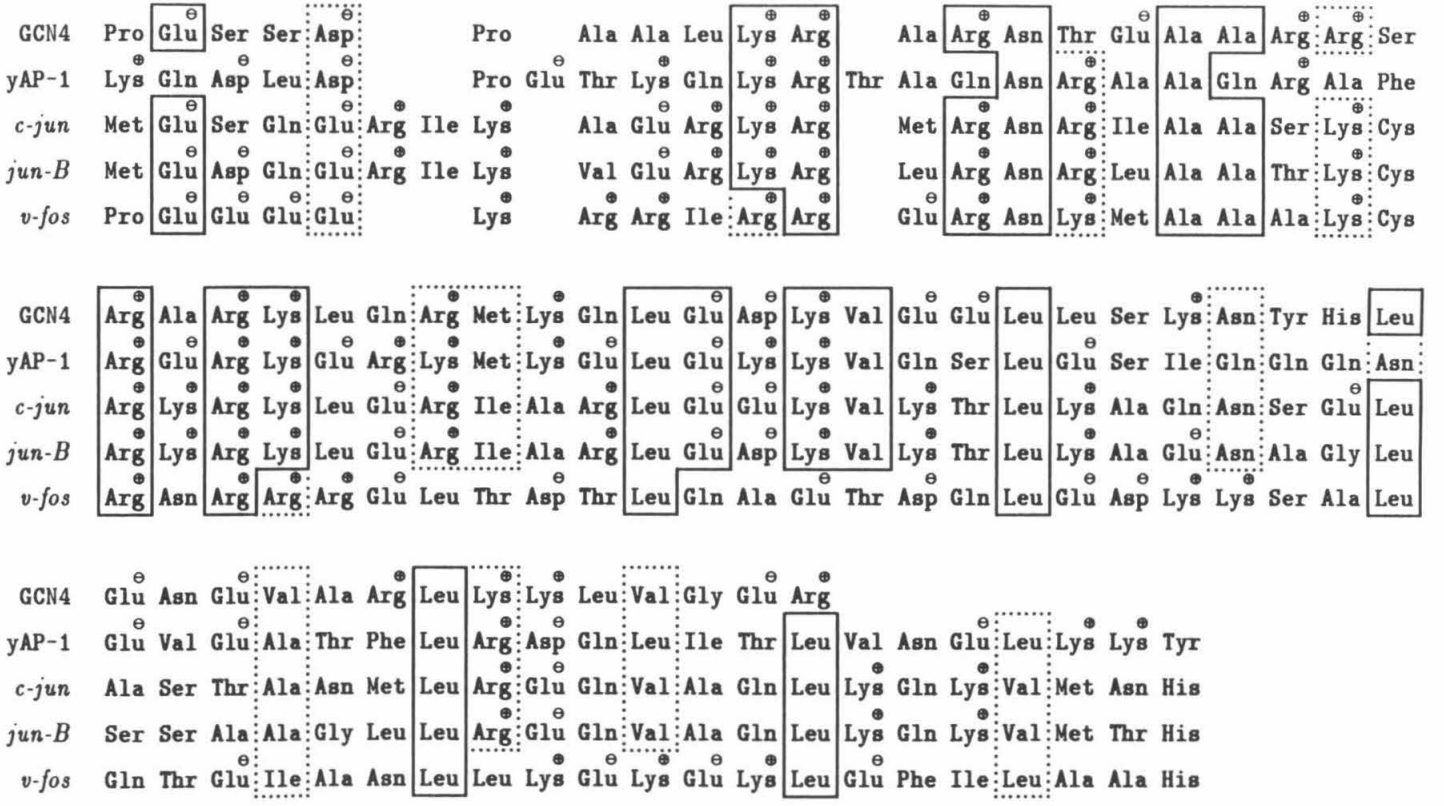

Figure 5 Homology comparison of proteins with known sequence which bind to the ARE. The alignment was generated by matching the N-terminal leucine of the the leucine zipper. Amino acids 217 to 281 of GCN4,[168,169] 59 to 127 of yAP-1,[170] 256 to 324 of *c-jun*,[171] 260 to 328 of *jun-B*,[163] and 134 to 200 of *v-fos*.[172]

GCN4 and AP-1 Structure

While these proteins have not been crystallized, comparisons between the various proteins that bind the ARE site have been used to assess structure. The putative DNA binding regions for the proteins with published sequences are shown in figure 5. Deletion analysis has shown that this region is responsible for most of the DNA specific contacts for GCN4,[140] *jun*[141] and yAP-1.[173] Given the degree of similarity between all these proteins, this is likely to carry over to the others as well. There appears to be no specific organization of this protein family. In GCN4 the binding domain is at the C terminus, while in yAP-1 the putative binding domain is near the N-terminus. The proteins also vary widely in size, from GCN4 at 281 aa to yAP-1 at $>$ 600 aa.

This family of proteins does not display significant homology to either the helix-turn-helix or zinc finger DNA binding proteins, so that new model DNA binding structural motif is indicated.[139] All of the proteins have a 45 aa region predicted to have high alpha helix content with a leucine at every seventh position. Homology comparisons between this portion of GCN4, *jun*, *fos*, and several other proteins led Landschulz *et al.* to propose a structure for this region.[174] In the model, leucines on a long alpha helix of one peptide chain interdigitate with the leucines on the same helix of a second peptide chain to form a stable dimer, which they term a leucine zipper (see figure 6). As proposed, the helices could be either parallel or antiparallel and still keep the C_2 symmetry seen in transcriptional activation. The

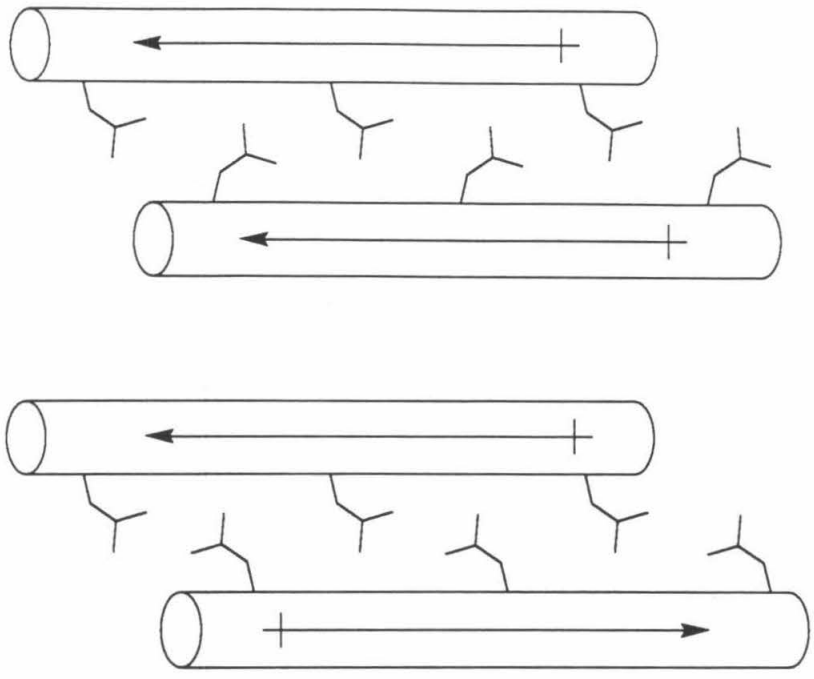

Figure 6 Proposed parallel and antiparallel leucine zipper structures.[174] Cylinders represent the alpha helix of each monomer.

authors favored the antiparallel conformation because it gave better overlap in the computer modeling.

Most available evidence suggests that the helices are actually aligned in the parallel orientation. Although binding and activation occur at the same DNA sites for both *jun* and GCN4, the number of leucines in the zipper region is different. For the antiparallel conformation, the dimer with maximum leucine overlap would moves the DNA binding regions of the *jun* monomers 7 aa (about 9 Å) farther apart than in the GCN4 case. It seems highly unlikely that the strong homology observed in the basic region adjacent to the zipper would exist with such a large

difference in complex geometry. More importantly, the antiparallel dimer would have no net helical dipole, whereas the parallel dimer would have a large dipole oriented so that the positive terminus is at the DNA. Such an arrangement has been proposed to be a major contributor to the stability of the *EcoR I*-DNA complex.[175]

Simple Binding Model for GCN4

The simplest binding model that explains all current data is shown in figure 7. To take advantage of the maximum effect of the helix dipole, the leucine zipper is shown perpendicular to the helix axis. In the dimer, the two zipper helices must be offset by 3–4 bp from one another. If the helices continue into the DNA-binding region, then the ends of the helix will create a three residue L-shaped pocket at the N terminus of the helix. Computer modeling[95] indicates that this structure can fit into the major groove of B DNA with potential for specific contacts to all the recognized bases.

The model predicts that residues forming specific contacts could be found at 3–4, 7, 10–11, or 14 aa from the end of the leucine zipper. It is interesting that two of the regions with the highest homology in the basic region are 7 and 10 residues from the N-terminal leucine. The model also explains the asymmetric specificity requirements seen in the mutagenesis experiments. Because of the offset α helix, one monomer helix will interact head-on with the DNA sequence, while the other will interact from the side. Thus, identical residues on identical monomers have different positions with respect to the DNA. The actual residues involved in base

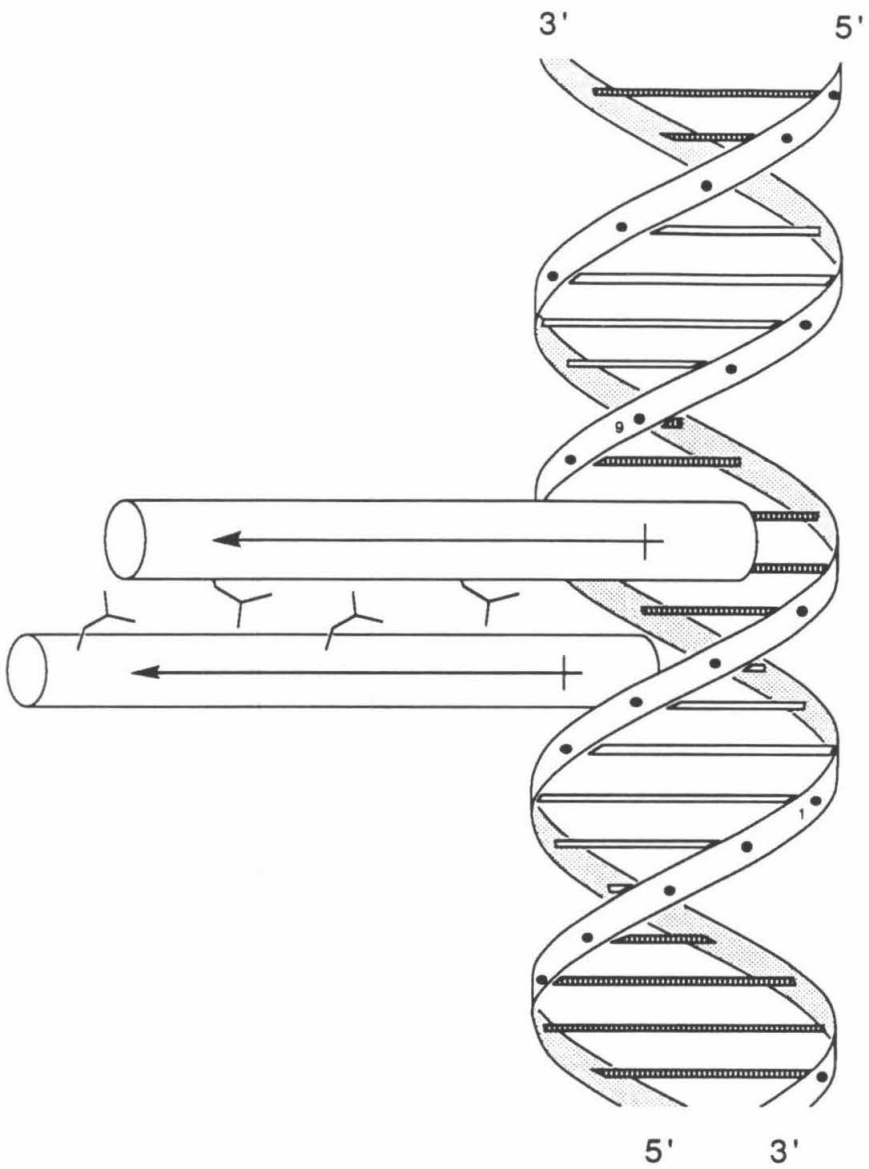

Figure 7 A Hypothetical leucine zipper DNA complex. The leucine containing alpha helices oriented parallel to each other and perpendicular to the major groove. The N-termini are placed near the DNA by analogy to the *Eco R* I crystal structure.[175] The proposed complex can interact readily with 9 bp, as observed by MPE·Fe(II) footprinting.[159] 2-ImN presumably binds in the minor groove at the right of the model.

contacts are not known. However, there are several highly conserved arginines present in the basic region. Experiments are currently underway in the Parker group to determine the specific contacts by replacing Arg by Lys using site directed mutagenesis techniques.[173]

Conformationally Isomeric Complexes?

An explanation for the difference of 2-ImNE cleavage based on electrostatic arguments predicts that yAP-1 would be more positively charged so as to inhibit 2-ImN binding. Figure 6 shows that this is not the case. Starting with the first proline shown, the basic region up to the leucine zipper has a +10 net charge, while the same region in yAP-1 is +8. The zipper regions of both proteins have a net −1 charge. Overall, both proteins are quite negatively charged (−11 for GCN4 and −33 for AP-1).

This leaves a change in DNA conformation as the most likely source of the cleavage differences. Increasing or decreasing the propeller twist would disrupt the optimum alignment of 2-ImN and the G,C bp it recognizes. Alternatively, decreasing the width of the minor groove would prevent 2-ImN from binding. The evidence best fits a decrease in propeller twist in yAP-1 complexes compared to GCN4 complexes. An increase in propeller twist or a narrower minor groove are predicted to be favored at the GCRE, yet yAP-1 prefers the ARE by a large factor. In addition, AP-1 binding sites that have been sequenced show an increased number of G,C bp outside the recognition sequence.[162, 164] Do the different proteins of the

AP-1 family bind varying conformations of the same sequences? Future studies with 2-ImNE and other probes might be able to answer this question.

Summary

A 2-ImN binding site is present in the consensus sequence of a family of transcriptional activators. Presence of 50 μM 2-ImN does not inhibit protein binding for two members of this family, GCN4 and yAP-1. MPE·Fe(II) cleavage is strongly inhibited in the presence of either protein. 2-ImNE cleavage is only slightly inhibited by GCN4. This indicates that both protein and small molecule are bound simultaneously by the same DNA sequence. yAP-1 inhibits 2-ImNE cleavage more efficiently. A simple model for the DNA-protein complex is proposed.

Chapter 6

Experimental Procedures

General DNA Procedures

Reagents

All water used was distilled, filtered through an organic removal cartridge (Corning) and redistilled. For DNA manipulations, the water and all buffers used were autoclaved for 20 min at 160°C. Acrylamide was purchased as a 30% solution from National Diagnostics. To each liter was added 15 g (1.5%) N, N'-methylene-bisacrylamide. Chloroform was prepared by adding 4% amyl alcohol to reagent grade chloroform. Recrystallized phenol was purchased from Bethesda Research Labs (BRL) and saturated with water. 5X TBE (acrylamide gel buffer) and 10X TAE (agarose gel buffer) were prepared by standard methods.[176] Formamide loading buffer was prepared by adding 100 μL 5X TBE to 1 mL twice recrystallized formamide containing 0.1% bromophenol blue and 0.1% xylene cyanol. Ficoll loading buffer was prepared by dissolving 12.5 g Ficoll in 100 mL water containing 0.25% bromophenol blue and 0.1% xylene cyanol. All other reagents were used as received.

Calf thymus DNA was sonicated for 1 min and extracted with equal volumes of phenol, 1:1 phenol:chloroform, chloroform, and butanol twice. The solution was exhaustively dialyzed against water and diluted to 1 mM-bp. Sigma type XX tRNA, was deproteinized by extraction with phenol, 1:1 phenol:chloroform, chloroform, and butanol twice, and diluted to 1 mg/mL. Poly(dG)·poly(dC) from Boehringer-Mannheim (25 AU) was dissolved in 5 mL water over 20 min with sonication

(cleaning bath), extracted with phenol, 1:1 phenol:chloroform, chloroform, and butanol 5 times, and lyophilized to 1 mL. The solution was diluted to 500 μM-bp with 5 min sonication (cleaning bath).

Plasmid pBR322 was grown in HB101 cells and purified by CsCl gradient.[176] Plasmid pAG, a pUC19 derived plasmid containing the *his3* GCN4 binding site and the SV40 ARE AP-1 binding site; GCN4, purified by phosphocellulose chromatography; and yAP-1, purified by ion exchange and DNA affinity chromatography,[159] were gifts of K. Harshman. ^{32}P labeled nucleotides were purchased from Amersham. Restriction endonucleases were purchased from New England Biolabs and Boehringer-Mannheim. Calf alkaline phosphatase, DNA polymerase I, Klenow fragment and T4 polynucleotide kinase were purchased from Boehringer-Mannheim.

Concentrations of all compounds studied were determined by UV. Mg quantities of the compounds studied were weighed on a Sartorius microbalance and diluted to 100 mL with water. The average molar extinction coefficient from three measurements was used to determine the concentration of a stock solution, which was lyophilized in 600 μL double-lock eppendorf tubes and stored dry at $-20°$C.

Ethanol Precipitation

To the DNA solution to be purified was added 1/10 volume 3 M sodium acetate at pH 5.2 and 3 volumes ethanol. The solution was vortexed and incubated at 0°C for 10 min. The solution was then centrifuged at 13,000 rpm for 25 min in an

Eppendorf model 5415 microcentrifuge, and the supernatant was decanted and discarded. 300 μL 70% ethanol was added and the tubes were centrifuged at 13,000 rpm for 10 min. The supernatant was discarded, and the DNA pellet was dried for 5 min on a Sorval Speedvac at <1 Torr.

Ammonium Acetate Ethanol Precipitation

To the DNA solution to be purified was added 1/2 volume 7.5 M ammonium acetate, pH 5.2, and 2 volumes ethanol. The solution was vortexed and incubated at 0°C for 10 min. The solution was then centrifuged at 13,000 rpm for 25 min, and the supernatant was decanted and discarded. The DNA was resuspended in 50 μL water and the procedure repeated. Finally, 300 μL 70% ethanol was added to the pellet and the tubes were centrifuged at 13,000 rpm for 10 min. The supernatant was discarded, and the DNA pellet was dried for 5 min on a Sorval Speedvac at <1 Torr.

Electrophoresis

Agarose Gels

For DNA purification, a horizontal agarose gel containing 2 μg ethidium bromide/ 100 mL was used. The appropriate amount of agarose in 200 mL 1X TAE buffer was heated to a rolling boil, cooled to 70°C, and poured into the UV transparent tray of a Pharmacia GNA 100 horizontal gel apparatus. For gels > 1%, a comb that gave 1 mm x 5 mm wells was used. For lower percentage gels, a 2 mm x 4 mm comb was necessary. The DNA was visualized on a Fotodyne

Transilluminator, and the bands were excised from the gel and purified by either electro-elution or melting followed by phenol extraction.

For cleavage assays, a 1% agarose vertical gel was used. 2 g agarose was suspended in 200 mL TAE buffer, heated to a rolling boil, and cooled slowly. The gel plates were clamped upright in a gel pouring stand, and an agarose plug was poured. When the plug had solidified and the temperature of the main agarose solution was between 50 and 55°C, the solution was poured between the plates and capped with a comb. Cooling gave a 14 cm x 21 cm x 4 mm gel with twelve wells 3 mm thick by 8 mm wide separated by 3 mm.

The gel was set vertically in a Watson Products EV300 apparatus and pre-electrophoresed with fan cooling at 120 V for 15 min. The DNA solution in 1X Ficoll buffer was added to the wells and the gel was electrophoresed at 120 V with fan cooling until the bromophenol blue was 3 cm from the bottom of the gel. The plates were separated, and the gel transferred to filter paper and dried at <1 Torr on a Bio-Rad model 483 Slab dryer for 30 min at 60°C, then 30 min at 80°C. X-ray film was exposed to the dried gel for 12–36 h at 25°C.

Polyacrylamide Gels

An 8% denaturing polyacrylamide gel was prepared from 36 g urea, 16 mL 5X TBE, 20 mL of a commercial 30% acrylamide solution containing 1.5% bis-acrylamide, 50 mg ammonium persulfate and water to make 80 mL. The solution was run through a 0.45 μm filter, 20 μL tetramethylethylenediamine was added,

and the solution was poured between glass plates using a standard 0.4 mm spacer and comb set (BRL). Polymerization gave a 31 cm x 37 cm x 0.4 mm 8% gel with 32 wells 6 mm wide separated by 3 mm.

The gel was set vertically on a BRL model S2 gel setup with aluminum backplate and pre-electrophoresed at the running voltage for 1 h. The DNA solutions in formamide buffer were heated to 90°C for 3 min, chilled on ice, and loaded into the wells. A typical 8% gel was electrophoresed at 1100 V for ~3 h until the bromophenol blue eluted from the bottom of the gel. X-ray film was exposed to the dried gel for 10–14 h at −80°C with one intensifying screen and for 4–10 d at 25°C without intensification.

Preparation of Labeled Restriction Fragments

A list of the labeled restriction fragments used is shown in table 1. The appropriate plasmid was linearized with a restriction enzyme, labeled on either strand, and cut with a second enzyme. The radioactive DNA was isolated on a 1% LMP agarose gel containing ethidium bromide, running at 32 V for 2.5 h. The band visualized by UV was cut out of the gel and eluted using a Schleicher and Schuell Elutrap (1X TAE, 100 V for 2.5 h). The DNA-containing solution was extracted with phenol, 1:1 phenol:chloroform, chloroform, and butanol 5 times, ethanol precipitated, resuspended in water and stored at −20°C.

Table 1 Restriction Fragments Utilized.

Plasmid Size	Fragment Enzyme	First *dNTP*	[α-^{32}P] dNTP	Cold Enzyme	Second
pBR322	167	*EcoR I*	dATP	TTP	*Rsa I*
	517	*EcoR I*	dATP	TTP	*Rsa I*
	279	*BamH I*	dATP, dGTP	dCTp, TTP	*Sal I*
	381	*BamH I*	dATP, dGTP	dCTP, TTP	*EcoR I*
	279r	*Sal I*	dCTP, TTP	dATP, dGTP	*BamH I*
	720	*Sal I*	dCTP, TTP	dATP, dGTP	*Sty I*
	550	*Hind III*	dATP, dGTP	dCTP, TTP	*Rsa I*
pA/G	280	*EcoR I*	dATP	TTP	*Pvu II*

Restriction Enzyme Digests

Conditions for restriction enzyme digestion are shown in table 2. All digests were performed on 15 μg plasmid DNA in 100 μL total volume. After the specified time at 37°C, the DNA was purified by ethanol precipitation.

3' Endlabeling

Labeling with Klenow fragment followed standard procedures.[176] To a solution of 15 μg linearized plasmid in 5 μL water was added 5 μL 10X HaeIII buffer, 5 μL 10 mg/mL DTT, 10 μL of each [α-^{32}P]nucleotide triphosphate needed, and 5 μL of each cold nucleotide triphosphate (10 mM, pH 7) needed. The presence of two radioactive nucleotides was generally sufficient. The volume was adjusted to 45 μL with water, 5 μL of a 5 U/μL solution of Klenow fragment was added, and the reaction was incubated at 25°C for 25 min. 2 μL of a 5 mM, pH 7 solution of all

Table 2 Restriction Enzyme Digest Conditions.

Enzyme	Units/ μg DNA	[Tris] (mM)	pH	[NaCl] (mM)	[$MgCl_2$] (mM)	DTT[a]	β-ME[b]	Time (h)
Bam HI	5	10	7.9	150	10			1.5
Eco RI	2	100	7.5	50	5			2
Hind III	4	10	7.5	50	10			2
Pst I	5	10	7.4	100	10	√		1
Pvu II	7	10	7.5	50	10	√		1.5
Rsa I	1.5	10	8.0	50	10	√		1
Sal I	10	10	7.9	150	10		√	2.5
Sty I	5	10	8.5	100	10	√		2
Xmn I	5	10	8.0	6	10	√		2

[a] Dithiothreitol. [b] 2-Mercaptoethanol.

four cold nucleotides was then added and the solution was incubated at 25°C for 10 min. The radioactive DNA was isolated by ammonium acetate precipitation.

5′ Endlabeling

Labeling of the 5′ end of a linearized plasmid by treatment with calf alkaline phosphatase and then T4 polynucleotide kinase followed standard procedures.[176] A solution of 15 μg linearized plasmid in 170 μL water and 20 μL 10X CAP buffer was treated with 10 μL of a 1 U/μL calf alkaline phosphatase solution, incubating at 37°C for 30 min. The solution was extracted with phenol, 1:1 phenol:chloroform, chloroform, and butanol twice, then ethanol precipitated. The DNA was redissolved in 28 μL water, 5 μL 10 mg/mL DTT, 5 μL 10X kinase salts and 10 μL [γ-^{32}P]ATP. The solution was treated with 2 μL 11 U/μL T4 polynucleotide ki-

nase and was incubated at 37°C for 45 min. The DNA was isolated by ammonium acetate/ethanol precipitation.

G Reaction[80]

A 1.5 mL eppendorf tube containing 100 μL 100 mM sodium cacodylate, pH 8; 40 μL 10 mM EDTA, pH 8; 3 μL 1 mM-bp calf thymus DNA; 100,000 cpm labeled restriction fragment and water to make 199 μL was cooled to 0°C. One μL dimethyl sulfate was added, the tube was shaken vigorously and incubated at 25°C for 2.5 min (3 min for fragments smaller than 300 bp). The reaction was quenched with 50 μL stop buffer (47 μL 4 M sodium acetate, pH 5.2, 9 μL 2-mercaptoethanol, 6 μL 1 mg/mL tRNA and water to make 125 μL) and 750 μL ethanol. After ethanol precipitation, the pellet was resuspended in 100 μL 10% piperidine and heated to 90°C for 30 min. The solution was lyophilized four times and diluted to 4000 cpm/μLwith formamide loading buffer.

A Reaction[81]

To a solution of 3 μL 1 mM-bp calf thymus DNA and 100,000 cpm labeled restriction fragment in a total of 160 μL water was added 40 μL of a pH 2 potassium tetrachloropalladate solution (1.6 mg K_2PdCl_4/100 μL of 100 mM NaCl/HCl, pH 2). The reaction was incubated for 40 min at 25°C, quenched with 50 μL G reaction stop buffer and 750 μL ethanol, precipitated, heated with 10% piperidine for 30 min, lyophilized four times and resuspended in formamide as for the G reaction.

Labeling of Linear pBR322

pBR322 was linearized as above with *Sty* I, and then labeled on the 3′ terminus of the clockwise strand with [α-^{32}P]dATP or on the 3′ terminus of the counterclockwise strand with [α-^{32}P]TTP using Klenow fragment. The radioactive plasmid was purified on a 0.7% agarose gel (16 V, 9 h) containing ethidium bromide. The linearized plasmid band was cut out, diluted with 500 μL TE buffer (20 mM Tris, 1 mM EDTA, pH 7.9), melted at 70°C for 10 min, extracted with phenol, 1:1 phenol:chloroform, chloroform, and butanol five times and ethanol precipitated. The pellet was resuspended in water, diluted to 4000 cpm/μL, and stored at −20°C.

Molecular Weight Standards

Equal amounts of the [α-^{32}P]A and [α-^{32}P]T labeled plasmid were combined with 1 μg λ DNA and digested with the restriction enzymes *Eco* RI, *Xmn* I, *BamH* I, and *Pst* I or *Pvu* II. The reactions were ethanol precipitated, counted, diluted to the same concentration (cpm/μL) and equal volumes were combined with the same cpm of intact pBR322.

DNA Binding Assays

MPE·Fe(II) Footprinting

MPE·Fe(II) footprinting followed the standard method.[14,45] A 100 μM MPE·Fe(II) solution was prepared by mixing 10 μL of a 1 mM MPE solution with 10 μL of a freshly prepared 2 mM ferrous ammonium sulfate solution in the dark, then diluting to 100 μL. This solution could be stored at −20°C for several months.

Just before use, the 100 μM stock solution was thawed and the appropriate amount diluted 1:5 with water.

A DNA cocktail was prepared containing 1 μL/tube 20X TA buffer (800 mM Tris, 100 mM sodium acetate, pH 7.9), 2 μL/tube 1mM-bp calf thymus DNA, 36,000 cpm labeled restriction fragment and water to make 8 μL/tube total solution. The solution was pipetted into individual 600 μL eppendorf tubes and 4 μL of a 5X solution of the compound was added. The tubes were vortexed, spun down and incubated in the dark for 30 min at 37°C. To each tube was added 4 μL of the 20 μM MPE·Fe(II) solution above and 4 μL of a freshly prepared 20 mM DTT solution in separated drops. Final concentrations: 40 mM pH 7.9 Tris·acetate, 5 mM sodium acetate, 100 μM-bp DNA, 4 μM MPE·Fe(II) and 4 mM DTT, in 20 μL. The reactions were incubated at 37°C for 10 min (15 min for fragments shorter than 300 bp). The solutions were frozen, lyophilized, Cerenkov counted on a Beckman LS 3801 scintillation counter, diluted to 3000 cpm/μL with formamide loading buffer, and electrophoresed on a denaturing polyacrylamide gel.

MPE·Fe(II) Footprinting at pH 6.0–10.0

A DNA cocktail was prepared for each pH studied from 2 μL/tube 10X CPB buffer (200 mM sodium citrate, 200 mM disodium hydrogen phosphate, 100 mM boric acid, 200 mM sodium hydroxide, adjusted to the proper pH with concentrated hydrochloric acid), 2 μL/tube 1 mM-bp calf thymus DNA and water to make 8 μL/tube. The procedure for MPE·Fe(II) footprinting was followed exactly

except that 4 μL 5 mM sodium ascorbate was added as the reducing agent. Final concentrations: 20 mM citrate, 20 mM phosphate, 10 mM borate, ~20 mM sodium chloride, 4 μM MPE·Fe(II) and 1 mM sodium ascorbate, in 20 μL. Cleavage time varied with pH. 18 min at pH 6, 4 min at pH 7–8, 8 min at pH 9 and 30 min at pH 10 gave comparable cleavage. The reactions were lyophilized, counted, diluted and electrophoresed.

EDTA·Fe(II) Footprinting[86]

A DNA cocktail was assembled from 1 μL/tube 20X TN buffer (400 mM Tris, 2 M NaCl, pH 7.4), 2 μL/tube 1 mM-bp calf thymus DNA, 36,000 cpm/tube labeled restriction fragment and water to make 8 μL/tube. This was pipetted into individual 600 μL eppendorf tubes and 4 μL of a 5X solution of the compound to be footprinted was added. The solutions were mixed and incubated at 37°C in the dark for 30 min. Three solutions were then added in separate drops: 2 μL of a 1 mM EDTA·Fe(II) solution (equal volumes of 2 mM EDTA, pH 8, and 2 mM freshly prepared ferrous ammonium sulfate), 4 μL of a 5 mM sodium ascorbate solution, and 2 μL of a 0.3% hydrogen peroxide solution. Final concentrations: 20 mM pH 7.4 Tris·HCl, 100 μM-bp DNA, 100 μM EDTA·Fe(II), 1 mM sodium ascorbate and 9 mM hydrogen peroxide, in 20 μL. The solutions were mixed, then incubated at 37°C. After 5 min, the reactions were lyophilized, counted, diluted to 3000 cpm/μL, and electrophoresed.

Affinity Cleaving

A DNA cocktail was prepared from 1 μL/tube 20X TA buffer (800 mM Tris, 200 mM sodium acetate, pH 7.9), 2 μL/tube calf thymus DNA, 36,000 cpm/tube labeled restriction fragment and water to make 12 μL/tube. This solution was pipetted into individual 600 μL eppendorf tubes. The compounds to be examined were loaded with Fe^{2+} by adding 10 μL of a 2 mM freshly prepared 2 mM ferrous ammonium sulfate solution to 10 μL of a 2 mM solution of the compound. The tube was vortexed and diluted to the appropriate 5X concentration. 4 μL of the compound was added to each tube, and the solutions were incubated at 37°C for 30 min in the dark. DTT (4 μL at 20 mM) was added, and the reactions were incubated in the dark at 37°C for 30 min. Final concentrations: 40 mM pH 7.9 Tris·acetate, 5 mM sodium acetate, 100 μM-bp DNA, 4 mM DTT, in 20 μL. The reactions were lyophilized, counted, diluted to 3000 cpm/μL, and electrophoresed in the usual manner.

DNase I Footprinting[14]

A DNA stock solution was prepared from 1 μL/tube 10X TKMC buffer (100 mM Tris, 100 mM potassium chloride, 100 mM magnesium chloride, 50 mM calcium chloride, pH 7.0), 2 μL/tube calf thymus DNA, 18,000 cpm/tube labeled 517 bp fragment and water to make 7 μL/tube. The compound to be footprinted was added in 2 μL of a 5X solution, and the tubes were incubated at 25°C for 30 min in the dark. A DNase I solution was prepared from 1 μL of a 0.33 mg/mL

stock solution, 20 μL 50 mM DTT and water to make 1 mL. 1 μL was added to each tube, and the reactions were incubated at 25°C for 3 min. Final concentrations: 10 mM pH 7.0 Tris·HCl, 10 mM potassium chloride, 10 mM magnesium chloride, 5 mM calcium chloride, 200 μM-bp DNA, 0.33 ng DNase and 100 μM DTT, in 10 μL. The cleavage was quenched with 2.5 μL of a 3 M ammonium acetate solution containing 250 mM EDTA, ethanol precipitated, dried, counted and prepared for electrophoresis as before.

Dimethyl Sulfate Footprinting[75]

A DNA solution was prepared from 0.5 μL/tube 20X TA buffer, 2 μL/tube 1 mM-bp calf thymus DNA, 18,000 cpm/tube labeled 517 bp fragment, and water to make 6 μL/tube. The footprinted compound was added as a 5X solution (2 μL), and the tubes were incubated for 30 min in the dark at 25°C. 2 μL of a 1:40 dimethyl sulfate:water solution was added to each tube and the reactions were incubated at 25°C for 5 min. Final concentrations: 40 mM pH 7.9 Tris·acetate, 5 mM sodium acetate, 200 μM-bp DNA and 53 mM dimethyl sulfate, in 10 μL. One μL of mercaptoethanol was added, and the reactions were ethanol precipitated. The pellet was taken up in 20 μL dilute hydrochloric acid, pH 2.2, and incubated at 0°C for 2 h with vortexing at 15 min intervals. The solution was diluted with 80 μL 200 mM sodium hydroxide containing 200 μM EDTA, heated to 90°C for 30 min, and ethanol precipitated. The precipitate was prepared for gel electrophoresis in the usual manner.

Diethyl Pyrocarbonate Reactions[177]

The same DNA solution used for dimethyl sulfate footprinting was divided into individual 600 μL eppendorf tubes. 2 μL of the compound to be tested was added as a 5X solution, and the tubes were incubated for 30 min at 37°C in the dark. Diethyl pyrocarbonate (2 μL of a 10% solution in methanol) was added, and the reactions were incubated at 37°C for 10 min in the dark. Final concentrations: 40 mM pH 7.9 Tris·acetate, 5 mM sodium acetate, 200 μM-bp DNA and 136 mM diethyl pyrocarbonate, in 10 μL. The reactions were ethanol precipitated, resuspended in 10% piperidine and heated to 90°C for 15 min. The solution was lyophilized twice to dryness, counted, diluted to 3000 cpm/μL and electrophoresed.

Potassium Permanganate Reactions[178]

The same DNA solution used for dimethyl sulfate footprinting was divided into individual 600 μL eppendorf tubes. The compound to be studied was added as a 5X solution in 2 μL, and the solution was incubated at 37°C for 30 min in the dark. A 2 μL portion of 500 μM potassium permanganate was added, and the tubes were incubated for 15 min at 37°C in the dark. Final concentrations: 40 mM pH 7.9 Tris·acetate, 5 mM sodium acetate, 200 μM-bp DNA and 100 μM potassium permanganate, in 10 μL. The reactions were ethanol precipitated, resuspended in 10% piperidine and heated to 90°C for 15 min. The solution was lyophilized twice to dryness, counted, diluted to 3000 cpm/μL, and electrophoresed.

Cleavage of Linear pBR322[16]

A DNA solution was prepared from 0.75 μL/tube 20X TA buffer, 1.5 μL 1 mM-bp calf thymus DNA, 30,000 cpm radioactive pBR322 and water to make 9 μL. The solution was pipetted into individual 600 μL eppendorf tubes, and 3 μL of a 5X solution of compound·Fe(II) was added. The tubes were incubated at 37°C for 30 min in the dark, then 3 μL of a 5 mM sodium ascorbate solution was added, and the reactions were incubated at 37°C for 2 h. Final concentrations: 40 mM pH 7.9 Tris·acetate, 5 mM sodium acetate, 100 μM-bp DNA, 1 mM sodium ascorbate, in 15 μL. The solutions were diluted with 4 μL 5X Ficoll loading buffer, and 18 μL were loaded on a 1% vertical agarose gel and electrophoresed in the usual manner.

Quantitative Footprinting[99]

DNA Preparation

Labeled 517 bp fragment was prepared by the standard procedure with two modifications. The linearized plasmid was labeled at the 3′ end using both [α-^{32}P]dATP and [α-^{32}P]TTP and no cold nucleotide triphosphates. After ethanol precipitation, the labeled fragment was resuspended in 100 μL 20 mM Tris·HCl, pH 7, and diluted to 2 mL with water. The solution was reconcentrated using an Amicon Centricon 30,000 MW cutoff membrane. The centricon was sterilized with 70% ethanol, and washed with water. The DNA solution was added to the top, and the Centricon spun in a 45° fixed rotor of a clinical centrifuge for 30 min. The DNA in 40 μL was collected, diluted to 4000 cpm/μL, and stored at −20°C.

Footprinting Reactions

Nineteen 600 μL eppendorf tubes were prepared containing the amount of water shown in the following table.

Table 3 2-PyN, 2-ImN Dilutions.

Lane No.	μL 4	μL H_2O	Lane No.	μL 9	μL H_2O	Lane No.	μL 14	μL H_2O	Lane No.	μL 19	μL H_2O
4		250									
5	50	50	**10**	50	75	**15**	50	50	**20**	50	50
6	50	150	**11**	50	200	**16**	50	200	**21**	50	150
7	10	90	**12**	10	90	**17**	10	90	**22**	10	90
8	10	190	**13**	10	240	**18**	10	190			
9	10	390	**14**	10	490	**19**	10	490			

Twenty three 1.5 mL eppendorf tubes were numbered sequentially and number 2 was set aside. Into the remaining tubes was placed 160 μL 1.25X Qfp buffer (200 mM Tris·HCl, 1 M NaCl, pH 7.0, diluted 12.5:100). Water was added to lanes 1 (control DNA, 25 μL), 3 and 23 (MPE standards, 20 μL). 10 μL of a DNA solution prepared from 25 μL 500 μM poly(dG)·poly(dC), 25 x 30,000 cpm labeled 517 bp restriction fragment and water to make 250 μL, was added to each tube. The compound to be footprinted was serially diluted as shown in the table above, and 20 μL of the appropriate concentration was added to each tube. The tubes were vortexed, spun down and incubated at 37°C for 30 min. Five μL of a freshly prepared 80 mM DTT solution and 5 μL of a 40 μM MPE·Fe(II) solution in

separate drops were added. The reactions were vortexed, spun down and incubated at 37°C for 10 min. Final concentrations: 20 mM pH 7.0 Tris·HCl, 100 mM sodium chloride, 2.5 μM-bp DNA, 1 μM MPE·Fe(II) and 2 mM DTT, in 200 μL. 25 μL of a tRNA solution (25 μL 1 mg/mL tRNA plus 600 μL water) was added, then 700 μL of ethanol, and the reactions were ethanol precipitated *without added salt* as above, counted and diluted to 3000 cpm/μL. Poly(dG)·poly(dC) proved difficult to resuspend. Best results were obtained by sonicating the formamide solutions for 5 min in a cleaning bath before loading, although most gels still contained at least one lane that did not resuspend. An 8% denaturing polyacrylamide gel was prepared with a special comb consisting of twenty 6 mm teeth separated by 6 mm, surrounded by seven 6 mm teeth separated by 3 mm. The standard and A lanes were loaded in wells separated by 3 mm. All other lanes were loaded in wells separated by 6 mm. The DNA was electrophoresed at 1100 V for 3 h until the bromophenol blue eluted from the bottom of the gel. The gel was dried as before and exposed to preflashed X-ray film at −78°C with one intensifying screen. Several exposures of varied duration were routinely prepared.

Densitometry

Normal footprinting and affinity cleaving autoradiograms were scanned on a LKB XL laser densitometer. Settings of X width 2, Y step 3 and no smoothing gave an absorbance value every 120 μm averaged over two 1 mm wide scans. The scans were output to an IBM printer, and footprints determined by comparison to

the MPE·Fe(II) standard lane. A horizontal line was drawn from the top of the nearest unprotected band, and the distance in AU from this line to the maximum peak height was determined for each band and plotted as a histogram. Affinity cleavage patterns were measured in similar fashion, using the peak heights of sites without specific cleavage as a baseline.

To determine the sites of cleavage in the linearized pBR322 assay, the cleavage lanes were scanned as above and output to the Hoefer program GS370 using sequential digital to analog and analog to digital conversions. Cleavage band molecular weights were determined by comparison to the molecular weight standard lane, and positions on pBR322 were calculated. The positions were averaged between labels and used, along with the average relative area of the peaks, to generate histograms.

For the quantitative footprinting gels, a suitable preflashed film was scanned using an X width of 7, Y step 2 and no smoothing for gel lanes, or X width 1, Y step 2 and no smoothing for background scans. Output was directed to the LKB program GSXL running on an IBM AT. The baseline was determined manually using a linear interpolation of the minimum number of points needed to reproduce the background curve shape (usually 3–4). The average of the baseline scans on both sides of the lane in question was subtracted by the program and the resultant peaks were integrated in signal mode. Peak areas were printed out and transferred to an Excel worksheet, running on a MacIntosh Plus.

The apparent fractions bound were calculated by the equations in chapter 3, and the data points transferred to the program BINDFIT, running on an IBM AT.

The best fit parameters were used to calculate a fitted curve (Excel), and the data points and the curve were transferred to Cricket Graf (MacIntosh) and printed. Average residuals were calculated from the Cricket Graf data sheet.

Synthesis

Instruments

Melting points were taken on a Thomas-Hoover apparatus and are uncorrected. Infrared spectra were recorded on a Shimadzu IR-435 spectrometer. ^{1}H NMR's were taken on a Jeol JNM-GX400 spectrometer at 400 MHz using partially deuterated solvent as an internal standard. Mass Spectrometry was performed at the Midwest Center for Mass Spectrometry, Lincoln, Nebraska. Ultraviolet and visible spectra were recorded on a Perkin-Elmer Lambda 4C spectrophotometer.

Reagents

Dry THF was distilled from sodium benzophenone ketyl. Dry DMF and dichloromethane were treated with activated 4Å Molecular Sieves.[179] N, N′-Carbonyldiimidazole was sublimed at 100°C and <1 Torr. All other reagents were used as received.

Methods

Oven-dried glassware was used for all non-aqueous reactions. All reactions except those containing thionyl chloride or other concentrated acids were performed under argon. The acidic reactions were flushed with argon, connected to a mineral bubbler, and heated to the reaction temperature. Reaction progress was monitored by TLC, using the following detection methods: UV, iodine (amines, pyrrole compounds), bromocresol purple (acids), or potassium permanganate (alkenes,

amines). Flash chromatography on silica gel was performed by the method of Still *et al.*[180] with flow rates slower than 1 cm/min for eluting solvents containing methanol or ethanol.

Procedures

Methyl 4-chloropyridine-2-carboxylate 9[117]

Pyridine-2-carboxylic acid (50 g, 0.41 mol) was suspended in 200 mL thionyl chloride and heated at reflux for 18 h. The excess thionyl chloride was removed *in vacuo*. The residue was cooled to 0°C, and 200 mL methanol was cautiously added. The methanol was removed, and the solid was taken up in 200 mL of water and extracted with dichloromethane (3 x 200 mL). The organic layers were combined, washed with saturated sodium bicarbonate (3 x 250 mL), dried over sodium sulfate, and evaporated to a brown oil. Distillation at <1 Torr (bp 75–82°C) gave a white solid, which was recrystallized from hexane to give 12 g (22%) of colorless flakes, **9**. ^{1}H NMR (DMSO-d_6) δ 8.61 (d, 1H, J= 5 Hz), 8.10 (d, 1H, J= 2 Hz), 7.46 (dd, 1H, J= 5, 2 Hz), 3.98 (s, 3H); IR (KBr) 1718 (s), 1568 (m), 1556 (w), 1440 (m), 1396 (w), 1302 (s), 1264 (m), 966 (w), 842 (w), 780 (w), 746 (m) cm^{-1}; FABMS m/e (relative intensity) 178 (73, M+Li), 172.0169 (72, M+H, 172.0165 calcd. for $C_7H_6NO_2{}^{35}Cl$).

4-Chloropyridine-2-carboxylic acid 10

A solution of 2.0 g (12 mmol) of **9** in 6 mL 6 M hydrochloric acid and 3 mL THF was heated at reflux for 8 h. The solvent was removed under reduced pressure

to give a white paste which was triturated with THF to give 2.3 g **10** (94%). ^{1}H NMR (DMSO-d_6) δ 8.68 (d, 1H, J= 5 Hz), 8.05 (d, 1H, J= 2 Hz), 7.79 (dd, 1H, J= 5, 2 Hz); IR (KBr) 3090 (m), 2850 (m), 1740 (m), 1620 (m), 1606 (s), 1438 (m), 1410 (s), 1338 (w), 1284 (m), 1260 (m), 1220 (m), 1166 (w), 1084 (w), 844 (w), 768 (w), 720 (w) cm^{-1}; FABMS m/e (relative intensity) 166 (41, M+2+Li), 164.0092 (78, M+Li, 164.0091 calcd. for $C_6H_4NO_2{}^{35}ClLi$), 160 (69, M+2+H), 158 (87, M+H), 140 (100, M+H$-H_2O$).

4-Dimethylaminopyridine-2-carboxylic acid 11

91 mg (0.47 mmol) of **10** and 5 mL of 40% dimethylamine in water were heated to 160°C for 12 h in a sealed tube.[118] The reaction was concentrated under reduced pressure and the residue purified by flash chromatography on silica gel with methanol, yielding 73 mg (94%) **11**, a white solid. ^{1}H NMR (DMSO-d_6) δ 7.96 (d, 1H, J= 7 Hz), 7.21 (d, 1H, J= 3 Hz), 6.88 (dd, 1H, J= 7, 3 Hz), 3.17 (s, 6H); IR (KBr) 3400 (w), 1628 (s), 1580 (m), 1560 (m), 1440 (w), 1392 (m), 1360 (m), 1250 (w), 1240 (w), 1002 (w), 860 (w), 812 (w), 796 (w) cm^{-1}; FABMS m/e (relative intensity) 167.0815 (100, M+H, 167.0821 calcd. for $C_8H_{11}N_2O_2$).

Sodium Pyrimidine-2-sulfite 12[119]

A suspension of 3.77 g (32.9 mmol) 2-chloropyrimidine and 4.4 g (34.9 mmol) sodium sulfite in 20 mL of water was heated at reflux for 1 h. The solution was concentrated to 10 mL and cooled to 0°C, precipitating 4.17 g (70%) **12** as a white solid. ^{1}H NMR (DMSO-d_6) δ 8.78 (d, 2H, J= 5 Hz), 7.46 (t, 1H, J= 5 Hz); IR

(KBr) 3500 (s), 3420 (m), 1568 (w), 1394 (w), 1238 (s), 1220 (s), 1058 (w), 1040 (w), 658 (w) cm^{-1}; FABMS m/e (relative intensity) 189 (35, M+Li), 160 (100, M+H−Na), 158.9862 (M−H−Na, 158.9864 calcd. for $C_4H_3N_2O_3S$).

2-Cyanopyrimidine 13[119]

Potassium cyanide (1.66 g, 25.5 mmol) and 3.47 g (19.1 mmol) **12** were intimately mixed in a mortar. The mixture was heated slowly to 300°C at <1 Torr. The solid distillate was dissolved in dichloromethane, filtered through Celite, and purified by flash chromatography on silica gel with 50% ether in hexane to give 0.578 g (29%) clear crystalline **13**. ^{1}H NMR (DMSO-d_6) δ 9.03 (d, 2H, J= 5 Hz), 7.87 (t, 1H, J= 5 Hz); IR (KBr) 1560 (s), 1500 (s), 1266 (w), 1084 (w), 988 (w), 816 (m), 786 (m), 640 (w) cm^{-1}; EIMS m/e (relative intensity) 105.0318 (100, M^+, 105.0319 calcd. for $C_5H_3N_3$), 78 (17, M−HCN).

Pyrimidine-2-carboxylic acid 14[120]

A 556 mg (5.30 mmol) sample of **13** was dissolved in 6 mL of 2 M sodium hydroxide and heated to reflux . After 5 h, the reaction was cooled to 25°C and neutralized with 6N hydrochloric acid. The water was lyophilized and the methanol soluble fraction sublimed at <1 Torr and 150°C to give 250 mg (38%) **14** as a white solid. ^{1}H NMR (DMSO-d_6) δ 8.95 (d, 2H, J= 5 Hz), 7.69 (t, 1H, J= 5 Hz); IR (KBr) 3050 (m), 2700 (s), 1744 (s), 1608 (s), 1596 (m), 1570 (m), 1442 (m), 1404 (m), 1306 (m), 1288 (m), 1272 (s), 1188 (s), 1166 (m), 1104 (w), 998 (m), 862 (w), 838 (w), 798 (w), 672 (m) cm^{-1}; FABMS m/e (relative intensity) 137 (74,

M−H+2Li), 131.0436 (81, M+Li, 131.0432 calcd. for $C_5H_4N_2O_2Li$), 125 (79, M+H).

Methyl 3-hydroxypyridine-2-carboxylate 15

3-Hydroxypyridine-2-carboxylic acid (5.0 g, 36 mmol) was heated at reflux for 72 h in 150 mL methanol containing 6 mL concentrated sulfuric acid. The methanol was removed, and the remainder diluted with 250 mL dichloromethane, washed with saturated sodium carbonate (2 x 250 mL) and water (1 x 200 mL). Drying over sodium sulfate and vacuum evaporation gave a light yellow solid, which was recrystallized from ether/hexane to give 1.76 g (32%) **15**. ^{1}H NMR ($CDCl_3$) δ 10.61 (s, 1H), 8.26 (dd, 1H, J= 4, 1 Hz), 7.40 (dd, 1H, J= 9, 4 Hz), 7.36 (dd, 1H, J= 9, 1 Hz), 4.04 (s, 3H); IR (KBr) 3100 (w), 1670 (s), 1596 (w), 1448 (s), 1366 (m), 1304 (s), 1240 (m), 1202 (s), 1098 (m), 960 (w), 860 (w), 820 (m), 804 (w), 736 (m), 688 (m), 662 (w) cm^{-1}; EIMS m/e (relative intensity) 153.0424 (100, M^+, 153.0426 calcd. for $C_7H_7NO_3$), 123 (98, M−CH_2O), 95 (98, M−$C_2H_2O_2$).

Methyl 3-methoxypyridine-2-carboxylate 16[121]

Sodium methoxide was freshly prepared from 200 mg (8.7 mmol) sodium metal and 10 mL of methanol. A 1.0 g (6.7 mmol) sample of **15** was added and then enough DMSO to give a clear solution. The methanol was removed at <1 Torr, 1 mL (16 mmol) iodomethane was added, and the reaction was stirred for 6 h. Another mL of iodomethane was added, and the reaction stirred for another 12 h. The DMSO was removed at <1 Torr pressure, and the residue was taken up in

75 mL of water and extracted with dichloromethane (3 x 80 mL). The organic layers were combined, dried over sodium sulfate, and concentrated. The resulting oil was distilled at <1 Torr and 130°C by Kügelrohr to yield 339 mg (31%) of **16**, a yellow oil. ^{1}H NMR ($CDCl_3$) δ 8.24 (d, 1H, J= 4 Hz), 7.39 (dd, 1H, J= 9, 4 Hz), 7.33 (d, 1H, J= 9 Hz), 3.94 (s, 3H), 3.89 (s, 3H); IR (film) 1736 (s), 1304 (s), 1100 (s) cm^{-1}; EIMS m/e (relative intensity) 167.0580 (16, M^+, 167.0583 calcd. for $C_8H_9NO_3$), 152 (17, $M-CH_3$), 108 (94, $M-C_2H_3O_2$).

3-Methoxypyridine-2-carboxylic Acid 17

A 239 mg (1.43 mmol) sample of **16** was dissolved in 4 mL 6 M hydrochloric acid and 2 mL THF and heated at reflux for 8 h. The solvent was removed *in vacuo* to give **17** in nearly quantitative yield. ^{1}H NMR (DMSO-d_6) δ 8.18 (d, 1H, J= 5 Hz), 7.70 (d, 1H, J= 9 Hz), 7.57 (dd, 1H, J= 9, 5 Hz), 3.85 (s, 3H); IR (KBr) 3360 (s), 2920 (s), 1720 (m), 1520 (s), 1480 (m), 1306 (m) cm^{-1}; FABMS m/e (relative intensity) 160.0584 (72, M+Li, 160.0586 calcd. for $C_7H_7NO_3Li$), 154 (83, M+H), 136 (100, $M+H-H_2O$).

2-Nitromalonaldehyde, sodium salt, 35[181]

To a solution of 102 g (1.5 mol) sodium nitrite in 100 mL water at 50°C was added dropwise over 1.25 h a solution of 100 g (0.38 mol) mucobromic acid in 100 mL 95% ethanol (heated to dissolve), keeping the temperature at 50 ±5°C. The solution was stirred for 10 min, then cooled to 0°C. The orange solid was collected, air-dried, and recrystallized from 200 mL 80% ethanol with a hot filtration to give

19.6 g **35** (36%) as orange needles. ^{1}H NMR (DMSO-d_6) δ 9.74 (s, 2H); IR (KBr) 3410 (s), 3200 (m), 1690 (s), 1652 (s), 1612 (m), 1544 (m), 1380 (m), 1322 (m), 860 (w), 690 (w), 548 (w) cm^{-1}.

Ethyl 4-Nitropyrrole-2-carboxylate 36[132]

An 8.1 g (58 mmol) sample of **35** and 7.9 g (57 mmol) ethyl glycinate hydrochloride were dissolved in 14 mL water and 28 mL methanol. 5 M sodium hydroxide (120 mL, 60 mmol) was added, and the reaction heated to 50°C for 0.5 h. The solution was cooled to 0°C and acidified to pH <1 with concentrated hydrochloric acid. The suspension was extracted with ethyl acetate (7 x 200 mL), keeping the pH <1 by adding concentrated hydrochloric acid as needed. The ethyl acetate was dried over sodium sulfate, removed under reduced pressure, and the residue was dissolved in 80 mL ethanol containing 1 mL concentrated sulfuric acid and heated at reflux. After 14 h, the solution was cooled to 25°C and 20 mL of water was added to start precipitation. Cooling to −20°C gave a tan precipitate, which was recrystallized from ethanol to give 2.79 g (27%) tan crystalline **36**. ^{1}H NMR (DMSO-d_6) δ 8.03 (d, 1H, J= 2 Hz), 7.22 (d, 1H, J= 2 Hz), 4.24 (q, 2H, J= 7 Hz), 1.30 (t, 3H, J= 7 Hz); IR (KBr) 3280 (s), 1690 (s), 1564 (w), 1506 (s), 1472 (w), 1420 (w), 1384 (m), 1362 (s), 1320 (s), 1264 (m), 1202 (s), 1016 (w), 766 (w), 752 (m) cm^{-1}; FABMS m/e (relative intensity) 197 (57, M−H+2Li), 191 (100, M+Li), 185.0564 (51, M+H, 185.0562 calcd. for $C_7H_9N_2O_4$).

Ethyl 4-Nitro-N-(3-dimethylaminopropyl)pyrrole-2-carboxylate 37

A solution of 523 mg (2.84 mmol) **36** in 25 mL acetone was stirred over 1.25 g (9.1 mmol) potassium carbonate for 1 h at 25°C.[133] Meanwhile, 520 mg (3.3 mmol) 3-chloro-1-dimethylaminopropane hydrochloride and 490 mg (3.3 mmol) sodium iodide were stirred in 15 mL acetone at 25°C for 1 h. The iodide solution was filtered, and the two solutions combined and heated at reflux for 14 h. Another portion of the iodide was prepared as above, added to the reaction mixture, and heated at reflux. After 5 h, the solution was filtered and the solvent removed *in vacuo* to produce a yellow solid, which was purified by flash chromatography on silica gel , eluting with 5% methanol in dichloromethane to give 626 mg (82%) of **37** as a white solid. ^{1}H NMR (DMSO-d_6) δ 8.28 (d, 1H, J= 2 Hz), 7.32 (d, 1H, J= 2 Hz), 4.35 (t, 2H, J= 7 Hz), 4.26 (q, 2H, J= 7 Hz), 2.20 (t, 2H, J= 7 Hz), 2.13 (s, 6H), 1.85 (quint, 2H, J= 7 Hz), 1.28 (t, 3H, J= 7 Hz); IR (KBr) 2980 (w), 2810 (w), 1720 (s), 1536 (m), 1508 (s), 1492 (m), 1424 (m), 1380 (m), 1362 (w), 1320 (s), 1250 (s), 1200 (m), 1172 (w), 1156 (w), 1100 (m), 1078 (w), 1022 (w), 840 (w), 802 (w), 744 (m) cm^{-1}; FABMS m/e (relative intensity) 270.1447 (100, M+H, 270.1454 calcd. for $C_{12}H_{20}N_3O_4$), 252 (23, M$-H_2O$).

4-Nitro-N-(3-dimethylaminopropyl)pyrrole-2-carboxylic acid 38

A 610 mg (2.3 mmol) sample of **37** was dissolved in 4 mL ethanol and treated with 2.5 mL 2.5 M sodium hydroxide at reflux for 2 h. The solvent was removed under reduced pressure and the residue purified by flash chromatography on silica

gel eluting with methanol to give the zwitterionic form of **38** in quantitative yield. ^{1}H NMR (DMSO-d_6) δ 7.87 (d, 1H, J= 2 Hz), 6.85 (d, 1H, J= 2 Hz), 4.49 (t, 2H, J= 7 Hz), 2.27 (t, 2H, J= 7 Hz), 2.22 (s, 6H), 1.91 (quint, 2H, J= 7 Hz); IR (KBr) 3420 (w), 1630 (m), 1600 (m), 1536 (w), 1500 (s), 1418 (w), 1390 (w), 1346 (s), 1292 (m), 820 (w), 750 (w) cm^{-1}; FABMS m/e (relative intensity) 242.1144 (8, M+H, 242.1141 calcd. for $C_{10}H_{16}N_3O_4$).

Ethyl 1-methylimidazole-2-carboxylate 3[122]

A solution of 1-methylimidazole (3.2 mL, 40 mmol) and triethylamine (10 mL, 72 mmol) in 20 mL acetonitrile was cooled to -30°C. A solution of 7 mL (73 mmol) ethyl chloroformate in 10 mL acetonitrile was added rapidly and the solution was warmed to 25°C and stirred for 18 h. The reaction mixture was filtered and the solvent removed under reduced pressure. The residue was dissolved in 50 mL water, extracted with chloroform (3 x 50 mL) and the organic layers combined, dried (sodium sulfate), and concentrated. Purification by flash chromatography on silica gel using ethyl acetate produced 3.11 g (51%) of **3** as a light yellow solid. ^{1}H NMR (DMSO-d_6) δ 7.43 (s, 1H), 7.04 (s, 1H), 4.26 (q, 2H, J= 7 Hz), 3.89 (s, 3H), 1.28 (t, 3H, J= 7 Hz); IR (KBr) 1706 (s), 1478 (m), 1420 (s), 1384 (m), 1260 (s), 1124 (m) cm^{-1}; FABMS m/e (relative intensity) 161.0900 (94, M+Li, 161.0902 calcd. for $C_7H_{10}N_2O_2Li$), 155 (100, M+H), 127 (79, M+H$-C_2H_4$), 109 (94, M+H$-$EtOH).

1-Methylimidazole-2-carboxylic acid 4[122]

To a solution of 1.95 g (10.0 mmol) **3** in 20 mL ethanol was added 20 mL 0.5 M lithium hydroxide (11.5 mmol). After 5 h, the ethanol was removed *in vacuo* and the remaining solution lyophilized to dryness. The white powder was taken up in a minimum amount of water, cooled to 0°C, acidified to pH 2 with 6 M hydrochloric acid, and a minimum amount of acetone was added to precipitate 1.04 g **4** containing ~10% 1-methylimidazole (77% yield). ^{1}H NMR (DMSO-d_6) δ 7.50 (s, 1H), 7.27 (s, 1H), 3.99 (s, 3H); IR (KBr) 3450 (w), 2600 (m), 1980 (w), 1652 (s), 1514 (m), 1462 (m), 1402 (s), 1354 (s), 1312 (s), 1276 (m), 1172 (w), 1014 (w), 906 (w), 800 (s), 778 (m), 632 (w) cm^{-1}; EIMS m/e (relative intensity) 126.0428 (17, M^+, 126.0430 calcd. for $C_5H_6N_2O_2$), 109 (6, M−OH), 108 (7, M−H_2O), 82 (100, M−CO_2).

Ethyl 4-nitro-1-methylimidazole-2-carboxylate 24[113]

A mixture of 1.05 g **3** (3.74 mmol), 4 mL concentrated sulfuric acid , and 4 mL fuming nitric acid was heated to 95°C for 1 h. The reaction was cooled, poured onto ice, and extracted with carbon tetrachloride (3 x 50 mL), then dichloromethane (3 x 50 mL). The dichloromethane layers were dried over sodium sulfate, concentrated under vacuum, and the solid was recrystallized from carbon tetrachloride containing a few drops of ethanol. Yield: 303 mg white crystals (22%). mp 124-127°C (lit[113] 130-131°C); ^{1}H NMR (DMSO-d_6) δ 8.63 (s, 1H), 4.34 (q, 2H, J= 7 Hz), 3.98 (s, 3H), 1.32 (t, 3H, J= 7 Hz); IR (KBr) 3130 (m),

1720 (s), 1538 (s), 1510 (m), 1496 (s), 1444 (m), 1380 (m), 1364 (m), 1340 (m), 1308 (s), 1260 (s), 1172 (w), 1140 (m), 1118 (s), 1008 (w), 992 (w), 858 (w), 840 (w), 822 (m), 756 (w), 652 (w) cm^{-1}; FABMS m/e (relative intensity) 206.0751 (100, M+Li, 206.0753 calcd. for $C_7H_9N_3O_4Li$), 200 (37, M+H).

4-Nitro-1-methylimidazole-2-carboxylic acid 25[113]

275 mg (1.38 mmol) **24** was heated at reflux in 2 mL 0.25 M sodium hydroxide for 15 min. The reaction was cooled to 50°C and acidified to pH 2. Further cooling gave 235 mg (99%) **25** as a white solid. ^1H NMR (DMSO-d_6) δ 8.58 (s, 1H), 3.97 (s, 3H); IR (KBr) 3000 (w), 1724 (s), 1548 (s), 1518 (m), 1502 (s), 1460 (w), 1390 (s), 1340 (m), 1300 (s), 1208 (m), 1154 (s), 1136 (m), 1070 (w), 1006 (w), 938 (w), 922 (w), 760 (w), 750 (w), 700 (s) cm^{-1}; FABMS m/e (relative intensity) 170.0204 (M−H, 170.0202 calcd. for $C_5H_4N_3O_4$).

1-(2-Chloroethyl)imidazole 18

A commercial sample of 60% sodium hydride (5.0 g, 125 mmol) was washed with hexane (3 x 75 mL) and dried *in vacuo*. THF (180 mL) then 5.0 g (73 mmol) imidazole were added cautiously with positive argon flow to remove hydrogen. 10 mL (120 mmol) 1-bromo-2-chloroethane was then added, and the mixture stirred for 30 min at 25°C and 4 h at reflux. After filtration and removal of the solvent under reduced pressure, the remaining oil was purified by flash chromatography on silica gel using 5% methanol in dichloromethane to yield 3.72 g (39%) **18** containing a small amount of 1-vinylimidazole. ^1H NMR (DMSO-d_6) δ 7.65 (s, 1H), 7.22 (d,

1H, J= 1 Hz), 6.89 (s, 1H), 4.30 (t, 2H, J= 6 Hz), 3.92 (t, 2H, J= 6 Hz); IR (film) 3100 (w), 1506 (s), 1458 (w), 1284 (w), 1226 (m), 1102 (w), 1076 (m), 922 (w), 816 (w), 738 (w), 660 (s), 580 (w) cm^{-1}; FABMS m/e (relative intensity) 139 (72, M+2+Li), 137.0457 (88, M+Li, 137.0458 calcd. for $C_5H_7N_2{}^{35}ClLi$), 133 (91, M+2+H), 131 (100, M+H).

4-Nitrophenyl 1-(2-chloroethyl)imidazole-2-carboxylate, 19

To a solution of 500 mg (3.8 mmol) **18** and 1.4 mL (8.1 mmol) diisopropylethylamine in 10 mL acetonitrile at −40°C was added rapidly a solution of 1.55 g (7.7 mmol) 4-nitrophenyl chloroformate in 10 mL acetonitrile at −40°C. The reaction solidified upon warming and was allowed to stand at 25°C for 18 h. The mixture was diluted with 50 mL acetonitrile, filtered and evaporated under reduced pressure to a yellow oil. Purification by flash chromatography on silica gel eluting with 40% ethyl acetate in hexane gave 563 mg (49%) of a yellow solid which was ~95% pure **19** (the rest is diisopropylammonium 4-nitrophenylate). An analytical sample was obtained by washing with ethyl acetate. ^1H NMR (DMSO-d_6) δ 8.35 (d, 2H, J= 9 Hz), 7.72 (s, 1H), 7.61 (d, 2H, J= 9 Hz), 7.26 (s, 1H), 4.74 (t, 2H, J= 6 Hz), 4.02 (t, 2H, J= 6 Hz); IR (KBr) 3100 (w), 1732 (s), 1615 (w), 1588 (m), 1512 (s), 1485 (m), 1470 (m), 1448 (w), 1436 (w), 1406 (s), 1386 (m), 1366 (w), 1345 (s), 1324 (w), 1308 (m), 1270 (w), 1240 (s), 1200 (s), 1160 (m), 1152 (m), 1140 (m), 1106 (m), 1082 (s), 1060 (s), 915 (w), 860 (m), 798 (w), 780 (w), 740 (w), 702 (w) cm^{-1}; FABMS m/e (relative intensity) 304 (65, M+2+Li), 302.0535

(88, M+Li, 302.0520 calcd. for $C_{12}H_{10}N_3O_4{}^{35}ClLi$), 298 (49, M+2+H), 296 (84, M+H).

1-(2-Chloroethyl)imidazole-2-carboxylic acid 20

A solution of 278 mg (0.94 mmol) **19** in 4 mL THF was treated with 2 mL of 1.25 M sodium hydroxide at 25°C for 45 min. The yellow solution was titrated with 6 M hydrochloric acid until clear, the THF was removed *in vacuo*, and the water layer washed with dichloromethane (3 x 5 mL). The water layer was lyophilized and the solid extracted with methanol (2 x 5 mL). The methanol was filtered through Celite and evaporated to give **20** as an unstable clear glass containing some sodium chloride. ^{1}H NMR (DMSO-d_6) δ 7.63 (s, 1H), 7.33 (s, 1H), 4.84 (t, 2H, J= 6 Hz), 4.01 (t, 2H, J= 6 Hz); IR (KBr) 3400 (s), 3100 (s), 2900 (s), 1655 (s), 1500 (w), 1460 (w), 1360 (m), 800 (m), 762 (w) cm^{-1}; FABMS m/e (relative intensity) 183 (16, M+2+Li), 181.0348 (38, M+Li, 181.0356 calcd. for $C_6H_7N_2O_2{}^{35}ClLi$), 177 (17, M+2+H), 175 (49, M+H), 157 (32, M+H$-H_2O$), 131 (72, ClEtIm+H).

Methyl 4-(1-(2-chloroethyl)imidazole-2-carboxamide)-N-methyl-pyrrole-2-carboxylate 22

Methyl 4-nitro-N-methylpyrrole-2-carboxylate (198 mg, 1.20 mmol) in 8 mL dry DMF was hydrogenated with 5% paladium on charcoal at 25°C and 1 atmosphere for 8 h. After filtration, the solvent was removed at <1 Torr. A solution of 130 mg (0.74 mmol) **20** and 208 mg (1.54 mmol) N-hydroxybenzotriazole at 0°C was treated with 149 mg (0.72 mmol) dicyclohexylcarbodiimide. The reaction was

warmed, stirred for 7 h at 25°C, and a solution of the pyrrole amine in 2 mL dry DMF was added. After 14 h, the reaction was filtered, and the solvent removed at <1 Torr. Purification by flash chromatography on silica gel using 40% ethyl acetate in hexane yielded 69 mg (31%) **22** as a yellow solid. ^{1}H NMR (DMSO-d_6) δ 10.62 (s, 1H), 7.53 (s, 1H), 7.50 (s, 1H), 7.07 (s, 1H), 7.03 (d, 1H, J= 2 Hz), 4.77 (t, 2H, J= 6 Hz), 3.98 (t, 2H, J= 6 Hz), 3.83 (s, 3H), 3.72 (s, 3H); IR (KBr) 3210 (m), 2930 (w), 1684 (s), 1652 (s), 1626 (m), 1578 (s), 1558 (s), 1508 (w), 1464 (s), 1448 (s), 1436 (m), 1420 (m), 1254 (s), 1195 (m), 1108 (s), 1094 (w), 780 (w), 756 (w), 650 (w), 620 (w) cm^{-1}; FABMS m/e (relative intensity) 319 (68, M+2+Li), 317 (87, M+Li), 313 (63, M+2+H), 311.0909 (88, M+H, 311.0911 calcd. for $C_{13}H_{16}N_4O_3{}^{35}Cl$), 295 (25, M+H−O), 281 (34, M+H−CH_2O).

Methyl 4-(Imidazo[1,2-a]pyrazinecarboxamide)-N-methyl-2-carboxylate 23

A solution of 27 mg (0.091 mmol) **22** in 15 mL dry THF containing 12 mg 60% sodium hydride and 5 mg sodium iodide was warmed to 35°C and stirred for 15 min. The solvent was removed under reduced pressure and the solid purified by flash chromatography on silica gel (5% methanol in dichloromethane) to give 17 mg (72%) white solid **23**. ^{1}H NMR (DMSO-d_6) δ 7.54 (d, 1H, J= 2 Hz), 7.39 (s, 1H), 7.13 (s, 1H), 7.02 (d, 1H, J= 2 Hz), 4.37 (t, 2H, J= 6 Hz), 4.11 (t, 2H, J= 6 Hz), 3.87 (s, 3H), 3.75 (s, 3H); IR (KBr) 1712 (m), 1680 (w), 1664 (s), 1510 (w), 1486 (m), 1456 (m), 1402 (m), 1260 (m), 1200 (w), 1148 (w), 1104 (w), 1058

(w), 762 (w) cm^{-1}; FABMS m/e (relative intensity) 281 (100, M+Li), 275.1143 (79, M+H, 275.1144 calcd. for $C_{13}H_{14}N_4O_3$), 263 (46, M+Li$-H_2O$).

General Procedure for Preparing ArN

A solution of 80 mg (0.21 mmol) 4-nitro-di-(N-methylpyrrole)-2-dimethylaminopropylcarboxamide and 15 mg of 5% paladium on charcoal in dry DMF (12 mL) was hydrogenated at atmospheric pressure for 12 h. The solution was filtered, and the DMF removed at <1 Torr. Several methods were used for acid activation:

Method A

Carbonyldiimidazole (68 mg, 0.42 mmol) was added separately to a solution of 0.42 mmol of the appropriate acid, and the solution stirred at 25°C for 1 h.

Method B

A solution of 0.42 mmol of the aromatic acid and 136 mg (1.0 mmol) N-hydroxybenzotriazole in 2 mL dry DMF was cooled to 0°C and 104 mg (0.5 mmol) dicyclohexylcarbodiimide was added. The solution was warmed to 25°C and stirred for 14 h.

Method C

The aromatic acid (0.42 mmol) was suspended in 10 mL thionyl chloride and heated to reflux for 1 h. The excess thionyl chloride was removed *in vacuo* and the residue cooled to 0°C and dissolved in 2 mL dry DMF containing 0.2 mL (1.4 mmol) triethylamine.

The pyrrole amine was dissolved in 2 mL dichloromethane, added to the activated acid, and the solution stirred for 14 h. The solvent was removed at <1 Torr, and the orange oil chromatographed with 0.25% concentrated aqueous ammonia in methanol. The products were lyophilized from dilute hydrochloric acid, and characterized as the hydrochloride salts.

Furan-2-carboxamide-netropsin (2-FuN)

Furan-2-carboxylic acid was activated by method A, yielding 35 mg 2-FuN, 35%. UV-vis $\lambda_{max}(\epsilon)$ 253 (21,000), 303 (25,000) nm; ^{1}H NMR (DMSO-d_6) δ 10.33 (s, 1H), 9.96 (s, 1H), 9.78 (bs, 1H), 8.17 (t, 1H, J= 6 Hz), 7.89 (s, 1H), 7.25 (d, 1H, J= 2 Hz), 7.22 (d, 1H, J= 3 Hz), 7.19 (s, 1H), 7.07 (s, 1H), 6.92 (s, 1H), 6.66 (dd, 1H, J= 3, 1 Hz), 3.85 (s, 3H), 3.81 (s, 3H), 3.24 (q, 2H, J= 6 Hz), 3.08 (t, 2H, J= 7 Hz), 2.74 (s, 6H), 1.84 (quint, 2H, J= 7 Hz); IR (KBr) 2920 (w), 2700 (w), 1650 (s), 1580 (m), 1526 (s), 1464 (m), 1436 (s), 1400 (m), 1260 (m) cm^{-1}; FABMS m/e (relative intensity) 441.2245 (56, M+H, 441.2250 calcd. for $C_{22}H_{29}N_6O_4$), 339 (20, M+H$-C_5H_{14}N_2$), 217 (27).

Furan-3-carboxamide-netropsin (3-FuN)

Furan-3-carboxylic acid was activated by method A, yielding 74 mg 3-FuN, 79%. UV-vis $\lambda_{max}(\epsilon)$ 246 (19,500), 299 (23,000) nm; ^{1}H NMR (DMSO-d_6) δ 10.12 (bs, 1H), 10.07 (s, 1H), 9.94 (s, 1H), 8.30 (s, 1H), 8.17 (t, 1H, J= 6 Hz), 7.75 (t, 1H, J= 1 Hz), 7.25 (d, 1H, J= 2 Hz), 7.19 (d, 1H, J= 2 Hz), 7.02 (d, 1H, J= 2 Hz), 6.97 (s, 1H), 6.91 (d, 1H, J= 2 Hz), 3.85 (s, 3H), 3.80 (s, 3H), 3.24 (q,

2H, J= 6 Hz), 3.04 (dt, 2H, J= 8, 6 Hz), 2.74 (d, 6H, J= 5 Hz), 1.85 (quint, 2H, J= 7 Hz); IR (KBr) 2920 (w), 2700 (w), 1640 (s), 1580 (m), 1528 (s), 1460 (m), 1436 (s), 1401 (m), 1260 (m), 1202 (w), 1158 (m) cm^{-1}; FABMS m/e (relative intensity) 441.2256 (7, M+H, 441.2250 calcd. for $C_{22}H_{29}N_6O_4$).

Thiophene-2-carboxamide-netropsin (2-ThN)

Thiophene-2-carboxylic acid was activated by method A, yielding > 47 mg 2-ThN, > 48%. UV-vis $\lambda_{max}(\epsilon)$ 246 (21,500), 300 (26,000) nm; ^1H NMR (DMSO-d_6) δ 10.43 (s, 1H), 10.17 (bs, 1H), 9.97 (s, 1H), 8.19 (t, 1H, J= 7 Hz), 7.97 (d, 1H, J= 4 Hz), 7.79 (dd, 1H, J= 5, 1 Hz), 7.27 (d, 1H, J= 2 Hz), 7.20 (d, 1H, J= 2 Hz), 7.19 (dd, 1H, J= 5, 1 Hz), 7.09 (d, 1H, J= 2 Hz), 6.93 (d, 1H, J= 2 Hz), 3.85 (s, 3H), 3.81 (s, 3H), 3.24 (q, 2H, J= 7 Hz), 3.06 (dt, 2H, J= 8, 6 Hz), 2.78 (d, 6H, J= 5 Hz), 1.86 (quint, 2H, J= 7 Hz); IR (KBr) 2940 (w), 2700 (w), 1640 (s), 1580 (m), 1532 (s), 1462 (m), 1436 (s), 1401 (m), 1260 (m), 1200 (w), 1100 (w) cm^{-1}; FABMS m/e (relative intensity) 457.1985 (67, M^+, 457.2804 calcd. for $C_{22}H_{29}N_6O_3S$), 355 (17, $M-C_5H_{14}N_2$).

Thiophene-3-carboxamide-netropsin (3-ThN)

Thiophene-3-carboxylic acid was activated by method A, yielding 74 mg 3-ThN, 75%. UV-vis $\lambda_{max}(\epsilon)$ 202 (23,500), 243 (22,500), 298 (25,000) nm; ^1H NMR (DMSO-d_6) δ 10.31 (s, 1H), 10.23 (s, 1H), 9.97 (s, 1H), 8.28 (t, 1H, J= 2 Hz), 8.19 (t, 1H, J= 6 Hz), 7.62 (d, 2H, J= 2 Hz), 7.29 (d, 1H, J= 2 Hz), 7.15 (d, 1H, J= 2 Hz), 7.07 (d, 1H, J= 2 Hz), 6.91 (d, 1H, J= 1 Hz), 3.85 (s, 3H), 3.80

(s, 3H), 3.24 (q, 2H, J= 6 Hz), 3.04 (dt, 2H, J= 8, 6 Hz), 2.73 (d, 6H, J= 7 Hz), 1.86 (quint, 2H, J= 7 Hz); IR (KBr) 2920 (w), 2700 (w), 1640 (s), 1580 (m), 1530 (s), 1460 (m), 1436 (s), 1401 (m), 1260 (m) cm^{-1}; FABMS m/e (relative intensity) 457.2003 (100, M^+, 457.2804 calcd. for $C_{22}H_{29}N_6O_3S$), 412 (8, $M-C_2H_7N$), 355 (27, $M-C_5H_{14}N_2$).

N-methylpyrrole-2-carboxamide-netropsin (2-PrN)

N-methylpyrrole-2-carboxylic acid was activated by method A, yielding 34 mg 2-PrN, 34%. UV-vis $\lambda_{max}(\epsilon)$ 240 (19,500), 297 (31,500) nm; ^1H NMR (DMSO-d_6) δ 9.90 (s, 1H), 9.83 (s, 1H), 9.70 (bs, 1H), 8.16 (t, 1H, J= 6 Hz), 7.22 (d, 1H, J= 2 Hz), 7.17 (d, 1H, J= 2 Hz), 7.03 (d, 1H, J= 2 Hz), 6.94 (t, 1H, J= 2 Hz), 6.92 (d, 1H, J= 2 Hz), 6.91 (dd, 1H, J= 4, 2 Hz), 6.05 (dd, 1H, J= 4, 2 Hz), 3.87 (s, 3H), 3.84 (s, 3H), 3.80 (s, 3H), 3.23 (q, 2H, J= 6 Hz), 3.04 (t, 2H, J= 6 Hz), 2.75 (s, 6H), 1.84 (quint, 2H, J= 7 Hz); IR (KBr) 3400 (m), 3300 (m), 2950 (w), 1640 (s), 1580 (m), 1536 (s), 1464 (m), 1436 (m), 1315 (w), 1252 (m), 1200 (w), 1108 (w), 740 (w) cm^{-1}; FABMS m/e (relative intensity) 454.2574 (55, M+H, 454.2567 calcd. for $C_{23}H_{32}N_7O_3$).

Pyridine-2-carboxamide-netropsin (2-PyN)

Pyridine-2-carboxylic acid was activated by method A, yielding 65 mg 2-PyN, 64%. UV-vis $\lambda_{max}(\epsilon)$ 223 (sh, 21,000), 238 (22,000), 296 (26,000) nm; ^1H NMR (DMSO-d_6) δ 10.73 (s, 1H), 9.95 (s, 1H), 8.71 (dd, 1H, J= 6, 2 Hz), 8.17 (t, 1H, J= 7 Hz), 8.11 (d, 1H, J= 8 Hz), 8.05 (ddd, 1H, J= 8, 8, 2 Hz), 7.64 (ddd, 1H,

J= 8, 5, 2 Hz), 7.37 (d, 1H, J= 2 Hz), 7.24 (d, 1H, J= 2 Hz), 7.18 (d, 1H, J= 2 Hz), 6.93 (d, 1H, J= 2 Hz), 3.85 (s, 3H), 3.81 (s, 3H), 3.23 (q, 2H, J= 7 Hz), 3.02 (t, 2H, J= 7 Hz), 2.74 (s, 6H), 1.84 (quint, 2H, J= 7 Hz); IR (KBr) 2910 (w), 2700 (w), 1640 (s), 1580 (s), 1530 (s), 1460 (m), 1432 (s), 1400 (m), 1260 (m), 1200 (w), 1120 (w) cm^{-1}; FABMS m/e (relative intensity) 452.2427 (60, M+H, 452.2410 calcd. for $C_{23}H_{30}N_7O_3$), 350 (28, M$-C_5H_{14}N_2$), 228 (46).

Pyridine-3-carboxamide-netropsin (3-PyN)

Pyridine-3-carboxylic acid was activated by method A, yielding > 31 mg 3-PyN, > 32%. UV-vis $\lambda_{max}(\epsilon)$ 213 (19,500), 246 (19,500), 300 (23,500) nm; ^1H NMR (DMSO-d_6) δ 10.64 (s, 1H), 9.98 (s, 1H), 9.77 (bs, 1H), 9.14 (d, 1H, J= 2 Hz), 8.77 (dd, 1H, J= 6, 5 Hz), 8.38 (d, 1H, J= 9 Hz), 8.17 (t, 1H, J= 6 Hz), 7.64 (dd, 1H, J= 9, 6 Hz), 7.35 (d, 1H, J= 2 Hz), 7.19 (d, 1H, J= 2 Hz), 7.10 (d, 1H, J= 2 Hz), 6.93 (d, 1H, J= 2 Hz), 3.87 (s, 3H), 3.81 (s, 3H), 3.24 (q, 2H, J= 5 Hz), 3.05 (dt, 2H, J= 8, 7 Hz), 2.76 (d, 6H, J= 5 Hz), 1.84 (quint, 2H, J= 8 Hz); IR (KBr) 3100 (w), 2940 (w), 2700 (w), 1670 (m), 1632 (s), 1575 (s), 1550 (s), 1530 (s), 1464 (m), 1434 (s), 1422 (s), 1260 (m), 1200 (w), 1120 (w) cm^{-1}; FABMS m/e (relative intensity) 452.2399 (2, M+H, 452.2410 calcd. for $C_{23}H_{30}N_7O_3$).

Pyridine-4-carboxamide-netropsin (4-PyN)

Pyridine-4-carboxylic acid was activated by method A, yielding 69 mg 4-PyN, 72%. UV-vis $\lambda_{max}(\epsilon)$ 209 (22,500), 241 (17,500), 293 (22,500) nm; ^1H NMR (DMSO-d_6) δ 10.82 (s, 1H), 10.00 (s, 1H), 8.84 (d, 2H, J= 6 Hz), 8.18 (t,

1H, J= 7 Hz), 8.01 (d, 2H, J= 6 Hz), 7.38 (d, 1H, J= 2 Hz), 7.20 (d, 1H, J= 2 Hz), 7.13 (d, 1H, J= 2 Hz), 6.93 (d, 1H, J= 2 Hz), 3.87 (s, 3H), 3.81 (s, 3H), 3.23 (q, 2H, J= 7 Hz), 3.02 (t, 2H, J= 7 Hz), 2.74 (s, 6H), 1.84 (quint, 2H, J= 7 Hz); IR (KBr) 3100 (w), 2950 (w), 2700 (w), 1660 (m), 1640 (s), 1573 (s), 1542 (s), 1462 (m), 1434 (s), 1402 (s), 1288 (w), 1260 (m), 1202 (w) cm^{-1}; FABMS m/e (relative intensity) 452.2431 (6, M+H, 452.2410 calcd. for $C_{23}H_{30}N_7O_3$).

1-Methylimidazole-2-carboxamide-netropsin (2-ImN)

Compound **4** was activated by method A, yielding 72 mg 2-ImN, 80%. UV-vis $\lambda_{max}(\epsilon)$ 255 (19,000), 302 (26,000) nm; ^1H NMR (DMSO-d_6) δ 10.92 (bs, 1H), 10.05 (bs, 1H), 9.89 (s, 1H), 8.18 (t, 1H, J= 6 Hz), 7.58 (s, 1H), 7.35 (s, 1H), 7.32 (d, 1H, J= 2 Hz), 7.18 (d, 1H, J= 2 Hz), 7.14 (d, 1H, J= 2 Hz), 6.92 (d, 1H, J= 2 Hz), 4.02 (s, 3H), 3.85 (s, 3H), 3.80 (s, 3H), 3.24 (q, 2H, J= 6 Hz), 3.04 (m, 2H), 2.74 (d, 6H, J= 5 Hz), 1.85 (quint, 2H, J= 7 Hz); FABMS m/e (relative intensity) 455.2519 (M+H, 0.8, 455.2519 calcd. for $C_{22}H_{31}N_8O_3$), 351 (8).

4-Chloropyridine-2-carboxamide-netropsin (4-ClPyN)

Compound **10** was activated by method A, yielding 90 mg 4-ClPyN, 79%. UV-vis $\lambda_{max}(\epsilon)$ 200 (45,500), 235 (23,000), 300 (26,500) nm; ^1H NMR (DMSO-d_6) δ 10.86 (s, 1H), 9.97 (s, 1H), 9.42 (bs, 1H), 8.69 (d, 1H, J= 5 Hz), 8.15 (t, 1H, J= 6 Hz), 8.10 (d, 1H, J= 2 Hz), 7.80 (dd, 1H, J= 5, 2 Hz), 7.37 (d, 1H, J= 2 Hz), 7.24 (d, 1H, J= 2 Hz), 7.18 (d, 1H, J= 2 Hz), 6.93 (d, 1H, J= 2 Hz), 3.85 (s, 3H), 3.80 (s, 3H), 3.25 (q, 2H, J= 6 Hz), 3.00 (m, 2H), 2.72 (bs,

6H), 1.81 (quint, 2H, J= 6 Hz); IR (KBr) 3330 (m), 1646 (s), 1580 (m), 1540 (s), 1462 (m), 1436 (m), 1406 (m), 1260 (m), 1202 (w), 774 (w) cm^{-1}; FABMS m/e (relative intensity) 486.2027 (65, M+H, 486.2020 calcd. for $C_{23}H_{29}N_7O_3{}^{35}Cl$), 384 (22, M+H$-C_5H_{14}N_2$).

4-Dimethylaminopyridine-2-carboxamide-netropsin (4-Me_2NPyN)

Compound **11** was activated by method C, yielding 41 mg 4-Me_2NPyN, 38%. UV-vis $\lambda_{max}(\epsilon)$ 226 (25,500), 287 (31,500) nm; ^{1}H NMR (DMSO-d_6+TFA) δ 11.25 (s, 1H), 10.02 (s, 1H), 9.50 (bs, 1H), 8.19 (d, 2H, J= 7 Hz), 7.74 (d, 1H, J= 3 Hz), 7.39 (d, 1H, J= 2 Hz), 7.18 (d, 1H, J= 2 Hz), 7.14 (d, 1H, J= 2 Hz), 7.05 (dd, 1H, J= 7, 3 Hz), 6.93 (d, 1H, J= 2 Hz), 3.89 (s, 3H), 3.81 (s, 3H), 3.26 (m, 8H), 3.06 (m, 2H), 2.77 (d, 6H, J= 5 Hz), 1.83 (quint, 2H, J= 7 Hz); IR (KBr) 3400 (m), 3300 (m), 3100 (w), 2950 (w), 1634 (s), 1570 (s), 1532 (m), 1464 (m), 1406 (m), 1262 (w), 1210 (w), 1006 (w), 804 (w), 776 (w) cm^{-1}; FABMS m/e (relative intensity) 517 (6, M+Na), 495.2834 (25, M+H, 495.2832 calcd. for $C_{25}H_{35}N_8O_3$), 393 (11, M+H$-C_5H_{14}N_2$).

3-Methoxypyridine-2-carboxamide-netropsin (3MeOPyN)

Compound **17** was activated by method B, and purified with the usual procedure. An additional chromatography step using 10% ammonia saturated methanol in dichloromethane as the eluent gave 21 mg 3-MeOPyN, 18%. UV-vis $\lambda_{max}(\epsilon)$ 192 (33,000), 234 (20,500), 300 (27,000) nm; ^{1}H NMR (DMSO-d_6) δ 10.34 (s, 1H), 9.94 (s, 1H), 9.80 (bs, 1H), 8.18 (dd, 1H, J= 5, 1 Hz), 8.16 (t, 1H, J= 6 Hz),

7.62 (dd, 1H, J= 9, 1 Hz), 7.51 (dd, 1H, J= 9, 5 Hz), 7.26 (d, 1H, J= 2 Hz), 7.18 (d, 1H, J= 2 Hz), 7.04 (d, 1H, J= 2 Hz), 6.92 (d, 1H, J= 2 Hz), 3.85 (s, 3H), 3.80 (s, 3H), 3.23 (q, 2H, J= 5 Hz), 3.04 (dt, 2H, J= 8, 6 Hz), 2.75 (d, 6H, J= 5 Hz), 1.84 (quint, 2H, J= 7 Hz); IR (KBr) 3400 (s), 1676 (m), 1644 (s), 1556 (m), 1520 (s), 1464 (m), 1436 (m), 1404 (m), 1308 (w), 1268 (m), 1212 (w), 1000 (w), 804 (w), 600 (w) cm^{-1}; FABMS m/e (relative intensity) 482.2514 (34, M+H, 482.2512 calcd. for $C_{24}H_{32}N_7O_4$), 380 (8, M+H$-C_5H_{14}N_2$).

Pyrimidine-2-carboxamide-netropsin (2-PmN)

Compound **14** was activated by method A, yielding 55 mg 2-PmN, 57%. UV-vis $\lambda_{max}(\epsilon)$ 209 (20,000), 238 (17,000), 297 (21,500) nm; ^1H NMR (DMSO-d_6) δ 10.87 (s, 1H), 9.98 (s, 1H), 9.01 (d, 2H, J= 5 Hz), 8.15 (t, 1H, J= 6 Hz), 7.71 (t, 1H, J= 5 Hz), 7.37 (d, 1H, J= 2 Hz), 7.21 (d, 1H, J= 2 Hz), 7.18 (d, 1H, J= 2 Hz), 6.92 (d, 1H, J= 2 Hz), 3.85 (s, 3H), 3.80 (s, 3H), 3.22 (q, 2H, J= 6 Hz), 2.92 (m, 2H), 2.66 (bs, 6H), 1.80 (quint, 2H, J= 7 Hz); IR (KBr) 3400 (m), 3300 (m), 2950 (w), 1640 (s), 1560 (s), 1530 (s), 1464 (m), 1436 (s), 1400 (s), 1262 (m), 1206 (w), 1138 (w), 1000 (w), 972 (w), 660 (w), 632 (w) cm^{-1}; FABMS m/e (relative intensity) 453.2352 (8, M+H, 453.2342 calcd. for $C_{22}H_{29}N_8O_3$), 371 (4).

4-Nitro-1-methylimidazole-2-carboxamide-netropsin (O_2NImN)

Compound **25** was activated by method A. Purification by flash chromatography on silica gel twice gave 39 mg O_2NImN, 37%. ^1H NMR (DMSO-d_6) δ 10.87 (s, 1H), 9.94 (s, 1H), 8.61 (s, 1H), 8.07 (t, 1H, J= 7 Hz), 7.31 (d, 1H, J= 2

Hz), 7.18 (s, 2H), 6.83 (d, 1H, J= 2 Hz), 4.04 (s, 3H), 3.84 (s, 3H), 3.79 (s, 3H), 3.18 (q, 2H, J= 7 Hz), 2.31 (m, 2H), 2.19 (s, 6H), 1.62 (quint, 2H, J= 7 Hz); IR (KBr) 3350 (w), 3120 (w), 2930 (w), 1642 (s), 1580 (m), 1536 (s), 1460 (m), 1436 (m), 1400 (m), 1382 (m), 1328 (w), 1304 (w), 1258 (w), 1200 (w), 1116 (w), 822 (w) cm^{-1}; FABMS m/e (relative intensity) 506.2461 (62, M+Li, 506.2451 calcd. for $C_{22}H_{29}N_9O_5Li$), 500 (25, M+H), 452 (23).

1-(2-Chloroethyl)imidazole-2-carboxamide-netropsin21

20 was activated by method B, yielding 20 mg **21**, 17%. ^1H NMR (DMSO-d_6) δ 10.55 (s, 1H), 9.90 (s, 1H), 8.05 (t, 1H, J= 7 Hz), 7.50 (s, 1H), 7.28 (d, 1H, J= 2 Hz), 7.17 (d, 1H, J= 2 Hz), 7.15 (d, 1H, J= 2 Hz), 7.08 (d, 1H, J= 1 Hz), 6.82 (d, 1H, J= 2 Hz), 4.78 (t, 2H, J= 6 Hz), 4.00 (t, 2H, J= 6 Hz), 3.83 (s, 3H), 3.78 (s, 3H), 3.17 (q, 2H, J= 7 Hz), 2.22 (t, 2H, J= 7 Hz), 2.12 (s, 6H), 1.59 (quint, 2H, J= 7 Hz); IR (KBr) 3350 (w), 2920 (w), 1646 (s), 1586 (m), 1530 (s), 1466 (s), 1432 (m), 1400 (w), 1258 (w), 1104 (w), 774 (w) cm^{-1}; FABMS m/e (relative intensity) 505 (23, M+2+H), 503.2283 (59, M+H, 503.2286 calcd. for $C_{23}H_{32}N_8O_3{}^{35}Cl$), 401 (14, M+H$-C_5H_{14}N_2$).

4-Acetomido-1-methylimidazole-2-carboxamide-netropsin (AcImN)

O_2NImN (18 mg, 0.036 mmol) was dissolved in 6 mL dry DMF containing 8 mg 5% paladium on charcoal and hydrogenated at 1 atmosphere and 25°C for 12 h. Acetic acid (10mg, 0.17 mmol) was activated by method A. The solutions were combined and stirred for 14 h. Application of the usual ArN purification

procedure gave 13 mg (69%) AcImN, characterized as the hydrochloride salt. UV-vis $\lambda_{max}(\epsilon)$ 207 (22,000), 241 (21,000), 305 (29,500) nm; ^{1}H NMR (DMSO-d_6) δ 10.24 (s, 1H), 9.97 (s, 1H), 9.93 (s, 1H), 9.81 (bs, 1H), 8.16 (t, 1H, J= 6 Hz), 7.42 (s, 1H), 7.25 (s, 1H), 7.17 (s, 1H), 7.13 (s, 1H), 6.93 (s, 1H), 3.94 (s, 3H), 3.84 (s, 3H), 3.80 (s, 3H), 3.23 (q, 2H, J= 6 Hz), 3.04 (dt, 2H, J= 8, 6 Hz), 2.75 (d, 6H, J= 5 Hz), 2.02 (s, 3H), 1.84 (quint, 2H, J= 7 Hz); IR (KBr) 3300 (m), 2960 (w), 1646 (s), 1580 (s), 1540 (s), 1464 (m), 1438 (s), 1322 (m), 1260 (m), 1206 (w), 1118 (w), 804 (w), 774 (w) cm^{-1}; FABMS m/e (relative intensity) 512.2743 (22, M+H, 512.2733 calcd. for $C_{24}H_{34}N_9O_4$), 371 (8).

Imidazo[1,2-a]pyrazinecarboxamide-netropsin (CycN)

A solution of 17 mg (0.034 mmol) ClEtImN in 15 mL dry THF containing 25 mg 60% sodium hydride and 5 mg sodium iodide was warmed to 35°C for 0.5 h. Flash chromatography on silica gel eluting with 0.5% concentrated aqueous ammonia in methanol produced 15 mg (95%) CycN, which was characterized as the hydrochloride salt. UV-vis $\lambda_{max}(\epsilon)$ 248 (16,000), 293 (23,000) nm; ^{1}H NMR (DMSO-d_6) δ 10.39 (bs, 1H), 10.05 (s, 1H), 8.21 (t, 1H, J= 6 Hz), 7.80 (s, 1H), 7.67 (s, 1H), 7.42 (s, 1H), 7.26 (s, 1H), 7.20 (s, 1H), 6.93 (s, 1H), 4.57 (t, 2H, J= 6 Hz), 4.24 (t, 2H, J= 6 Hz), 3.90 (s, 3H), 3.81 (s, 3H), 3.24 (q, 2H, J= 6 Hz), 3.04 (m, 2H), 2.72 (d, 6H, J= 6 Hz), 1.87 (quint, 2H, J= 7 Hz); IR (KBr) 3400 (m), 3100 (w), 2960 (w), 2700 (w), 1676 (s), 1640 (s), 1574 (m), 1540 (s), 1468 (s), 1440 (s), 1404 (m), 1365 (m), 1260 (m), 1214 (w), 1142 (w), 1100 (w), 1060 (w),

778 (w), 612 (w) cm^{-1}; FABMS m/e (relative intensity) 489 (30, M+Na), 467.2521 (29, M+H, 467.2521 calcd. for $C_{23}H_{31}N_8O_3$), 413 (17), 371 (34).

Synthesis of ArD

The synthesis of ArD followed the procedure for ArN exactly except that the nitro-tri-N-methylpyrrole starting material was hydrogenated for 18 h. Purification by flash chromatography on silica gel used 1% concentrated aqueous ammonia in methanol as the eluting solvent.

Pyridine-2-carboxamide-distamycin (2-PyD)

Pyridine-2-carboxylic acid was activated by method A, yielding 53 mg 2-PyD, 57%. UV-vis $\lambda_{max}(\epsilon)$ 241 (28,500), 310 (38,500) nm; ^1H NMR (DMSO-d_6) δ 10.74 (s, 1H), 10.00 (s, 1H), 9.93 (s, 1H), 9.89 (bs, 1H), 8.71 (d, 1H, J= 4 Hz), 8.17 (t, 1H, J= 6 Hz), 8.12 (d, 1H, J= 8 Hz), 8.03 (ddd, 1H, J= 8, 8, 2 Hz), 7.64 (ddd, 1H, J= 7, 5, 2 Hz), 7.39 (d, 1H, J= 2 Hz), 7.25 (d, 1H, J= 2 Hz), 7.24 (d, 1H, J= 2 Hz), 7.18 (d, 1H, J= 2 Hz), 7.07 (d, 1H, J= 2 Hz), 6.93 (d, 1H, J= 2 Hz), 3.87 (s, 3H), 3.84 (s, 3H), 3.81 (s, 3H), 3.24 (q, 2H, J= 7 Hz), 3.06 (m, 2H), 2.75 (d, 6H, J= 5 Hz), 1.84 (quint, 2H, J= 7 Hz); IR (KBr) 3300 (m), 1640 (s), 1580 (s), 1522 (s), 1464 (m), 1432 (s), 1404 (m), 1258 (m), 1204 (w), 1100 (w), 772 (w) cm^{-1}; FABMS m/e (relative intensity) 574.2872 (0.6, M+H, 574.2890 calcd. for $C_{29}H_{36}N_9O_4$), 351 (0.8).

1-Methylimidazole-2-carboxamide-distamycin (2-ImD)

4 was activated by method A, yielding 51 mg 2-ImD, 47%. UV-vis $\lambda_{max}(\epsilon)$ 248 (27,500), 307 (41,000) nm; ^{1}H NMR (DMSO-d_6) δ 10.74 (bs, 1H), 9.99 (s, 1H), 9.91 (s, 1H), 9.88 (bs, 1H), 8.16 (t, 1H, J= 6 Hz), 7.51 (s, 1H), 7.31 (d, 1H, J= 2 Hz), 7.23 (d, 2H, J= 2 Hz), 7.18 (d, 1H, J= 2 Hz), 7.17 (d, 1H, J= 2 Hz), 7.06 (d, 1H, J= 2 Hz), 6.93 (d, 1H, J= 2 Hz), 4.01 (s, 3H), 3.86 (s, 3H), 3.83 (s, 3H), 3.80 (s, 3H), 3.24 (q, 2H, J= 5 Hz), 3.05 (m, 2H), 2.75 (d, 6H, J= 5 Hz), 1.85 (quint, 2H, J= 8 Hz); IR (KBr) 3400 (m), 3300 (m), 3130 (w), 2960 (w), 2700 (w), 1680 (m), 1642 (s), 1580 (s), 1540 (s), 1466 (s), 1436 (s), 1404 (s), 1348 (w), 1258 (m), 1204 (w), 1138 (w), 1100 (w), 775 (w), 604 (w) cm^{-1}; FABMS m/e (relative intensity) 577.2984 (12, M+H, 577.2970 calcd. for $C_{28}H_{37}N_{10}O_4$).

3-Dimethylaminopropyl-4-(1-methylimidazole-2-carboxamide)-N-methylpyrrole-2-carboxamide (2-ImP)

The synthesis of 2-ImP followed the exact procedure for ArN, except that the 4-nitro-N-methylpyrrole-2-(3-dimethylaminopropyl)carboxamide starting material was hydrogenated for 18 h. Yield(method A): 50 mg 2-ImP, 48%. UV-vis $\lambda_{max}(\epsilon)$ 259 (15,000), 286 (18,500) nm; ^{1}H NMR (DMSO-d_6) δ 11.08 (s, 1H), 10.33 (bs, 1H), 8.27 (t, 1H, J= 6 Hz), 7.64 (s, 1H), 7.44 (s, 1H), 7.29 (d, 1H, J= 1 Hz), 7.00 (d, 1H, J= 1 Hz), 4.02 (s, 3H), 3.82 (s, 3H), 3.23 (q, 2H, J= 6 Hz), 3.03 (m, 2H), 2.72 (d, 6H, J= 6 Hz), 1.86 (quint, 2H, J= 7 Hz); IR (KBr) 3470 (m), 3320 (m), 3250 (m), 3100 (s), 2940 (m), 2700 (m), 1684 (s), 1646 (s), 1574 (m), 1530

(s), 1478 (m), 1460 (m), 1440 (s), 1408 (m), 1356 (w), 1282 (w), 1260 (s), 1204 (w), 1140 (w), 800 (w), 750 (w), 590 (w) cm^{-1}; FABMS m/e (relative intensity) 333.2036 (73, M+H, 333.2033 calcd. for $C_{16}H_{25}N_6O_2$).

N-Methyl, N-(2,2-diethoxyethyl)guanadinium acetate 27[131]

A 5.6 g (38 mmol) sample of N-methylaminoacetaldehyde diethyl acetal and 5.1 g (121 mmol) cyanamide were dissolved in 20 mL water, and acidified to pH 5 with acetic acid (> 3 mL). The solution was heated to 75°C and stirred for 45 min. The solvent was removed at <1 Torr and the residue triturated with ether and washed with acetone. The solid product was recrystallized from ethanol/ethyl acetate to give 2.1 g (22%) **27** as a white powder. ^1H NMR (DMSO-d_6) δ 4.62 (t, 1H, J= 5 Hz), 3.64 (dq, 2H, J= 9, 7 Hz), 3.50 (dq, 2H, J= 9, 7 Hz), 3.35 (d, 2H, J= 5 Hz), 2.90 (s, 3H), 1.62 (s, 3H), 1.10 (t, 6H, J= 7 Hz); IR (KBr) 3100 (s), 1688 (m), 1606 (s), 1575 (s), 1410 (s), 1122 (m), 1060 (m), 1020 (w), 692 (w) cm^{-1}; FABMS m/e (relative intensity) 190 (100, M+), 176.1400 (24, M−CH_2, 176.1399 calcd. for $C_7H_{18}N_3O_2$), 144 (76, M−EtOH).

2-Amino-1-methylimidazole hydrochloride 28[131]

A solution of 2.0 g (8.0 mmol) **27** in 7 mL concentrated hydrochloric acid was heated to 75°C for 15 min. The solution was concentrated to dryness under reduced pressure and recrystallized from ethanol/ether to give 782 mg (73%) **28** as white needles. ^1H NMR (DMSO-d_6) δ 12.21 (bs, 1H), 7.72 (bs, 2H), 6.94 (d, 1H, J= 3 Hz), 6.87 (d, 1H, J= 3 Hz), 3.45 (s, 3H); IR (KBr) 3270 (s), 3130 (s),

1664 (s), 1614 (m), 1544 (w), 1360 (w), 1080 (w), 742 (m), 598 (w), 588 (m) cm^{-1}; EIMS m/e (relative intensity) 97.0641 (100, M^+, 97.0640 calcd. for $C_4H_7N_3$), 82 (11, $M-NH_3$).

Synthesis of O_2NPAr

Acylation of the amino heterocycles followed the published procedure for acylation of 2-aminopyridine.[130]

4-Nitro-N-methylpyrrole-2-(1-methylimidazole)carboxamide, 29

4-Nitro-N-methylpyrrole-2-carboxylic acid (513 mg, 3.2 mmol) was heated at reflux in thionyl chloride for 1 h. The excess was removed *in vacuo* and the residual solid dissolved in 15 mL pyridine. **28** (503 mg, 3.8 mmol) was added, and the reaction heated at reflux for 5 h. The liquid was poured onto ice, the precipitate was collected, washed with water (3 x 20 mL) and dried to give 0.66 g (85%) **29**, a brown solid. ^1H NMR (DMSO-d_6+TFA) δ 8.31 (d, 1H, J= 2 Hz), 7.84 (d, 1H, J= 2 Hz), 7.54 (d, 1H, J= 2 Hz), 7.45 (d, 1H, J= 2 Hz), 3.95 (s, 3H), 3.75 (s, 3H); IR (KBr) 3230 (w), 1602 (s), 1560 (m), 1530 (m), 1500 (s), 1432 (w), 1416 (w), 1378 (s), 1320 (s), 1304 (s), 1285 (m), 1066 (w), 876 (w), 818 (w) cm^{-1}; FABMS m/e (relative intensity) 250.0945 (4, M+H, 250.0940 calcd. for $C_{10}H_{12}N_5O_3$), 195 (42).

4-Nitro-N-methylpyrrole-2-pyridinecarboxamide 30

4-Nitro-N-methylpyrrole-2-carboxylic acid (600 mg, 3.8 mmol) was heated at reflux in thionyl chloride for 1 h. The excess was removed *in vacuo* and the remain-

ing tan solid dissolved in 15 mL pyridine. 2-Aminopyridine (540 mg, 5.7 mmol) was added, and the reaction heated to reflux and stirred for 5 h. The liquid was poured onto ice, the precipitate was collected, washed with water (3 x 20 mL) and dried to give 0.76 g (86%) **30**, a tan solid. ^{1}H NMR (DMSO-d_6) δ 10.78 (s, 1H), 8.37 (dd, 1H, J= 5, 1 Hz), 8.24 (d, 1H, J= 2 Hz), 8.08 (dd, 1H, J= 9, 1 Hz), 7.90 (d, 1H, J= 2 Hz), 7.82 (ddd, 1H, J= 9, 9, 2 Hz), 7.16 (ddd, 1H, J= 9, 6, 1 Hz), 3.96 (s, 3H); IR (KBr) 1680 (m), 1582 (m), 1536 (s), 1500 (s), 1460 (m), 1435 (m), 1420 (m), 1402 (w), 1320 (s), 1302 (s), 1234 (w), 1198 (w), 770 (w), 748 (w) cm^{-1}; FABMS m/e (relative intensity) 247.0829 (35, M+H, 247.0831 calcd. for $C_{11}H_{11}N_4O_3$), 195 (44).

4-Nitro-N-methylpyrrole-2-methyl(2-pyridine)carboxamide 31

Alkylation of the heterocyclic amide followed the procedure of Pachter and Kloetzel.[124] A solution of 203 mg (0.868 mmol) **30** in 25 mL acetone was treated with 242 mg (4.3 mmol) powdered potassium hydroxide and 0.5 mL iodomethane (8 mmol). After 10 min at reflux, the reaction was filtered and 25 mL water was added to the filtrate. The acetone was removed *in vacuo* and the solid collected and dried, yielding 139 mg **31** (65%), a tan solid. ^{1}H NMR (DMSO-d_6) δ 8.29 (d, 1H, J= 9 Hz), 8.18 (d, 1H, J= 7 Hz), 8.06 (d, 1H, J= 2 Hz), 7.75 (ddd, 1H, J= 7, 7, 2 Hz), 7.27 (d, 1H, J= 2 Hz), 6.76 (ddd, 1H, J= 7, 7, 2 Hz), 4.00 (s, 3H), 3.82 (s, 3H); IR (KBr) 1640 (w), 1608 (w), 1556 (w), 1512 (m), 1485 (s), 1452 (m), 1416 (w), 1380 (s), 1308 (s), 1254 (w), 1152 (w), 764 (w) cm^{-1}; FABMS

m/e (relative intensity) 261.0989 (4, M+H, 261.0988 calcd. for $C_{12}H_{13}N_4O_3$), 195 (42).

Synthesis of O_2NNAr

Synthesis of the nitro-dipyrrole compounds followed that of the general ArN method. The nitro-monopyrrole compounds were stirred under with 5% paladium on charcoal under 1 atm hydrogen until TLC showed the disappearance of the nitro compound. After filtration, the DMF was removed at <1 Torr. 4-Nitro-N-methylpyrrole-2-carboxylic acid was activated by method C with thionyl chloride. Both the amine and the acid chloride were dissolved in dry DMF, combined and stirred with 3 equivalents of triethylamine for 18 h. The reactions were diluted with water and the precipitate was collected and further purified by flash chromatography on silica gel eluting with 4% methanol in dichloromethane to give the corresponding dipyrrole compound.

4-(4-Nitro-N-methylpyrrole-2-carboxamide)-N-methylpyrrole-N-(1-methylimidazole)carboxamide 32

199 mg **29** was hydrogenated for 48 h, yielding 36 mg (12%) **32** after coupling. ^{1}H NMR (DMSO-d_6+TFA) δ 11.27 (bs, 1H), 10.42 (s, 1H), 8.19 (s, 1H), 7.60 (d, 1H, J= 2 Hz), 7.55 (d, 1H, J= 2 Hz), 7.48 (d, 1H, J= 2 Hz), 7.46 (d, 1H, J= 2 Hz), 7.38 (s, 1H), 3.95 (s, 3H), 3.89 (s, 3H), 3.73 (s, 3H); IR (KBr) 3300 (w), 3130 (w), 1660 (w), 1588 (m), 1540 (m), 1506 (m), 1484 (m), 1440 (m), 1400

(m), 1310 (s), 1110 (w), 750 (w) cm^{-1}; FABMS m/e (relative intensity) 372.1420 (5, M+H, 372.1420 calcd. for $C_{16}H_{18}N_7O_4$).

4-(4-Nitro-N-methylpyrrole-2-carboxamide)-N-methylpyrrole-2-pyridinecarboxamide 33

202 mg **30** was hydrogenated for 11 h, yielding 129 mg (43%) **33** after coupling. ^1H NMR (DMSO-d_6) δ 10.35 (s, 1H), 10.32 (s, 1H), 8.35 (d, 1H, J= 6 Hz), 8.19 (d, 1H, J= 2 Hz), 8.07 (d, 1H, J= 9 Hz), 7.77 (ddd, 1H, J= 9, 9, 2 Hz), 7.61 (d, 1H, J= 2 Hz), 7.41 (d, 1H, J= 2 Hz), 7.16 (d, 1H, J= 2 Hz), 7.09 (ddd, 1H, J= 7, 7, 1 Hz), 3.95 (s, 3H), 3.87 (s, 3H); IR (KBr) 1660 (m), 1578 (m), 1518 (s), 1504 (s), 1470 (w), 1436 (w), 1404 (m), 1310 (s), 1200 (w), 1106 (w), 780 (w) cm^{-1}; FABMS m/e (relative intensity) 369.1333 (5, M+H, 369.1311 calcd. for $C_{17}H_{17}N_6O_4$), 195 (38).

4-(4-Nitro-N-methylpyrrole-2-carboxamide)-N-methylpyrrole-2-methyl(2-pyridine)carboxamide 34

120 mg **31** was hydrogenated for 56 h to produce 99 mg (57%) **34** after coupling. ^1H NMR (DMSO-d_6) δ 10.15 (s, 1H), 8.18 (d, 1H, J= 9 Hz), 8.16 (d, 1H, J= 2 Hz), 8.05 (dd, 1H, J= 5, 2 Hz), 7.61 (ddd, 1H, J= 9, 7, 2 Hz), 7.56 (d, 1H, J= 2 Hz), 7.27 (d, 1H, J= 2 Hz), 6.87 (d, 1H, J= 2 Hz), 6.60 (ddd, 1H, J= 7, 7, 2 Hz), 3.95 (s, 3H), 3.91 (s, 3H), 3.76 (s, 3H); IR (KBr) 1638 (m), 1570 (m), 1504 (s), 1436 (s), 1396 (s), 1372 (s), 1308 (s), 1254 (m), 1150 (w), 1110 (w), 750

(w) cm^{-1}; FABMS m/e (relative intensity) 383.1456 (3, M+H, 383.1468 calcd. for $C_{18}H_{19}N_6O_4$), 351 (2).

4-(4-Nitro-N-(3-dimethylaminopropyl)pyrrole-2-carboxamide)-N-methylpyrrole-2-pyridinecarboxamide 39

A 146 mg (0.62 mmol) sample of **30** in 12 mL dry DMF containing 40 mg 5% paladium on charcoal was hydrogenated for 1 h at 25°C and 1 atm. The solution was filtered, and the solvent removed at <1 Torr. 150 mg (0.62 mmol) **38** that had been lyophilized from dilute hydrochloric acid was suspended in 4 mL dry DMF. The acid was activated by addition of 204 mg (1.5 mmol) N-hydroxybenzotriazole and then 156 mg (0.75 mmol) dicyclohexylcarbodiimide at 0°C. After 6 h, the amine dissolved in 2 mL dichloromethane was added, and the reaction stirred at 25°C. At 20 h, 0.2 mL (2.1 mmol) acetic anhydride was added. At 32 h, the solvent was removed at <1 Torr pressure and the residue purified by flash chromatography, loading with methanol and eluting with 0.25% concentrated aqueous ammonia in methanol to give 170 mg (64%) **39**. ^{1}H NMR (DMSO-d_6) δ 10.35 (bs, 2H), 8.34 (dd, 1H, J= 5, 1 Hz), 8.18 (d, 1H, J= 2 Hz), 8.07 (d, 1H, J= 8 Hz), 7.77 (ddd, 1H, J= 8, 8, 2 Hz), 7.60 (d, 1H, J= 2 Hz), 7.41 (d, 1H, J= 2 Hz), 7.16 (d, 1H, J= 2 Hz), 7.10 (ddd, 1H, J= 6, 6, 1 Hz), 4.42 (t, 2H, J= 7 Hz), 3.87 (s, 3H), 2.15 (t, 2H, J= 7 Hz), 1.86 (quint, 2H, J= 7 Hz); IR (KBr) 1668 (m), 1650 (w), 1576 (m), 1508 (s), 1464 (w), 1434 (s), 1400 (m), 1308 (s), 1220 (w), 775 (w), 746 (w) cm^{-1}.

Synthesis of NAr

The synthesis of NAr compounds followed closely the ArN synthesis. The nitro-dipyrrole compounds (80 mg, ~0.2 mmol) were hydrogenated at 25°C and 1 atm for 14 h. The solution was filtered and evaporated to dryness under <1 Torr. 4-Dimethylaminobutyric acid hydrochloride (75 mg, 0.45 mmol) was dissolved in 2 mL dry DMF and treated with 73 mg (0.45 mmol) N,N′-carbonyldiimidazole for 1 h at 25°C. The amine was dissolved in 2 mL dichloromethane, added to the acyl imidazole and stirred for 14 h. After solvent removal *in vacuo*, purification by flash chromatography on silica gel with 0.25% concentrated aqueous ammonia in methanol gave the product, which was characterized as the hydrochloride salt.

4-Dimethylaminobutylcarboxamide-netropsin-2-(1-methylimidazole)-carboxamide (NIm)

31 mg **32** yielded 17 mg (44%) NIm after coupling. UV-vis $\lambda_{max}(\epsilon)$ 235 (20,000), 308 (26,000) nm; ^{1}H NMR (DMSO-d_6) δ 11.33 (bs, 1H), 10.34 (bs, 1H), 10.11 (s, 1H), 10.06 (s, 1H), 7.57 (s, 1H), 7.49 (s, 1H), 7.47 (s, 1H), 7.44 (s, 1H), 7.19 (s, 1H), 6.94 (s, 1H), 3.88 (s, 3H), 3.83 (s, 3H), 3.75 (s, 3H), 3.04 (q, 2H, J= 5 Hz), 2.75 (d, 6H, J= 6 Hz), 2.36 (t, 2H, J= 6 Hz), 1.93 (quint, 2H, J= 6 Hz); IR (KBr) 3400 (m), 2950 (w), 1660 (s), 1616 (s), 1580 (m), 1550 (m), 1488 (m), 1430 (s), 1400 (m), 1240 (w), 1200 (w), 1048 (w) cm^{-1}; FABMS m/e (relative intensity) 455.2519 (46, M+H, 455.2519 calcd. for $C_{22}H_{31}N_8O_3$).

4-Dimethylaminobutylcarboxamide-netropsin-2-pyridine-carboxamide (NPy)

Yield: 51 mg, 52%. UV-vis $\lambda_{max}(\epsilon)$ 235 (21,000), 305 (29,000) nm; ^{1}H NMR (DMSO-d_6) δ 11.17 (bs, 1H), 10.37 (bs, 1H), 10.07 (s, 1H), 10.06 (s, 1H), 8.40 (d, 1H, J= 5 Hz), 8.13 (t, 1H, J= 7 Hz), 8.02 (d, 1H, J= 9 Hz), 7.47 (d, 1H, J= 2 Hz), 7.40 (s, 1H), 7.35 (t, 1H, J= 7 Hz), 7.19 (d, 1H, J= 2 Hz), 6.93 (d, 1H, J= 2 Hz), 3.90 (s, 3H), 3.83 (s, 3H), 3.02 (m, 2H), 2.74 (d, 6H, J= 5 Hz), 2.36 (t, 2H, J= 7 Hz), 1.93 (quint, 2H, J= 7 Hz); IR (KBr) 1652 (s), 1610 (m), 1560 (s), 1436 (s), 1400 (m), 1236 (m), 1205 (w), 1048 (w), 780 (w) cm^{-1}; FABMS m/e (relative intensity) 452.2436 (4, M+H, 452.2410 calcd. for $C_{23}H_{30}N_7O_3$).

4-Dimethylaminobutylcarboxamide-netropsin-2-methyl(2-pyridine)-carboxamide (NMePy)

Yield: 22 mg, 25%. UV-vis $\lambda_{max}(\epsilon)$ 230 (20,000), 301 (24,000) nm; ^{1}H NMR (DMSO-d_6) δ 11.09 (bs, 1H), 10.57 (bs, 1H), 10.13 (s, 1H), 10.10 (s, 1H), 8.92 (d, 1H, J= 6 Hz), 8.52 (t, 1H, J= 6 Hz), 8.18 (d, 1H, J= 8 Hz), 7.84 (d, 1H, J= 7 Hz), 7.49 (s, 1H), 7.44 (s, 1H), 7.18 (s, 1H), 6.96 (d, 1H, J= 2 Hz), 4.25 (s, 3H), 3.87 (s, 3H), 3.83 (s, 3H), 3.05 (q, 2H, J= 6 Hz), 2.73 (d, 6H, J= 6 Hz), 2.36 (t, 2H, J= 6 Hz), 1.94 (quint, 2H, J= 7 Hz); IR (KBr) 3400 (s), 2950 (m), 1690 (m), 1640 (m), 1580 (m), 1550 (w), 1510 (m), 1425 (m), 1400 (m), 1280 (w), 1230 (w), 1195 (w), 1030 (w), 760 (w) cm^{-1}; FABMS m/e (relative intensity) 466.2539 (3, M+H, 466.2567 calcd. for $C_{24}H_{32}N_7O_3$).

Pyridine-2-carboxamide-netropsin-2-pyridinecarboxamide (PyP^+PPy)

The procedure above was followed exactly except that pyridine-2-carboxylic acid was used as the acid component. Yield: 44 mg, 47%. UV-vis $\lambda_{max}(\epsilon)$ 239 (20,500), 309 (32,500) nm; ^{1}H NMR (DMSO-d_6) δ 11.48 (bs, 1H), 10.80 (s, 2H), 10.42 (bs, 1H), 8.72 (d, 1H, J= 5 Hz), 8.43 (d, 1H, J= 5 Hz), 8.23 (t, 1H, J= 7 Hz), 8.17 (d, 1H, J= 7 Hz), 8.07 (d, 1H, J= 5 Hz), 8.04 (ddd, 1H, J= 7, 7, 2 Hz), 7.65 (ddd, 1H, J= 6, 6, 1 Hz), 7.54 (d, 1H, J= 2 Hz), 7.51 (s, 1H), 7.48 (s, 1H), 7.41 (t, 1H, J= 6 Hz), 7.35 (d, 1H, J= 2 Hz), 4.40 (t, 2H, J= 6 Hz), 3.92 (s, 3H), 3.03 (q, 2H, J= 7 Hz), 2.74 (d, 6H, J= 6 Hz), 2.14 (quint, 2H, J= 7 Hz); IR (KBr) 2950 (w), 1646 (s), 1608 (m), 1560 (s), 1522 (m), 1438 (s), 1404 (s), 1230 (m), 1200 (w), 1092 (w), 1050 (w), 780 (w) cm^{-1}; FABMS m/e (relative intensity) 515.2524 (7, M+H, 515.2519 calcd. for $C_{27}H_{31}N_8O_3$).

Ethyl 4-(1-methylimidazole-2-carboxamide)-N-(3-dimethylamino-pyrrole-2-carboxylate 39

A 198 mg (0.74 mmol) portion of **36** was hydrogenated for 8 h at 1 atm and 25°C in 8 mL dry DMF containing 20 mg 5% paladium on charcoal. The reaction was filtered and the solvent removed at <1 Torr. 154 mg (1.2 mmol) **4** was activated by 205 mg (1.3 mmol) N,N′-carbonyldiimidazole in 4 mL dry DMF. After 1 h, the pyrrole amine was redissolved in dichloromethane, and the solutions combined and stirred for 10 h. Removal of the solvent and flash chromatography on silica gel eluting with 0.25% concentrated aqueous ammonia in 1:1 methanol:ethanol gave

206 mg (81%) **39** as a yellow solid. ^{1}H NMR (DMSO-d_6) δ 10.52 (s, 1H), 7.52 (d, 1H, J= 2 Hz), 7.38 (s, 1H), 7.06 (d, 1H, J= 2 Hz), 4.25 (t, 2H, J= 7 Hz), 4.19 (q, 2H, J= 7 Hz), 3.97 (s, 3H), 2.13 (t, 2H, J= 7 Hz), 2.11 (s, 6H), 1.76 (quint, 2H, J= 7 Hz), 1.26 (t, 3H, J= 7 Hz); IR (KBr) 3320 (m), 1680 (s), 1668 (s), 1580 (m), 1555 (m), 1512 (w), 1460 (w), 1418 (s), 1396 (w), 1274 (w), 1224 (w), 1206 (w), 1106 (w), 1084 (m), 784 (w) cm^{-1}; FABMS m/e (relative intensity) 354 (87, M+Li), 348.2037 (100, M+H, 348.2036 calcd. for $C_{17}H_{26}N_5O_3$), 325 (70).

4-(1-Methylimidazole-2-carboxamide)-N-(3-dimethylaminopropyl)-pyrrole-2-carboxylic acid 40

To a solution of 190 mg (0.55 mmol) **39** in 10 mL ethanol was added 2 mL 1.25 M sodium hydroxide and the mixture heated at reflux for 1 h. The solvent was removed *in vacuo* and the residue purified by flash chromotography. Eluting with methanol yielded 170 mg (97%) **40**, which was lyophilized from dilute hydrochloric acid and characterized as the hydrochloride salt. ^{1}H NMR (DMSO-d_6) δ 12.30 (bs, 1H), 10.58 (s, 1H), 9.90 (s, 1H), 7.60 (d, 1H, J= 2 Hz), 7.41 (s, 1H), 7.06 (s, 1H), 7.01 (d, 1H, J= 2 Hz), 4.33 (t, 2H, J= 7 Hz), 3.97 (s, 3H), 3.00 (m, 2H), 2.73 (d, 6H, J= 5 Hz), 2.07 (quint, 2H, J= 7 Hz); IR (KBr) 3400 (w), 3260 (w), 3100 (w), 2950 (m), 2680 (w), 1676 (s), 1664 (s), 1576 (m), 1470 (m), 1416 (m), 1398 (m), 1282 (w), 1258 (m), 1182 (w), 1108 (w), 780 (w) cm^{-1}; FABMS m/e (relative intensity) 326 (44, M+Li), 320.1716 (74, M+H, 320.1723 calcd. for $C_{15}H_{22}N_5O_3$).

***bis*-4-(1-Methylimidazole-2-carboxamide)-N-(3-dimethylamino-propyl)-pyrrole-2-carboxamide (ImP^+P^+Im)**

A solution of 161 mg (0.45 mmol) **40** and 148 mg (1.09 mmol) N-hydroxybenzotriazole in 10 mL dry DMF was cooled to 0°C. A 118 mg (0.57 mmol) portion of dicyclohexylcarbodiimide was added, and the mixture stirred for 6 h. 1,2-Diaminoethane (20 μL, 0.30 mmol) was added and the solution was stirred for 14 h at 25°C. Evaporation to dryness followed by purification by flash chromatography on silica gel using 2% concentrated aqueous ammonia in methanol yielded 38 mg (25%) white solid ImP^+P^+Im, which was lyophilized from dilute hydrochloric acid to be characterized as the hydrochloride salt. UV-vis $\lambda_{max}(\epsilon)$ 257 (sh, 28,000), 285 (36,500) nm; ^{1}H NMR (DMSO-d_6) δ 10.93 (s, 2H), 10.27 (s, 2H), 8.30 (bs, 2H), 7.57 (s, 2H), 7.40 (d, 2H, J= 2 Hz), 7.32 (bs, 2H), 7.03 (d, 2H, J= 2 Hz), 4.34 (t, 4H, J= 6 Hz), 4.01 (s, 6H), 3.33 (bs, 4H), 2.98 (q, 4H, J= 6 Hz), 2.71 (d, 12H, J= 6 Hz), 2.08 (quint, 4H, J= 7 Hz); IR (KBr) 3400 (m), 3300 (m), 3050 (m), 2950 (m), 2700 (m), 1680 (s), 1640 (s), 1578 (s), 1520 (s), 1460 (m), 1412 (s), 1340 (w), 1260 (m), 1236 (w), 1120 (w), 770 (w), 608 (w) cm^{-1}; FABMS m/e (relative intensity) 661.3679 (4, M+H, 661.3672 calcd. for $C_{32}H_{45}N_{12}O_4$).

Synthesis of ArNE

A suspension of 20 mg (26 μmol) **2** and 15 mg 5% Pd/C was hydrogenated for 18 h at 50 psi in a Parr Rocker. The solution was filtered and the DMF was removed *in vacuo*. Carbonyldiimidazole (12.5 mg, 77 μmol) was added to a

solution of the appropriate acid (3 equiv.) and the reaction stirred for 1 h. The amine was dissolved in dry dichloromethane, added to the activated acid, and the solution was stirred for 18 h in the dark. The solvent was removed, and the residue chromatographed with 0.25% concentrated aqueous ammonia in 1:1 methanol:ethanol to give a 50–65% yield of $ArNE(OEt)_3$. This was dissolved in 1 mL of ethanol, and 1 mL of 0.5 M lithium hydroxide was added. After 18 h, the solvent was removed, and the solid chromatographed on silica gel using 1% concentrated aqueous ammonia in 1:1 methanol:ethanol as the eluent to give a 65% yield of ArNE.

Pyridine-2-carboxamide-netropsin-EDTA (2-PyNE)

UV-vis $\lambda_{max}(\epsilon)$ 245, 305 nm; ^{1}H NMR (DMSO-d_6+TFA) δ 10.78 (s, 1H), 9.95 (s, 1H), 9.33 (bs, 1H), 8.70 (dd, 1H, J= 4, 1 Hz), 8.48 (t, 1H, J= 7 Hz), 8.18 (m, 1H), 8.15 (d, 1H, J= 8 Hz), 8.06 (ddd, 1H, J= 8, 8, 2 Hz), 7.64 (ddd, 1H, J= 8, 5, 1 Hz), 7.37 (d, 1H, J= 2 Hz), 7.24 (d, 1H, J= 2 Hz), 7.17 (d, 1H, J= 2 Hz), 6.96 (d, 1H, J= 2 Hz), 4.01 (s, 2H), 3.88 (s, 2H), 3.85 (s, 3H), 3.80 (s, 7H), 3.3-3.0 (m, 12H), 2.75 (d, 3H, J= 5 Hz), 1.82 (m, 4H); FABMS m/e (relative intensity) 769.3634 (2, M+H, 769.3633 calcd. for $C_{35}H_{49}N_{10}O_{10}$).

Pyridine-3-carboxamide-netropsin-EDTA (3-PyNE)

UV-vis $\lambda_{max}(\epsilon)$ 238, 296 nm; ^{1}H NMR (DMSO-d_6+TFA) δ 10.88 (s, 1H), 9.99 (s, 1H), 9.35 (bs, 1H), 9.32 (s, 1H), 9.01 (d, 1H, J= 6 Hz), 8.88 (dd, 1H, J= 8, 1 Hz), 8.47 (t, 1H, J= 7 Hz), 8.18 (t, 1H, J= 7 Hz), 8.08 (dd, 1H, J= 8, 6

Hz), 7.36 (d, 1H, J= 2 Hz), 7.17 (d, 1H, J= 2 Hz), 7.12 (d, 1H, J= 2 Hz), 6.96 (d, 1H, J= 2 Hz), 4.01 (s, 2H), 3.88 (s, 5H), 3.81 (s, 4H), 3.80 (s, 3H), 3.3-3.0 (m, 12H), 2.76 (d, 3H, J= 5 Hz), 1.83 (m, 4H); FABMS m/e (relative intensity) 769.3606 (10, M+H, 769.3633 calcd. for $C_{35}H_{49}N_{10}O_{10}$), 743 (20, M+H−CN).

Pyridine-4-carboxamide-netropsin-EDTA (4-PyNE)

UV-vis $\lambda_{max}(\epsilon)$ 245, 305 nm; ^{1}H NMR (DMSO-d_6+TFA) δ 11.09 (s, 1H), 9.98 (s, 1H), 9.33 (bs, 1H), 9.08 (d, 1H, J= 7 Hz), 8.49 (t, 1H, J= 7 Hz), 8.46 (d, 1H, J= 7 Hz), 8.18 (bs, 1H), 7.38 (d, 1H, J= 2 Hz), 7.15 (d, 1H, J= 4 Hz), 6.97 (d, 1H, J= 2 Hz), 4.04 (s, 2H), 3.91 (s, 2H), 3.88 (s, 3H), 3.86 (s, 4H), 3.79 (s, 3H), 3.4-3.0 (m, 12H), 2.75 (d, 3H, J= 5 Hz), 1.82 (m, 4H); FABMS m/e (relative intensity) 769.3638 (0.4, M+H, 769.3633 calcd. for $C_{35}H_{49}N_{10}O_{10}$).

4-Chloropyridine-2-carboxamide-netropsin-EDTA (4-ClPyNE)

UV-vis $\lambda_{max}(\epsilon)$ 199, 236, 300 nm; ^{1}H NMR (DMSO-d_6+TFA) δ 10.82 (s, 1H), 9.96 (s, 1H), 9.33 (bs, 1H), 8.67 (d, 1H, J= 5 Hz), 8.47 (t, 1H, J= 5 Hz), 8.17 (t, 1H, J= 5 Hz), 8.09 (d, 1H, J= 2 Hz), 7.76 (dd, 1H, J= 5, 2 Hz), 7.36 (d, 1H, J= 2 Hz), 7.25 (d, 1H, J= 2 Hz), 7.17 (d, 1H, J= 2 Hz), 6.95 (d, 1H, J= 2 Hz), 4.01 (s, 2H), 3.87 (s, 2H), 3.85 (s, 3H), 3.80 (s, 4H), 3.79 (s, 3H), 3.3–2.9 (m, 12H), 2.76 (d, 3H, J= 4 Hz), 1.83 (m, 4H); FABMS m/e (relative intensity) 812 (14, M+2+Li), 810 (28, M+Li), 805 (40, M+2+H), 803.3269 (89, M+H, 803.3243 calcd. for $C_{35}H_{48}N_{10}O_{10}{}^{35}Cl$), 384 (52).

4-Dimethylaminopyridine-2-carboxamide-netropsin-EDTA (4-Me_2NPyNE)

UV-vis $\lambda_{max}(\epsilon)$,pH 4, 225, 289 nm; ^{1}H NMR (DMSO-d_6+TFA) δ 11.12 (s, 1H), 10.01 (s, 1H), 9.36 (bs, 1H), 8.47 (t, 1H, J= 6 Hz), 8.19 (d, 2H, J= 7 Hz), 7.66 (d, 1H, J= 3 Hz), 7.38 (d, 1H, J= 2 Hz), 7.16 (d, 1H, J= 2 Hz), 7.12 (d, 1H, J= 2 Hz), 7.05 (dd, 1H, J= 7, 3 Hz), 6.95 (d, 1H, J= 2 Hz), 4.01 (s, 2H), 3.89 (s, 3H), 3.87 (s, 2H), 3.81 (s, 4H), 3.79 (s, 3H), 3.3 (bs, 6H), 3.3–2.9 (m, 12H), 2.76 (d, 3H, J= 4 Hz), 1.84 (m, 4H); FABMS m/e (relative intensity) 812.4050 (13, M+H, 812.4055 calcd. for $C_{37}H_{54}N_{11}O_{10}$), 621 (4).

3-Methoxypyridine-2-carboxamide-netropsin-EDTA (3-MeOPyNE)

UV-vis $\lambda_{max}(\epsilon)$ 191, 238, 300 nm; ^{1}H NMR (DMSO-d_6+TFA) δ 10.44 (s, 1H), 9.94 (s, 1H), 9.32 (bs, 1H), 8.47 (t, 1H, J= 6 Hz), 8.31 (d, 1H, J= 4 Hz), 8.17 (t, 1H, J= 6 Hz), 7.92 (d, 1H, J= 9 Hz), 7.73 (dd, 1H, J= 9, 5 Hz), 7.31 (d, 1H, J= 2 Hz), 7.15 (d, 1H, J= 2 Hz), 7.08 (d, 1H, J= 2 Hz), 6.95 (d, 1H, J= 2 Hz), 4.01 (s, 2H), 3.93 (s, 3H), 3.87 (s, 2H), 3.86 (s, 3H), 3.80 (s, 7H), 3.3–2.9 (m, 12H), 2.76 (d, 3H, J= 5 Hz), 1.83 (m, 4H); FABMS m/e (relative intensity) 821 (2, M+Na), 799.3730 (17, M+H, 799.3739 calcd. for $C_{36}H_{51}N_{10}O_{11}$), 608 (5).

Pyrimidine-2-carboxamide-netropsin-EDTA (2-PmNE)

UV-vis $\lambda_{max}(\epsilon)$ 206, 237, 296 nm; ^{1}H NMR (DMSO-d_6+TFA) δ 10.86 (s, 1H), 9.97 (s, 1H), 9.32 (bs, 1H), 8.99 (d, 2H, J= 5 Hz), 8.47 (t, 1H, J= 6 Hz), 8.17 (t, 1H, J= 6 Hz), 7.68 (t, 1H, J= 5 Hz), 7.36 (d, 1H, J= 2 Hz), 7.23 (d, 1H, J=

2 Hz), 7.17 (d, 1H, J= 2 Hz), 6.95 (d, 1H, J= 2 Hz), 4.01 (s, 2H), 3.87 (s, 2H), 3.86 (s, 3H), 3.80 (s, 7H), 3.4–2.9 (m, 12H), 2.75 (d, 3H, J= 5 Hz), 1.84 (m, 4H); FABMS m/e (relative intensity) 814 (3, M+2Na), 792 (5, M+Na), 770.3574 (8, M+H, 770.3586 calcd. for $C_{34}H_{48}N_{11}O_{10}$).

1-Methylimidazole-2-carboxamide-netropsin-diaminoazaheptane-tBoc 6

A solution of 125mg (0.24 mmol) 4-nitro-di-(N-methylpyrrole)-2-diaminoazaheptane-tBoc **5**[76] and 35mg of 5% paladium on charcoal in dry DMF (15 mL) was hydrogenated at atmospheric pressure for 9 h. The solution was filtered, and the DMF removed *in vacuo*. To a solution of the hydrochloride salt of imidazole-2-carboxylic acid (75 mg, 0.50 mmol) and N-hydroxybenzotriazole (183 mg, 1.36 mmol) at 0°C was added dicyclohexylcarbodiimide and the solution allowed to warm to 25°C over 14 h. The hydrogenation residue was dissolved in dichloromethane, added to the activated acid, and the solution stirred for 16 h. The solvent was removed and the solid chromatographed with 8% ammonia saturated methanol in dichloromethane to give 119 mg (84%) of **6**. ^{1}H NMR (DMSO-d_6) δ 10.44 (s, 1H), 9.89 (s, 1H), 8.01 (t, 1H, J= 7 Hz), 7.38 (s, 1H), 7.27 (d, 1H, J= 2 Hz), 7.17 (d, 1H, J= 2 Hz), 7.14 (d, 1H, J= 2 Hz), 6.82 (d, 1H, J= 2 Hz), 6.77 (t, 1H, J= 6 Hz), 3.98 (s, 3H), 3.83 (s, 3H), 3.78 (s, 3H), 3.17 (q, 2H, J= 7 Hz), 2.93 (q, 2H, J= 7 Hz), 2.28 (t, 2H, J= 7 Hz), 2.27 (t, 2H, J= 7 Hz), 2.10 (s, 3H), 1.59 (quint, 2H, J= 7 Hz), 1.50 (quint, 2H, J= 7 Hz), 1.35 (s, 9H); FABMS

m/e (relative intensity) 598.3447 (41, M+H, 598.3464 calcd. for $C_{29}H_{44}N_9O_5$), 498 (19, M+H$-C_5H_8O_2$).

1-Methylimidazole-2-carboxamide-netropsin-diaminoazaheptane 7

To a solution of 110 mg **6** (0.188 mmol) in 8 mL of dichloromethane was added 1 mL of trifluoroacetic acid and the solution allowed to stand for 0.25 h. Ether was added and the solid collected, dissolved in 8% concentrated aqueous ammonia in methanol and purified by flash chromatography on silica gel to yield 79 mg (87%) **7** as a white foam. ^{1}H NMR (DMSO-d_6) δ 10.44 (s, 1H), 9.92 (s, 1H), 8.03 (t, 1H, J= 7 Hz), 7.37 (d, 1H, J= 1 Hz), 7.27 (d, 1H, J= 2 Hz), 7.16 (d, 2H, J= 2 Hz), 7.13 (s, 1H), 7.02 (d, 1H, J= 2 Hz), 3.97 (s, 3H), 3.82 (s, 3H), 3.77 (s, 3H), 3.3 (q, 2H, J= 7 Hz), 3.17 (q, 2H, J= 7 Hz), 2.50 (m, 2H), 2.28 (t, 2H, J= 7 Hz), 2.10 (s, 3H), 1.59 (quint, 2H, J= 7 Hz), 1.47 (quint, 2H, J= 7 Hz); FABMS m/e (relative intensity) 498.2947 (22, M+H, 498.2941 calcd. for $C_{24}H_{36}N_9O_3$).

1-Methylimidazole-2-carboxamide-netropsin-EDTA, triethyl ester 8

A solution of 128 mg (0.34 mmol) EDTA triethylester and 55 mg (0.34 mmol) N,N′-carbonyldiimidazole in 4 mL dry dichloromethane was stirred at 25°C for 1 h. **7** was added and the solution stirred in the dark for 12 h. Purification by flash chromatography on silica gel using 0.25% concentrated aqueous ammonia in 1:1 methanol:ethanol gave 17 mg (15%) of **8**. ^{1}H NMR (DMSO-d_6) δ 10.43 (s, 1H), 9.90 (s, 1H), 8.01 (t, 1H, J= 7 Hz), 7.95 (t, 1H, J= 7 Hz), 7.39 (s, 1H), 7.28

(d, 1H, J= 2 Hz), 7.17 (d, 1H, J= 2 Hz), 7.13 (d, 1H, J= 2 Hz), 7.03 (d, 1H, J= 2 Hz), 6.83 (d, 1H, J= 2 Hz), 4.05 (q, 6H, J= 7 Hz), 3.98 (s, 3H), 3.83 (s, 3H), 3.74 (s, 3H), 3.49 (s, 4H), 3.43 (s, 2H), 3.18 (s, 2H), 3.15 (m, 2H), 3.11 (q, 2H, J= 7 Hz), 2.69 (m, 4H), 2.31 (t, 2H, J= 7 Hz), 2.29 (t, 2H, J= 7 Hz), 2.13 (s, 3H), 1.6 (m, 4H), 1.16 (t, 9H, J= 7 Hz).

1-Methylimidazole-2-carboxamide-netropsin-EDTA (2-ImNE)

Compound **8** (14 mg, 0.016 mmol) was stirred in a mixture of 1:2 0.5 M lithium hydroxide to ethanol at 25°C for 16 h. Flash chromatography on silica gel using 1% concentrated aqueous ammonia in 1:1 methanol:ethanol yielded 3.4 mg (27%) of 2-ImNE. UV-vis $\lambda_{max}(\epsilon)$ 252, 304 nm; ^{1}H NMR (DMSO-d_6+TFA) δ 10.96 (s, 1H), 9.98 (s, 1H), 9.36 (bs, 1H), 8.47 (t, 1H, J= 7 Hz), 8.19 (t, 1H, J= 7 Hz), 7.70 (s, 1H), 7.54 (s, 1H), 7.32 (d, 1H, J= 2 Hz), 7.16 (d, 1H, J= 2 Hz), 7.12 (d, 1H, J= 2 Hz), 6.95 (d, 1H, J= 2 Hz), 4.02 (2s, 5H), 3.87 (s, 5H), 3.81 (s, 4H), 3.79 (s, 2H), 3.78 (s, 3H), 3.3-3.0 (m, 12H), 2.75 (s, 3H), 1.84 (m, 4H); FABMS m/e (relative intensity) 772.3746 (14, M+H, 772.3742 calcd. for $C_{34}H_{50}N_{11}O_{10}$), 549 (39), 507 (17).

References

[1] Watson, J.D. & Crick, F.H.C. (1953) *Nature* **171**, 737–8.

[2] Seemen, N.C., Rosenberg, J. & Rich, A. (1976) *Proc. Natl. Acad. Sci., U.S.A.* **73**, 804–8.

[3] Pabo, C.O., Jordan, S.R. & Frankel, A.D. (1983) *J. Biomol. Struc. Dyn.* **1**, 1039–49.

[4] For a review of DNA single crystal structures see Dickerson, R.E. (1988) in *Unusual DNA Structures*, Wells, R.D. & Harvey, S.C., eds. (Springer-Verlag, New York) , pp. 287–306.

[5] Wells, R.D. & Harvey, S.C., eds (1988) in *Unusual DNA Structures*, (Springer-Verlag, New York), pp. 1–311.

[6] Calladine, C.R. (1982) *J. Mol. Biol.* **161**, 343–52.

[7] Dickerson, R.E. (1983) *J. Mol. Biol.* **166**, 419–41.

[8] Sarai, A., Mazur, J., Nussinov, R. & Jernigan, R.L. (1988) *Biochemistry* **27**, 8498–502.

[9] Zimmer, C. & Wähnert, U. (1986) *Prog. Biophys. Molec. Biol.* **47**, 31–112.

[10] Neidle, S., Pearl, L.H. & Skelly, J.V. (1987) *Biochem. J.* **243**, 1–13.

[11] Neidle, S.R. (1984) *CRC Crit. Rev. Biochem.* **17**, 73–121.

[12] Kolchinsky, A.M., Mirzabekov, A.D., Zasedatelev, A.S., Gursky, G.V., Grokhovsky, S.L., Zhuze, A.L. & Gottikh, B.P. (1975) *Molec. Biol. (USSR)* **9**, 19–27.

[13] Van Dyke, M.W., Hertzberg, R.P. & Dervan, P.B. (1982) *Proc. Natl. Acad. Sci., U.S.A.* **79**, 5470–4.

[14] Van Dyke, M.W. & Dervan, P.B. (1982) *Cold Spring Harbor Symposium on Quantitative Biology* **47**, 347–53.

[15] Lane, M.J., Dobrowiak, J.C. & Vournakis, J. (1983) *Proc. Natl. Acad. Sci., U.S.A.* **80**, 3260–4.

[16] Youngquist, R.S. (1988) Ph.D. thesis, California Institute of Technology.

[17] Youngquist, R.S. & Dervan, P.B. (1985) *Proc. Natl. Acad. Sci., U.S.A.* **82**, 2565–69.

[18] Kopka, M.L., Yoon, C., Goodsell, D., Pjura, P. & Dickerson, R.E. (1985) *J. Mol. Biol.* **183**, 553–563.

[19] Kopka, M.L., Yoon, C., Goodsell, D., Pjura, P. & Dickerson, R.E. (1985) *Proc. Natl. Acad. Sci., U.S.A.* **82**, 1376–80.

[20] Coll, M., Frederick, C.A., Wang, A.H.-J. & Rich, A. (1987) *Proc. Natl. Acad. Sci., U.S.A.* **84**, 8385–9.

[21] Goodsell, D. & Dickerson, R.E. (1986) *J. Med. Chem.* **29**, 727–33.

[22] Patel, D.J., Shapiro, L. & Hare, D. (1986) *Biopolymers* **25**, 693–706.

[23] Patel, D.J. & Shapiro, L. (1986) *J. Biol. Chem.* **261**, 1230–40.

[24] Klevitt, R.E., Wemmer, D.E. & Reid, B.R. (1986) *Biochemistry* **25**, 3296–303.

[25] Marky, L.A. & Breslauer, K.J. (1987) *Proc. Natl. Acad. Sci., U.S.A.* **84**, 4359–63.

[26] Marky, L.A., Blumenfeld, K.S. & Breslauer, K.J. (1983) *Nucl. Acids Res.* **11**, 2857–70.

[27] Breslauer, K.J., Remeta, D.P., Chou, W.-Y., Ferrante, R., Curry, J., Zaunckowski, D. & Marky, L.A. (1987) *Proc. Natl. Acad. Sci., U.S.A.* **84**, 8922–6.

[28] Mahendrasingham, A., Rhodes, N.J., Goodwin, G.C., Nave, C., Pigram, W.J., Fuller, W., Brahms, J. & Vergne, J. (1983) *Nature* **301**, 535–7.

[29] Arnott, S. & Selsing, E. (1974) *J. Mol. Biol.* **88**, 509–21.

[30] Arcamone, F., Lazzari, E., Menozzi, M., Soranzo, C. & Verini, M.A. (1986) *Anti-Cancer Drug Des.* **1**, 235–44.

[31] Arcamone, F., Penco, S. & Delle Monache, F. (1969) *Gazz. chim. italiana* **99**, 620–631.

[32] Arcamone, F. (1972) in *Medicinal Chemistry*, Pratesi, P., ed. (Butterworths, London), pp. 29–45.

[33] Arcamone, F., Nicolella, V., Penco, S. & Redaelli, S. (1969) *Gazz. chim. italiana* **99**, 620–631.

[34] Rao, K.E., Dasgupta, D. & Sasiskeharan, V. (1988) *Biochemistry* **27**, 3018–24.

[35] Zimmer, C., Luck, G. & Burckhardt, G. (1984) *Studia Biophys.*, 247–51.

[36] Luck, G., Zimmer, C. & Baguley, B. (1984) *Biochim. Biophys. Acta* **782**, 41–8.

[37] Burckhardt, G., Zimmer, C. & Baguley, B. (1987) *J. Biomol. Struc. Dyn.* **4**, 813–31.

[38] Harshman, K.D. & Dervan, P.B. (1985) *Nucl. Acids Res.* **13**, 4825–35.

[39] Pjura, P., Grzeskowiak, K. & Dickerson, R.E. (1987) *J. Mol. Biol.* **197**, 257–71.

[40] Teng, M., Usman, N., Frederick, C.A. & Wang, A.H.-J. (1988) *Nucl. Acids Res.* **16**, 2671–90.

[41] Remers, W.A. (1979) in *The Chemistry of Antitumor Antibiotics*, (Wiley and Sons, New York) Vol. 1, pp. 133–75.

[42] Ward, D.C., Reich, E. & Goldberg, I.H. (1965) *Science* **149**, 1259–65.

[43] Weinberger, S., Shafer, R. & Berman, E. (1988) *Biopolymers* **27**, 831–42.

[44] Waring, M. (1970) *J. Mol. Biol.* **54**, 247–79.

[45] Van Dyke, M.W. & Dervan, P.B. (1983) *Biochemistry* **22**, 2373–7.

[46] Fox, K.R. & Howarth, N.R. (1985) *Nucl. Acids Res.* **13**, 8695–714.

[47] Prasad, K.S. & Nayak, R. (1976) *FEBS Lett.* **71**, 171–4.

[48] Shafer, R.H., Roques, B.P., LePecq, J.B. & Delepierre, M. (1988) *Eur. J. Biochem.* **173**, 377–82.

[49] Kam, M., Schafer, R.H. & Berman, E. (1988) *Biochemistry* **27**, 3581–8.

[50] Keniry, M.A., Brown, S.C., Berman, E. & Shafer, R.H. (1987) *Biochemistry* **26**, 1058-67.

[51] Berman, E., Brown, S.C., James, T.L. & Shafer, R.H. (1985) *Biochemistry* **24**, 6887–93.

[52] Patel, D.J. (1978) *Proc. Natl. Acad. Sci., U.S.A.* **75**, 5483–7.

[53] Gao, X. & Patel, D.J. (1989) *Biochemistry* **28**, 751–62.

[54] For recent examples from the Dervan group see Dervan, P.B. (1988) in *Nucleic Acids and Molecular Biology*, Eckstein, F. & Lilley, D.M.J. eds. (Springer-Verlag, Berlin) Vol. 2, pp. 49–64.

[55] Dervan, P.B. (1986) *Pont. Acad. Sci. Scr. Var.* **70**, 365–84.

[56] Schultz, P.G. & Dervan, P.B. (1983) *J. Am. Chem. Soc.* **105**, 7748–50.

[57] Youngquist, R.S. & Dervan, P.B. (1985) *J. Am. Chem. Soc.* **107**, 5528–9.

[58] Griffin, J.H. & Dervan, P.B. (1986) *J. Am. Chem. Soc.* **108**, 5008–9.

[59] Parrack, P., Dasgupta, D., Ayyer, J. & Sasisekharan, V. (1987) *FEBS Lett.* **212**, 297–301.

[60] Khorlin, A.A., Krylov, A.S., Grokhovsky, S.L., Zhuse, A.L., Zasedatelev, A.S., Gursky, G.V. & Gottikh, B.P. (1980) *FEBS Lett.* **118**, 311–4.

[61] Khorlin, A.A., Grokhovsky, S.L., Zhuze, A.L. & Gottikh, B.P. (1982) *Bioorgan. Khim.* **8**, 1063–9.

[62] Youngquist, R.S. & Dervan, P.B. (1987) *J. Am. Chem. Soc.* **109**, 7564–6.

[63] Griffin, J.H., Mack, D.P. & Dervan, P.B., unpublished results.

[64] Lown, J.W., Krowicki, K., Bhat, U.G., Skorobogaty, A., Ward, B. & Dabrowiak, J.C. (1986) *Biochemistry* **25**, 7408–16.

[65] Kissinger, K., Krowicki, K., Dabrowiak, J.C. & Lown, J.W. (1987) *Biochemistry* **26**, 5590–5.

[66] Van Dyke, M.W. (1984) Ph.D. thesis, California Institute of Technology.

[67] Wade, W.S. & Dervan, P.B. (1987) *J. Am. Chem. Soc.* **109**, 1574–5.

[68] Lee, M., Pon, R.T., Krowicki, K. & Lown, J.W. (1988) *J. Biomol. Struc. Dyn.* **5**, 939–49.

[69] Patel, D.J., Pardi, A. & Itakura, K. (1982) *Science* **216**, 581–90.

[70] Lee, M., Krowicki, K., Hartley, J.A., Pon, R.T. & Lown, J.W. (1988) *J. Am. Chem. Soc.* **110**, 3641–9.

[71] Zakrzewska, K., Lavery, R. & Pullman, B. (1987) *J. Biomol. Struc. Dyn.* **4**, 833–43.

[72] Lee, M., Hartley, J.A., Pon, R.T., Krowicki, K. & Lown, J.W. (1988) *Nucl. Acids Res.* **16**, 665–84.

[73] Lee, M., Coulter, D.M., Pon, R.T., Krowicki, K. & Lown, J.W. (1988) *J. Biomol. Struc. Dyn.* **5**, 1059–87.

[74] Galas, D. & Schmitz, A. (1978) *Nucl. Acids Res.* **5**, 3157–70.

[75] Gilbert, W., Maxam, A. & Mirzabekov, A. (1976) in *Control of Ribosome Synthesis*, Kjelgaard, N.O. & Malløe, O., eds. (Munksgaard, Copenhagen), pp. 139–48.

[76] Taylor, J.S., Schultz, P.G. & Dervan, P.B. (1984) *Tetrahedron* **40**, 457–65.

[77] Dervan, P.B. (1986) *Science* **232**, 464–71.

[78] Strobel, S.A., Moser, H.E. & Dervan, P.B. (1988) *J. Am. Chem. Soc.* **110**, 7927–7929.

[79] Gursky, G., Zasedatelev, A.S., Zhuze, A.L., Khorlin, A.A., Grokhovsky, S.L., Streltsov, S.A., Surovaya, A.N., Nikitin, S.M., Krylov, A.S., Retchinsky, V.O., Mikhailov, M.V., Beabealashvili, R.S. & Gottikh, B.P. (1982) *Cold Spring Harbor Symposium on Quantitative Biology* **74**, 367–78.

[80] Maxam, A.M. & Gilbert, W.S. (1980) *Methods in Enzymology* **65**, 499–560.

[81] Iverson, B.L. & Dervan, P.B. (1987) *Nucl. Acids Res.* **15**, 7823–30.

[82] Sutcliffe, J.G. (1978) *Cold Spring Harbor Symposium on Quantitative Biology* **43**, 77–90.

[83] Peden, K.W.C. (1983) *Gene* **22**, 277–80.

[84] Fox, K.R. & Waring, M.J. (1984) *Nucl. Acids Res.* **12**, 9271–85.

[85] Ceccarelli, C., Jeffrey, G.A. & Taylor, R. (1981) *J. Mol. Struct.* **70**, 255–71.

[86] Tullius, T.D. & Dombroski, B.A. (1986) *Proc. Natl. Acad. Sci., U.S.A.* **83**, 5469–73.

[87] Nelson, H.C.M., Finch, J.T., Luisi, B.F. & Klug, A. (1987) *Nature* **330**, 221–6.

[88] Wu, H-M. & Crothers, D.M. (1984) *Nature* **308**, 509–13.

[89] Beranek, D.T., Weis, C.C. & Swenson, D.H. (1980) *Carcinogenesis* **1**, 595–605.

[90] Zimmerman, S.B. (1982) *Ann. Rev. Biochem.* **51**, 395–427.

[91] Cornish-Bowden, A. (1985) *Nucl. Acids Res.* **13**, 3021–30.

[92] Griffin, J.H., unpublished results.

[93] MACROMODEL is a graphic based program developed by W.C. Still at Columbia University for the purpose of modeling macromolecules. A complete conformational search was done on the aromatic portion of each structure studied. The conformer list was refined by molecular mechanics techniques using the AMBER forcefield.

[94] Arnott, S. & Hukins, D.W.L. (1973) *J. Mol. Biol.* **81**, 93–105.

[95] BIOGRAF is a graphic based program developed by W.A. Goddard III, S. Mayo and B. Olafson at BioDesign for the purpose of modeling macromolecules. All structures were refined by molecular mechanics techniques to a local minimum using the Dreiding force field supplied with the program.

[96] Koudelka, G.B., Harrison, S.C. & Ptashne, M. (1987) *Nature* **326**, 886–8.

[97] Aggarwal, A.K., Rodgers, D.W., Drottar, M., Ptashne, M. & Harrison, S.C. (1988) *Science* **242**, 899–907.

[98] Koudelka, G.B., Harbury, P., Harrison, S.C. & Ptashne M. (1988) *Proc. Natl. Acad. Sci., U.S.A.* **85**, 4633–7.

[99] Brenowitz, M., Senear, D.F., Shea, M.A. & Ackers, G.K. (1986) *Methods in Enzymology* **130**, 133–181.

[100] Brenowitz, M., Senear, D.F., Shea, M.A. & Ackers, G.K. (1986) *Proc. Natl. Acad. Sci., U.S.A.* **83**, 8462–6.

[101] Lasky, R. & Mills, D.A. (1975) *Eur. J. Biochem.* **56**, 335–41.

[102] Hertzberg, R.P. & Dervan, P.B. (1983) *Biochemistry* **23**, 3934–45.

[103] Krylov, A.S., Grokhovsky, S.L., Zasedatelev, A.S., Zhuze, A.L., Gursky, G.V. & Gottikh, B.P. (1979) *Nucl. Acids Res.* **6**, 289–304.

[104] Zimmer, C., Luck, G., Birch-Hirschfeld, E., Weiss, R., Arcamone, F. & Guschlbauer, W. (1983) *Biochim. Biophys. Acta* **741**, 15–22.

[105] Lindahl, T. & Andersson, A. (1972) *Biochemistry* **11**, 3618–23.

[106] Pharmacia Molecular Biologicals Catalog, (1988) 135.

[107] Bevington, P.R. (1969) in *Data Reduction and Error Analysis for the Physical Sciences*, (McGraw Hill, New York), pp. 204–45.

[108] Marquardt, D.W. (1963) *J. Soc. Ind. Appl. Math.* **11**, 431–41.

[109] Cantor, C.R. & Schimmel, P.R. (1980) in *Biophysical Chemistry*, (W.H. Freeman, San Francisco) Part III, pp. 849–78.

[110] Luck, G., Triebel, H., Waring, M. & Zimmer, C. (1974) *Nucl. Acids Res.* **1**, 503–30.

[111] Hogan, M., Dattagupta, N. & Crothers, D. (1979) *Nature* **278**, 521–4.

[112] Baker, B. (1988) Ph.D. thesis, California Institute of Technology.

[113] Krowicki, K. & Lown, J.W. (1987) *J. Org. Chem.* **52**, 3493–501.

[114] Crothers, D.M. (1968) *Biopolymers* **6**, 575–84.

[115] Pages, M.J.M. & Roizès, G.P. (1984) *J. Mol. Biol.* **173**, 143–57.

[116] Fried, M. & Crothers, D.M. (1981) *Nucl. Acids Res.* **9**, 6506–25.

[117] De Roos, K.B. & Salemink, C.A. (1969) *Recuil. Trav. Chim. Pays-Bas* **88**, 1263–74.

[118] Den Hertog, H.J. & Jouwersma, C. (1953) *Recuil. Trav. Chim. Pays-Bas* **72**, 44–49.

[119] Ochia, E. & Yamanaka, H. (1955) *Chem. Pharm. Bull.* **3**, 173–4.

[120] Deady, L.W., Foskey, D.J. & Shanks, R.J. (1971) *J. Chem. Soc. (B)*, 1962–3.

[121] Nedenskov, P., Clauson-Kaas, N., Lei, J., Heide, H., Olsen, G. & Jansen, G. (1969) *Acta Chem. Scand.* **23**, 1791–1796.

[122] Regel, E. & Buchel, K.M. (1977) *Justus Liebigs Ann. Chem.*, 145–58.

[123] Jones, R.G. (1949) *J. Am. Chem. Soc.* **71**, 383–6.

[124] Pachter, I.J. & Kloetzel, M.C. (1952) *J. Am. Chem. Soc.* **74**, 1321–5.

[125] Barbieri, G., Benassi, R., Grandi, R., Pagnoni, U.M. & Taddei, F. (1979) *Org. Magn. Reson.* **12**, 159–62.

[126] Katritzky, A.R. & Reavill, R.E. (1965) *J. Chem. Soc.*, 3825–7.

[127] Green, R.W. & Tong, H.K. (1956) *J. Am. Chem. Soc.* **78**, 4896–900.

[128] Jellinek, H.H.G. & Urwin, J.R. (1954) *J. Phys. Chem.* **58**, 548–50.

[129] Essery, J.M. & Schofield, K. (1961) *J. Chem. Soc.*, 3939–53.

[130] Shirley, D.A. & Cameron, M.D. (1952) *J. Am. Chem. Soc.* **74**, 664–5.

[131] Lawson, A. (1956) *J. Chem. Soc.*, 307–310.

[132] Morgan, K.J. & Morrey, D.P. (1966) *Tetrahedron* **22**, 57–62.

[133] Gellman, S.H., final report.

[134] Evans, R.F. (1964) *J. Chem. Soc.*, 2450–5.

[135] Pullman, B. (1984) in *Specificity and Biological Interactions, Int. Symp. at the Pontifical Acad. Sci.*, Chagas, C. & Pullman, B., eds. (Vatican Press) Vol. 55, pp. 1–20.

[136] Weller, R.D. (1987) *NATO ASI, ser. A* **137**, 63–83.

[137] Struhl, K., Chen, W., Hill, D.E., Hope, I.A. & Oettinger, M.A. (1986) *Cold Spring Harbor Symposium on Quantitative Biology* **50**, 489–503.

[138] Jones, E.W. & Fink, G.R. (1982) in *The molecular biology of the yeast* Saccharomyces: *Metabolism and gene expression*, Strathern, J.N., *et al.* eds. (Cold Spring Harbor Laboratory, New York), pp. 181–299.

[139] Hope, I.A. & Struhl, K. (1986) *Cell* **46**, 885–94.

[140] Hope, I.A. & Struhl, K. (1987) *EMBO J.* **6**, 2781–4.

[141] Struhl, K. (1987) *Cell* **50**, 841–6.

[142] Crabeel, M., Huygen, R., Verschueren, K., Messenguy, F., Tinel, K., Cunin, R. & Glansdorff, N. (1985) *Mol Cell. Biol.* **5**, 3139–48.

[143] Beacham, I.R., Schweitzer, B.W., Warrick, H.M. & Carbon, J. (1984) *Gene* **29**, 271–9.

[144] Werner, M., Feller, A. & Pierard, A. (1985) *Eur. J. Biochem.* **146**, 371–81.

[145] Hinnebusch, A.G. & Fink, G.R. (1983) *J. Biol. Chem.* **258**, 5238–47.

[146] Hill, D.E., Hope, I.A., Macke, J.P. & Struhl, K. (1986) *Science* **234**, 451–7, and references therein.

[147] Donahue, T.F., Daves, R.S., Lucchini, G.R. & Fink, G.R. (1983) *Cell* **32**, 89–98.

[148] Nishiwaki, K., Hayashi, N., Irie, S., Chung, D.H., Harashima, S. & Oshima, Y. (1987) *Mol. Gen. Genet.* **208**, 159–67.

[149] Holmberg, S., Kielland-Brandt, M.C., Nilsson-Tillgren, T. & Petersen, J.G.L. (1985) *Carlsberg Res. Commun.* **50**, 163–78.

[150] Falco, S.C., Dumas, K.S. & Livak, K.J. (1985) *Nucl. Acids Res.* **13**, 4011–27.

[151] Hsu, Y.-P. & Schimmel, P. (1984) *J. Biol. Chem.* **259**, 3714–9.

[152] Zhou, K., Brisco, P.R.G., Hinkkanen, A.E. & Kohlhaw, G.B. (1987) *Nucl. Acids Res.* **15**, 5261–73.

[153] Beltzer, J.P., Chang, L.L., Hinkkanen, A.E. & Kohlhaw, G.B. (1986) *J. Biol. Chem.* **261**, 5160–7.

[154] Zalkin, H., Paluh, J.L., van Cleemput, M., Moye, W.S. & Yanofsky, C. (1984) *J. Biol. Chem.* **259**, 3985–92.

[155] Aebi, M., Furtur, R., Prantl, F., Niederberger, P. & Hütter, R. (1984) *Curr. Genet.* **8**, 165–72.

[156] Lee, W., Mitchell, P. & Tjian, R. (1987) *Cell* **49**, 741–52.

[157] Andreadis, A., Hsu, Y.-P., Kohlhaw, G.B. & Schimmel, P. (1982) *Cell* **31**, 319–25.

[158] Zalkin, H. & Yanofsky, C. (1982) *J. Biol. Chem.* **257**, 1491–1500.

[159] Harshman, K.D., Moye-Rowley, W.S. & Parker, C.S. (1988) *Cell* **53**, 321–30.

[160] Hai, T., Liu, F., Allegretto, E.A., Karin, M. & Green, M.R. (1988) *Genes and Development* **2**, 1216–26.

[161] Marx, J.L. (1988) *Science* **242**, 1377–8.

[162] Angel, P., Imagawa, M., Chiu, R., Stein, B., Imbra, R.J., Rahmsdorf, H.J., Jonat, C., Herrlich, P. & Karin, M. (1987) *Cell* **49**, 729–39.

[163] Ryder, K., Lau, L.F. & Nathans, D. (1988) *Proc. Natl. Acad. Sci., U.S.A.* **85**, 1487–91.

[164] Rauscher III, F.J., Sambucetti, L.C., Curran, T., Distel, R.J. & Spiegelman, B.M. (1988) *Cell* **52**, 471–80.

[165] Franza, B.R., Jr., Rauscher III, F.J., Josephs, S.F. & Curran, T. (1988) *Science* **239**, 1150–3.

[166] Burkoff, A.M. & Tullius, T.D. (1987) *Cell* **48**, 935–43.

[167] Burkoff, A.M. & Tullius, T.D. (1988) *Nature* **331**, 455–7.

[168] Thireos, G., Penn, M.D. & Greer, H. (1984) *Proc. Natl. Acad. Sci., U.S.A.* **81**, 5096-100.

[169] Hinnebusch, A.G. (1984) *Proc. Natl. Acad. Sci., U.S.A.* **81**, 6442–6.

[170] Harshman, K.D. (1989) Ph.D. thesis, California Institute of Technology.

[171] Bohmann, D., Bos, T.J., Admon, A., Nishimwo, T., Vogt, P.K. & Tjian, R. (1987) *Science* **238**, 1386–92.

[172] Van Beveren, C., von Stroaken, F., Curran, T., Müller, R. & Verma, I.M. (1983) *Cell* **32**, 1241–55.

[173] Harshman, K.D., unpublished data.

[174] Landschulz, W.H., Johnson, P.F. & McKnight, S.L. (1988) *Science* **240**, 1759–64.

[175] McClarin, J.A., Frederick, C.A., Wang, B-C., Greene, P., Boyer, H.W., Grable, J. & Rosenberg, J.M. (1986) *Science* **234**, 1526–41.

[176] Maniatis, T., Fritsch, E.F. & Sambrook, J. (1982) in *Molecular Cloning, A Laboratory Manual*, (Cold Spring Harbor Laboratory, New York), pp. 1–542.

[177] Mendel, D.M. & Dervan, P.B. (1987) *Proc. Natl. Acad. Sci., U.S.A.* **84**, 910–4.

[178] Haniford, D.B. & Pulleyblank, D.E. (1985) *Nucl. Acids Res.* **13**, 4343–63.

[179] Stewart, J.M. & Young, S.D. (1984) in *Solid Phase Peptide Synthesis*, (Pierce, Rockford, Illinois) 2nd ed., pp. 1–158.

[180] Still, W.C., Kahn, M. & Mitra, A. (1978) *J. Org. Chem.* **40**, 2923–5.

[181] Fanta, P. (1963) *Org. Syn. Coll. Vol. IV*, 844–5.

Appendix A

Summary of Gel Data

Table 1 Footprinting Gel Data.

Compound	5′ gel	Notebook Page	Thesis Figure	3′ gel	Notebook Page	Thesis Figure
N	298	IV-144	4.14	284	IV-128	A.7
D	168	II-262	2.4	284	IV-128	A.7
HyN	122	II-194	A.1	121	II-193	A.2
MeN	122	II-194	A.1	121	II-193	A.2
2-FuN	184	II-275	2.4	121	II-193	A.2
3-FuN	184	II-275	2.4	121	II-193	A.2
2-ThN	184	II-275	2.4	121	II-193	A.2
3-ThN	184	II-275	2.4	121	II-193	A.2
2-PyN	168	II-262	2.6	290	IV-135	A.8
720 bp	100	II-161	A.4	100	II-161	A.4
3-PyN	295	IV-141	2.5	290	IV-135	A.8
4-PyN	295	IV-141	2.5	290	IV-135	A.8
2-ImN	168	II-262	2.6	284	IV-128	A.7
4-ClPyN	297	IV-143	A.5	283	IV-127	4.3
2-PmN	297	IV-143	A.5	283	IV-127	4.3
4-Me_2NPyN	297	IV-143	A.5	283	IV-127	4.3
pH gel	199	IV-30	4.12			
CycN	297	IV-143	A.5	283	IV-127	4.3
3-MeOPyN	297	IV-143	A.5	283	IV-127	4.3
2-ImP	298	IV-144	4.14	284	IV-128	A.7
2-PrN	298	IV-144	4.14	284	IV-128	A.7
AcImN	298	IV-144	4.14	284	IV-128	A.7
2-ImD	298	IV-144	4.14	284	IV-128	A.7
NPy	295	IV-141	4.19	290	IV-135	A.8
NMePy	295	IV-141	4.19	290	IV-135	A.8
NIm	295	IV-141	4.19	290	IV-135	A.8
PyP^+PPy	295	IV-141	4.19	290	IV-135	A.8
Quantitative Footprinting						
D				277	IV-119	3.2
2-PyN				264	IV-101	3.3
2-ImN				279	IV-121	3.4

Table 2 Affinity Cleaving Gel Data.

Compound	5′ gel	Notebook Page	Thesis Figure	3′ gel	Notebook Page	Thesis Figure
ED	296	IV-142	2.6	291	IV-136	A.6
HyNE	122	II-194	A.1	121	II-193	A.2
MeNE	122	II-194	A.1	121	II-193	A.2
2-FuNE	122	II-194	A.1	121	II-193	A.2
3-FuNE	122	II-194	A.1	121	II-193	A.2
2-PyNE	296	IV-142	2.6	291	IV-136	A.6
3-PyNE	296	IV-142	2.5	291	IV-136	A.6
4-PyNE	296	IV-142	2.5	291	IV-136	A.6
2-ImNE	296	IV-142	2.6	291	IV-136	A.6
3-PyNE	296	IV-142	4.4	291	IV-136	A.6
4-PyNE	296	IV-142	4.4	291	IV-136	A.6
4-ClPyNE	296	IV-142	4.4	291	IV-136	A.6
2-PmNE	296	IV-142	4.4	291	IV-136	A.6
4-Me_2NPyNE	296	IV-142	4.4	291	IV-136	A.6
3-MeOPyNE	296	IV-142	4.4	291	IV-136	A.6
Double Strand Assay						
ED				293	IV-138	2.13
2-PyNE				293	IV-138	2.13
3-PyNE				293	IV-138	2.13
4-PyNE				293	IV-138	2.13
2-ImNE				293	IV-138	2.13
4-ClPyNE				213	IV-38	4.6
2-PmNE				213	IV-38	4.6
4-Me_2NPyNE				213	IV-38	4.6
3-MeOPyNE				213	IV-38	4.6

Figure 1 Footprinting and affinity cleaving of the furan and thiophene analogs of D. Autoradiogram of an 8% high resolution denaturing polyacrylamide gel. All reactions contain 4 mM DTT, 100 μM-bp calf thymus DNA, and 12 kcpm 5′ labeled 517 bp restriction fragment in 40 mM Tris·acetate pH 7.9 buffer. Lane 1, intact DNA; lane 2, Maxam-Gilbert G reaction;[80] lanes 3–11 contain 4 μM MPE·Fe(II), lane 3, MPE·Fe(II) standard; lane 4, 1 μM D; lane 5, 10 μM N, lane 6, 25 μM Hydroxyacetamide-netropsin (HyN); lane 7, 25 μM Methoxyacetamide-netropsin (MeN); lane 8, 10 μM 2-FuN; lane 9, 10 μM 3-FuN; lane 10, 5 μM 2-ThN; lane 11, 5 μM 3-ThN; lane 12, 2 μM ED; lane 13, 40 μM NE; lane 14, 60 μM HyNE; lane 15, 60 μM MeNE; lane 16, 40 μM 2-FuNE; lane 17, 80 μM 3-FuNE.

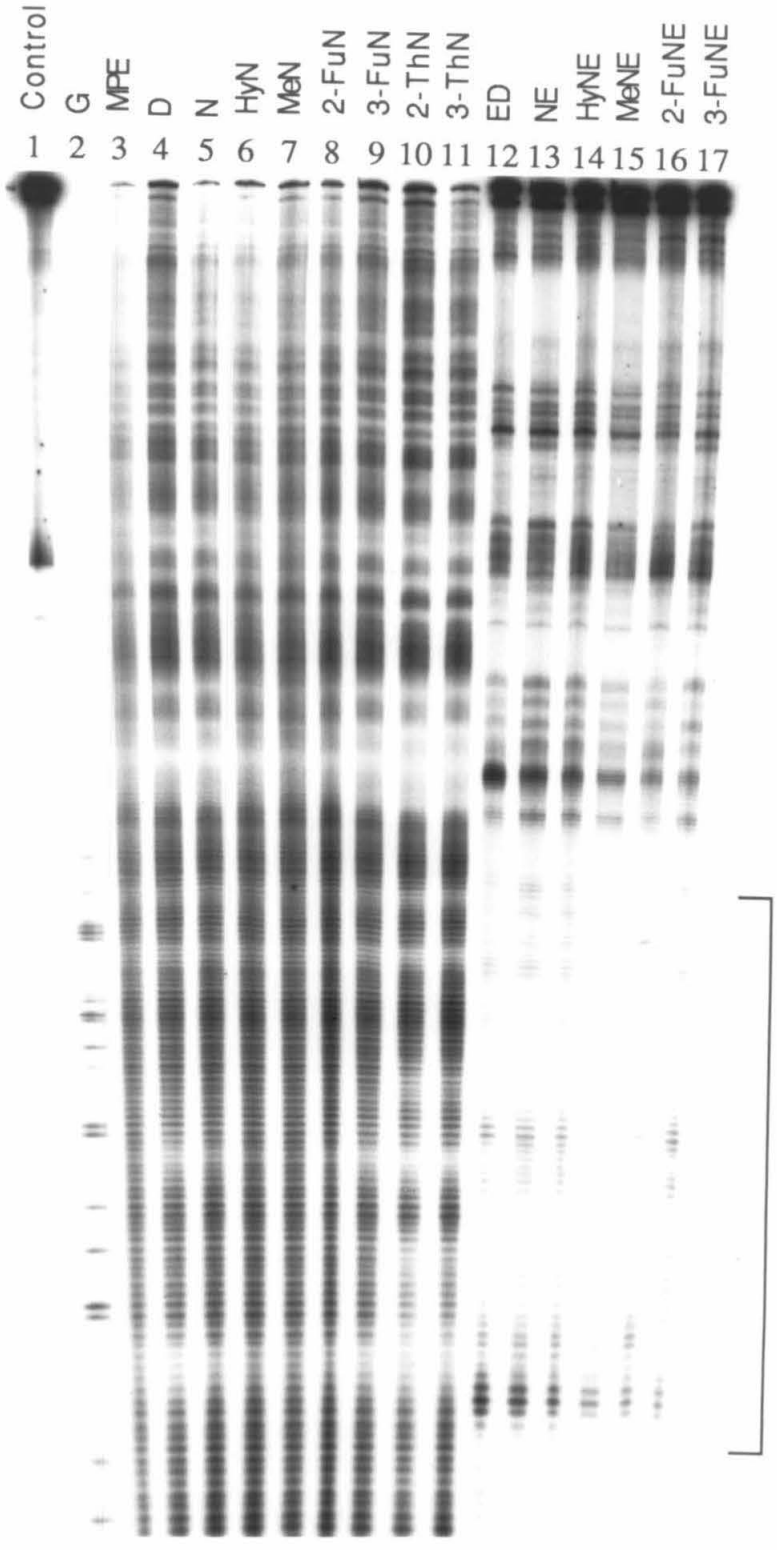
Control
G
MPE
D
N
HyN
MeN
2-FuN
3-FuN
2-ThN
3-ThN
ED
NE
HyNE
MeNE
2-FuNE
3-FuNE
1 2 3 4 5 6 7 8 9 10 11 12 13 14 15 16 17

Figure 2 Footprinting and affinity cleaving of the furan and thiophene analogs of D. Autoradiogram of an 8% high resolution denaturing polyacrylamide gel. All reactions contain 4 mM DTT, 100 μM-bp calf thymus DNA, and 12 kcpm 3′ labeled 517 bp restriction fragment in 40 mM Tris·acetate pH 7.9 buffer. Lane 1, intact DNA; lane 2, Maxam-Gilbert G reaction;[80] lanes 3–11 contain 4 μM MPE·Fe(II), lane 3, MPE·Fe(II) standard; lane 4, 1 μM D; lane 5, 10 μM N, lane 6, 25 μM Hydroxyacetamide-netropsin (HyN); lane 7, 25 μM Methoxyacetamide-netropsin (MeN); lane 8, 10 μM 2-FuN; lane 9, 10 μM 3-FuN; lane 10, 5 μM 2-ThN; lane 11, 5 μM 3-ThN; lane 12, 2 μM ED; lane 13, 40 μM NE; lane 14, 60 μM HyNE; lane 15, 60 μM MeNE; lane 16, 40 μM 2-FuNE; lane 17, 80 μM 3-FuNE.

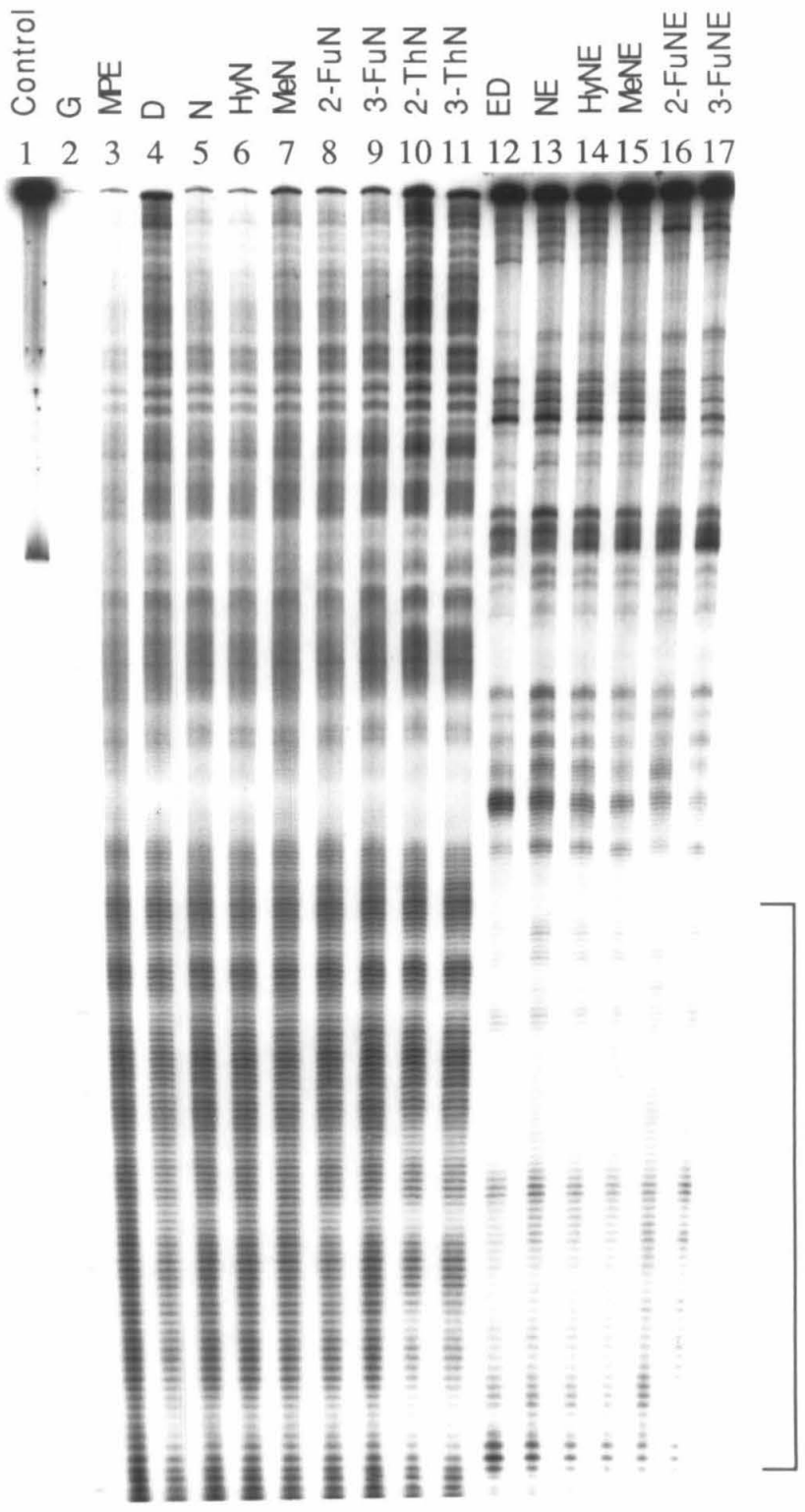
Control
G
MPE
D
N
HyN
MeN
2-FuN
3-FuN
2-ThN
3-ThN
ED
NE
HyNE
MeNE
2-FuNE
3-FuNE
1 2 3 4 5 6 7 8 9 10 11 12 13 14 15 16 17

Figure 3 Structural features of 2-PyN and 2-ImN binding. Autoradiogram of an 8% denaturing polyacrylamide gel. All reactions contain 12 kcpm 5′ labeled 517 bp restriction fragment. Lanes 1, 3–6, 12–24, and 26–28 contain 200 μM-bp calf thymus DNAin 40 mM tris acetate pH 7.9 buffer; Lanes 7–11, and 25 contain 200 μM-bp calf thymus DNA in TKMC buffer; Lane 1, intact DNA; lane 2, G reaction;[80] lanes 3–6 contain 4 μM MPE·Fe(II), and 4 mM DTT, cleavage time 20 min at 37°C; lanes 7–11, and 25 contain 1 ng DNase I reacted for 3 min at 25°C; lanes 12–15, and 26 contain 53 mM dimethyl sulfate, reacted for 5 min at 25°C, then A>G workup;[80] lanes 16–19, and 27 contain 136 mM diethyl pyrocarbonate, 10 min at 37°C; lanes 20–23, and 28 contain 100 μM potassium permanganate, 15 min at 37°C; lanes 4, 9, 13, 17, and 21 contain 20 μM D; lanes 5, 10, 14, 18, and 22 contain 20 μM 2-PyN; lanes 6, 11, 15, 19, and 23 contain 20 μM 2-ImN; lanes 25–28 contain 20 μM echinomycin.

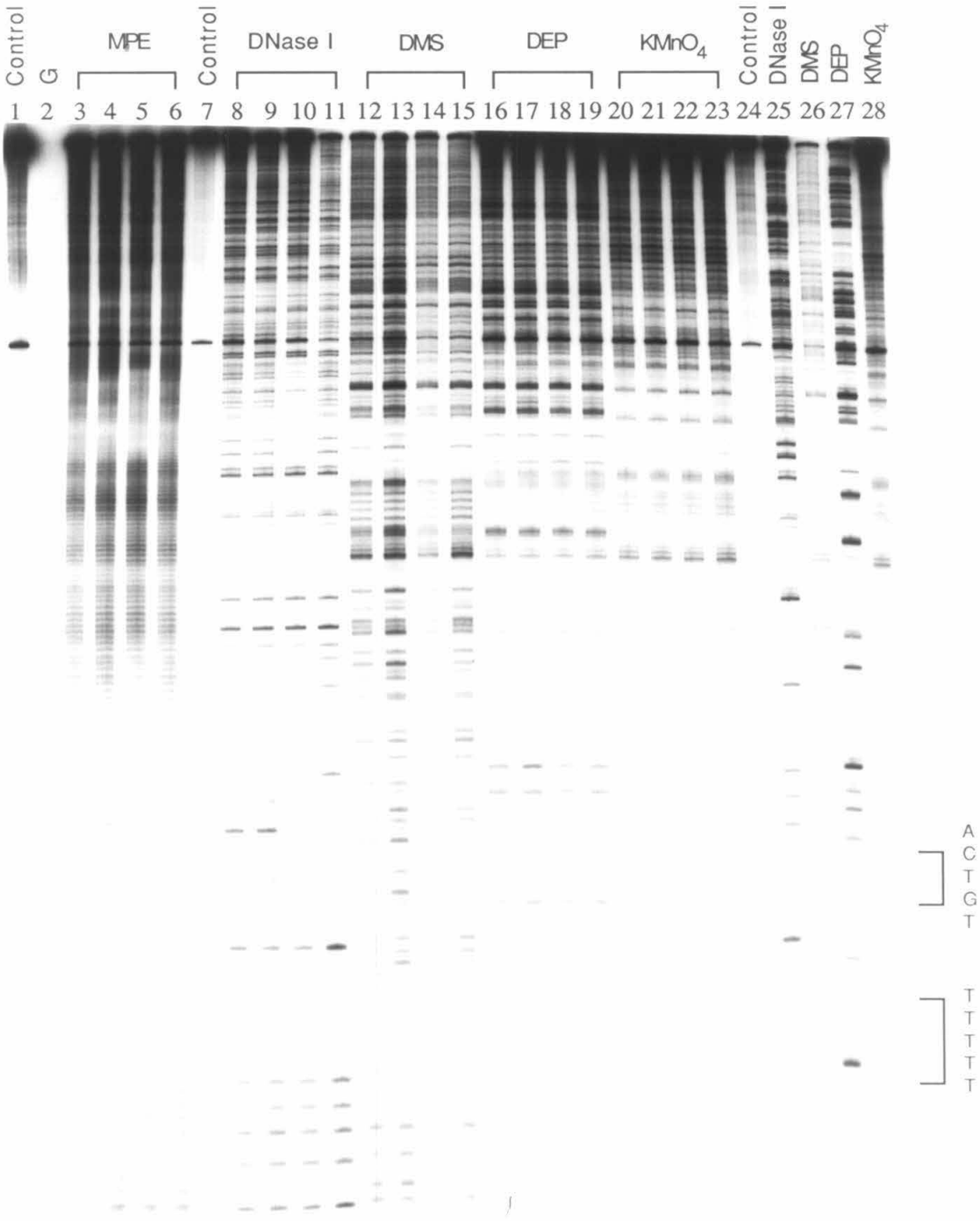
Control
G
MPE
Control
DNase I
DMS
DEP
KMnO4
Control
DNase I
DMS
DEP
KMnO4
1 2 3 4 5 6 7 8 9 10 11 12 13 14 15 16 17 18 19 20 21 22 23 24 25 26 27 28
A
C
T
G
T
T
T
T
T
T

Figure 4 Footprinting and affinity cleaving of 2-PyN on the *Sal* I/*Sty* I restriction fragment of pBR322. Autoradiogram of an 8% denaturing polyacrylamide gel. All reactions contain 4 mM DTT, 100 μM-bp calf thymus DNA, and 12 kcpm labeled 720 bp restriction fragment in 40 mM Tris·acetate pH 7.9 buffer. Lanes 1–9, 5′ labeled fragment; lanes 10–18, 3′ labeled fragment; Lanes 1 and 18, intact DNA; lanes 2 and 17, G reaction;[80] lanes 3 and 10, contain 10 μM ED; lanes 4–6 and 15–13 contain 2-PyNE at 50 μM, 25 μM, and 10 μM, respectively; lanes 7–12 contain 4 μM MPE·Fe(II), lanes 7 and 12, MPE·Fe(II) standards; lanes 8 and 11, 1 μM D; lanes 9–10, 10 μM 2-PyN.

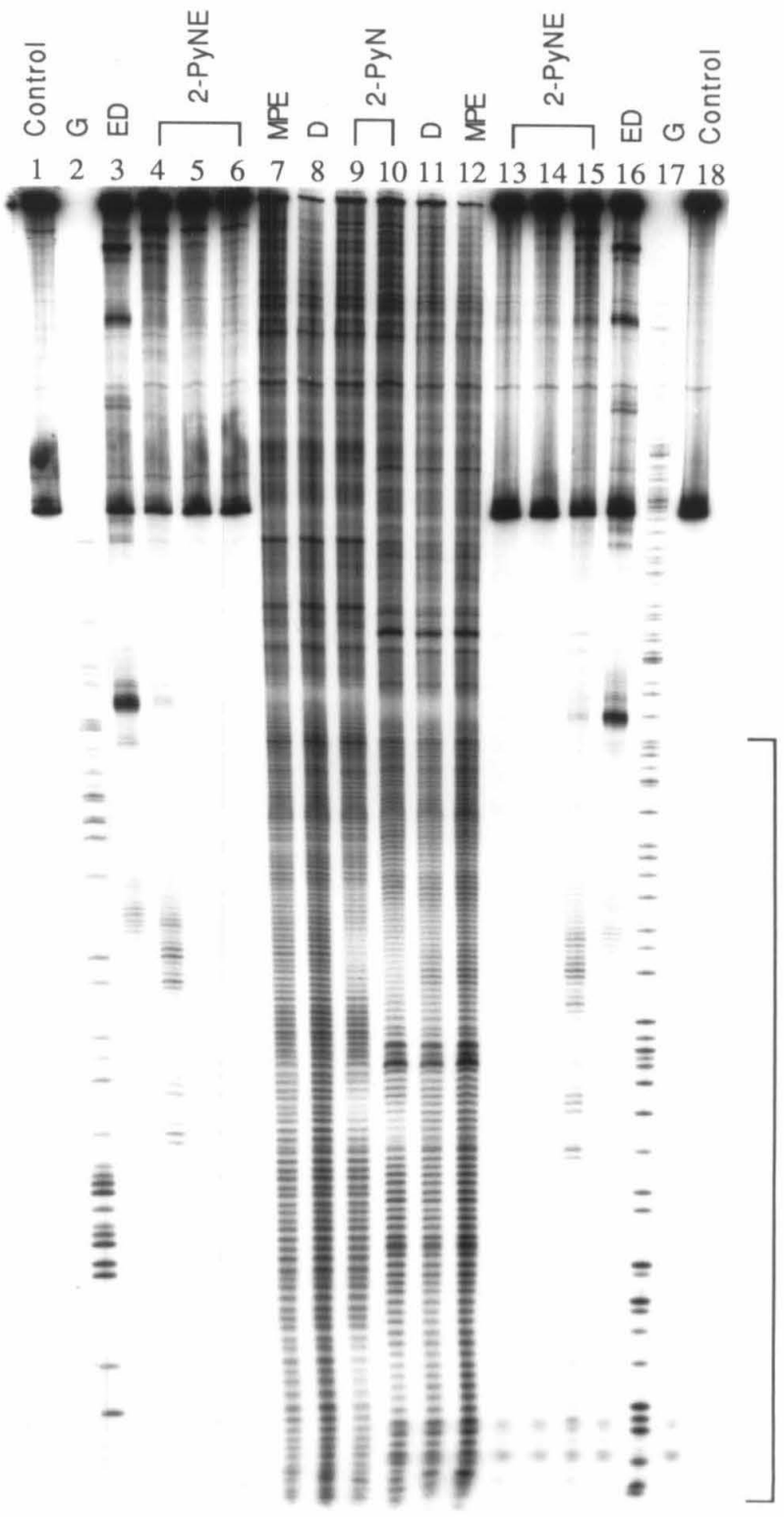
Control
G
ED
2-PyNE
MPE
D
2-PyN
D
MPE
2-PyNE
ED
G
Control
1 2 3 4 5 6 7 8 9 10 11 12 13 14 15 16 17 18

Figure 5 Footprinting of substituted derivatives of 2-PyN and 2-ImN. Autoradiogram of an 8% denaturing polyacrylamide gel. All reactions contain 4 mM DTT, 100 μM-bp calf thymus DNA, and 12 kcpm 5′ labeled 517 bp restriction fragment in 40 mM Tris·acetate pH 7.9 buffer. Lane 1, intact DNA; lane 2, G reaction;[80] lane 3, A reaction;[81] lanes 4–22 contain 4 μM MPE·Fe(II): lane 4, MPE·Fe(II) standard; lane 5 4 μM D; lane 6, 20 μM 2-PyN; lane 6, 20 μM 2-ImN; lanes 8–10 contain 35 μM, 10 μM, and 1 μM 4-ClPyN respectively; lanes 11–13, 35 μM, 10 μM, and 1 μM 2-PmN respectively; lanes 14–16, 35 μM, 10 μM, and 1 μM 4-Me_2NPyN respectively; lanes 17–19, 35 μM, 10 μM, and 1 μM CycN respectively.

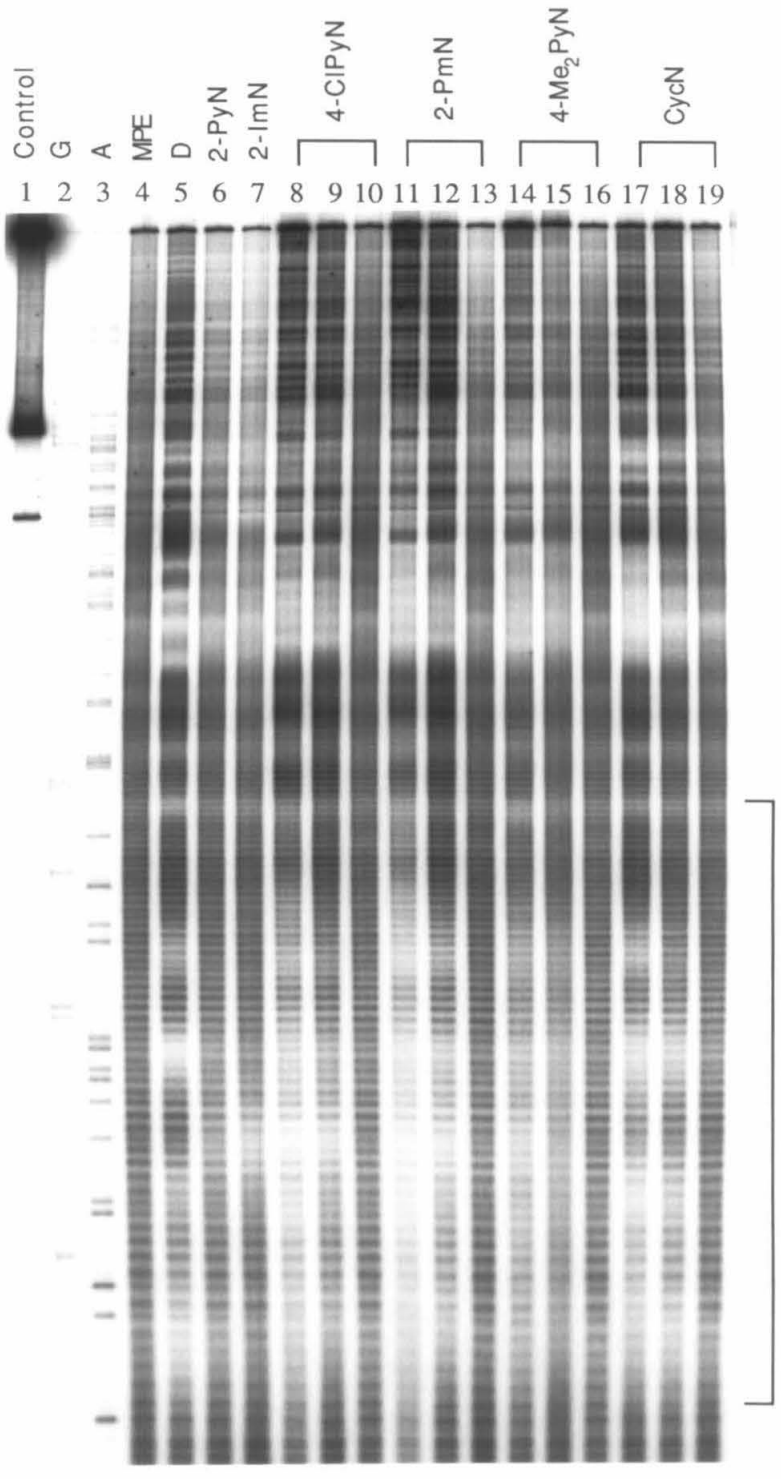
Control
G
A
MPE
D
2-PyN
2-ImN
4-ClPyN
2-PmN
4-Me2PyN
CycN
1 2 3 4 5 6 7 8 9 10 11 12 13 14 15 16 17 18 19

Figure 6 Affinity cleaving of the substituted pyridine derivatives. Autoradiogram of an 8% denaturing polyacrylamide gel. All reactions contain 4 mM DTT, 100 μM-bp calf thymus DNA, and 12 kcpm 3′ labeled 517 bp restriction fragment in 40 mM Tris·acetate pH 7.9 buffer. Lane 1, intact DNA; lane 2, G reaction;[80] lane 3, A reaction;[81] lane 4, 2 μM ED; lane 5, 50 μM 2-PyNE, lane 6, 70 μM 2-ImNE; lane 7, 10 μM 3-PyNE; lane 8, 7 μM 4-PyNE; lane 9, 70 μM 4-ClPyNE; lane 10, 25 μM 2-PmNE; lane 11, 50 μM 4-Me_2NPyNE; lane 12, 70 μM 3-MeOPyNE.

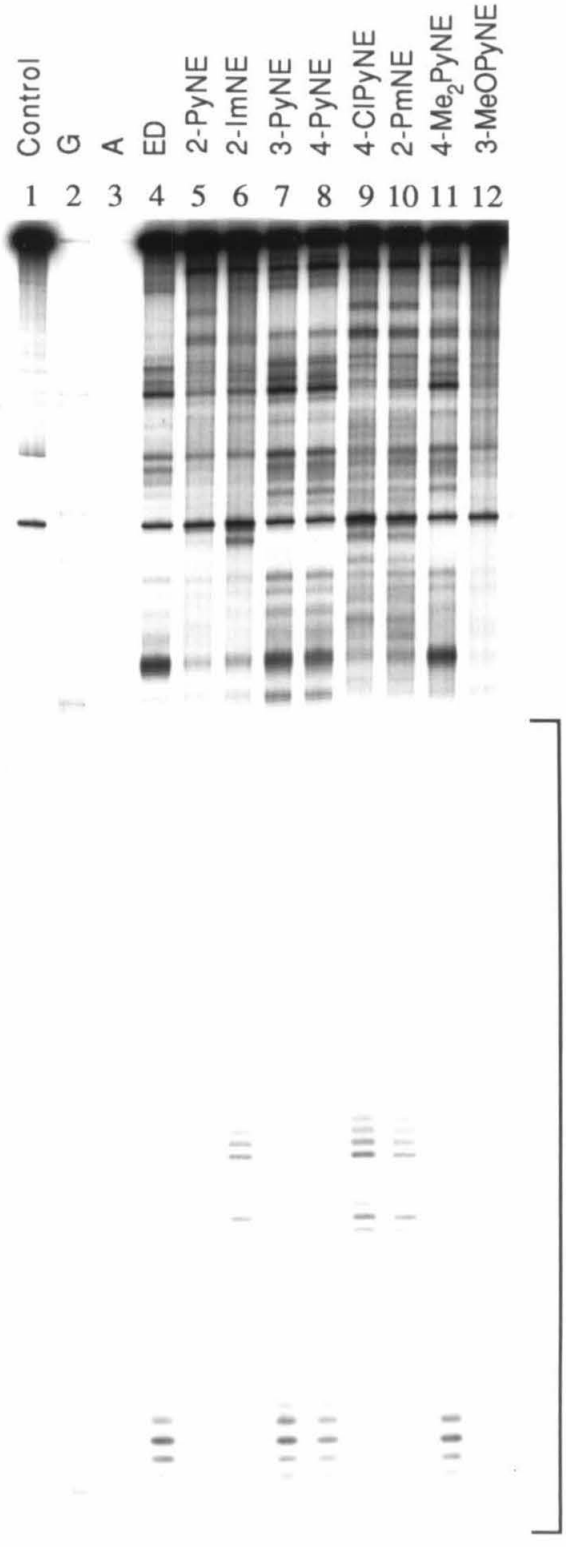
Control
G
A
ED
2-PyNE
2-ImNE
3-PyNE
4-PyNE
4-ClPyNE
2-PmNE
4-Me2PyNE
3-MeOPyNE
1 2 3 4 5 6 7 8 9 10 11 12

Figure 7 Footprinting of varying length D and 2-ImN derivatives. Autoradiogram of an 8% denaturing polyacrylamide gel. All reactions contain 4 mM DTT, 100 μM-bp calf thymus DNA, and 12 kcpm 3′ labeled 517 bp restriction fragment in 40 mM Tris·acetate pH 7.9 buffer. Lane 1, intact DNA; lane 2, G reaction;[80] lane 3, A reaction;[81] lanes 4–22 contain 4 μM MPE·Fe(II): lane 4, MPE·Fe(II) standard lanes 5–7 contain 35 μM, 10 μM, and 1 μM N respectively; lanes 8–10, 35 μM, 10 μM, and 1 μM 2-PrN respectively; lanes 11–13, 5 μM, 2 μM, and 1 μM D respectively; lanes 14–16, 50 μM, 35 μM, and 10 μM 2-PrN respectively; lanes 17–19, 35 μM, 10 μM, and 1 μM 2-ImN respectively; lanes 20–22, 35 μM, 10 μM, and 1 μM AcImN respectively; lanes 23–25, 35 μM, 10 μM, and 1 μM 2-ImD respectively.

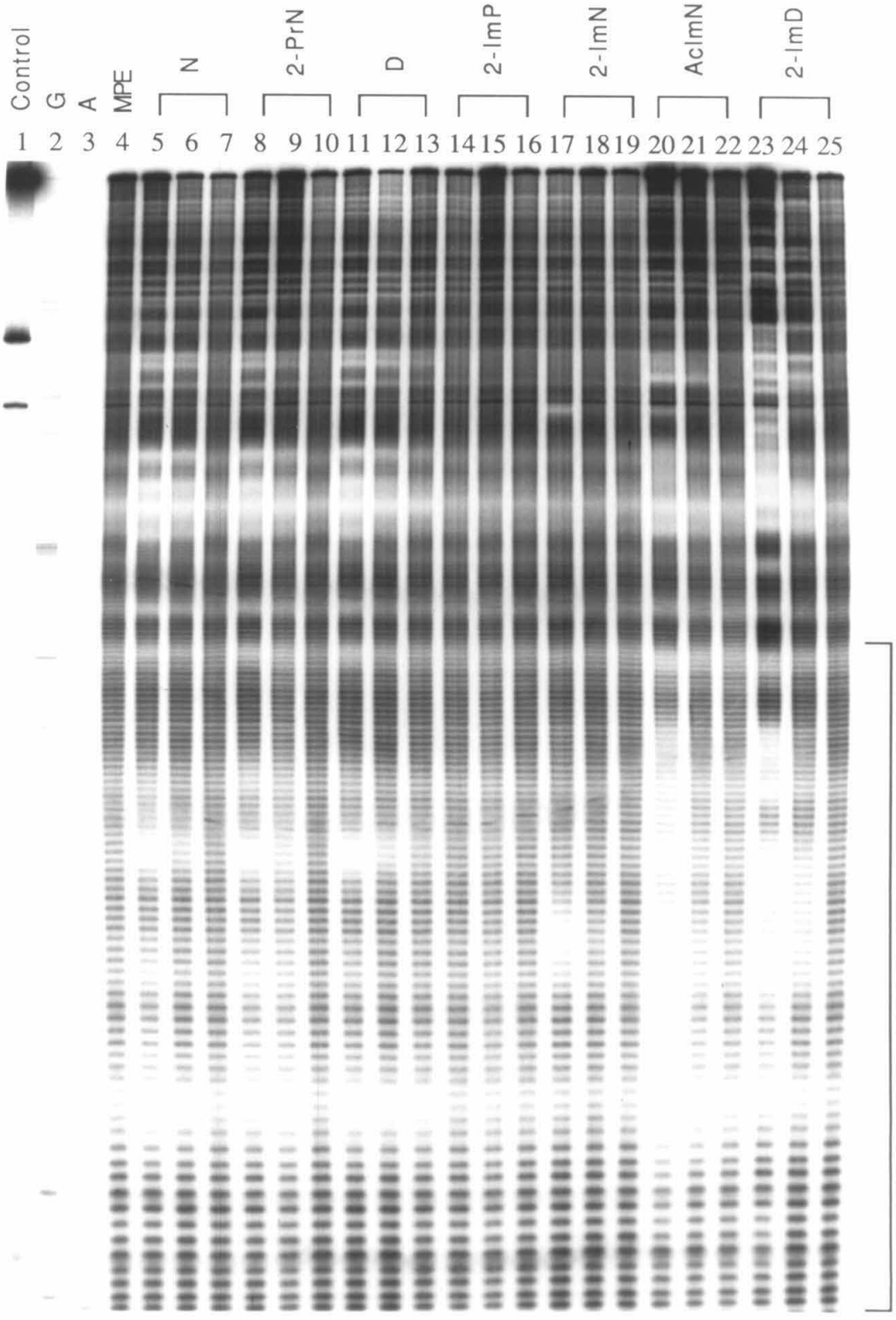
Control
G
A
MPE
N
2-PrN
D
2-ImP
2-ImN
AcImN
2-ImD
1 2 3 4 5 6 7 8 9 10 11 12 13 14 15 16 17 18 19 20 21 22 23 24 25

Figure 8 Footprinting of C-terminal analogs of 2-PyN and 2-ImN. Autoradiogram of an 8% denaturing polyacrylamide gel. All reactions contain 4 mM DTT, 100 μM-bp calf thymus DNA, and 12 kcpm 3′ labeled 517 bp restriction fragment in 40 mM Tris·acetate pH 7.9 buffer. Lane 1, intact DNA; lane 2, G reaction;[80] lane 3, A reaction;[81] lanes 4–25 contain 4 μM MPE·Fe(II): lane 4, MPE·Fe(II) standard; lane 5 4 μM D; lane 6, 20 μM 2-PyN; lane 6, 20 μM 2-ImN; lanes 8–10 contain 35 μM, 10 μM, and 1 μM 3-PyN respectively; lanes 11–13, 35 μM, 10 μM, and 1 μM 4-PyN respectively; lanes 14–16, 35 μM, 10 μM, and 1 μM NPy respectively; lanes 17–19, 35 μM, 10 μM, and 1 μM NMePy respectively; lanes 20–22, 50 μM, 35 μM, and 10 μM PyP^+PPy respectively; and lanes 23–25, 35 μM, 10 μM, and 1 μM NIm respectively.

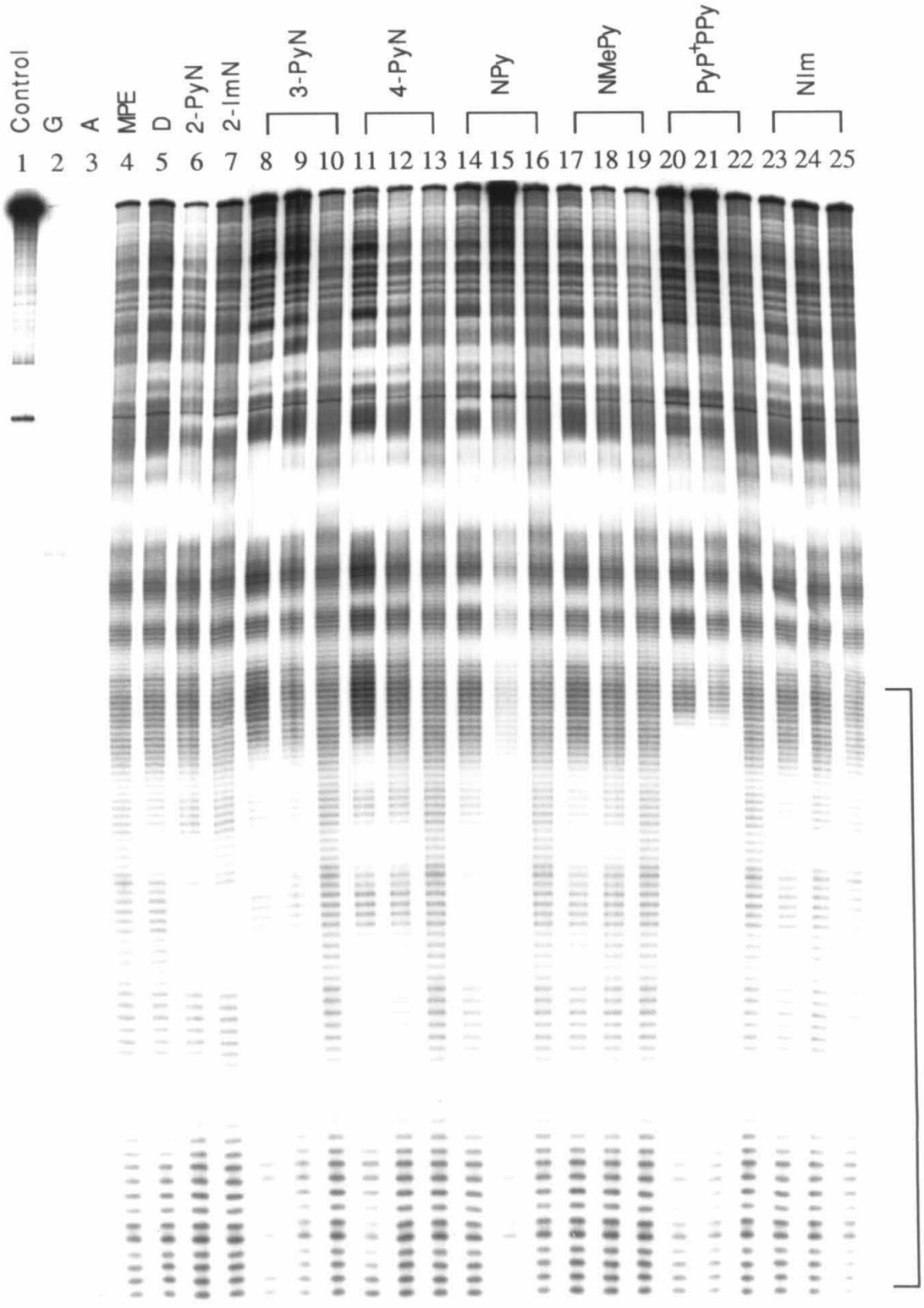
Control
G
A
MPE
D
2-PyN
2-ImN
3-PyN
4-PyN
NPy
NMePy
PyP+PPy
NIm
1 2 3 4 5 6 7 8 9 10 11 12 13 14 15 16 17 18 19 20 21 22 23 24 25

Appendix B

Summary of Quantitative Footprinting Data

2-PyN Quantitative Footprinting Data

[MPE]	Site	Data File	Gel #	K_a Monomer	χ^2	K_a Dimer	χ^2
1 μM	TGTCA	qfpp523w	264	2.0×10^5	1.71	2.5×10^5	0.71
		qfpp78a	278	1.8×10^5	0.87	2.1×10^5	0.66
		qfpp82a	262	1.4×10^5	1.99	1.9×10^5	1.40
		Average		1.7×10^5	18[a]	2.2×10^5	14[a]
	TTTTT	qfpp523x	264	3.6×10^5	1.19	3.0×10^5	1.06
		qfpp78c	278	1.1×10^5	1.36	1.2×10^5	1.12
		qfpp82b	262	2.1×10^5	1.18	3.2×10^5	0.94
		Average		2.3×10^5	50[a]	2.5×10^5	44[a]
	TTAAT	qfpp523y	264	4.2×10^4	1.28	7.2×10^4	1.27
		qfpp78b	278	7.4×10^4	1.13	9.9×10^4	1.54
		qfpp82c	262	5.4×10^4	1.28	8.7×10^4	1.03
		Average		5.7×10^4	28[a]	8.6×10^9	16[a]
	AATAA	qfpp523z	264	8.6×10^4	2.59	1.2×10^5	1.31
		qfpp78d	278	8.4×10^4	3.06	1.1×10^5	2.27
		qfpp82d	262	7.8×10^4	2.97	1.1×10^5	1.93
		Average		8.3×10^4	5[a]	1.2×10^5	5[a]
0.5 μM	TGTCA	qfpp106a	314	1.9×10^5	3.15	2.4×10^5	0.93
	TTTTT	qfpp106b	314	1.5×10^5	0.71	1.9×10^5	0.58
	TTAAT	qfpp106c	314	2.6×10^4	2.23	6.4×10^4	1.79
	AATAA	qfpp106d	314	1.3×10^5	3.00	1.7×10^5	1.58
0.38 μM	TGTCA	qfpp825a	285	3.0×10^5	0.93	3.1×10^5	0.26
		qfpp103a	312	1.6×10^5	2.32	2.4×10^5	0.67
	TTTTT	qfpp825b	285	6.1×10^5	0.61	2.3×10^5	0.55
		qfpp103b	312	1.3×10^5	1.42	1.3×10^5	1.19
	AATAA	qfpp825d	285	2.1×10^5	1.44	2.5×10^5	0.92
		qfpp103d	312	6.8×10^4	2.18	1.2×10^5	1.41
	TTAAT	qfpp103c	312	2.2×10^4	0.48	2.7×10^4	0.59

[a] Standard Deviation (%).

D, 2-ImN Quantitative Footprinting Data

L	Site	Data File	Gel #	K_a Monomer	χ^2	K_a Dimer	χ^2
D	TTTTT	qfpd614k	273	4.4×10^7	2.84	6.3×10^7	2.28
		qfpd615k	275	7.7×10^7	0.96	9.0×10^7	1.06
		qfpd618k	276	4.7×10^7	1.60	5.8×10^7	2.19
		qfpd78k	277	3.6×10^7	0.69	4.7×10^7	1.04
		Average		5.1×10^7	35[a]	6.5×10^7	28[a]
	TTAAT	qfpd614l	273	2.7×10^6	1.32	3.3×10^6	0.81
		qfpd615l	275	1.9×10^6	1.88	1.9×10^6	1.89
		qfpd618l	276	1.6×10^6	1.35	1.8×10^6	0.78
		qfpd78l	277	6.9×10^5	1.02	1.2×10^6	0.85
		Average		1.7×10^6	49[a]	2.1×10^6	42[a]
	AATAA	qfpd614m	273	1.9×10^7	0.92	2.0×10^7	0.57
		qfpd615m	275	2.7×10^7	0.68	2.3×10^7	1.44
		qfpd618m	276	1.3×10^7	0.42	1.4×10^7	1.62
		qfpd78m	277	5.4×10^6	1.10	6.7×10^6	1.40
		Average		1.6×10^7	57[a]	1.6×10^7	45[a]
2-ImN	TGTCA	qfpi64	268	1.4×10^5	1.40	1.5×10^5	0.63
		qfpi612a	271	1.6×10^5	1.63	1.9×10^5	0.64
		qfpi712	279	1.1×10^5	1.39	1.3×10^5	0.46
		Average		1.4×10^5	18[a]	1.6×10^5	19[a]

[a] Standard Deviation (%).

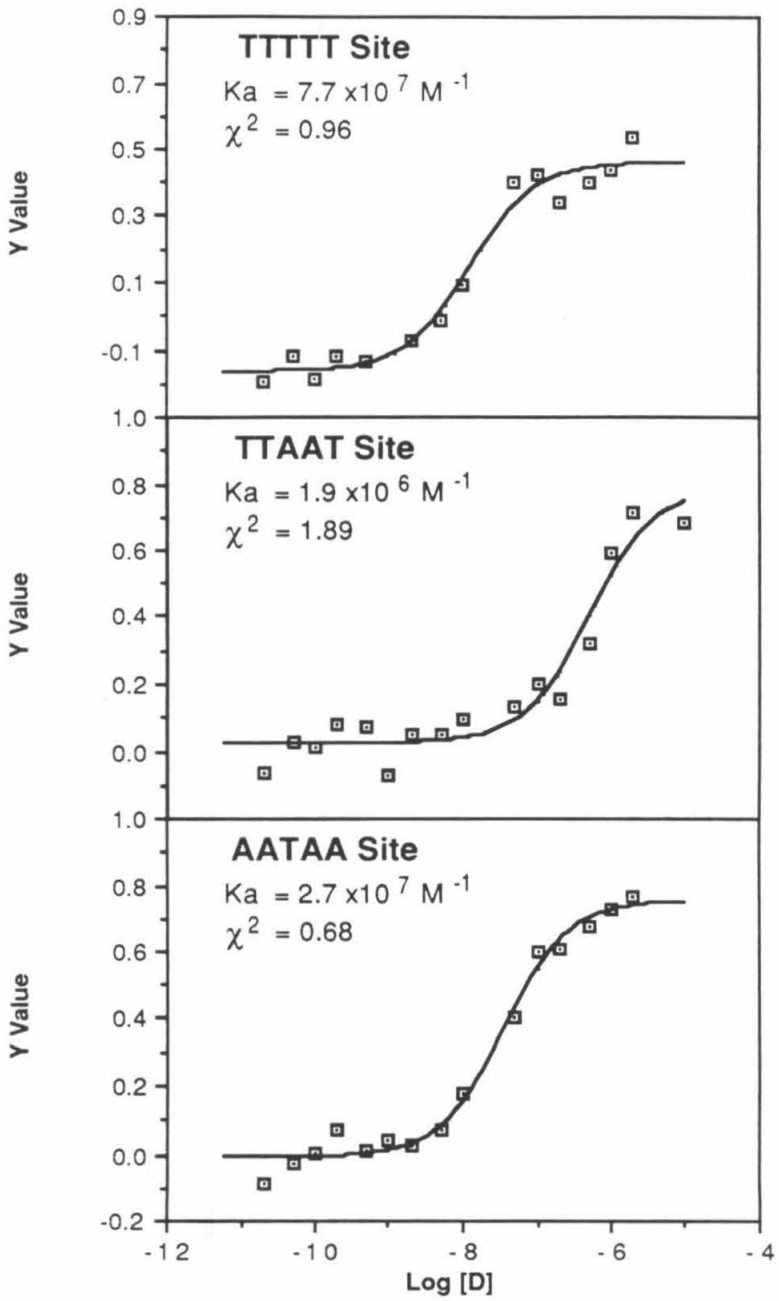

D, Gel #275, 1 μM MPE·Fe(II), qfpd615 Data

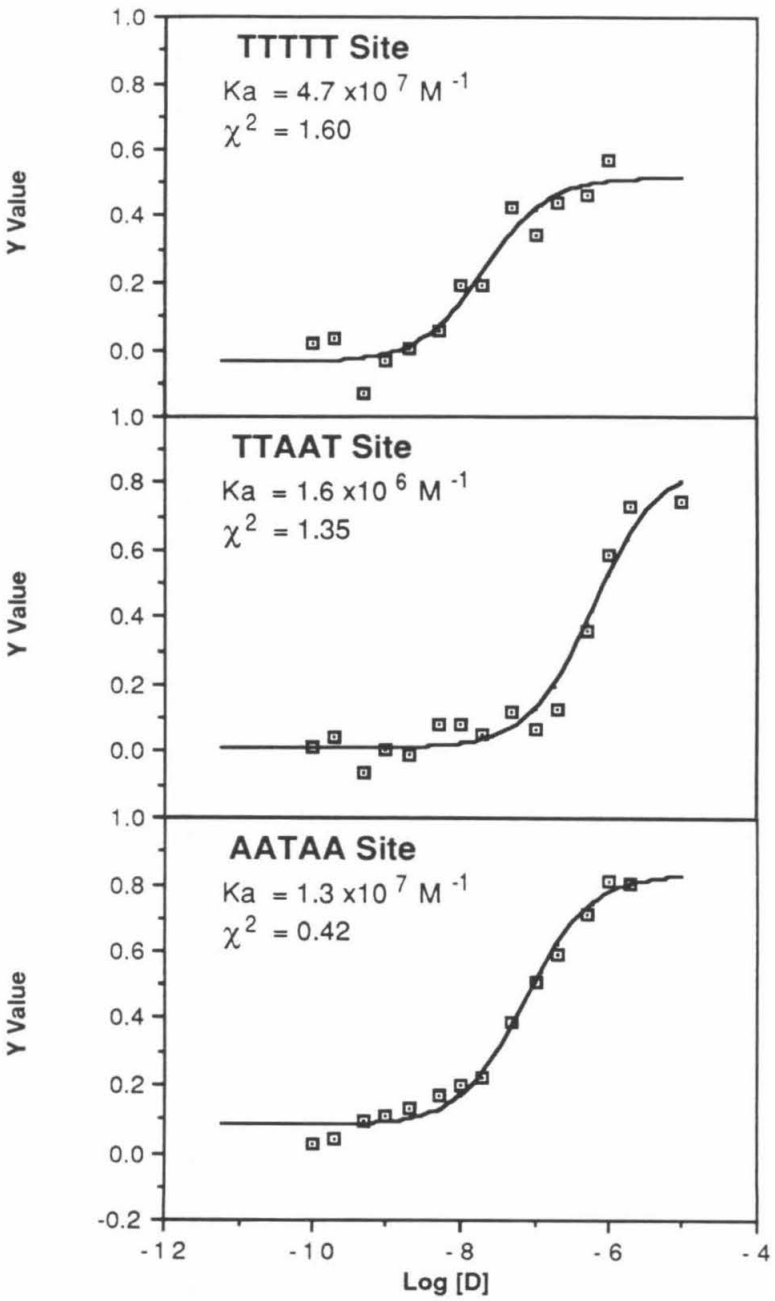

D, Gel #276, 1 μM MPE·Fe(II), qfpd618 Data

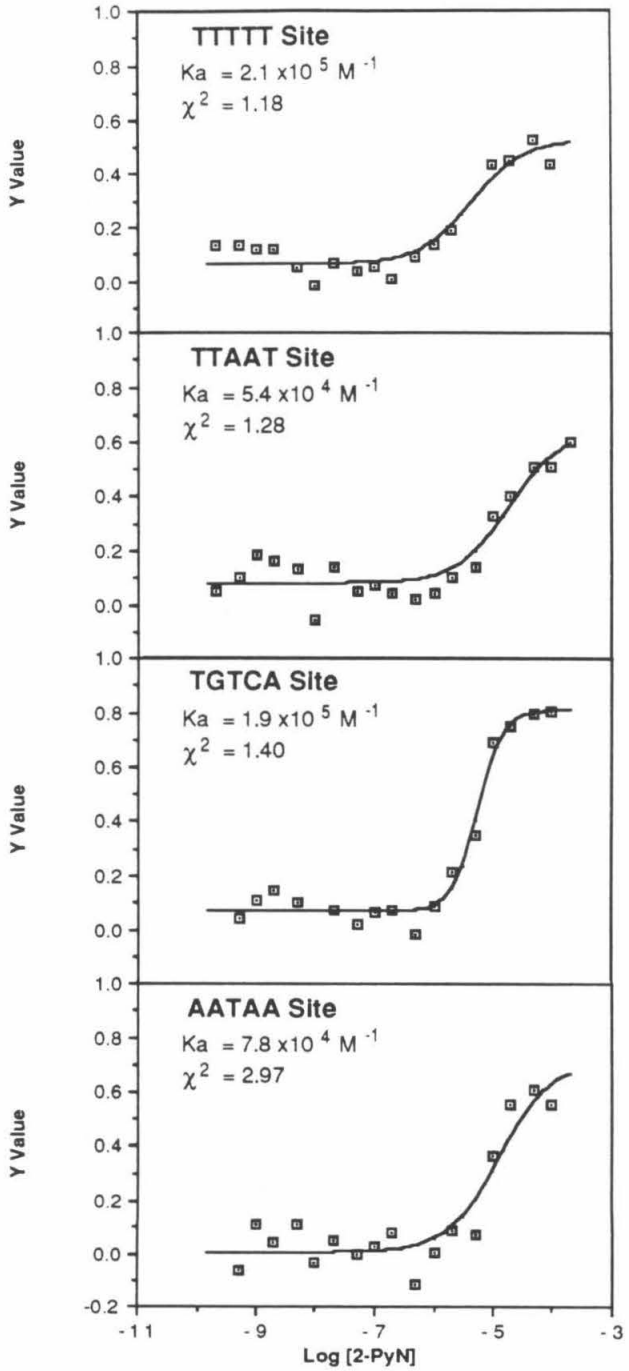

2-PyN, Gel #262, 1 μM MPE·Fe(II), qfpp82 Data

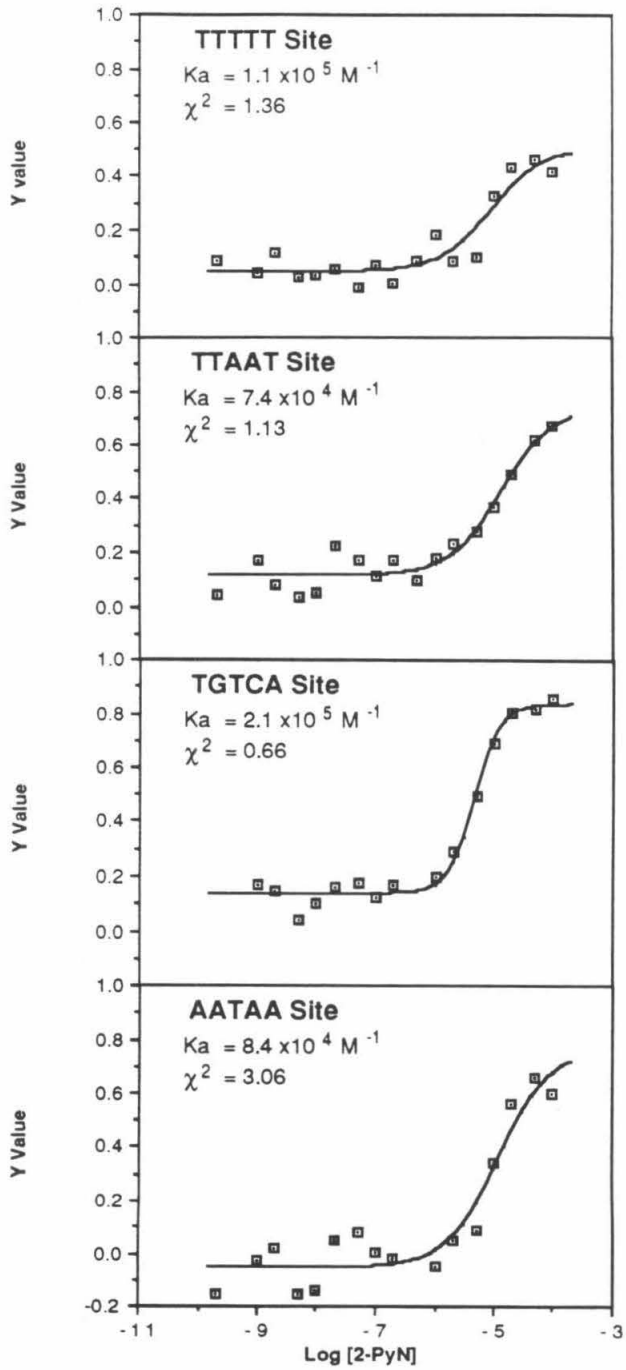

2-PyN, Gel #278, 1 μM MPE·Fe(II), qfpp78 Data

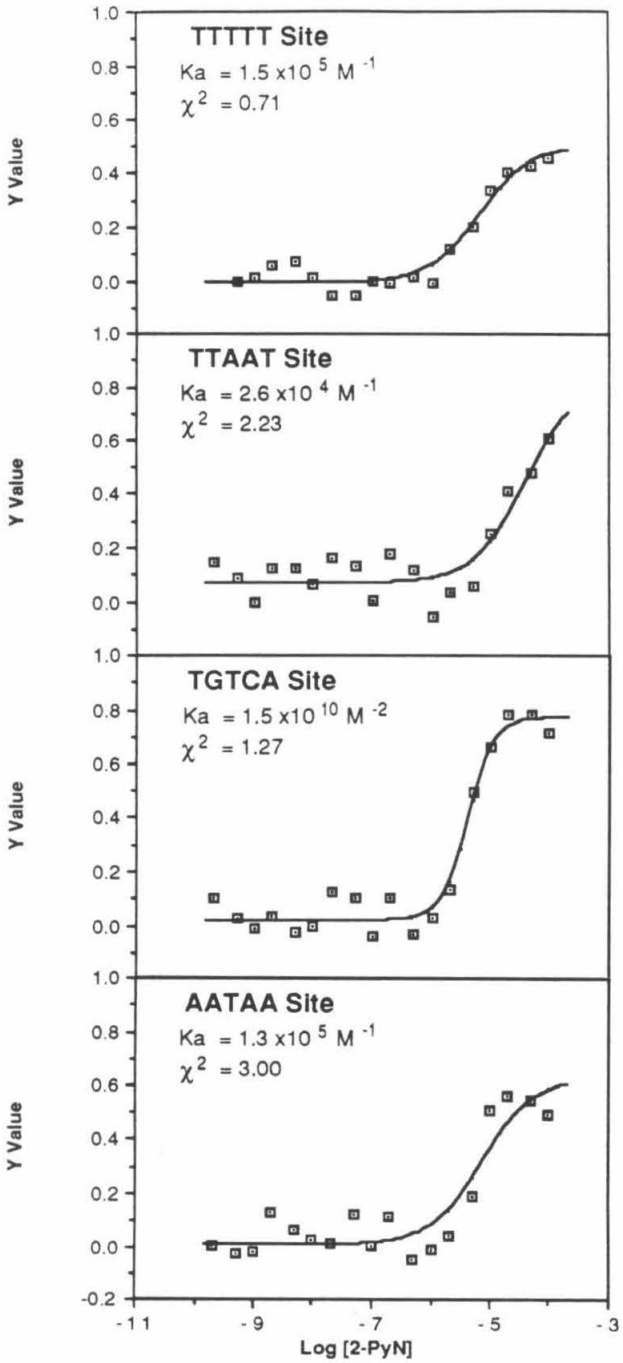

2-PyN, Gel #314, 0.5 μM MPE·Fe(II), qfpp106 Data

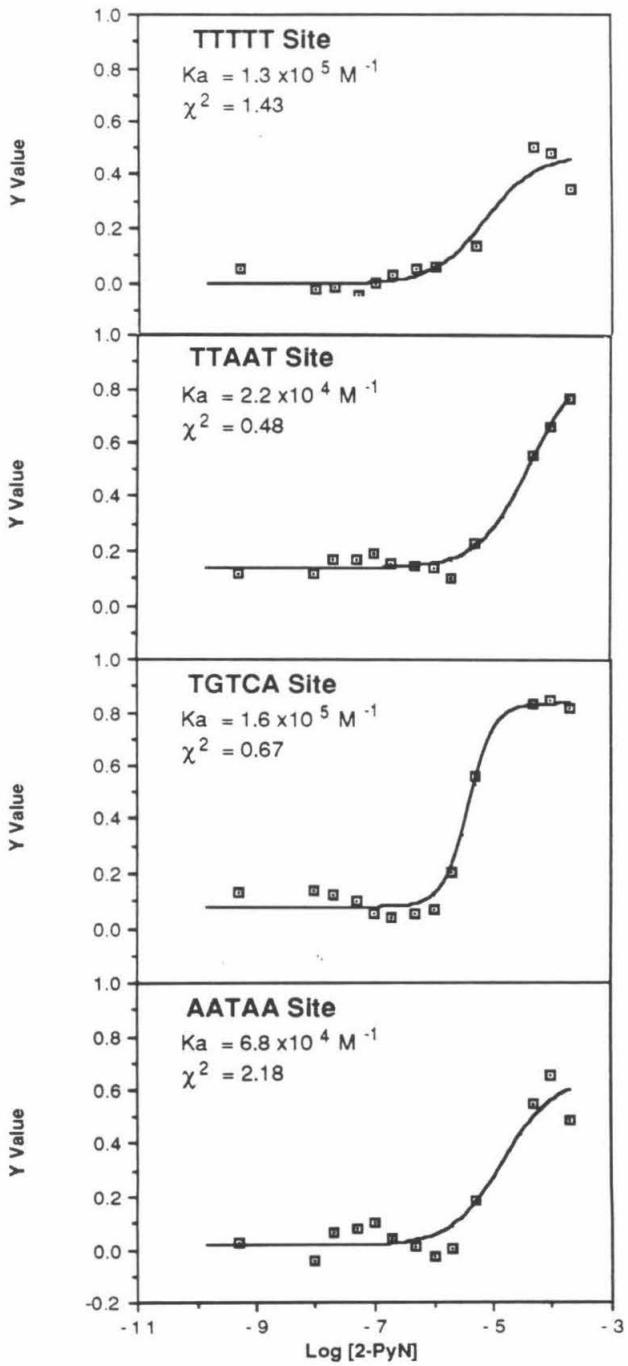

2-PyN, Gel #285, 0.375 μM MPE·Fe(II), qfpp825 Data

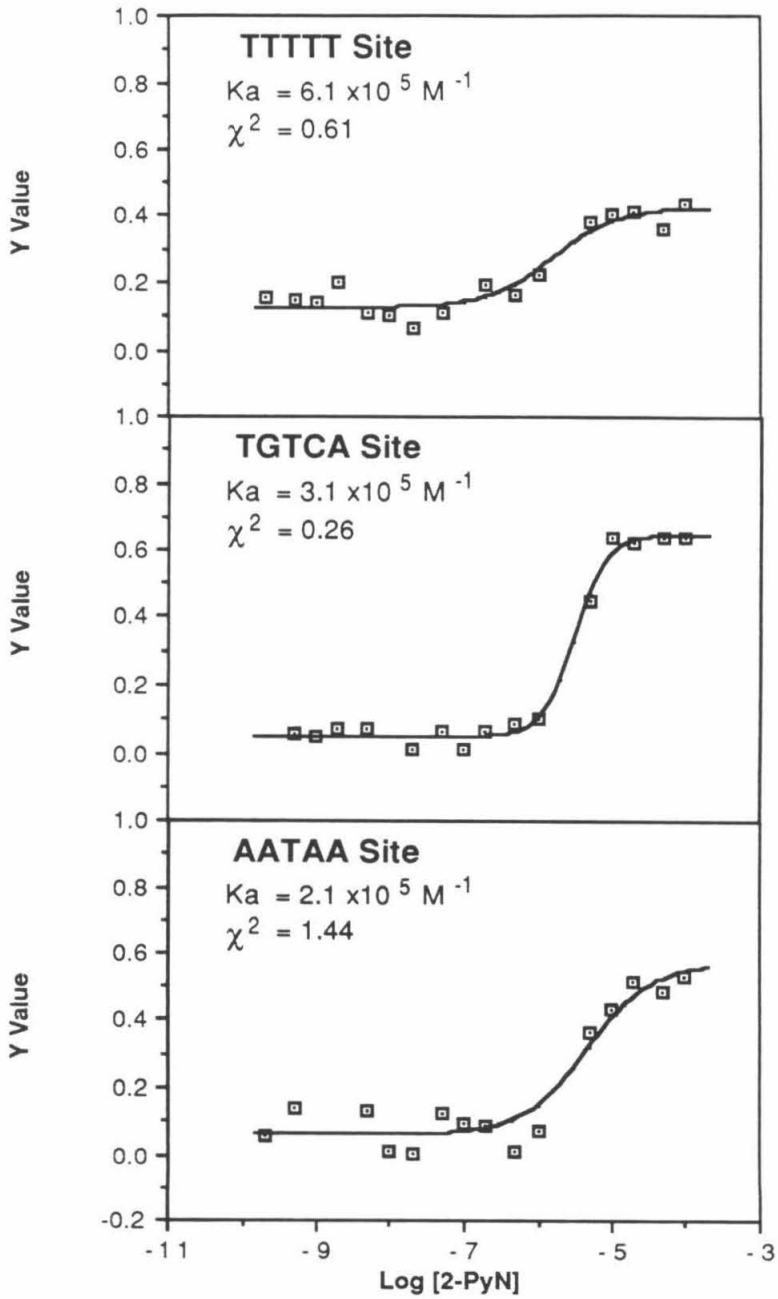

2-PyN, Gel #312, 0.375 μM MPE·Fe(II), qfpp103 Data

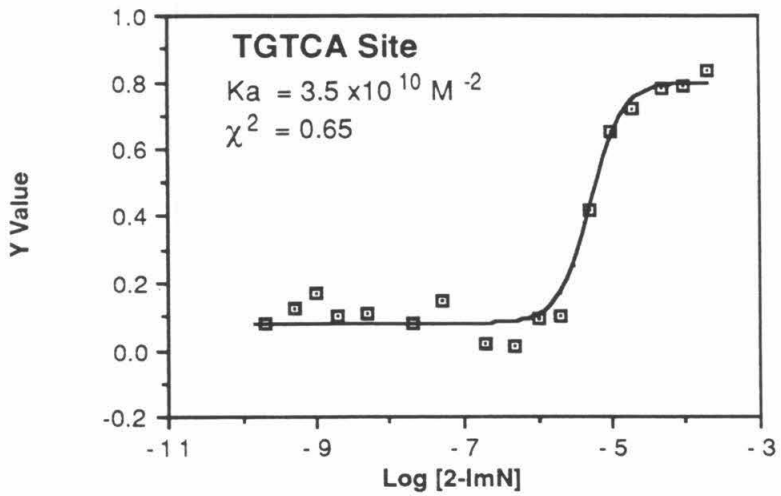

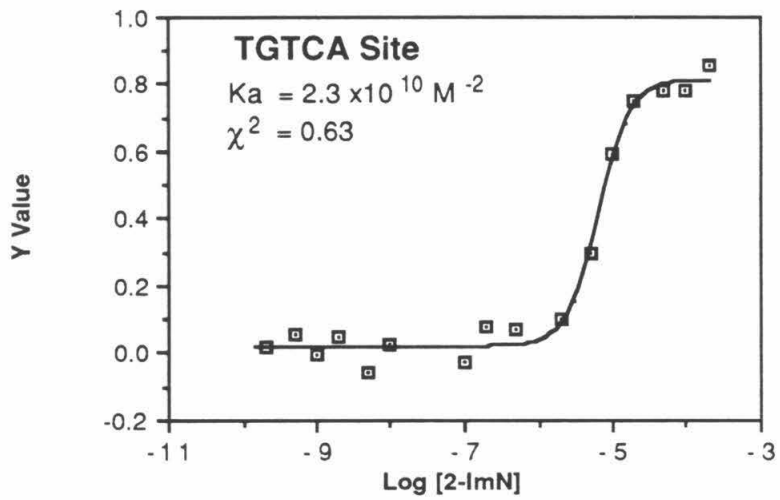

2-ImN, Gel #268, 1 μM MPE·Fe(II), qfpi64 Data
2-ImN, Gel #271, 1 μM MPE·Fe(II), qfpi712 Data

Appendix C

Proposed G·C Binding Molecules

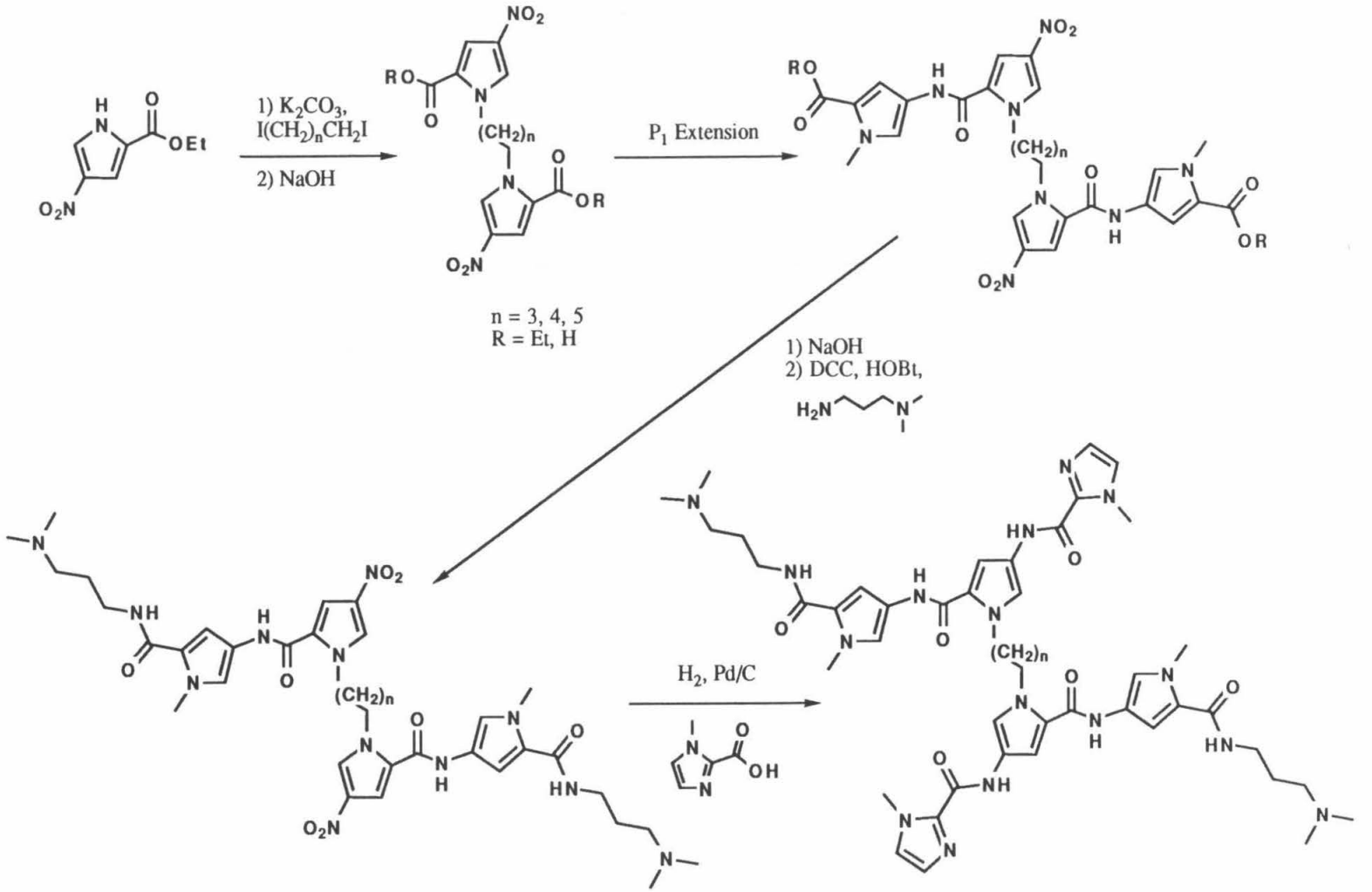
1) K_2CO_3,
$I(CH_2)_nCH_2I$
2) NaOH
P_1 Extension
n = 3, 4, 5
R = Et, H
1) NaOH
2) DCC, HOBt,
H_2, Pd/C

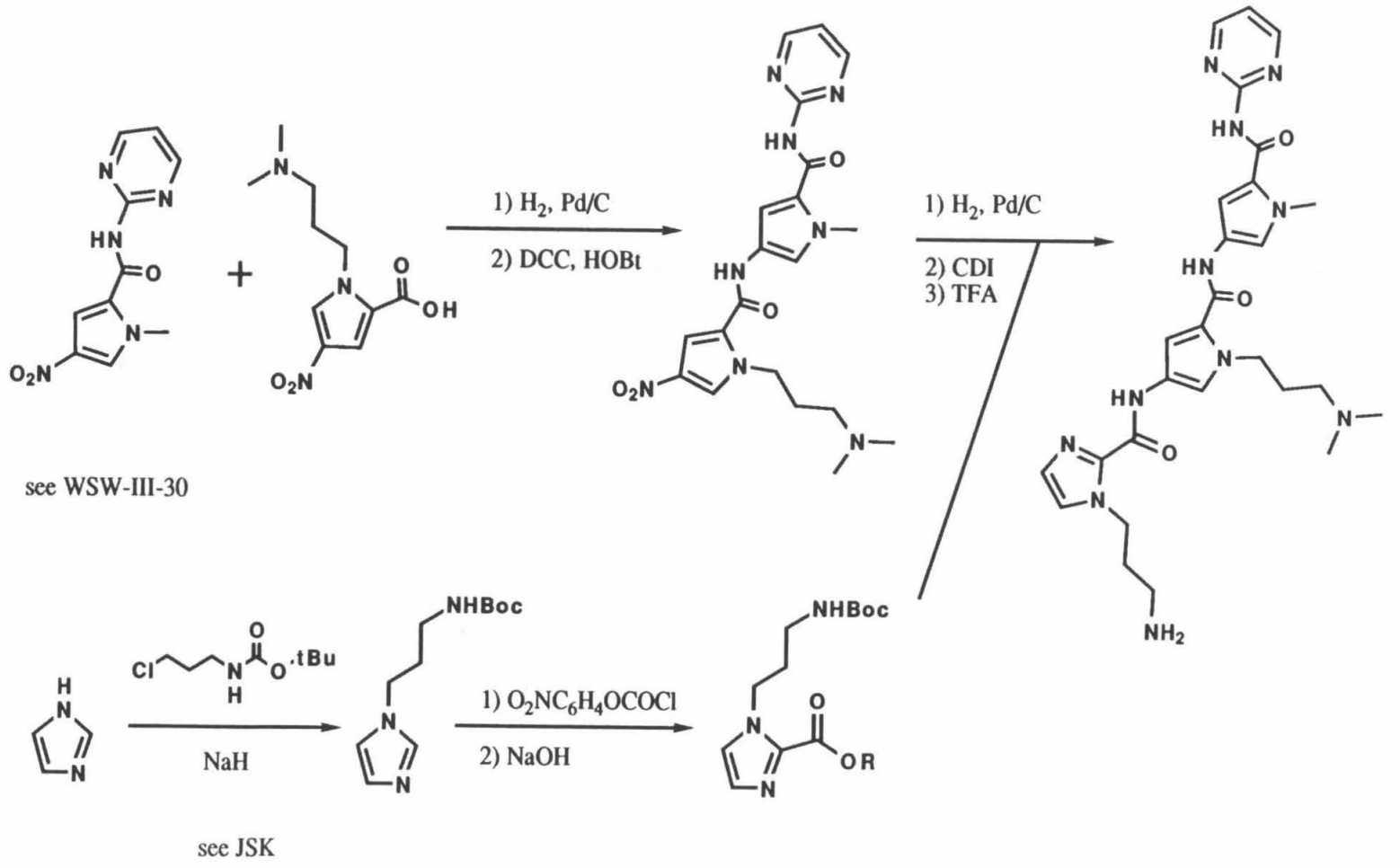

see WSW-III-30

see JSK

Appendix D

Other Potential G·C Binding Molecules Synthesized

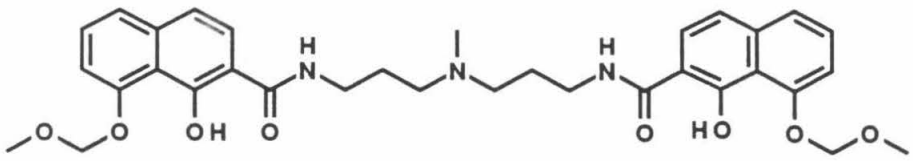

I-230, II-88

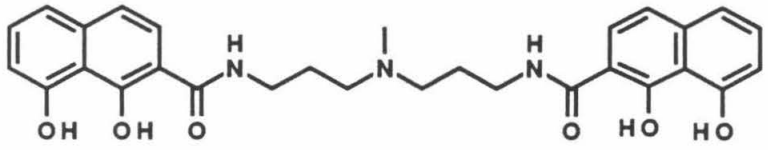

I-230, II-88

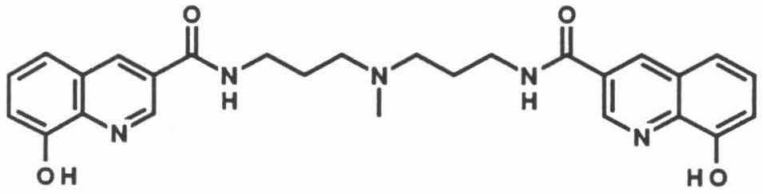

I-226, II-80, 82

Compounds Which Do Not Bind Detectably to DNA. References are to key notebook pages with synthesis and characterization respectively.

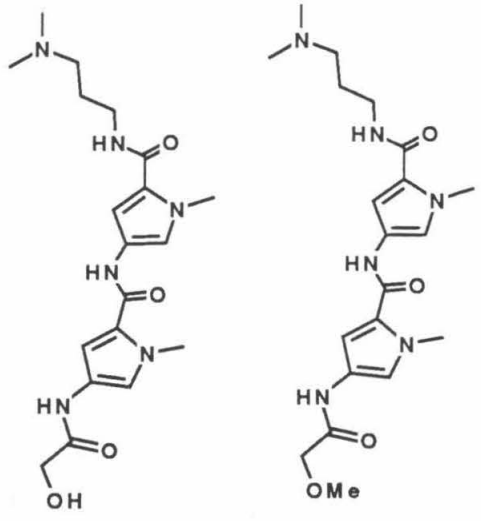

I-270, appendix A

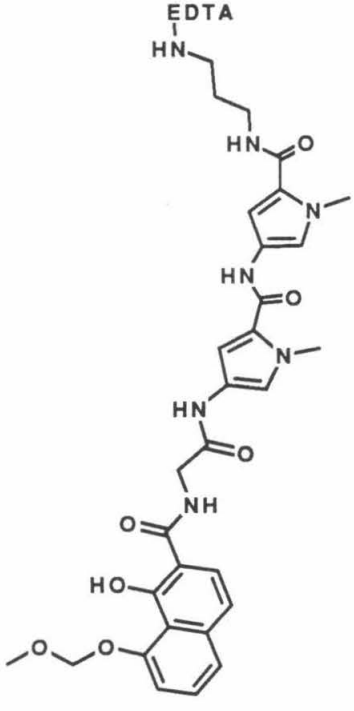

I-176, II-39, 43

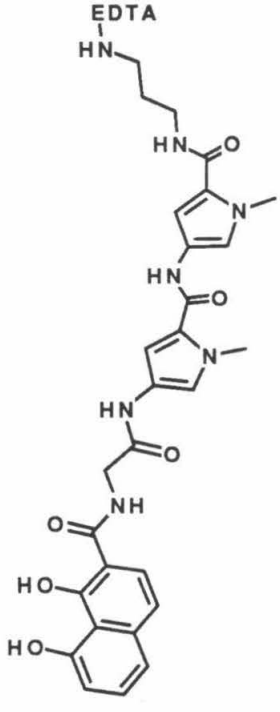

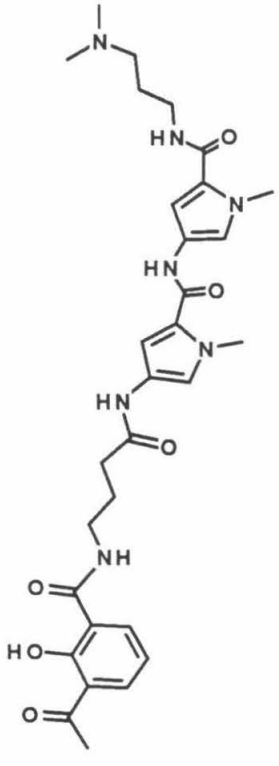

III-23, II-177

Additional compounds which appear to bind weakly to DNA with the normal distamycin A specificity. References are to key notebook pages with synthesis and characterization respectively.

Appendix E

Computer Programs

A Commentary on Hist80.tex

Hist80.tex is a TEX program which takes an input sequence of DNA and generates a bar or arrow histogram to be output on the laser printer. The software was originally written by Jim Sluka, and has been modified several times since. Because the understanding of TEX is a hard-won process, I will attempt to describe hist80 in such a way as to make future modification easier.

WARNING Even simple changes can produce far-reaching effects. Make all changes on a copied version of the program. A spare copy will be kept on my thesis disk for emergency recovery.

For those few brave souls who wish to use the power of TEX, I commend you. I urge you to start by reading the first twenty-three chapters of the TEXbook and do as many exercises as are humanly possible. TEXing is just not agreeable without much practice. I will also leave a copy of this thesis on floppy disk which is designed to run off the floppy. The disk is intended to be an extended example of TEX in action. I do not claim to be an expert and therefore it is highly likely that there is plenty of inefficient code and more than one lapse of insight. Still, this thesis should be a reasonable example of what can be done with TEX. The following discussion will be divided into two parts. The general introduction to the program is relatively straightforward, but the design portion assumes an acquaintance with the TEXbook.

Histogram Production

The average user of hist80 needs to know very little about the actual process in order to generate a histogram. Basically any file following the described format will generate the appropriate output. Two conventions of TEX must be mentioned at this point. The backslash is used as an escape character. It alerts the program that the next characters to be input are a command to be acted upon. TEX reads the next characters until the first non-letter as a single unit, and then takes appropriate action based on the current definition of the command. Conversely, % is the comment character. All symbols on a line after a % will be ignored by the program. TEX also ignores blank lines and most spaces. To make the program readable, I have added more lines and spaces than are necessary.

Suppose that the sequence in figure 1 is to be typeset.

Figure 1 Output of the files listed in figures 2 and 3.

The file in figure 2 produces the above output (with an optional title). Some of the statements (like**setscale**) were not used to generate the sequence, but keeping this general form will give enough flexibility for normal use. \input is the command that tells TEX to add a file to the current one. In this case, we want

```
\input d:/programs/his/hist80

\title {Short Sequence}

\bars

\start
\setscale{100}

\A{0}{0}
\A{0}{0}
\T{0}{0}
\G{0}{0}
\T{0}{0}
\C{0}{0}
\A{0}{0}
\T{0}{0}
\stop

\vfill\eject\end
```

Figure 2 A typical sequence file used by hist80.tex.

to process the file with definitions and macros present in hist80, and so the file is added first. `\vfill\eject\end` are commands that should occur at the end of all TEX files. They finish out the page and end the program without complaint.

The rest of the commands relate directly to histograms and are defined by hist80. `\start` tells TEX that a histogram is being made and adds the ^{32}P label and the lefthand side 5′ and 3′. Next comes the sequence arranged so that the lefthand side of the top strand in the display is at the top of the file. The numbers in curly brackets are parameters which will be described later. `\stop` then tells the program that the histogram is finished and adds the right hand side 5′ and 3′.

To utilize the other macros it is necessary to construct a histogram like the one shown below. Suppose that we have an MPE·Fe(II) footprint such that on the 5′ strand the GTCAT bases of the previous example are protected by 5, 10, 15, 10, and 5 mAU respectively, and on the 3′ strand the ACAT bases are protected 5, 6, 7 and 1 mAU respectively. This would give a 5 bp binding site, which can be boxed as shown in figure 1 using both bars and arrows.

```
\input d:/programs/his/hist80

\title {Short Sequence}

\bars

\start
\setscale{100}

\A{0}{0}
\A{0}{1}
\boxit{5}
\T{0}{7}
\G{5}{6}
\T{10}{5}
\C{15}{0}
\A{10}{0}
\T{5}{0}
\stop

\vfill\eject\end
```

Figure 3 A typical histogram file used by hist80.tex.

The file which produces this output is shown in figure 3. `\bars` tells TEX to choose bars for the histogram (`\arrows` chooses arrows). The parameters after

each base in the sequence now determine the height of the histogram. To place a bar above the sequence, *i.e.*, to represent a protection of the top 5′ labeled strand, the first parameter is made nonzero. To place a bar below the sequence (3′ labeled strand), the second parameter is made nonzero. `\setscale` controls the total height of the histogram. When its parameter is 100, the heights of the histograms in mm corresponds to the numbers after each nucleotide in the sequence. Changing to `\setscale{40}` gives histogram heights which are 40% of the typed numbers, and so forth. To draw a box around a particular sequence, place a `\boxit` directly before the first nucleotide to be boxed. The argument of `\boxit` determines how long a sequence will be boxed.

To get a printout of a file, type **total** filename (no .tex) and hit return several times. TEX printing actually calls three separate programs. TEX itself uses a *.tex input file and produces a *.dvi output file. The dvi extension means that the output is independent of the output device, and so another program, dvips, is used to translate into PostScript to use with the LaserWriter. The program spr then sends the file to the printer. To print successfully, make sure that the connections are set properly. The LaserWriter switch must be set at 9600 baud, and the box(es?) under the countertop must be turned properly.

Certain errors turn up frequently. If spr produces the message VMerror BeginDviLaserDoc, the LaserWriter has been re-initialized, and needs to be reloaded to run TEX properly. Type either **lsrinit** or **initlsr** and wait for the page to be

printed. If spr produces the error Nostringval, ignore it. Everything should print as usual. If any other error occurs, the LaserWriter memory is probably jammed. First try spr again. Sometimes data gets garbled on the way to the printer, and sending it twice will fix the problem. Next try printing a small file from the Mac. If this doesn't help, check the status of the LaserWriter by typing **status**. This command will dump the amount of memory used to the screen. If less than 20K remains before the purge, then the memory needs to be unjammed. Turn off the LaserWriter, turn it back on, wait for the boot page, and **lsrinit** as before. If this does not work, trying panicking, calling CCO, buying a new LaserWriter, etc. You are now a fully qualified user of hist80.

WARNING The rest of this appendix will deal with the hist80 macros themselves. Consider the rest of this a dangerous bend section (see Knuth, D.E. *The TEXbook*).

In the original design of hist80, the designer, Jim Sluka, was faced with a number of different specifications which needed to be met simultaneously. The sequence needs to be evenly spaced, and ideally both strands should be produced from one strand sequence. Histograms can contain either bars (footprinting) or arrows (affinity cleaving) or both, which must be centered on the proper bp. Binding sites need to be boxed, and the left and right sides of the box must be centered between two bp. To address these challenges, Jim used some of the advanced capabilities of TEX.

Each position of the sequence was conceived as a vertical series of boxes. At the top is the cleavage or protection pattern for the 5′ strand, followed by the 5′ base, followed by the 3′ base, followed by the cleavage or protection pattern of the 3′ strand. Horizontal equal spacing was readily accomplished by using the TEX `\setbox` facility. The width of all bp was set by determining the width of a G plus a little extra space (`\charwidth`). The vertical boxes of any given sequence position are then placed in a `\hbox` of width `\charwidth`. These boxes are then tightly packed horizontally so that there is no glue between them, ensuring equal spacing.

Vertical spacing is determined using the strut concept. (A strut is a vertical line of zero width.) Jim chose a maximum height for the histogram above and below the sequence of 50 mm. The sequence itself contains struts which are just slightly higher than a single character. Thus the total height of the histogram is 50 mm for the 5′ data, 2 `\charheight` for the sequence, and 50 mm for the 3′ data, but only the heights of the bars or arrows are visible.

Alignment of arrows over the middle of the sequence proved more difficult, since boxes have a single horizontal reference point. However, TEX does not require that the contents of a box reside in that box. This allows for the constructions `\rlap`, `\mlap`, and `\llap`, which are boxes of zero width with the contents of the box just to the right of the box, centered on the box or just to the left of the box. Hist80 places the the entire contents of a sequence position box inside an

\mlap, then fills the sequence box with glue (of width \charwidth). This has the effect of placing the \mlap box at the extreme left of the sequence box, and the \mlap ensures that the contents are centered there. This also means that the positions of the printed sequence do not correspond to the postions that the computer calculates (Oh well). To reach the actual midpoint between two bp, the program must skip either forward or backward by \halfcharwidth.

Boxing a binding site is also a lesson in using TEX commands. Again, hist80 uses \mlap so that no physical space is taken up by the box itself. Four lines need to be drawn to produce the proper box. The vertical two are readily accomplished, with a skip of one \halfcharwidth backwards or one \halfcharwidth backwards followed by the appropriate number of \charwidth forward giving the correct horizontal positions for \vrule's. Hist80 handles the top of the box by drawing a rule with a large height, a negative depth of slightly smaller magnitude, and a width of the right number of \charwidth's. This yields a visible line of thickness *height* − *depth* which is drawn *depth* units above the baseline. Similar use of a negative height and a positive (and larger depth) gives the bottom line of the box.

So far, there has been no distinction made between arrow and bar histograms, and for most practical purposes none is needed. Any differences which do exist can be handled using the \ifcase construction of TEX. One caveat remains, however. Jim did not like the available arrowheads of TEX, and so he wrote his own definition. For each arrowhead constructed, the program must draw a set of twenty nested

\vrule's of gradually increasing width. As a consequence, arrowheads take up most of the programs processing memory, and a common error seen is "Sorry, TEX main memory capacity exceeded." When this happens, placement of a \page in the middle of a sequence should permit printing.

The rest of hist80 is relatively straightforward, and its understanding will be left for the reader. As a further example of this general approach to alignment, I offer the hom.def program used to contruct the protein homology figure in chapter 5. This program uses exactly the same strategy as hist80, with the added complication that boxes can have dotted boundaries as well as solid ones, and a box may not be square or rectangular. The reader is referred to the file gjfig2.tex for usage of hom.def definitions.

The rest of this appendix contains the source code for hist80.tex, hom.def, and a representative sample of the programs used in this thesis, which will not be discussed in detail.

Hist80.tex

```
\magnification=\magstep1 \nopagenumbers
\special{ps: landscape}\ \par\vfill\eject
\tracingstats=1 \pageno=1
% ============================= HISTOGRAM Macros ================================
%                          80bp/line version, April 1986
% ===============================================================================

\baselineskip=0pt
\lineskiplimit=0pt
\lineskip=0pt
\parindent=0pt
\parskip=0pt plus0pt minus20truemm

\pretolerance=10000
\tolerance=10000
\exhyphenpenalty=0
\linepenalty=0
\adjdemerits=0
\doublehyphendemerits=0
\finalhyphendemerits=0

% FONTS -----------------------------------------
\font\rm=amr10
\font\tt=amtt10
\font\srm=amr8

% ignore CR'c and spaces
\def\nocrsp{\begingroup\catcode\^^L=9\catcode\ =9\catcode\^^M=9\endlinechar=-1}
\def\crsp{\endgroup}

\newdimen\charheight
\newdimen\charwidth
\newdimen\halfchar
\newdimen\shortdbl
\newdimen\topboxit
\newdimen\scale
\newdimen\scaledht
\newcount\arrowbarcharseq
\newcount\printer \printer=0
\newcount\colcount \colcount=1
\newcount\maxcount \maxcount=80
\newcount\linecount \linecount=0

\setbox0=\hbox{{\tt G}}\charheight=\ht0\charwidth=\wd0\setbox0=\null
\advance\charwidth by1.5pt
\advance\charheight by2pt
\advance\halfchar by\charwidth\divide\halfchar by2
\advance\shortdbl by2\charheight\advance\shortdbl by-0.5pt
\advance\topboxit by2\charheight\advance\topboxit by0.2pt

\def\mlap#1{\hbox to0pt{\hss #1\hss}}

\def\dh{\hskip 3sp plus1sp minus1sp\penalty-200}%allow breaks after bp's


% ============================ PRINTER TYPE ============================
%\def\laser{\global\printer=0\setprinter}
%\def\versatec{\global\printer=1\setprinter}
%\def\epson{\global\printer=2\setprinter}
%
```

```
% ========================== TYPE OF HISTOGRAM ========================
\def\arrows{\global\arrowbarcharseq=0}
\def\bars{\global\arrowbarcharseq=1}
\def\characters{\global\arrowbarcharseq=2}
\def\sequence{\global\arrowbarcharseq=3}
\sequence % default output type
%
\endlinechar=-1

\def\a{\A{0}{0}}
\def\t{\T{0}{0}}
\def\c{\C{0}{0}}
\def\g{\G{0}{0}}

\def\start{\message{START OF PROCESSING}
\leavevmode\parshape=1 0pt 80\charwidth\leftlbl}

\def\stop{\rightlbl\hfill\break}

\def\page{\par\vfill\eject\leavevmode\parshape=1 0pt 80\charwidth}

\def\downarrowhead{\dimen50=0pt\relax
\loop\ifdim\dimen50<4pt\advance\dimen50 by0.2pt
\mlap{\raise\dimen50\hbox{\vrule height0.2pt depth0pt width\dimen50}}
\repeat}

\def\uparrowhead{\dimen50=0pt\relax
\loop\ifdim\dimen50<4pt\advance\dimen50 by0.2pt
\mlap{\lower\dimen50\hbox{\vrule height0pt depth0.2pt width\dimen50}}
\repeat}

\def\boxit#1{\rlap{\hskip-\halfchar\mlap{\vrule
height\topboxit width0.7pt depth1.7pt}\rlap{\vrule
 height\topboxit width#1\charwidth depth-\shortdbl}\rlap{\vrule
height-1pt width#1\charwidth depth1.7pt}\hskip#1\charwidth\mlap{\vrule
height\topboxit width0.7pt depth1.7pt}
\hskip-#1\charwidth\hskip\halfchar}}

\def\bboxit#1{{\advance\topboxit by1pt \advance\shortdbl by1pt
\rlap{\hskip-\halfchar\mlap{\vrule
height\topboxit width0.7pt depth2.7pt}\rlap{\vrule
 height\topboxit width#1\charwidth depth-\shortdbl}\rlap{\vrule
height-2pt width#1\charwidth depth2.7pt}\hskip#1\charwidth\mlap{\vrule
height\topboxit width0.7pt depth2.7pt}
\hskip-#1\charwidth\hskip\halfchar}}}

\def\setscale#1{\global\scale=#1sp\relax}
\setscale{100}

\def\calc#1{\scaledht=#1truemm
\multiply\scaledht by\scale\global\divide\scaledht by100}

%\def\curline{\ifnum\colcount>\maxcount\endlinechar=13\par
%\ \unskip\colcount=2\advance\linecount by1
%\message{
%NEW LINE -- \number\linecount}\endlinechar=-1
%\else\advance\colcount by1\fi}

%\def\setprinter{\ifcase\printer
% case 0; output for LASER PRINTER (LANDSCAPE MODE) ---------------------
%\message{LASER}
\hoffset=0.5truein
\hsize=80\charwidth
```

```
\topskip=0.5truein
\voffset=0.01truein
\vsize=6truein
%\or
% case 1; output for VERSATEC (LANDSCAPE MODE) -------------------------
%\message{VERSATEC}
%\hoffset=0.5truein
%\hsize=80\charwidth
%\topskip=0.1truein
%\vsize=10truein
%\or
% case 2; output for EPSON (PORTRAIT MODE) ----------------------------
%\message{output set for EPSON printer}
%\hoffset=0.75truein
%\hsize=80\charwidth
%\topskip=0.5truein
%\vsize=10truein
%\voffset=0.5truein
%\fi}
%\laser % default printer

\def\lstrut{\ifcase\arrowbarcharseq
\vrule height\charheight depth0pt width0pt
\or
\vrule height\charheight depth0pt width0pt
\or
\vrule height\charheight depth0pt width0pt
\or
\vrule height\charheight depth0pt width0pt
\fi}

\def\astrutt{\ifcase\arrowbarcharseq
\vrule height50truemm depth1.5pt width0pt
\or
\vrule height50truemm depth1.5pt width0pt
\or
{}
\or
{}
\fi}

\def\astrutb{\ifcase\arrowbarcharseq
\vrule height0pt depth50truemm width0pt %see also vskip in uparrow
\or
\vrule height0pt depth50truemm width0pt %see also vskip in upbar
\or
\vrule height0pt depth50truemm width0pt %see also vskip in upbar
\or
\hbox{\vrule height0pt depth8mm width0pt}
\fi}

\def\downarrow#1{\ifcase\arrowbarcharseq
\hbox{\astrutt\vbox{\ifnum#1>0\calc{#1}
\mlap{\vrule height\scaledht depth1.5pt width0.8pt}
\mlap{\downarrowhead}\fi\vskip 0.4pt\relax}}
\or
\hbox{\astrutt\vbox{\ifnum#1>0\calc{#1}\mlap{\vrule
 height\scaledht depth1.5pt width\charwidth}\fi\vskip 0.4pt\relax}}
\or
{}
\or
{}
\fi}
```

```
\fi}

\def\uparrow#1{\ifcase\arrowbarcharseq
\hbox{\astrutb\vbox{\vskip 3.2pt\ifnum#1>0\calc{#1}
\mlap{\uparrowhead}\mlap{\vrule height\scaledht depth1pt width0.8pt}\fi}}
\or
\hbox{\astrutb\vbox{\vbox to 3.2pt{}\ifnum#1>0\calc{#1}
\mlap{\vrule height1.5pt depth\scaledht width\charwidth}\fi}}
\or
{}
\or
{}
\fi}

\def\A#1#2{\ifcase\arrowbarcharseq
\hbox to\charwidth{\vtop{\vbox{\downarrow{#1}\mlap{\lstrut A}
\mlap{\lstrut T}}\uparrow{#2}}\hfil}\dh
\or
\hbox to\charwidth{\vtop{\vbox{\downarrow{#1}\mlap{\lstrut A}
\mlap{\lstrut T}}\uparrow{#2}}\hfil}\dh
\or
\hbox to\charwidth{\vtop{\mlap{\lstrut A}\mlap{\lstrut T}}\hfil}\dh
\or
\hbox to\charwidth{\vtop{\vbox{\mlap{\lstrut A}
\mlap{\lstrut T}}\astrutb}\hfil}\dh
\fi}

\def\T#1#2{\ifcase\arrowbarcharseq
\hbox to\charwidth{\vtop{\vbox{\downarrow{#1}
\mlap{\lstrut T}\mlap{\lstrut A}}\uparrow{#2}}\hfil}\dh
\or
\hbox to\charwidth{\vtop{\vbox{\downarrow{#1}
\mlap{\lstrut T}\mlap{\lstrut A}}\uparrow{#2}}\hfil}\dh
\or
\hbox to\charwidth{\vtop{\mlap{\lstrut T}
\mlap{\lstrut A}}\hfil}\dh
\or
\hbox to\charwidth{\vtop{\vbox{\mlap{\lstrut T}
\mlap{\lstrut A}}\astrutb}\hfil}\dh
\fi}

\def\G#1#2{\ifcase\arrowbarcharseq
\hbox to\charwidth{\vtop{\vbox{\downarrow{#1}
\mlap{\lstrut G}\mlap{\lstrut C}}\uparrow{#2}}\hfil}\dh
\or
\hbox to\charwidth{\vtop{\vbox{\downarrow{#1}
\mlap{\lstrut G}\mlap{\lstrut C}}\uparrow{#2}}\hfil}\dh
\or
\hbox to\charwidth{\vtop{\mlap{\lstrut G}
\mlap{\lstrut C}}\hfil}\dh
\or
\hbox to\charwidth{\vtop{\vbox{\mlap{\lstrut G}
\mlap{\lstrut C}}\astrutb}\hfil}\dh
\fi}

\def\C#1#2{\ifcase\arrowbarcharseq
\hbox to\charwidth{\vtop{\vbox{\downarrow{#1}
\mlap{\lstrut C}\mlap{\lstrut G}}\uparrow{#2}}\hfil}\dh
\or
\hbox to\charwidth{\vtop{\vbox{\downarrow{#1}
\mlap{\lstrut C}\mlap{\lstrut G}}\uparrow{#2}}\hfil}\dh
\or
\hbox to\charwidth{\vtop{\mlap{\lstrut C}
```

```
\mlap{\lstrut G}}\hfil}\dh
\or
\hbox to\charwidth{\vtop{\vbox{\mlap{\lstrut C}
\mlap{\lstrut G}}\astrutb}\hfil}\dh
\fi}

\def\p32{\ifcase\arrowbarcharseq
\hbox{\raise 4.2pt\hbox{$^{32}$\rm P\hskip1pt}}
\or
\hbox{\raise 4.2pt\hbox{$^{32}$\rm P\hskip1pt}}
\or
\hbox{\raise 4.2pt\hbox{$^{32}$\rm P\hskip1pt}}
\or
{}
\fi}

\def\leftlbl{\ifcase\arrowbarcharseq
\llap{\p32\vtop{\vbox{\downarrow0\hbox{\lstrut\rm 5$^\prime$-}
\hbox{\lstrut\rm 3$^\prime$-}}\vskip 2pt\uparrow0}\ }
\or
\llap{\p32\vtop{\vbox{\downarrow0\hbox{\lstrut\rm 5$^\prime$-}
\hbox{\lstrut\rm 3$^\prime$-}}\vskip 2pt\uparrow0}\ }
\or
\llap{\vbox{\hbox{\lstrut \rm 5$^\prime$-}\hbox{\lstrut\rm 3$^\prime$-}}\ }
\or
\llap{\vbox{\hbox{\lstrut \rm 5$^\prime$-}\hbox{\lstrut\rm 3$^\prime$-}}\ }
\fi}

\def\rightlbl{\ifcase\arrowbarcharseq
\hskip-\halfchar\hbox{\vtop{\vbox{\downarrow0
\hbox{\lstrut\rm -3$^\prime$}\hbox{\lstrut\rm -5$^\prime$}}
\vskip 2pt\uparrow0}\hfill}
\or
\hskip-\halfchar\hbox{\vtop{\vbox{\downarrow0
\hbox{\lstrut\rm -3$^\prime$}\hbox{\lstrut\rm -5$^\prime$}}
\vskip 2pt\uparrow0}\hfill}
\or
\hskip-\halfchar\hbox{\vbox{\hbox{\lstrut\rm -3$^\prime$}
\hbox{\lstrut\rm -5$^\prime$}}\hfil}
\or
\hskip-\halfchar\hbox{\vbox{\hbox{\lstrut\rm -3$^\prime$}
\hbox{\lstrut\rm -5$^\prime$}}\hfil}
\fi}

\def\title#1{\ifcase\arrowbarcharseq
\endlinechar=13\rm #1\tt\par\endlinechar=-1
\or
\endlinechar=13\rm #1\tt\par\endlinechar=-1
\or
\endlinechar=13\rm #1\tt\par\endlinechar=-1
\or
\divide\hoffset by2
\hsize=80\charwidth \topskip=1truein \voffset=0.5truein
\headline={{\rm #1}\hfil{\rm pg.~\folio}}\footline={\hfill}
\fi}

\tt

% ============================== end HISTO Macros ======================
```

Hom.def

```
% ================================================
%
%  in DVIPS use:
%              MAG 820
%              XY 0.5IN 1IN
%  Not necess. as now written 30 aa/line in \threecode mode
% ================================================

\nopagenumbers
\special{ps: landscape}\ \par\vfill\eject
\tracingstats=1
\parskip=0pt
\parindent=0pt
\headline={\hfill}
\footline={\hfill}
\hsize=310truemm
\vsize=235truemm
\baselineskip=17pt
\lineskiplimit=0pt
\lineskip=2pt

\tt
\font\boldtt=ambx6


\newdimen\tempdim
\newdimen\charwidth
\newdimen\halfcharwidth
\newdimen\charheight
\newdimen\chardepth
\newdimen\shorttop
\newdimen\topboxit
\newdimen\shortbot
\newdimen\botboxit
\newdimen\htdots
\newcount\code
\newcount\tempcount
\newcount\strand
%
\def\nocrsp{\begingroup\catcode\^^L=9\catcode\ =9\catcode\^^M=9
\ignorespaces\endlinechar=-1}
\def\crsp{\endgroup}
\def\threecode{\global\code=2\sizing}
\def\onecode{\global\code=0\sizing}
\def\ul#1{\setbox70=\hbox{#1}\tempdim=\wd70 \box70\hskip-\tempdim %
 \lower1.5pt\hbox to\tempdim{\hrulefill}}
\def\bstr{$\beta_{\strand}$}
\def\aa#1{\hbox to\charwidth{\mlap{#1}\hfil}}
\def\hdrseq#1{\leavevmode\hbox to30pt{\hss #1\quad\ }}


\def\plus{\mlap{$^{^{^\oplus}}$\hskip3.3pt}}
\def\minus{\mlap{$^{^{^\ominus}}$\hskip3.3pt}}
\def\dots{\xleaders\hbox to 3pt{\hss .\hss}}
\def\lcor#1{\mlap{#1}\hbox to1.5pt{\hss}\kern 0pt}
\def\rcor#1{\kern 0pt\hbox to1.5pt{\hss}\mlap{#1}}
\def\boxstrut{\hrule height\topboxit width0pt depth\botboxit\relax}

\def\sizing{\ifcase\code
\setbox69=\hbox{M\plus\ }
```

```
\charheight=\ht69
\shorttop=\charheight\advance\shorttop by.8pt
\topboxit=\charheight\advance\topboxit by1.5pt
\chardepth=\dp69\advance\chardepth by2pt
\charwidth=\wd69
\halfcharwidth=\charwidth\divide\halfcharwidth by2
\or
\or
\setbox69=\hbox{Arg\plus\ }
\charheight=\ht69
\shorttop=\charheight\advance\shorttop by.8pt
\topboxit=\charheight\advance\topboxit by1.5pt
\chardepth=\dp69\advance\chardepth by2pt
\charwidth=\wd69
\halfcharwidth=\charwidth\divide\halfcharwidth by2
\fi
}
\def\mlap#1{\hbox to0pt{\hss #1\hss}}

\def\id#1,#2{\nocrsp
\tempcount=#2\advance\tempcount by-1
\botboxit=\chardepth\advance\botboxit by\tempcount\baselineskip
\shortbot=\botboxit\advance\shortbot by-0.7pt
\rlap{\vbox to 0pt{\vss\hrule height\topboxit width0pt depth\botboxit%
\hskip-\halfcharwidth%
\mlap{\vrule height\topboxit width0.7pt depth\botboxit}%
\rlap{\raise\shorttop\hbox to#1\charwidth{\leaders\vrule height0.7pt
depth0pt\hfil}}%
\rlap{\lower\shortbot\hbox to#1\charwidth{\leaders\vrule height0pt
depth0.7pt\hfil}}%
\hskip#1\charwidth\mlap{\vrule height\topboxit width0.7pt
depth\botboxit}\hskip-#1\charwidth\hskip\halfcharwidth\vskip-\botboxit}}%
\crsp}

\def\ib#1,#2{\nocrsp
\tempcount=#2\advance\tempcount by-1
\botboxit=\chardepth\advance\botboxit by\tempcount\baselineskip
\shortbot=\botboxit\advance\shortbot by-0.7pt
\rlap{\vbox to 0pt{\vss\hrule height\topboxit width0pt depth\botboxit
\hskip-\halfcharwidth%
\rlap{\lower\shortbot\hbox to#1\charwidth{\leaders\vrule height0pt
depth0.7pt\hfil}}%
\hskip\halfcharwidth\vskip-\botboxit}}%
\crsp}

\def\iu#1,#2{\nocrsp
\botboxit=\chardepth
\rlap{\vbox to 0pt{\vss\boxstrut
\hskip-\halfcharwidth%
\mlap{\vrule height\topboxit width0pt depth\botboxit}%
\rlap{\raise\shorttop\hbox to#1\charwidth{\leaders
\vrule height0.7pt depth0pt\hfil}}%
\hskip\halfcharwidth\vskip-\botboxit}}%
\crsp}

\def\il#1,#2{\nocrsp
\tempcount=#2\advance\tempcount by-1
\botboxit=\chardepth\advance\botboxit by\tempcount\baselineskip
\shortbot=\botboxit\advance\shortbot by-0.7pt
\rlap{\vbox to 0pt{\vss\boxstrut
\hskip-\halfcharwidth%
\mlap{\vrule height\topboxit width0.7pt depth\botboxit}%
\hskip\halfcharwidth\vskip-\botboxit}}%
```

```
\crsp}

\def\ir#1,#2{\nocrsp
\tempcount=#2\advance\tempcount by-1
\botboxit=\chardepth\advance\botboxit by\tempcount\baselineskip
\shortbot=\botboxit\advance\shortbot by-0.7pt
\rlap{\vbox to 0pt{\vss\boxstrut
\hskip-\halfcharwidth\hskip#1\charwidth\mlap{\vrule height\topboxit
width0.7pt depth\botboxit}\hskip-#1\charwidth\hskip\halfcharwidth%
\vskip-\botboxit}}%
\crsp}

\def\iN#1,#2{\il{#1},{#2}\iu{#1},{#2}\ir{#1},{#2}}
\def\iU#1,#2{\il{#1},{#2}\ib{#1},{#2}\ir{#1},{#2}}
\def\iL#1,#2{\il{#1},{#2}\ib{#1},{#2}\iu{#1},{#2}}
\def\iR#1,#2{\iu{#1},{#2}\ib{#1},{#2}\ir{#1},{#2}}
\def\iM#1,#2{\il{#1},{#2}\ir{#1},{#2}}
\def\iB#1,#2{\il{#1},{#2}\iu{#1},{#2}\ib{#1},{#2}\ir{#1},{#2}}

\def\sm#1,#2{\nocrsp
\tempcount=#2\advance\tempcount by-1
\botboxit=\chardepth\advance\botboxit by\tempcount\baselineskip
\shortbot=\botboxit\advance\shortbot by-0.7pt
\tempdim=\topboxit\advance\tempdim by\botboxit\advance\tempdim by-3pt
\htdots=\topboxit\advance\htdots by-1.5pt
\setbox71=\vbox to\tempdim{
\xleaders\mlap{.\vrule height1.5pt
 depth1.5pt width0pt}\vfill}\ht71=\htdots%
\rlap{\vbox to 0pt{\vss\boxstrut
\hskip-\halfcharwidth\mlap{\copy71}%
\rlap{\raise\topboxit\hbox to#1\charwidth{\lcor{.}\dots\hfil\rcor{.}}}%
\rlap{\lower\shortbot\hbox to#1\charwidth{\lcor{.}\dots\hfil\rcor{.}}}%
\hskip#1\charwidth\mlap{\copy71}%
\hskip-#1\charwidth\hskip\halfcharwidth\vskip-\botboxit}}%
\crsp}

\def\su#1,#2{\nocrsp
\tempcount=#2\advance\tempcount by-1
\botboxit=\chardepth\advance\botboxit by\tempcount\baselineskip
\shortbot=\botboxit\advance\shortbot by-0.7pt
\tempdim=\topboxit\advance\tempdim by\botboxit\advance\tempdim by-3pt
\htdots=\topboxit\advance\htdots by-1.5pt
\setbox71=\vbox to\tempdim{\vfill}\ht71=\htdots%
\rlap{\vbox to 0pt{\vss\boxstrut
\hskip-\halfcharwidth\mlap{\copy71}%
\rlap{\raise\topboxit\hbox to#1\charwidth{\lcor{.}\dots\hfil\rcor{.}}}%
\rlap{\lower\shortbot\hbox to#1\charwidth{\hfil}}%
\hskip\halfcharwidth\vskip-\botboxit}}%
\crsp}

\def\sb#1,#2{\nocrsp
\tempcount=#2\advance\tempcount by-1
\botboxit=\chardepth\advance\botboxit by\tempcount\baselineskip
\shortbot=\botboxit\advance\shortbot by-0.7pt
\tempdim=\topboxit\advance\tempdim by\botboxit\advance\tempdim by-3pt
\htdots=\topboxit\advance\htdots by-1.5pt
\setbox71=\vbox to\tempdim{\vfill}\ht71=\htdots%
\rlap{\vbox to 0pt{\vss\boxstrut%
\hskip-\halfcharwidth\mlap{\copy71}%
\rlap{\lower\shortbot\hbox to#1\charwidth{\lcor{.}\dots\hfil\rcor{.}}}%
\hskip\halfcharwidth\vskip-\botboxit}}%
\crsp}
```

```
\def\sl#1,#2{\nocrsp
\tempcount=#2\advance\tempcount by-1
\botboxit=\chardepth\advance\botboxit by\tempcount\baselineskip
\shortbot=\botboxit\advance\shortbot by-0.7pt
\tempdim=\topboxit\advance\tempdim by\botboxit\advance\tempdim by-3pt
\htdots=\topboxit\advance\htdots by-1.5pt
\setbox71=\vbox to\tempdim{
\xleaders\mlap{.\vrule height1.5pt
 depth1.5pt width0pt}\vfill}\ht71=\htdots%
\rlap{\vbox to 0pt{\vss\boxstrut
\hskip-\halfcharwidth\mlap{\copy71}%
\rlap{\raise\topboxit\hbox to#1\charwidth{\lcor{.}\hfil}}%
\rlap{\lower\shortbot\hbox to#1\charwidth{\lcor{.}\hfil}}%
\hskip\halfcharwidth\vskip-\botboxit}}%
\crsp}

\def\sr#1,#2{\nocrsp
\tempcount=#2\advance\tempcount by-1
\botboxit=\chardepth\advance\botboxit by\tempcount\baselineskip
\shortbot=\botboxit\advance\shortbot by-0.7pt
\tempdim=\topboxit\advance\tempdim by\botboxit\advance\tempdim by-3pt
\htdots=\topboxit\advance\htdots by-1.5pt
\setbox71=\vbox to\tempdim{
\xleaders\mlap{.\vrule height1.5pt
 depth1.5pt width0pt}\vfill}\ht71=\htdots%
\rlap{\vbox to 0pt{\vss\boxstrut%
\hskip-\halfcharwidth\rlap{\raise\topboxit\hbox to#1\charwidth{\hfil\rcor{.}}}}%
\rlap{\lower\shortbot\hbox to#1\charwidth{\hfil\rcor{.}}}%
\hskip#1\charwidth\mlap{\copy71}%
\hskip-#1\charwidth\hskip\halfcharwidth\vskip-\botboxit}}%
\crsp}

\def\lm#1,#2{\nocrsp
\tempcount=#2\advance\tempcount by-1
\botboxit=\chardepth\advance\botboxit by\tempcount\baselineskip
\shortbot=\botboxit\advance\shortbot by-0.7pt
\tempdim=\topboxit\advance\tempdim by\botboxit\advance\tempdim by-3pt
\htdots=\topboxit\advance\htdots by-1.5pt
\setbox71=\vbox to\tempdim{
\xleaders\mlap{.\vrule height1.5pt
 depth1.5pt width0pt}\vfill}\ht71=\htdots%
\rlap{\vbox to 0pt{\vss\boxstrut
\hskip-\halfcharwidth\mlap{\copy71}%
\rlap{\raise\topboxit\hbox to#1\charwidth{\lcor{.}\dots\hfil\rcor{}}}%
\rlap{\lower\shortbot\hbox to#1\charwidth{\lcor{.}\dots\hfil\rcor{}}}%
\vskip-\botboxit}}%
\crsp}

\def\rm#1,#2{\nocrsp
\tempcount=#2\advance\tempcount by-1
\botboxit=\chardepth\advance\botboxit by\tempcount\baselineskip
\shortbot=\botboxit\advance\shortbot by-0.7pt
\tempdim=\topboxit\advance\tempdim by\botboxit\advance\tempdim by-3pt
\htdots=\topboxit\advance\htdots by-1.5pt
\setbox71=\vbox to\tempdim{
\xleaders\mlap{.\vrule height1.5pt
 depth1.5pt width0pt}\vfill}\ht71=\htdots%
\rlap{\vbox to 0pt{\vss\boxstrut
\hskip-\halfcharwidth\mlap{}%
\rlap{\raise\topboxit\hbox to#1\charwidth{\lcor{}\dots\hfil\rcor{.}}}%
\rlap{\lower\shortbot\hbox to#1\charwidth{\lcor{}\dots\hfil\rcor{.}}}%
\hskip#1\charwidth\mlap{\copy71}%
\hskip-#1\charwidth\hskip\halfcharwidth\vskip-\botboxit}}%
```

```
\crsp}

\def\sU#1,#2{\sl{#1},{#2}\sb{#1},{#2}\sr{#1},{#2}}
\def\sN#1,#2{\sl{#1},{#2}\su{#1},{#2}\sr{#1},{#2}}
\def\sL#1,#2{\sl{#1},{#2}\sb{#1},{#2}\su{#1},{#2}}
\def\sR#1,#2{\su{#1},{#2}\sb{#1},{#2}\sr{#1},{#2}}
\def\sB#1,#2{\sl{#1},{#2}\su{#1},{#2}\sb{#1},{#2}\sr{#1},{#2}}

\def\A{\ifcase\code
\aa{\ul{A}}
\or
\or \aa{\ul{Ala}}\fi}
\def\R{\ifcase\code
\aa{R\plus}
\or
\or\aa{Arg\plus}\fi}
\def\N{\ifcase\code
\aa{N}
\or
\or \aa{Asn}\fi}
\def\D{\ifcase\code
\aa{D\minus}
\or
\or \aa{Asp\minus}\fi}
\def\C{\ifcase\code
\aa{C}
\or
\or \aa{Cys}\fi}
\def\Q{\ifcase\code
\aa{Q}
\or
\or \aa{Gln}\fi}
\def\E{\ifcase\code
\aa{E\minus}
\or
\or\aa{Glu\minus}\fi}
\def\G{\ifcase\code
\aa{G}
\or
\or \aa{Gly}\fi}
\def\H{\ifcase\code
\aa{H}
\or
\or \aa{His}\fi}
\def\I{\ifcase\code
\aa{\ul{I}}
\or
\or\aa{\ul{Ile}}\fi}
\def\L{\ifcase\code
\aa{\ul{L}}
\or
\or \aa{\ul{Leu}}\fi}
\def\K{\ifcase\code
\aa{K\plus}
\or
\or \aa{Lys\plus}\fi}
\def\M{\ifcase\code
\aa{\ul{M}}
\or
\or \aa{\ul{Met}}\fi}
\def\F{\ifcase\code
\aa{\ul{F}}
\or
```

```
\or\aa{\ul{Phe}}\fi}
\def\P{\ifcase\code
\aa{P}
\or
\or \aa{Pro}\fi}
\def\S{\ifcase\code
\aa{S}
\or
\or \aa{Ser}\fi}
\def\T{\ifcase\code
\aa{T}
\or
\or \aa{Thr}\fi}
\def\W{\ifcase\code
\aa{\ul{W}}
\or
\or \aa{\ul{Trp}}\fi}
\def\Y{\ifcase\code
\aa{\ul{Y}}
\or
\or \aa{\ul{Tyr}}\fi}
\def\V{\ifcase\code
\aa{\ul{V}}
\or
\or \aa{\ul{Val}}\fi}
\def\J{\ifcase\code
\aa{B}
\or
\or \aa{Asx}\fi}
\def\Z{\ifcase\code
\aa{Z}
\or
\or \aa{Glx}\fi}
\def\X{\ifcase\code
\aa{X}
\or
\or \aa{Xxx}\fi}
\def\B{\aa{\ }}
\def\?{\aa{?}}
\def\U{\aa{\hrulefil}}


%\def\BA{\aa{$\beta_1$}}
%\def\BB{\aa{$\beta_2$}}
%\def\BC{\aa{$\beta_3$}}
%\def\BD{\aa{$\beta_4$}}
%\def\BE{\aa{$\beta_5$}}
%\def\BF{\aa{$\beta_6$}}
%\def\BG{\aa{$\beta_7$}}


\onecode
\sizing
%\obeylines
%\vskip 1truemm
%
%\ \ \ I \F\P\D\G\M\L\I\L\V\D\P\E\Q\A\V\E\P\G\D\F\C\I\A\R\L\G\G\D\E\F\T
% \ \ II \F\P\D\G\M\L\I\L\V\D\P\E\Q\A\V\E\P\G\D\F\C\I\A\R\L\G\G\D\E\F\T
%  \ III \F\P\D\G\M\L\I\L\V\D\P\E\Q\A\V\E\P\G\D\F\C\I\A\R\L\G\G\D\E\F\T
% \ \ IV \F\P\D\G\M\L\I\L\V\D\P\E\Q\A\V\E\P\G\D\F\C\I\A\R\L\G\G\D\E\F\T
%\ \ \ V
% \ \ VI
% \ \ VII

%\vskip 1truemm
%
%\ \ \ \ \ \ Hydrophobic residues are \ul{underlined}.
%
%
```

BINDFIT.FOR

```
C     PROGRAM BINDFIT
C
C     PURPOSE
C         FITS A SERIES OF [L], Y VALUE POINTS TO A BINDING CURVE
C             USING Ka, YL, AND YH AS FITTING PARAMETERS
C
C     VARIABLES
C
C     SUBROUTINES NEEDED
C         CURFIT (X, Y, SIGMAY, A, DELTAA, SIGMAA,
C             FLAMDA, YFIT, CHISQR)
C             MAKES LEAST SQUARES FIT TO BINDING CURVE (ONE ITERATION)
C
C
C
      PROGRAM BINDFIT
          REAL*8 CONC, YVAL, SIGMAY, A, DELTAA, SIGMAA, FLAMDA, YFIT
          REAL*8 CHINEW, CHIOLD, MULT, KA
          INTEGER*2 NPTS, NTERMS, MODE, NFREE, I
          CHARACTER*40 NDAT, WDISK, FNAME, SAVEFILE, BANNER*60
          DIMENSION CONC(60), YVAL(60), SIGMAY(60), A(3), DELTAA(3),
     &              SIGMAA(3), YFIT(60)
          COMMON NPTS, NTERMS, MODE, NFREE
           COMMON /PARS/ A, DELTAA ,SIGMAA ,FLAMDA, MULT
          COMMON /DEPV/ YVAL, YFIT, SIGMAY
C
       FLAMDA= 0.0001
      NTERMS= 3
      I= 0
C
C     INPUT DATA
C
          OPEN (1,FILE='CON')
          OPEN (5,FILE='DUMP.DAT')
          OPEN (4,FILE='NAME.JNK',STATUS='OLD',ERR=6)
          READ (4, 15) FNAME
          IF (INDEX(FNAME,'.').EQ.1) GOTO 6
          CLOSE (4)
          SAVEFILE= 'INPUT.DAT'
          OPEN (4, FILE= SAVEFILE, STATUS='OLD', ERR=55)
          READ (4,*) MODE, NPTS
          READ (4,*) A(1), A(2), A(3)
          IF (MODE.EQ.1) THEN
              DO 8 I= 1,NPTS
                  READ (4,*) CONC(I),YVAL(I),SIGMAY(I)
8                  CONTINUE
              PRINT 10, 'MODE 1 READING'
           ELSE
              DO 9 I= 1,NPTS
                  READ (4,*) CONC(I), YVAL(I)
9                   CONTINUE
              PRINT 10, 'MODE NOT 1 READING'
          ENDIF
          CLOSE (4)
          SAVEFILE='CHIFIT.OUT'
          GOTO 92
6              PRINT 10, 'IS THIS NEW DATA [N]? '
10              FORMAT (2X,A)
          READ (1,FMT=15) NDAT
15          FORMAT (A)
```

```
      IF (NDAT(1:1).EQ.'Y'.OR.NDAT(1:1).EQ.'y') THEN
          PRINT 10, 'INPUT WEIGHTING MODE:'
          PRINT 10, '1 - (INSTRUMENTAL) WEIGHT= 1/SIGMAY**2'
          PRINT 10, '2 - (NONE)         WEIGHT= 1'
          PRINT 10, '3 - (STATISTICAL)  WEIGHT= 1/Y  '
          PRINT 10, 'MODE? '
          READ (1,*) MODE
          MODEC= MODE
          IF (MODE.EQ.1) THEN
              BANNER= 'INPUT POINTS AS TRIPLETS:'
              BANNER= BANNER(1:26)//'CONCENTRATION, Y VALUE, SIGMA Y'
              PRINT 10, BANNER
              PRINT 10, 'A NEGATIVE CONCENTRATION SIGNALS END OF DATA'
20              I= I+1
              PRINT 10, 'NEXT POINT '
              READ (1,*) CONC(I), YVAL(I), SIGMAY(I)
              IF (CONC(I).GE.0.0) GOTO 20
              NPTS= I-1
              NFREE= NPTS-NTERMS
          ELSE
              PRINT 10, 'INPUT POINTS AS PAIRS: CONCENTRATION, YVALUE '
              PRINT 10, 'A NEGATIVE CONCENTRATION SIGNALS END OF DATA'
30              I= I+1
              PRINT 10, 'NEXT POINT '
              READ (1,*) CONC(I), YVAL(I)
              IF (CONC(I).GE.0.0) GOTO 30
              NPTS= I-1
              NFREE= NPTS-NTERMS
          ENDIF
          PRINT 10, 'INPUT INITIAL GUESSES FOR Ka, YL, YH'
          READ (1,*) A(1), A(2), A(3)
          PRINT 10, 'WRITE TO DISK? '
          READ (1,FMT=15) WDISK
          IF (WDISK(1:1).EQ.'Y'.OR.WDISK(1:1).EQ.'y') THEN
              PRINT 10, 'FILENAME? (NO EXTENSION)'
              READ (1,FMT=15) FNAME
              LNAME= INDEX(FNAME,' ')-1
              FNAME= FNAME(1:LNAME)//'.DAT'
              SAVEFILE= FNAME
              PRINT 10, SAVEFILE
              OPEN (4, FILE=SAVEFILE)
              WRITE (4,*) MODE, NPTS
              WRITE (4,*) A(1), A(2), A(3)
              IF (MODE.EQ.1) THEN
                  DO 40 I= 1,NPTS
                      WRITE (4,*) CONC(I), YVAL(I), SIGMAY(I)
40                      CONTINUE
              ELSE
                  DO 50 I= 1,NPTS
                      WRITE (4,*) CONC(I), YVAL(I)
50                      CONTINUE
              ENDIF
              CLOSE (4)
          ENDIF
      ELSE
          BANNER= 'FILE NAME (NO EXTENSION)  '
          PRINT 10, BANNER(1:25)
C          PRINT 10, 'FILE='
          READ (1,FMT=15) FNAME
          LNAME= INDEX(FNAME,' ')-1
          SAVEFILE= FNAME(1:LNAME)//'.DAT'
          FNAME= FNAME(1:LNAME)//'.DAT'
          OPEN (4, FILE=SAVEFILE, STATUS='OLD', ERR=55)
```

```
            GOTO 57
55            CONTINUE
            BANNER= 'I CAN''T FIND FILE '//SAVEFILE
            PRINT 10, BANNER
            PRINT 10, 'PLEASE INPUT ANOTHER FILE (RETURN TO EXIT)  '
C            PRINT 10, 'INCLUDE PATH IF NOT IN D:\PROGRAMS\BINDFIT  '
            READ (1,FMT=15) FNAME
            LNAME= INDEX(FNAME,' ')-1
            IF (LNAME.LE.0) GOTO 999
            SAVEFILE= FNAME(1:LNAME)//'.DAT'
            FNAME= FNAME(1:LNAME)//'.DAT'
            OPEN (4, FILE= SAVEFILE, STATUS='OLD', ERR=55)
57            CONTINUE
            PRINT 10, SAVEFILE
            WRITE (5, FMT=10) SAVEFILE
            READ (4,*) MODE, NPTS
            READ (4,*) A(1), A(2), A(3)
            IF (MODE.EQ.1) THEN
                DO 60 I= 1,NPTS
                    READ (4,*) CONC(I),YVAL(I),SIGMAY(I)
60                    CONTINUE
                PRINT 10, 'MODE 1 READING'
             ELSE
                DO 70 I= 1,NPTS
                    READ (4,*) CONC(I), YVAL(I)
70                    CONTINUE
                PRINT 10, 'MODE NOT 1 READING'
            ENDIF
            CLOSE (4)
        ENDIF
92           CONTINUE
        NFREE= NPTS-NTERMS
        PRINT 85, MODE, NTERMS, NPTS, NFREE
        MULT= 1.0
85        FORMAT (2X, 4(I5))
        PRINT *
        DO 80 I= 1,NPTS
            PRINT 90, CONC(I), YVAL(I), SIGMAY(I)
            WRITE (5, FMT= 90) CONC(I), YVAL(I), SIGMAY(I)
90            FORMAT (10X, 1PE12.4, 5X, 0PF8.4, 4X, F8.4)
80            CONTINUE
C
C       FIT BINDING CURVE
C
        LNAME= INDEX(SAVEFILE,'.')-1
        SAVEFILE= SAVEFILE(1:LNAME)//'.OUT'
        OPEN (3,FILE= SAVEFILE, STATUS='NEW', ERR=95)
        GOTO 98
95           CONTINUE
            IF (SAVEFILE(LNAME-5:LNAME).EQ.'CHIFIT') THEN
C                FNAME= SAVEFILE(1:LNAME-5)//'CHIFIT.OUT'
                OPEN (3, FILE= 'CHIFIT.OUT')
            ELSE
                PRINT 620, 'SHOULD OUTPUT REPLACE PREVIOUS FILE ',
     1                      SAVEFILE(1:LNAME+4),' [N]? '
                READ (1, FMT=15) WDISK
                IF (WDISK(1:1).EQ.'Y'.OR.WDISK(1:1).EQ.'y') THEN
                    OPEN (3, FILE= SAVEFILE)
                     FNAME= SAVEFILE(1:LNAME+4)
                ELSE
                    PRINT 10, 'WRITING TO CHIFIT.OUT'
                    OPEN (3, FILE= 'CHIFIT.OUT')
                     FNAME= SAVEFILE(1:LNAME+4)
```

```
            ENDIF
         ENDIF
98        CONTINUE
        LNAME= INDEX(FNAME,'.')-1
        WRITE (3,*)
        WRITE (3, FMT=600) 'LEAST SQUARES ANALYSIS OF FILE ',
     1           FNAME(1:LNAME)//'.DAT'
        IF (MODE.EQ.1) THEN
            WRITE (3, FMT=600)'INSTRUMENTAL WEIGHTING','= 1/SIGMAY**2'
        ELSEIF (MODE.EQ.3) THEN
            WRITE (3, FMT=600) 'STATISTICAL WEIGHTING','= 1/Y'
        ELSE
            WRITE (3, FMT=600) 'NO WEIGHTING',' '
        ENDIF
        WRITE (3,*)
        WRITE (3,*)
C        WRITE (3, FMT=600) 'DATA ','POINTS'
        WRITE (3, FMT=630) 'CONCENTRATION', 'YVALUE','SIGMA(YVAL)'
        WRITE (3,*)
        DO 140 I= 1,NPTS
            WRITE (3, FMT=90) CONC(I), YVAL(I), SIGMAY(I)
140          CONTINUE
        WRITE (3,*)
        WRITE (3,*)
        WRITE (3, FMT=610) 'RUN','CHISQR','Ka','SIGMA(KA)','YL',
     1           'SIGMA(YL)', 'YH', 'SIGMA(YH)'
        WRITE (3,*)
600        FORMAT (10X,A,A)
610        FORMAT (5X,A,3X,A,6X,A,7X,A,4X,A,3X,A,2X,A,3X,A)
620        FORMAT (2X,A,A,A)
630        FORMAT (10X,A,6X,A,5X,A)
        I= 1
        CALL CURFIT (CONC, CHIOLD)
        PRINT 110, I, CHIOLD, A(1), SIGMAA(1), A(2), SIGMAA(2), A(3),
     1      SIGMAA(3)
        WRITE (3,FMT=110) I, CHIOLD, A(1), SIGMAA(1), A(2),
     1       SIGMAA(2), A(3), SIGMAA(3)
        I= I+1
100          CONTINUE
            CALL CURFIT (CONC, CHINEW)
        IF ((CHIOLD-CHINEW).GT.0.0001) THEN
            PRINT 120, CHIOLD, CHINEW, CHIOLD-CHINEW
            PRINT 110, I, CHINEW,A(1), SIGMAA(1), A(2), SIGMAA(2), A(3),
     1           SIGMAA(3)
            WRITE (3,FMT=110) I, CHINEW, A(1), SIGMAA(1), A(2),
     1           SIGMAA(2), A(3), SIGMAA(3)
110            FORMAT (2X, I5, F10.4, 1PE12.4, E12.4, 0P, 4(2X,F6.4))
130            FORMAT (2X, A, F10.4)
120            FORMAT (2X, 3(F10.4))
            CHIOLD= CHINEW
            I=I+1
            GOTO 100
        ENDIF
        CLOSE (5)
        CLOSE (3)
999        CONTINUE
        END
```

CURFIT.FOR

```
C     SUBROUTINE CURFIT
C
C     MAKE LEAST SQUARES FIT TO A NON-LINEAR FUNCTION (FUNCTN)
C         WITH A LINEARIZATION OF THE FITTING FUNCTION
C     REF: BEVINGTON, P.R., "DATA REDUCTION AND ERROR ANALYSIS FOR
C         THE PHYSICAL SCIENCES", MCGRAW-HILL,1969, CHAP 11.
C
C     DESCRIPTION OF PARAMETERS
C         X             -    ARRAY OF DATA POINTS FOR INDEPENDENT VARIABLE
C         Y             -    ARRAY OF DATA POINTS FOR DEPENDENT VARIABLE
C         SIGMAY     - ARRAY OF STANDARD DEVIATIONS FOR Y DATA POINTS
C         NPTS          -    NUMBER OF DATA POINT PAIRS
C         NTERMS     -    NUMBER OF PARAMETERS TO BE FIT
C         MODE          -    DETERMINES METHOD OF WEIGHTING LEAST SQUARES FIT
C                          1 (INSTRUMENTAL) WEIGHT(I)= 1/SIGMAY(I)**2
C                          2 (NONE)              WEIGHT(I)= 1
C                          3 (STATISTICAL)  WEIGHT(I)= 1/Y(I)
C         A             -    ARRAY OF PARAMETERS
C         DELTAA     -    ARRAY OF INCREMENTS FOR PARAMETERS A
C         SIGMAA     -    ARRAY OF STANDARD DEVIATIONS FOR PARAMETERS A
C         FLAMDA -    PROPORTION OF GRADIENT SEARCH INCLUDED
C         YFIT          -    ARRAY OF CALCULATED VALUES FOR Y
C         CHISQR     -    REDUCED CHI SQUARE FOR FIT
C         MULT          -    EXPONENT OF Ka (A(1))
C
C     SUBROUTINES AND FUNCTIONS REQUIRED
C         FUNCTN (X, I, A)
C             EVALUATES THE FITTING FUNCTION FOR THE Ith TERM
C         FCHISQ (Y, SIGMAY, YFIT)
C             EVALUATES REDUCED CHI SQUARE FOR FIT TO DATA
C         FDERIV (X, I, A, DELTAA, DERIV)
C             EVALUATES THE DERIVATIVES OF THE FITTING FUNCTION
C             FOR THE Ith TERM WRT EACH PARAMETER
C         MATINV (ARRAY, NTERMS, DET)
C             INVERTS A SYMMETRIC TWO-DIMENSIONAL MATRIX OF DEGREE
C             NTERMS AND CALCULATES ITS DETERMINANT
C
C
      SUBROUTINE CURFIT (X, CHISQR)
C     1     SIGMAA, YFIT, CHISQR)
         REAL*8 X, Y, SIGMAY, A, DELTAA, SIGMAA, FLAMDA, YFIT, CHISQR
         REAL*8 WEIGHT, ALPHA, BETA, DERIV, ARRAY, B, CHISQ1, DET
          REAL*8 CHIOLD, MULT
         INTEGER*2 NPTS, NTERMS, MODE, NFREE, NORDER, I, J, K
         DIMENSION X(60), Y(60), SIGMAY(60), A(3), DELTAA(3), SIGMAA(3),
     1             YFIT(60)
         DIMENSION WEIGHT(60), ALPHA(3,3), BETA(3), DERIV(3),
     1             ARRAY(3,3), B(3)
         COMMON  NPTS, NTERMS, MODE, NFREE
         COMMON /PARS/ A, DELTAA, SIGMAA, FLAMDA, MULT
         COMMON /DEPV/ Y, YFIT, SIGMAY
C
C     PRINT 2, NPTS, NTERMS, MODE, NFREE
2         FORMAT (2X, 4(I5))
C         NORDER= NTERMS
         CHIOLD= 1E15
C         FLAMDA= 0.0001
C         A(1)= A(1)/MULT
         WRITE (5, FMT=123) 'A(1)=' , A(1)
         WRITE (5, FMT= 123) 'MULT=' ,MULT
```

```
      IF (NFREE.GT.0) GOTO 5
      CHISQR=0.0
      GOTO 999
7      FORMAT (2X,A)
C
C    EVALUATE WEIGHTS
C
5      CONTINUE
      WRITE (5, FMT= 7) 'EVALUATE WEIGHTS'
      DO 10 I= 1,NPTS
          IF (MODE.EQ.1) THEN
              WEIGHT(I)=1.0/SIGMAY(I)**2
          ELSEIF ((MODE.EQ.3).AND.(Y(I).NE.0.0)) THEN
              WEIGHT(I)= 1.0/ABS(Y(I))
          ELSE
              WEIGHT(I)=1.0
          ENDIF
10          CONTINUE
C      WRITE (5, FMT= 7) 'EVALUATE ALPHA AND BETA MATRICES'
C
C    EVALUATE ALPHA AND BETA MATRICES
C
      DO 20 J= 1,NTERMS
          BETA(J)= 0.
          DO 30 K= 1,J
              ALPHA(J,K)=0.
30              CONTINUE
20          CONTINUE
C
      DO 50 I= 1,NPTS
          CALL FDERIV (X, I, DERIV)
          DO 60 J= 1,NTERMS
              BETA(J)= BETA(J)+WEIGHT(I)*(Y(I)-FUNCTN(X, I, A, MULT)
     1                    )*DERIV(J)
              DO 70 K= 1,J
                  ALPHA(J,K)= ALPHA(J,K)+WEIGHT(I)*DERIV(J)*DERIV(K)
70                  CONTINUE
60              CONTINUE
50          CONTINUE
C
      DO 80 J= 1,NTERMS
          DO 90 K=1,J
          ALPHA(K,J)=ALPHA(J,K)
90              CONTINUE
80          CONTINUE
          DO 91 J=1, NTERMS
          WRITE (5, FMT= 92) ALPHA(J,1), ALPHA(J,2), ALPHA(J,3),
     1                BETA(J)
91          CONTINUE
92          FORMAT (2X, 4(E12.4))
C      PRINT 7, 'EVALUATE CHI SQUARE AT STARTING POINT'
C
C    EVALUATE CHI SQUARE AT STARTING POINT
C
      DO 100 I= 1,NPTS
          YFIT(I)= FUNCTN(X, I, A, MULT)
          WRITE (5, FMT= 89) Y(I), SIGMAY(I), NPTS, NFREE, MODE, YFIT(I)
89          FORMAT (2X, 2(E12.4), 3(I5), E12.4)
100          CONTINUE
      CHISQ1 = FCHISQ ()
      WRITE (5, FMT= 123) 'CHISQR AT START=', CHISQ1
8      FORMAT (2X, F8.6)
      WRITE (5, FMT= 7) 'INVERT CURVATURE MATRIX'
```

```
C
C     INVERT MODIFIED CURVATURE MATRIX TO FIND NEW PARAMETERS
C
170         CONTINUE
          DO 110 J= 1,NTERMS
              DO 120 K=1,NTERMS
                  ARRAY(J,K)= ALPHA(J,K)/SQRT(ALPHA(J,J)*ALPHA(K,K))
C                  IF (J.NE.K) PRINT 124, J, K, ARRAY(J,K)
124                   FORMAT (2X, I5, I5, E14.6)
120                   CONTINUE
              ARRAY(J,J)=1.0+FLAMDA
C              PRINT 124, J, J, ARRAY(J,J)
123               FORMAT (2X, A, E14.6)
110               CONTINUE
              WRITE (5, FMT= 123) 'FLAMDA=',FLAMDA
C
C         PRINT 135, 'NORDER=',NORDER
135         FORMAT (2X, A, I5)
          CALL MATINV(ARRAY, DET)
          DO 130 J= 1,NTERMS
              B(J)=A(J)
              DO 140 K= 1,NTERMS
                  B(J)= B(J)+BETA(K)*ARRAY(J,K)/SQRT(ALPHA(J,J)*ALPHA(K,K))
140                   CONTINUE
              WRITE (5, FMT= 123) 'B(J)=', B(J)
130               CONTINUE
C
C     IF CHI SQUARE INCREASED, INCREASE FLAMDA AND TRY AGAIN
C
C         PRINT 7, 'REEVALUATE CHI SQUARE'
          DO 150 I= 1,NPTS
              YFIT(I) = FUNCTN (X, I, B, MULT)
C              PRINT 123, 'YFIT=', YFIT(I)
150               CONTINUE
          CHISQR = FCHISQ ()
          WRITE (5, FMT= 123) 'REEVALUATE CHISQR=', CHISQR
          IF (CHISQR.LE.CHISQ1) GOTO 160
          IF (ABS(CHIOLD-CHISQR).LT.0.001) GOTO 160
          CHIOLD= CHISQR
          FLAMDA= 10.*FLAMDA
          WRITE (5, FMT= 7) ' CHI SQUARE INCREASED, TRYING AGAIN'
C         WRITE (3, FMT= 7) ' CHI SQUARE INCREASED, TRYING AGAIN'
          PRINT 7, 'CHI SQUARE INCREASED, TRYING AGAIN'
          GOTO 170
C
C     EVALUATE PARAMETERS AND UNCERTAINTIES
C
160         CONTINUE
          WRITE (5, FMT= 7) 'EVALUATE PARAMETERS AND UNCERTAINTIES'
          DO 180 J= 1, NTERMS
              A(J)=B(J)
              SIGMAA(J)= SQRT(ARRAY(J,J)/ALPHA(J,J))
              WRITE (5, FMT= 123) 'A(J)=',A(J)
              WRITE (5, FMT= 123) 'ARRAY=',ARRAY(J,J)
              WRITE (5, FMT= 123) 'ALPHA=',ALPHA(J,J)
              WRITE (5, FMT= 123) 'SIGMAA=',SIGMAA(J)
180               CONTINUE
          FLAMDA=FLAMDA/10.
999         RETURN
          END
```

CHI.FOR

```
C     SUBROUTINE MATINV
C
C     INVERT A SYMMETRIC MATRIX AND CALCULATE ITS DETERMINANT
C
C     USAGE
C         CALL MATINV(ARRAY, DET)
C
C     DESCRIPTION OF PARAMETERS
C         ARRAY         -     INPUT MATRIX, REPLACED BY INVERSE
C         NORDER     -     DEGREE OF MATRIX
C         DET         -     DETERMINANT OF INPUT MATRIX
C
C
      SUBROUTINE MATINV(ARRAY, DET)
         REAL*8 ARRAY, DET, AMAX, SAVE
         INTEGER*2 NPTS, NORDER, IK, JK, I, J, K
         DIMENSION ARRAY(3,3), IK(3), JK(3)
         COMMON NPTS, NORDER
C
         DET=1.
C         PRINT 5, ARRAY(1,2), NORDER, DET
5         FORMAT (2X, E12.4, I5, F8.4)
C
C     FIND LARGEST ELEMENT ARRAY(I,J) IN REST OF MATRIX
C
         DO 10 K=1,NORDER
             AMAX=0.0
25             DO 20 I=K,NORDER
                 DO 30 J=K,NORDER
                     IF (ABS(AMAX).GT.ABS(ARRAY(I,J))) GOTO 30
                     AMAX= ARRAY(I,J)
                     IK(K)=I
                     JK(K)=J
30                  CONTINUE
20               CONTINUE
             DO 33 I= K, NORDER
                 DO 35 J=K, NORDER
C                     PRINT 37, K, IK(K), JK(K)
37                    FORMAT (2X, 3(I5))
35                    CONTINUE
33               CONTINUE
C
C     INTERCHANGE ROWS AND COLUMNS TO PUT AMAX IN ARRAY(K,K)
C
         IF (AMAX.EQ.0.0) THEN
             DET= 0.
             GOTO 999
             ENDIF
         I= IK(K)
         IF (I.LT.K) GOTO 25
         IF (I.GT.K) THEN
             DO 40 J= 1,NORDER
                 SAVE= ARRAY(K,J)
                 ARRAY(K,J)= ARRAY(I,J)
                 ARRAY(I,J)= -SAVE
40               CONTINUE
             ENDIF
         J= JK(K)
         IF (J.LT.K) GOTO 25
         IF (J.GT.K) THEN
```

```
            DO 50 I= 1,NORDER
                SAVE= ARRAY(I,K)
                ARRAY(I,K)= ARRAY(I,J)
                ARRAY(I,J)= -SAVE
50                CONTINUE
            ENDIF
C
C     ACCUMULATE ELEMENTS OF INVERSE MATRIX
C
         DO 60 I= 1,NORDER
             IF (I.NE.K) ARRAY(I,K)= -ARRAY(I,K)/AMAX
60           CONTINUE
         DO 70 I=1,NORDER
             DO 80 J=1,NORDER
                 IF ((I.NE.K).AND.(J.NE.K)) THEN
                     ARRAY(I,J)= ARRAY(I,J)+ARRAY(I,K)*ARRAY(K,J)
                     ENDIF
80                 CONTINUE
70           CONTINUE
         DO 90 J=1,NORDER
             IF (J.NE.K) ARRAY(K,J)= ARRAY(K,J)/AMAX
90           CONTINUE
         ARRAY(K,K)= 1./AMAX
         DET= DET*AMAX
10       CONTINUE
C
C     RESTORE ORDERING OF MATRIX
C
         DO 100 L=1, NORDER
             K= NORDER-L+1
             J= IK(K)
             IF (J.GT.K) THEN
                 DO 110 I=1,NORDER
                     SAVE= ARRAY(I,K)
                     ARRAY(I,K)= -ARRAY(I,J)
                     ARRAY(I,J)= SAVE
110                    CONTINUE
                 ENDIF
             I= JK(K)
             IF (I.GT.K) THEN
                 DO 120 J=1,NORDER
                     SAVE= ARRAY(K,J)
                     ARRAY(K,J)= -ARRAY(I,J)
                     ARRAY(I,J)= SAVE
120                    CONTINUE
                 ENDIF
100          CONTINUE
999       RETURN
         END
C
C
C
C     FUNCTION FCHISQ
C
C     PURPOSE
C         EVALUATE REDUCED CHI SQUARE FOR FIT TO DATA
C         FCHISQ = SUM((Y-YFIT)**2/SIGMA**2)/NFREE
C
C     USAGE
C         RESULT = FCHISQ (Y, SIGMAY, YFIT)
C
C     DESCRIPTION OF PARAMETERS
C         Y             -     ARRAY OF DATA POINTS
```

```
C        SIGMAY    - ARRAY OF STANDARD DEVIATIONS FOR Y DATA POINTS
C        NPTS        -    NUMBER OF DATA POINTS
C        NFREE     -    NUMBER OF DEGREES OF FREEDOM
C        MODE        -    DETERMINES METHOD OF WEIGHTING LEAST SQUARES FIT
C                        1 (INSTRUMENTAL) WEIGHT(I)= 1/SIGMAY(I)**2
C                        2 (NONE)              WEIGHT(I)= 1
C                        3 (STATISTICAL)  WEIGHT(I)= 1/Y(I)
C        YFIT        -    ARRAY OF CALCULATED VALUES FOR Y
C
    REAL*8 FUNCTION FCHISQ()
        REAL*8 Y,SIGMAY,YFIT,WEIGHT,CHISQ
        INTEGER*2 NPTS,NFREE,MODE,NTERMS, I, J
        DIMENSION Y(60), SIGMAY(60), YFIT(60)
        COMMON NPTS, NTERMS, MODE, NFREE
        COMMON /DEPV/ Y, YFIT, SIGMAY
C
        CHISQ= 0.0
110        FORMAT (2X,A,I5)
C         PRINT 110, 'NPTS(FCHISQ)', NPTS
C         PRINT 110, 'NTERMS(FCHISQ)', NTERMS
C         PRINT 110, 'MODE(FCHISQ)', MODE
C         PRINT 110, 'NFREE(FCHISQ)', NFREE
        IF (NFREE.LE.0) THEN
            FCHISQ= 0.0
            GOTO 999
            ENDIF
C
C    ACCUMULATE CHI SQUARE
C
        DO 10 I= 1,NPTS
            IF (MODE.EQ.1) THEN
                WEIGHT = 1.0/SIGMAY(I)**2
            ELSEIF ((MODE.EQ.3).AND.(Y(I).NE.0.0)) THEN
                WEIGHT = 1.0/ ABS(Y(I))
            ELSE
                WEIGHT= 1.0
            ENDIF
            CHISQ= CHISQ+WEIGHT*(Y(I)-YFIT(I))**2
C            PRINT 100, 'CHISQ=', CHISQ
10            CONTINUE
100        FORMAT (2X,A,E12.4)
C
C    DIVIDE BY THE NUMBER OF DEGREES OF FREEDOM
C
C         PRINT 100, 'FCHISQ=', CHISQ/REAL(NFREE)
        FCHISQ= CHISQ/REAL(NFREE)
C         PRINT 100, 'CRASH???', CHISQ
999         CONTINUE
        RETURN
        END
```

BINDF.FOR

```
C     FUNCTIONS NEEDED FOR LEAST SQUARES FIT TO BINDING CURVES
C     FUNCTION FUNCTN EVALUATES Yapp=(YH-YL)*KA*[L]/(1+KA*[L])
C
C     VARIABLES
C     L     -     LIGAND CONCENTRATION ARRAY (INDEPENDENT VARIABLE)
C     I     -     INDEX
C     A     -     PARAMETER ARRAY A(1)=Ka, A(2)=YL, A(3)=YH
C     MULT- EXPONENT OF Ka
C
      REAL*8 FUNCTION FUNCTN (L, I, A, MULT)
         REAL*8 LI,L,A,MULT
         INTEGER*2 I
         DIMENSION L(60), A(3)
         LI= L(I)
         FUNCTN= (A(3)-A(2))*A(1)*LI/(1+A(1)*LI)+A(2)
100         FORMAT (2X,F8.4,F8.4,F8.4)
         RETURN
         END
C
C
C     SUBROUTINE FDERIV EVALUATES PARTIAL DERIVATIVES OF EACH
C     PARAMETER IN EQUATION FOR Yapp
C
C     VARIABLES
C     L             -     LIGAND CONCENTRATION ARRAY (INDEPENDENT VARIABLE)
C     I             -     INDEX
C     A             -     PARAMETER ARRAY A(1)=Ka, A(2)=YL, A(3)=YH
C     DELTAA     -     PARAMETER INCREMENT ARRAY
C     NTERMS     -     NUMBER OF PARAMETERS (3 FOR BINDING CURVES)
C     DERIV(I)     -   Ith PARTIAL DERIVATIVE OF BINDING CURVE
C                       WRT PARAMETERS
C
      SUBROUTINE FDERIV (L, I, DERIV)
         REAL*8 LI, Z, L, A, DELTAA, DERIV, SIGMAA, FLAMDA, MULT
         INTEGER*2 I
         DIMENSION L(60), A(3), DELTAA(3), DERIV(3), SIGMAA(3)
         COMMON /PARS/ A, DELTAA, SIGMAA, FLAMDA, MULT
C
         LI= L(I)
         Z= 1+A(1)*LI
         RANGE= A(3)-A(2)
         DERIV(1)= RANGE*LI/Z-RANGE*A(1)*LI**2/Z**2
         DERIV(3)= A(1)*LI/Z
         DERIV(2)= 1.0-DERIV(3)
C         WRITE (5, *) 'A(1), Z=', A(1), Z
C         WRITE (5, *) 'DERIVS 1,3=', DERIV(1), DERIV(3)
100         FORMAT (2X, A, 2(F8.4))
         RETURN
         END
```

HILLFIT.FOR

```
C     PROGRAM BINDFIT
C
C     PURPOSE
C         FITS A SERIES OF [L], Y VALUE POINTS TO A BINDING CURVE
C             USING Ka, YL, AND YH AS FITTING PARAMETERS
C
C     VARIABLES
C
C     SUBROUTINES NEEDED
C         CURFIT (X, Y, SIGMAY, A, DELTAA, SIGMAA,
C             FLAMDA, YFIT, CHISQR)
C             MAKES LEAST SQUARES FIT TO BINDING CURVE (ONE ITERATION)
C
C
C
      PROGRAM BINDFIT
          REAL*8 CONC, YVAL, SIGMAY, A, DELTAA, SIGMAA, FLAMDA, YFIT
          REAL*8 CHINEW, CHIOLD, MULT, KA
          INTEGER*2 NPTS, NTERMS, MODE, NFREE, I
          CHARACTER*40 NDAT, WDISK, FNAME, SAVEFILE, BANNER*60
          DIMENSION CONC(60), YVAL(60), SIGMAY(60), A(3), DELTAA(3),
     &              SIGMAA(3), YFIT(60)
          COMMON NPTS, NTERMS, MODE, NFREE
           COMMON /PARS/ A, DELTAA ,SIGMAA ,FLAMDA, MULT
          COMMON /DEPV/ YVAL, YFIT, SIGMAY
C
       FLAMDA= 0.0001
      NTERMS= 3
      I= 0
C
C     INPUT DATA
C
          OPEN (1,FILE='CON')
          OPEN (5,FILE='DUMP.DAT')
          OPEN (4,FILE='NAME.JNK',STATUS='OLD',ERR=6)
          READ (4, 15) FNAME
          IF (INDEX(FNAME,'.').EQ.1) GOTO 6
          CLOSE (4)
          SAVEFILE= 'INPUT.DAT'
          OPEN (4, FILE= SAVEFILE, STATUS='OLD', ERR=55)
          READ (4,*) MODE, NPTS
          READ (4,*) KA, A(2), A(3)
          IF (MODE.EQ.1) THEN
              DO 8 I= 1,NPTS
                  READ (4,*) CONC(I),YVAL(I),SIGMAY(I)
8                  CONTINUE
              PRINT 10, 'MODE 1 READING'
           ELSE
              DO 9 I= 1,NPTS
                  READ (4,*) CONC(I), YVAL(I)
9                   CONTINUE
              PRINT 10, 'MODE NOT 1 READING'
          ENDIF
          CLOSE (4)
          SAVEFILE='HILLFIT.OUT'
          GOTO 92
6               PRINT 10, 'IS THIS NEW DATA [N]? '
10               FORMAT (2X,A)
          READ (1,FMT=15) NDAT
15          FORMAT (A)
```

```
      IF (NDAT(1:1).EQ.'Y'.OR.NDAT(1:1).EQ.'y') THEN
          PRINT 10, 'INPUT WEIGHTING MODE:'
          PRINT 10, '1 - (INSTRUMENTAL) WEIGHT= 1/SIGMAY**2'
          PRINT 10, '2 - (NONE)         WEIGHT= 1'
          PRINT 10, '3 - (STATISTICAL)  WEIGHT= 1/Y  '
          PRINT 10, 'MODE? '
          READ (1,*) MODE
          MODEC= MODE
          IF (MODE.EQ.1) THEN
              BANNER= 'INPUT POINTS AS TRIPLETS:'
              BANNER= BANNER(1:26)//'CONCENTRATION, Y VALUE, SIGMA Y'
              PRINT 10, BANNER
              PRINT 10, 'A NEGATIVE CONCENTRATION SIGNALS END OF DATA'
20              I= I+1
              PRINT 10, 'NEXT POINT '
              READ (1,*) CONC(I), YVAL(I), SIGMAY(I)
              IF (CONC(I).GE.0.0) GOTO 20
              NPTS= I-1
              NFREE= NPTS-NTERMS
          ELSE
              PRINT 10, 'INPUT POINTS AS PAIRS: CONCENTRATION, YVALUE '
              PRINT 10, 'A NEGATIVE CONCENTRATION SIGNALS END OF DATA'
30              I= I+1
              PRINT 10, 'NEXT POINT '
              READ (1,*) CONC(I), YVAL(I)
              IF (CONC(I).GE.0.0) GOTO 30
              NPTS= I-1
              NFREE= NPTS-NTERMS
          ENDIF
          PRINT 10, 'INPUT INITIAL GUESSES FOR Ka, YL, YH'
          READ (1,*) KA, A(2), A(3)
          PRINT 10, 'WRITE TO DISK? '
          READ (1,FMT=15) WDISK
          IF (WDISK(1:1).EQ.'Y'.OR.WDISK(1:1).EQ.'y') THEN
              PRINT 10, 'FILENAME? (NO EXTENSION)'
              READ (1,FMT=15) FNAME
              LNAME= INDEX(FNAME,' ')-1
              FNAME= FNAME(1:LNAME)//'.DAT'
              SAVEFILE= FNAME
              PRINT 10, SAVEFILE
              OPEN (4, FILE=SAVEFILE)
              WRITE (4,*) MODE, NPTS
              WRITE (4,*) KA, A(2), A(3)
              IF (MODE.EQ.1) THEN
                  DO 40 I= 1,NPTS
                      WRITE (4,*) CONC(I), YVAL(I), SIGMAY(I)
40                      CONTINUE
              ELSE
                  DO 50 I= 1,NPTS
                      WRITE (4,*) CONC(I), YVAL(I)
50                      CONTINUE
              ENDIF
              CLOSE (4)
          ENDIF
      ELSE
          BANNER= 'FILE NAME (NO EXTENSION)  '
          PRINT 10, BANNER(1:25)
C          PRINT 10, 'FILE='
          READ (1,FMT=15) FNAME
          LNAME= INDEX(FNAME,' ')-1
          SAVEFILE= FNAME(1:LNAME)//'.DAT'
          FNAME= FNAME(1:LNAME)//'.DAT'
          OPEN (4, FILE=SAVEFILE, STATUS='OLD', ERR=55)
```

```
            GOTO 57
55            CONTINUE
            BANNER= 'I CAN''T FIND FILE '//SAVEFILE
            PRINT 10, BANNER
            PRINT 10, 'PLEASE INPUT ANOTHER FILE (RETURN TO EXIT)  '
C            PRINT 10, 'INCLUDE PATH IF NOT IN D:\PROGRAMS\BINDFIT  '
            READ (1,FMT=15) FNAME
            LNAME= INDEX(FNAME,' ')-1
            IF (LNAME.LE.0) GOTO 999
            SAVEFILE= FNAME(1:LNAME)//'.DAT'
            FNAME= FNAME(1:LNAME)//'.DAT'
            OPEN (4, FILE= SAVEFILE, STATUS='OLD', ERR=55)
57            CONTINUE
            PRINT 10, SAVEFILE
            WRITE (5, FMT=10) SAVEFILE
            READ (4,*) MODE, NPTS
            READ (4,*) KA, A(2), A(3)
            IF (MODE.EQ.1) THEN
                DO 60 I= 1,NPTS
                    READ (4,*) CONC(I),YVAL(I),SIGMAY(I)
60                    CONTINUE
                PRINT 10, 'MODE 1 READING'
             ELSE
                DO 70 I= 1,NPTS
                    READ (4,*) CONC(I), YVAL(I)
70                    CONTINUE
                PRINT 10, 'MODE NOT 1 READING'
            ENDIF
            CLOSE (4)
        ENDIF
92           CONTINUE
        NFREE= NPTS-NTERMS
        PRINT 85, MODE, NTERMS, NPTS, NFREE
        MULT= 1.0
85        FORMAT (2X, 4(I5))
        PRINT *
        DO 80 I= 1,NPTS
            PRINT 90, CONC(I), YVAL(I), SIGMAY(I)
            WRITE (5, FMT= 90) CONC(I), YVAL(I), SIGMAY(I)
90            FORMAT (10X, 1PE12.4, 5X, 0PF8.4, 4X, F8.4)
80            CONTINUE
C
C       FIT BINDING CURVE
C
        LNAME= INDEX(SAVEFILE,'.')-1
        SAVEFILE= SAVEFILE(1:LNAME)//'.OUT'
        OPEN (3,FILE= SAVEFILE, STATUS='NEW', ERR=95)
        GOTO 98
95           CONTINUE
            IF (SAVEFILE(LNAME-5:LNAME).EQ.'CHIFIT') THEN
C                FNAME= SAVEFILE(1:LNAME-5)//'HILLFIT.OUT'
                OPEN (3, FILE= 'CHIFIT.OUT')
            ELSE
                PRINT 620, 'SHOULD OUTPUT REPLACE PREVIOUS FILE ',
     1                      SAVEFILE(1:LNAME+4),' [N]? '
                READ (1, FMT=15) WDISK
                IF (WDISK(1:1).EQ.'Y'.OR.WDISK(1:1).EQ.'y') THEN
                    OPEN (3, FILE= SAVEFILE)
                     FNAME= SAVEFILE(1:LNAME+4)
                ELSE
                    PRINT 10, 'WRITING TO HILLFIT.OUT'
                    OPEN (3, FILE= 'HILLFIT.OUT')
                     FNAME= SAVEFILE(1:LNAME+4)
```

```
            ENDIF
         ENDIF
98        CONTINUE
        LNAME= INDEX(FNAME,'.')-1
        WRITE (3,*)
        WRITE (3, FMT=600) 'LEAST SQUARES ANALYSIS OF FILE ',
     1           FNAME(1:LNAME)//'.DAT'
        IF (MODE.EQ.1) THEN
            WRITE (3, FMT=600)'INSTRUMENTAL WEIGHTING','= 1/SIGMAY**2'
        ELSEIF (MODE.EQ.3) THEN
            WRITE (3, FMT=600) 'STATISTICAL WEIGHTING','= 1/Y'
        ELSE
            WRITE (3, FMT=600) 'NO WEIGHTING',' '
        ENDIF
        WRITE (3, 600) 'COOPERATIVE CURVE FITTING',' '
        WRITE (3,*)
        WRITE (3,*)
C        WRITE (3, FMT=600) 'DATA ','POINTS'
        WRITE (3, FMT=630) 'CONCENTRATION', 'YVALUE','SIGMA(YVAL)'
        WRITE (3,*)
        DO 140 I= 1,NPTS
            WRITE (3, FMT=90) CONC(I), YVAL(I), SIGMAY(I)
140          CONTINUE
        MULT= 1.0
150        CONTINUE
        A(1)= KA**MULT
        WRITE (3,*)
        WRITE (3, 635) 'COOPERATIVITY COEFFICIENT',MULT
        WRITE (3,*)
        WRITE (3, FMT=610) 'RUN','CHISQR','Ka','SIGMA(KA)','YL',
     1           'SIGMA(YL)', 'YH', 'SIGMA(YH)'
        WRITE (3,*)
600        FORMAT (10X,A,A)
610        FORMAT (5X,A,3X,A,6X,A,7X,A,4X,A,3X,A,2X,A,3X,A)
620        FORMAT (2X,A,A,A)
630        FORMAT (10X,A,6X,A,5X,A)
635        FORMAT (2X,A,2X,F7.3)
        I= 1
        CALL CURFIT (CONC, CHIOLD)
        PRINT 110, I, CHIOLD, A(1)**(1/MULT), SIGMAA(1), A(2),
     1       SIGMAA(2), A(3), SIGMAA(3)
        WRITE (3,FMT=110) I, CHIOLD, A(1)**(1/MULT), SIGMAA(1), A(2),
     1       SIGMAA(2), A(3), SIGMAA(3)
        I= I+1
100          CONTINUE
            CALL CURFIT (CONC, CHINEW)
        IF ((CHIOLD-CHINEW).GT.0.0001) THEN
            PRINT 120, CHIOLD, CHINEW, CHIOLD-CHINEW
            PRINT 110, I, CHINEW, A(1)**(1/MULT), SIGMAA(1), A(2),
     1           SIGMAA(2), A(3), SIGMAA(3)
            WRITE (3,FMT=110) I, CHINEW, A(1)**(1/MULT), SIGMAA(1), A(2),
     1           SIGMAA(2), A(3), SIGMAA(3)
110            FORMAT (2X, I5, F10.4, 1PE12.4, E12.4, 0P, 4(2X,F6.4))
130            FORMAT (2X, A, F10.4)
120            FORMAT (2X, 3(F10.4))
            CHIOLD= CHINEW
            I=I+1
            GOTO 100
        ENDIF
        IF (MULT.LE.3.0) THEN
            MULT= MULT+0.1
            GOTO 150
            ENDIF
        CLOSE (5)
        CLOSE (3)
999        CONTINUE
        END
```

HILLF.FOR

```
C    FUNCTIONS NEEDED FOR LEAST SQUARES FIT TO TERTIARY COMPLEX
C    BINDING FUNCTION
C    FUNCTION FUNCTN EVALUATES Yapp=(YH-YL)*KA*[L]/(1+KA*[L])
C
C    VARIABLES
C    L    -    LIGAND CONCENTRATION ARRAY (INDEPENDENT VARIABLE)
C    I    -    INDEX
C    A    -    PARAMETER ARRAY A(1)=Ka, A(2)=YL, A(3)=YH
C    MULT- EXPONENT OF Ka
C
    REAL*8 FUNCTION FUNCTN (L, I, A, MULT)
        REAL*8 LI,L,A,MULT
        INTEGER*2 I
        DIMENSION L(60), A(3)
        LI= L(I)**MULT
        FUNCTN= (A(3)-A(2))*A(1)*LI/(1+A(1)*LI)+A(2)
100        FORMAT (2X,F8.4,F8.4,F8.4)
        RETURN
        END
C
C
C    SUBROUTINE FDERIV EVALUATES PARTIAL DERIVATIVES OF EACH
C    PARAMETER IN EQUATION FOR Yapp
C
C    VARIABLES
C    L            -    LIGAND CONCENTRATION ARRAY (INDEPENDENT VARIABLE)
C    I            -    INDEX
C    A            -    PARAMETER ARRAY A(1)=Ka, A(2)=YL, A(3)=YH
C    DELTAA    -    PARAMETER INCREMENT ARRAY
C    NTERMS    -    NUMBER OF PARAMETERS (3 FOR BINDING CURVES)
C    DERIV(I)    -  Ith PARTIAL DERIVATIVE OF BINDING CURVE
C                    WRT PARAMETERS
C
    SUBROUTINE FDERIV (L, I, DERIV)
        REAL*8 LI, Z, L, A, DELTAA, DERIV, SIGMAA, FLAMDA, MULT
        INTEGER*2 I
        DIMENSION L(60), A(3), DELTAA(3), DERIV(3), SIGMAA(3)
        COMMON /PARS/ A, DELTAA, SIGMAA, FLAMDA, MULT
C
        LI= L(I)**MULT
        Z= 1+A(1)*LI
        RANGE= A(3)-A(2)
        DERIV(1)= RANGE*LI/Z-RANGE*A(1)*LI*LI/Z**2
        DERIV(3)= A(1)*LI/Z
        DERIV(2)= 1.0-DERIV(3)
C        WRITE (5, *) 'A(1), Z=', A(1), Z
C        WRITE (5, *) 'DERIVS 1,3=', DERIV(1), DERIV(3)
100        FORMAT (2X, A, 2(F8.4))
        RETURN
        END
```

SIXMER.FOR

```
C     MERS TAKES A MICROGENIE SINGLE SEQUENCE OUTFILE AND DETERMINES
C     THE DISTRIBUTION OF SIXMERS WITHIN IT.  CURRENTLY, NO
C     POSITIONAL DATA IS STORED.  MERS USES A 6D ARRAY AS A THE
C     SIXMER FREQUENCY STORAGE ELEMENT.  USING A=1, C=2, G=3, AND T=4,
C     TO DESCRIBE EACH SEQUENCE, IE SMERS(1,1,2,3,4,4) = AACGTT.
C      MERS FIRST INPUTS A STRING OF 50 BASES, THEN MOVES SEQUENTIALLY
C     FORWARD COUNTING SIXMERS.  THE LAST FIVE BASES ARE SAVED TO
C     START THE NEXT INPUT LINE.  THE PROGRAM THEN REMOVES COMPLEMENTS
C     SO THAT ONLY THE ALPHABETICALLY FIRST OF A PAIR IS WRITTEN.
C     OUTPUT CONSISTS OF THE FILE C:\WSW\FORT\SEQLS6.OUT.
C
C     ********DATA PREPARATION**********
C
C      IF THE SEQUENCE IS LINEAR, THE FIRST LINE OF THE FILE MUST BE
C     XXXXX (OR MORE X'S) IF THE SEQUENCE IS CIRCULAR,
C     PUT THE LAST FIVE BASES IN
C      THE SEQUENCE AT THE FRONT.  ALL FILES MUST HAVE END AS THE FIRST
C     THREE CHARACTERS OF THE LAST LINE. CURRENTLY THE INPUT FILE IS
C     NAMED DATA.SEQ. IF THE BATCH FILES ARE USED TO RUN MERS, THE
C     .SEQ FILE OF YOUR CHOICE IS COPIED TO THE PROGRAMS DIRECTORY
C     AND THE END COMMAND IS AUTOMATICALLY ADDED. THE OUTPUT FILE IS
C     THEN COPIED BACK TO YOUR DIRECTORY WITH A 5.OUT APPENDED TO THE
C     NAME. TO PRODUCE A SUITABLE DATA FILE ON MICROGENIE,
C     ENTER ANALYZE, AND CHANGE A SET OF PARAMETERS TO THE FOLLOWING
C     NWIDTH=5, NFREQ=0, NSKIP=0. ANALYZE THE DESIRED SEQUENCE USING
C     ONLY PROCEDURE 1, EXIT MICROGENIE AND COPY OUTFILE TO YOUR
C     DIRECTORY .SEQ.  THEN EDIT THE FILE AND REMOVE THE SEQUENCE NAME
C     (IT APPEARS PERIODICALLY). PLACE EITHER MORE THAN FIVE X'S (OR
C     THE LAST FIVE BASES FOR CIRCULAR DNA) AT THE FRONT OF THE FILE.
C     IT IS NOT NECESSARY TO REMOVE COMPLETELY BLANK LINES.

      PROGRAM MERS
       INTEGER*2 I,J,K(6),L,M,N,Q,SMERS,COUNT
       DIMENSION SMERS(5,5,5,5,5,5)
       CHARACTER*4 BP*5, TEMP, SITE*10
       CHARACTER*60 LAST, SEQ, ISEQ

          PRINT 3,'STARTING'
       CALL INIT(SMERS)
       COUNT=0
       BP= 'ACGTX'
3             FORMAT (2X,A)
       CALL INPUT(LAST)
       CALL INPUT(ISEQ)
       SEQ=LAST(1:5)//ISEQ(1:50)
       PRINT 3,SEQ
7           CONTINUE
C
C         SORT SIXMERS OF SEQUENCE IN ORDER INTO ARRAY
          DO 10 I=1,50
              DO 20 J=1,6
                  K(J)=INDEX(BP,SEQ(I+J-1:I+J-1))
20                   CONTINUE
              SMERS(K(1),K(2),K(3),K(4),K(5),K(6))=SMERS(K(1),K(2),
     1             K(3),K(4),K(5),K(6))+1
C              IF (K(1).NE.5.AND.K(2).NE.5.AND.K(3).NE.5.AND.K(4).NE.5
C     1                .AND.K(5).NE.5.AND.K(6).NE.5) COUNT=COUNT+1
10              CONTINUE

C     INPUT SEQUENCE UNTIL 'END'
```

```
        CALL INPUT(ISEQ)
        IF (ISEQ(1:3).EQ.'END') GOTO 5
        LAST=SEQ(51:55)
        SEQ=LAST(1:5)//ISEQ(1:50)
        PRINT 3,SEQ
        GOTO 7

5       CONTINUE
C          REMOVE COMPLEMENTS OF SEQUENCES
    DO 50 I=1,4
        DO 60 J=1,4
            DO 70 L=1,4
                DO 80 M=1,4
                    DO 90 N=1,4
                        DO 98 Q=1,4
                            IF ((I.NE.5-Q.OR.J.NE.5-N.OR.L.NE.5-M)
     1                             .AND.SMERS(I,J,L,M,N,Q).GE.0) THEN
                               SMERS(I,J,L,M,N,Q)=SMERS(I,J,L,M,N,
     1                                Q)+SMERS(5-Q,5-N,5-M,5-L,5-J,
     2                                     5-I)
                               SMERS(5-Q,5-N,5-M,5-L,5-J,5-I)=-1
                               ENDIF
98                                CONTINUE
90                             CONTINUE
80                         CONTINUE
70                     CONTINUE
60                 CONTINUE
50             CONTINUE

        CALL OUTPUT(SMERS)
1000        FORMAT (2X,I5)
        PRINT 1000,SMERS(1,1,1,1,1,1)
        PRINT 1000,SMERS(4,4,4,4,4,4)
        END

    SUBROUTINE INIT (AR)
        INTEGER*2 I,J,K,L,M,N,AR
        DIMENSION AR(5,5,5,5,5,5)
        DO 9 I=1,4
            DO 19 J=1,4
                DO 29 K=1,4
                    DO 39 L=1,4
                        DO 49 M=1,4
                            DO 59 N=1,4
                                AR(I,J,K,L,M,N)=0
59                                CONTINUE
49                             CONTINUE
39                         CONTINUE
29                     CONTINUE
19                 CONTINUE
9                  CONTINUE
        RETURN
        END

    SUBROUTINE INPUT(STRG)
        CHARACTER STRG*55
        OPEN (4,FILE='DATA.SEQ')
10        READ (4,FMT=200) STRG
        IF (STRG(1:5).EQ.'     ') THEN
            GOTO 10
            ENDIF
200            FORMAT (A)
        RETURN
```

```
      END

    SUBROUTINE OUTPUT(SSEQ)
      INTEGER*2 SSEQ,I,J,L,M,N,P,Q,COUNT,SUMMARY,SUM
      CHARACTER*5 BP,SITE*6
      DIMENSION SSEQ(5,5,5,5,5,5),SITE(6),SUM(6),SUMMARY(0:1000)

C      OUTPUT TO FILE LIST OF SIXMERS,FREQUENCY AND SUMMARY
      BP='ACGT'
      COUNT=0
      P=1
      OPEN (3,FILE='SEQLS6.OUT')
      DO 6 I=1,4
        DO 17 J=1,4
          DO 27 L=1,4
            DO 37 M=1,4
              DO 47 N=1,4
                DO 57 Q=1,4
                  IF (SSEQ(I,J,L,M,N,Q).GT.0) THEN
                    COUNT=COUNT+SSEQ(I,J,L,M,N,Q)
                    ENDIF
57                CONTINUE
47              CONTINUE
37            CONTINUE
27             CONTINUE
17          CONTINUE
6         CONTINUE
      WRITE (3,FMT=134) 'TOTAL SITES SCANNED=',COUNT
134     FORMAT (A,1X,I6)
      DO 8 I=1,4
        DO 18 J=1,4
          DO 28 L=1,4
            DO 38 M=1,4
              DO 48 N=1,4
                DO 58 Q=1,4
                  IF (SSEQ(I,J,L,M,N,Q).GE.0) THEN
                    SITE(P)=BP(I:I)//BP(J:J)//BP(L:
     1                L)//BP(M:M)//BP(N:N)//BP(Q:Q)
                    COUNT=COUNT+1
                    SUM(P)=SSEQ(I,J,L,M,N,Q)
                    P=P+1
                    SUMMARY(SSEQ(I,J,L,M,N,Q))=
     1                SUMMARY(SSEQ(I,J,L,M,N,Q))+1
                    ENDIF
                  IF (P.GT.6) THEN
                    WRITE (3,FMT=130) SITE(1),SUM(1),
     1                SITE(2),SUM(2),SITE(3),SUM(3),
     2               SITE(4),SUM(4),SITE(5),SUM(5),
     3                 SITE(6),SUM(6)
130                FORMAT (6(2X,A,I5),:)
                    P=1
                    ENDIF
58                CONTINUE
48              CONTINUE
38            CONTINUE
28             CONTINUE
18          CONTINUE
8         CONTINUE
      WRITE (3,FMT=132) SITE(1),SUM(1),SITE(2),SUM(2),SITE(3),SUM(
     1      3),SITE(4),SUM(4)
132        FORMAT (4(2X,A,I5),:)

      DO 200 I=0,1000
```

```
            IF (SUMMARY(I).GT.0) THEN
                WRITE (3,FMT=120) 'SIXMERS FOUND',I,'TIMES =',
     1                    SUMMARY(I)
120                 FORMAT (A,1X,I3,1X,A,I5)
                ENDIF
200             CONTINUE
        RETURN
        END
```

WEAKSX.FOR

```
C     FOR A DESCRIPTION OF PROGRAM, SEE SIXMER.FOR. THIS PROGRAM
C     TREATS A AND T AS INTERCHANGEABLE.

      PROGRAM MERS
       INTEGER*2 I,J,K(6),L,M,N,Q,II,JJ,LL,MM,NN,QQ,SMERS,COUNT
       DIMENSION SMERS(5,5,5,5,5,5)
       CHARACTER*4 BP*5, TEMP, SITE*10
       CHARACTER*60 LAST, SEQ, ISEQ

          PRINT 3,'STARTING'
          CALL INIT(SMERS)
          OPEN (4,FILE='DATA.SEQ')
          BP= 'ACGTX'
3              FORMAT (2X,A)
          CALL INPUT(LAST)
          CALL INPUT(ISEQ)
          SEQ=LAST(1:5)//ISEQ(1:50)
          PRINT 3,SEQ
7          CONTINUE
C
C          SORT SIXMERS OF SEQUENCE IN ORDER INTO ARRAY
          DO 10 I=1,50
              DO 20 J=1,6
                  K(J)=INDEX(BP,SEQ(I+J-1:I+J-1))
C                     COMBINES ALL A,T BP AS A'S
                      IF (K(J).EQ.4) K(J)=1
20                  CONTINUE
              SMERS(K(1),K(2),K(3),K(4),K(5),K(6))=SMERS(K(1),K(2),
     1              K(3),K(4),K(5),K(6))+1
10                CONTINUE

C     INPUT SEQUENCE UNTIL 'END'
          CALL INPUT(ISEQ)
          IF (ISEQ(1:3).EQ.'END') THEN
              GOTO 5
              ENDIF
          LAST=SEQ(51:55)
          SEQ=LAST(1:5)//ISEQ(1:50)
          PRINT 3,'  ',SEQ
          GOTO 7

5         CONTINUE
          PRINT 1000,SMERS(1,2,2,1,2,2)
          PRINT 1000,SMERS(3,3,1,3,3,1)
          PRINT 1000,SMERS(4,4,4,4,4,4)
C            REMOVE COMPLEMENTS OF SEQUENCES
      DO 50 I=1,3
          DO 60 J=1,3
              DO 70 L=1,3
                  DO 80 M=1,3
```

```
                    DO 90 N=1,3
                        DO 98 Q=1,3
                            II=5-Q
                            JJ=5-N
                            LL=5-M
                            MM=5-L
                            NN=5-J
                            QQ=5-I
                            IF (II.EQ.4) II=1
                            IF (JJ.EQ.4) JJ=1
                            IF (LL.EQ.4) LL=1
                            IF (MM.EQ.4) MM=1
                            IF (NN.EQ.4) NN=1
                            IF (QQ.EQ.4) QQ=1
                            IF ((I.NE.II.OR.J.NE.JJ.OR.L.NE.LL)
     1                           .AND.SMERS(I,J,L,M,N,Q).GE.0) THEN
                            SMERS(I,J,L,M,N,Q)=SMERS(I,J,L,M,N,
     1                           Q)+SMERS(II,JJ,LL,MM,NN,QQ)
                            SMERS(II,JJ,LL,MM,NN,QQ)=-1
                            ENDIF
98                             CONTINUE
90                          CONTINUE
80                      CONTINUE
70                  CONTINUE
60                CONTINUE
50            CONTINUE

        CALL OUTPUT(SMERS)
1000        FORMAT (2X,I5)
        PRINT 1000,SMERS(1,2,2,1,2,2)
        PRINT 1000,SMERS(3,3,1,3,3,1)
        PRINT 1000,SMERS(4,4,4,4,4,4)
        END

    SUBROUTINE INIT (AR)
        INTEGER*2 I,J,K,L,M,N,AR
        DIMENSION AR(5,5,5,5,5,5)
        DO 9 I=1,4
            DO 19 J=1,4
                DO 29 K=1,4
                    DO 39 L=1,4
                        DO 49 M=1,4
                            DO 59 N=1,4
                                AR(I,J,K,L,M,N)=0
59                              CONTINUE
49                          CONTINUE
39                      CONTINUE
29                  CONTINUE
19                CONTINUE
9               CONTINUE
        RETURN
        END

    SUBROUTINE INPUT(STRG)
        CHARACTER STRG*55
10        READ (4,FMT=200) STRG
        IF (STRG(1:5).EQ.'     ') THEN
            GOTO 10
            ENDIF
200           FORMAT (A)
        RETURN
        END
```

```
      SUBROUTINE OUTPUT(SSEQ)
          INTEGER*2 SSEQ,I,J,L,M,N,P,Q,COUNT,SUMMARY,SUM
          CHARACTER*5 BP,SITE*6
          DIMENSION SSEQ(5,5,5,5,5,5),SITE(6),SUM(6),SUMMARY(0:1000)

C          OUTPUT TO FILE LIST OF SIXMERS,FREQUENCY AND SUMMARY
          BP='WCGT'
          P=1
          COUNT=0
          OPEN (3,FILE='SEQLS6W.OUT')
          DO 6 I=1,3
              DO 17 J=1,3
                  DO 27 L=1,3
                      DO 37 M=1,3
                          DO 47 N=1,3
                              DO 57 Q=1,3
                                  IF (SSEQ(I,J,L,M,N,Q).GT.0) THEN
                                      COUNT=COUNT+SSEQ(I,J,L,M,N,Q)
                                      ENDIF
57                                  CONTINUE
47                                CONTINUE
37                              CONTINUE
27                               CONTINUE
17                          CONTINUE
6                       CONTINUE
          WRITE (3,FMT=136) ' '
136           FORMAT (A)
          WRITE (3,FMT=134) 'TOTAL SITES SCANNED=',COUNT
          WRITE (3,FMT=136) ' '
134           FORMAT (A,1X,I6)
          DO 8 I=1,3
              DO 18 J=1,3
                  DO 28 L=1,3
                      DO 38 M=1,3
                          DO 48 N=1,3
                              DO 58 Q=1,3
                                  IF (SSEQ(I,J,L,M,N,Q).GE.0) THEN
                                      SITE(P)=BP(I:I)//BP(J:J)//BP(L:
     1                                     L)//BP(M:M)//BP(N:N)//BP(Q:Q)
                                      COUNT=COUNT+1
                                      SUM(P)=SSEQ(I,J,L,M,N,Q)
                                      P=P+1
                                      SUMMARY(SSEQ(I,J,L,M,N,Q))=
     1                                    SUMMARY(SSEQ(I,J,L,M,N,Q))+1
                                      ENDIF
                                  IF (P.GT.6) THEN
                                      WRITE (3,FMT=130) SITE(1),SUM(1),
     1                                    SITE(2),SUM(2),SITE(3),SUM(3),
     2                                   SITE(4),SUM(4),SITE(5),SUM(5),
     3                                    SITE(6),SUM(6)
130                                  FORMAT (6(2X,A,I5),:)
                                      P=1
                                      ENDIF
58                                  CONTINUE
48                                CONTINUE
38                              CONTINUE
28                               CONTINUE
18                          CONTINUE
8                       CONTINUE
C         WRITE (3,FMT=132) SITE(1),SUM(1),SITE(2),SUM(2),SITE(3),SUM(
C     1         3),SITE(4),SUM(4),SITE(5),SUM(5),SITE(6),SUM(6)
132           FORMAT (6(2X,A,I5))
          WRITE (3,FMT=136) ' '
```

```
      DO 200 I=0,1000
          IF (SUMMARY(I).GT.0) THEN
              WRITE (3,FMT=120) 'SIXMERS FOUND',I,'TIMES =',
     1                    SUMMARY(I)
120               FORMAT (A,1X,I3,1X,A,I5)
              ENDIF
200           CONTINUE
      RETURN
      END
```

PROBSITE.FOR

```
C     PROBSITE COMPARES TWO SEQUENCE DISTRIBUTIONS TO SCREEN FOR
C     FREQUENCY DIFFERENCES HIGHER THAN A DEFINED THRESHOLD.
C     TO INCREASE RESULT SIGNIFICANCE, THE MINIMUM NUMBER OF CORRECT
C     MATCHES IS ALSO DETERMINED BY THE USER.
C     THIS PROGRAM IS BEST ACCESSED THROUGH THE BATCH FILES PROB AND
C     PROBSITE.
C
      PROGRAM PROBSITE
          INTEGER*2 I,P,ONUM(6),OSTD(6),COUNT
          REAL PROB,TNUM,TSTD,STDNUM,NUM,THRESH,PROBMULT
          CHARACTER*10 STDSITE,TEMP,INSITE,OSITE
          DIMENSION OSITE(8)

          OPEN (3,FILE='PROBSQ.DAT')
          OPEN (4,FILE='PROBSTD.DAT')
          OPEN (2,FILE='PROBLS.OUT')
          OPEN (1,FILE='CON')

          READ (3,FMT=100) TNUM
          READ (4,FMT=100) TSTD
100               FORMAT (F6.0)
          PRINT 100,TNUM
          PRINT 100,TSTD
          PROB= TNUM/TSTD
          PRINT 104,' CURRENT FREQUENCY LOWER LIMIT IS ',PROB
          PRINT 110,' CHANGE TO? (ADD DECIMAL POINT) '
104               FORMAT (A,F6.3)
          READ (1,FMT=106) PROB
106              FORMAT (F6.3)
102               FORMAT (F2.0)
          PRINT 110,' ENTER SMALLEST NUMBER TO KEEP '
          READ (1,FMT=115) THRESH
          PRINT 115,THRESH
          PRINT 104,' PROB=',PROB
          P=1
          COUNT=1
          WRITE (2,FMT=110) ' '
          WRITE (2,FMT=152) 'AVERAGE SINGLE SITE FREQUENCY (IF RANDOM) IS '
     1              ,TNUM,' /',TSTD,' = ',TNUM/TSTD
152               FORMAT (A,F6.0,A,F6.0,A,F6.3)
          WRITE (2,FMT=110) ' '
          WRITE (2,FMT=150) 'SITES PRESENT ',THRESH,
     1              ' TIMES OR GREATER WITH A HIGHER FREQUENCY THAN ',PROB
150              FORMAT (A,F5.0,A,F5.3)
          WRITE (2,FMT=110) ' '
          WRITE (2,FMT=160) 'SITE ','NO.','STD#','SITE ','NO.','STD#'
     1              ,'SITE ','NO.','STD#','SITE ','NO.','STD#'
160              FORMAT (4(2X,A6,2(A5)))
```

```
      WRITE (2,FMT=110) ' '

10          CONTINUE
      READ (3,FMT=110) INSITE
      READ (3,FMT=115) NUM
      READ (4,FMT=110) STDSITE
      READ (4,FMT=115) STDNUM
110       FORMAT (A)
115       FORMAT (F5.0)
C      PRINT 140,INSITE,STDSITE
140       FORMAT (2X,A,2X,A)
      IF (INSITE(1:3).EQ.'END') GOTO 30
          IF (INSITE.EQ.STDSITE) THEN
              IF (NUM/STDNUM.GE.PROB.AND.NUM.GE.THRESH) THEN
                  OSITE(P)=INSITE
                  ONUM(P)=NUM
                  OSTD(P)=STDNUM
                  P=P+1
                  COUNT=COUNT+1
                  IF (P.GT.4) THEN
                      WRITE (2,FMT=120) OSITE(1)(1:6),ONUM(1),OSTD(1),
     1                         OSITE(2)(1:6),ONUM(2),OSTD(2),OSITE(3)(1:6),
     2                        ONUM(3),OSTD(3),OSITE(4)(1:6),ONUM(4),OSTD(4)
                      PRINT 120,OSITE(1)(1:6),ONUM(1),OSTD(1),
     1                         OSITE(2)(1:6),ONUM(2),OSTD(2),OSITE(3)(1:6),
     2                        ONUM(3),OSTD(3),OSITE(4)(1:6),ONUM(4),OSTD(4)
120                          FORMAT (4(2X,A6,I5,I5))
                      DO 40 I=1,4
                          OSITE(I)=' '
40                              CONTINUE
                      P=1
                      ENDIF
                  ENDIF
              ENDIF
               GOTO 10
30          CONTINUE
      IF (OSITE(1).EQ.' ') GOTO 50
      IF (OSITE(2).EQ.' ') GOTO 70
      IF (OSITE(3).EQ.' ') GOTO 60
      WRITE (2,FMT=170) OSITE(1),ONUM(1),OSTD(1),
     1          OSITE(2),ONUM(2),OSTD(2),OSITE(3),
     2         ONUM(3),OSTD(3)
170         FORMAT (3(2X,A6,I5,I5))
      GOTO 50
60           CONTINUE
      WRITE (2,FMT=172) OSITE(1),ONUM(1),OSTD(1),
     1          OSITE(2),ONUM(2),OSTD(2)
172         FORMAT (2(2X,A6,I5,I5))
      GOTO 50
70           CONTINUE
      WRITE (2,FMT=174) OSITE(1),ONUM(1),OSTD(1)
174         FORMAT (1(2X,A6,I5,I5))
50           CONTINUE
      END
```